UNIVERSITY OF SOUTHERN QUEENSLAND

DEVELOPMENT AND VALIDATION OF A MECHANICAL THORAX SURROGATE FOR THE EVALUATION OF THE BLUNT TRAUMA DUE TO BALLISTIC IMPACTS

A Dissertation submitted by

Narasimha Murthy Thota

B.Tech (Mech. Engg.), M.Sc (Physics), ME (Engg. Design), B.A.M.S

For the award of

Engineering Doctorate

2014

Dedication

To my father Late Sri. Venkaiah, my mother Late Smt. Anantha Laxmi and my aunt Narsamma for their divine love and blessings, my wife Smiti and lovely kids Curie and Cura aka Mihir for their love and unconditional support

Abstract

Although fruits of few decades worth of research carried out worldwide by scientists, engineers and researchers, have been available to everybody with a mouse click, engineering problems have not always been easy to accomplish. The complexities of the real life problems are due to lack of resources, lack of applicability of the available data and also due to the increasingly innovative and competitive marketplace. Therefore, engineers always face challenges and strive to accomplish the tasks to obtain desired outcome with continuous research and innovative approach. Two of such challenges, one related to the validation of a closed cell foam material for fabrication of non-lethal munitions and the other related to the development of compliant vehicle front protection systems (VFPS) for modern passenger cars, necessitated extensive research study and led to the development of the finite element (FE) model of thorax surrogate (Mechanical THOrax for Trauma Assessment – MTHOTA) and development a computer aided engineering (CAE) based method for the development of airbag compatible and ADR 69/00 (Australian Design Rule for vehicle occupant safety) compliant multi-variant vehicle front protection systems for a vehicle with multi-variants, with a minimum number of crash tests. These two challenging problems, pertinent research, development, and the outcome, have been presented in this thesis.

Initially, four anthropomorphic test devices (ATDs) were reviewed for their suitability for the evaluation of the blunt trauma. As they were found unsuitable for the intended application, novel concepts for the thorax surrogate were developed and studied for their feasibility. One of the novel ideas was pursued further and developed into a fully correlated (validated) FE model of a thorax surrogate (MTHOTA). Robustness and efficacy of the MTHOTA surrogate was verified for many cases studies from the published literature. Biomechanical responses obtained for the MTHOTA surrogate have shown a correlation with the respective cases. Due to its simplicity, accuracy, easy setup, fast solving and non-ambiguity, the MTHOTA surrogate was successfully used for the evaluation of:

1. the blunt thoracic trauma due to ballistic impacts and the risk of commotio-cordis due to solid sports ball impacts

2. the effect of material, spin and impact speed of the solid sports ball on the thoracic trauma

3. projectile – thorax energy interactions and their relation with the viscous criterion

4. the performance of new non-lethal weapons and foam materials

5. the effect of the energy-absorbing mechanisms on the blunt thoracic trauma caused by Kinetic Energy Non-Lethal Weapons (KENLW)

Concerning the second challenge mentioned above, a systematic procedure based on the non-linear finite element analysis simulations was devised for the development of compliant front protection systems for vehicles with and without airbags. The devised method has successfully been implemented and made commercially non-viable and extremely cumbersome FPS development projects into reality.

By exploiting the non-linear FE simulations expertise and foam material data, effect of foam embellishments on the pedestrian safety characteristics of the FPS was examined highlighting the benefits of garnishing FPS with such semi-rigid foam parts and presented in the thesis. Effect of FPS on the crash compatibility between vehicles was also studied and made recommendations for reaping the benefits of the VFPS.

Certification of Thesis

I certify that the research work and the outcome presented in this thesis are entirely my own work, except where otherwise acknowledged. I also certify that the work is original and has not been previously submitted for any other award, except where otherwise acknowledged.

_____ _____

Signature of Narasimha Murthy Thota Date

ENDORSEMENT

_____ _____

Signature of Dr. Jayantha A Epaarachchi Date

_____ _____

Signature of Prof. Kin-Tak Lau Date

Acknowledgements

The list of persons I wish to thank is, indeed, overwhelmingly long. So, if I have chosen a few whose contribution is conspicuous, it is not because I have forgotten others.

First of all, I am extremely grateful to Ms. Smiti Malik, Chairman of then Krish Engineering Services Pty Ltd (South Australia) and Mr Srinivasa Rao Koya, CEO of Amerigo Structural Engineers Private Limited (Bangalore, India) for sponsoring the research work and extending unconditional support. I am also extremely grateful to Ms. Lakshmi, Mr. Baskaran, one and all of Mindglow India Pvt Ltd (Bangalore, India) for providing unconditional support with never-say-die spirits.

It is with a deep sense of respect and reverence that I express my sincere thanks to my principal supervisor Dr. Jayantha A Epaarachchi and associate supervisor Prof. Kin-Tak Lau for their continuous encouragement and guidance. My profound and sincere thanks to the panel members Dr. Sourish Banerjee, Dr. Kazem Ghabraie, Dr. Mainul Islam and Dr. Cahn-Dung Tran for their valuable suggestions, during the review of the research proposal. I extend my sincere thanks to Dr. Mihir Dilip Wechalekar (Consultant Rheumatologist) for his reviews and valuable advices to ameliorate the quality of the presentation.

I am thankful to Ms. Jaunita Ryan and one and all of the esteemed USQ, for their continuous support and for providing necessary extensions and prompt responses to my numerous queries. I am also thankful for my siblings, friends, relatives and treating doctors for their immense support during all these years of debilitating illness.

I convey my heartfelt thanks to my lovely wife Smiti for her excellent support and patience. Without her support, with my current health condition, I would be very far from the submission of the thesis.

At last, but not least, I thank and bless my lovely kids Miss Curie and Master Cura aka Mihir for patiently tolerating me while I was unavailable and engrossed in the research work.

Thank you one and all.

Table of Contents

List of Figures

List of Tables

Notations, Units, and Abbreviations

Notations and Abbreviations

3-RCS	3 Rib Chest Structure
AIS	Abbreviated Injury Scale
ASA	Average Spinal Acceleration
ATD	Anthropomorphic Test Dummy or Anthropomorphic Test Device
BC	Blunt Criterion
CAE	Computer Aided Engineering
COR	Coefficient of Restitution
D	Dummy constant (measured in length dimension)
DSTO	Department of Science and Technology Organization
EA	Energy Absorbing
ECU	Electronic Control Unit
FEA	Finite Element Analysis
GAW	Gross Axle Weight
GVM	Gross Vehicle Mass
HSTM	Human Surrogate Torso Model
KENLW	Kinetic Energy Non-Lethal Weapons
LSTC	Livermore Software Technology Corporation
LP	Long Projectile
LV	Left Ventricle
MTHOTA	Mechanical THOrax for Trauma Assessment
P(AIS3+)	Probability for level 3 or more injuries on AIS
P(AIS4+)	Probability for level 4 or more injuries on AIS

PMHS	Post Mortem Human Subject
PVC	Poly Vinyl Chloride
S	Scale factor of the ATD (a dimensionless multiplication factor)
SP	Short Projectile
TPE	Thermo Plastic Elastomer
TTI	Thoracic Trauma Index
VC	Viscous Criterion = Product of the instantaneous 'Velocity of chest deformation' and instantaneous 'Chest compression'
VC_{max}	Max of Viscous Criterion
VF	Ventricular Fibrillation
VFPS	Vehicle Front Protection System

Units

9	9.81 m/s^2
GPa	Giga Pascal
kgf	kilogram-force
kPa	kilo Pascal
kN	kilo Newton
m	meter
m/s	meter per second
ms	millisecond
N	Newton
s	second

CHAPTER-1: INTRODUCTION

The research work presented in this thesis has been concerned with two major innovations. They are:

1. Development and validation of an FE model of the thorax for the evaluation of the blunt thoracic trauma due to ballistic impacts.
2. Development of a CAE based method for the design, development and validation of AS 4876.1-2002 compliant, airbag compatible and ADR 69/00 compliant multi-variant FPS for multi-variant vehicle with a minimum number of physical crash tests.

1.1 Statement of the problem related to thoracic trauma caused by impacts of non-lethal munitions

Various military research organizations and weapons manufacturers have been developing non-lethal munitions of different kinds, due to increasing demand for such munitions which can temporarily incapacitate the subjects of interest during peace-keeping missions, civilian riot control scenarios and other situations that do not warrant the usage of lethal force (Bir 2000; Koene, Id-Boufker & Papy 2008; Lyon, Bir & Patton 1999; Papy et al. 2012). Of numerous non-lethal munitions, foam nosed projectiles (for instance, eXact iMpact 1006 grenade, NS, NP and B&T) are some of the latest munitions available to the military and law enforcement officials in the USA and many other countries.

Though validated with experiments using clay signature tests, ballistic gelatin penetration tests and anesthetized animal surrogates, due to erroneous correlation with the human thorax, many so called non-lethal munitions have been reported causing fatal chest injuries, both blunt and penetrating. The record of injuries caused by impacts of non-lethal munitions is available dates back to the early 70's. Rubber ball projectile impacts have caused serious lung contusions as secondary injury, caused by penetration of the lungs by broken ribs (Millar et al. 1975; Shaw 1972). Plastic baton projectile impacts have been reported causing 147 cases of serious injuries, of which 21 were pertaining to thoracic trauma (Sheridan, S. M. & Whitlock, R. I. 1983). Similarly, many medical professionals (Ritchie 1992; Ritchie & Gibbons 1990; Rocke 1983) treating the victims have reported that plastic baton projectile impacts have caused 5 deaths and more than 200 serious injuries, of which 80 were serious thoracic injuries.

Wayne State University's researchers (Bir, Viano & King 2004; Bir 2000) have carried out extensive tests by subjecting the thoraces of cadavers with wood baton projectile impacts and developed biomechanical response corridors of the human thorax and also a reusable thoracic surrogate (3-Rib Chest Structure, popularly known as 3-RCS) for the evaluation of the blunt thoracic trauma due to blunt ballistic impacts. Though 3-RCS is widely used by various military organizations for the development and validation of novel non-lethal munitions, the latest plastic attenuated energy munitions (Maguire et al. 2007), 8 gram rubber balls (Chowaniec et al. 2008), 19 gram rubber attenuated energy (Rezende-Neto et al. 2009), 28 gram foam nose grenades, have been reported causing serious thoracic trauma to some of the victims. This performance related short-comings of the novel non-lethal munitions could be due to the effect of various factors such as age, build, race,

gender and clothes worn at the time of impact on the blunt thoracic trauma or could be due to the limitations of the surrogate used for validating the munitions or could be due to erroneous scaling or correlation of the clay signature tests and gelatin penetration tests with the human thorax. From the published research (Bir, Viano & King 2004; Bir 2000; Dau 2012; Lyon, Bir & Patton 1999) it is clear that 3-RCS, which is widely used by US military research organizations, has many limitations and has shown erroneous correlation with the cadaver tests. Such problems necessitate the development of an easy to use thorax surrogate that accurately predicts blunt trauma due to ballistic impacts. Such surrogate can be useful not only for the validation of the non-lethal munitions, but also for the validation of chest protectors for sports personnel and also development of safe solid sports balls and related material research. Physical surrogates will have some inherent disadvantages and limitations such as costly equipment (high-speed cameras, sensors and gauges, signal processing unit and software, etc.) and require preparation of the prototypes. At the same, very limited amount of data can be measured, as every measurement entails relevant hardware. All these limitations can be addressed through the development of appropriate finite element models of the thoracic surrogates that perfectly correlate with the cadaver test results (for example, human response corridors of all biomechanical responses; force-time, deflection-time and force-deflection).

1.1.1 Research goals

1.1.1.1 Review of anthropomorphic test dummies

Both physical and finite element models of the ATDs have been developed by various organizations involved in the vehicle occupant safety related research and development. Only two years after the development of human thorax responses and tolerance limits by Kroell et al. 1974, the Hybrid III dummy appeared for the first time in simulated tests. Now, Hybrid III has evolved into a family of dummies that were developed to be used as human surrogates in the simulated front crash tests of vehicles. Similarly, different dummies such as, ES-2Re, SID, Bio-SID, World-SID, etc. were developed for the simulated vehicle side impact tests. Both Hybrid III and Side Impact Dummies facilitate the quantification of blunt thoracic trauma in terms of the sternal deflection, chest compression and viscous criterion (VC) and head trauma in terms of head injury criterion (HIC).This led Janda et al. 1992 to use a Hybrid III child crash test dummy for the evaluation of the blunt thoracic trauma caused by baseball impacts. Viano et al. 2004 have studied facial injuries of the forehead, zygoma and mandible, due to blunt ballistic impacts by impacting the frangible face of the Hybrid III dummy with an instrumented 35 g, 37 mm blunt projectile. Similar experiments were conducted with cadavers and after comparison it was concluded that Hybrid III dummy's frangible face emulated the human head, as far as the injuries concerned. Using the Hybrid III dummy, Walilko et al. 2005 have studied the head injuries caused by an Olympic boxer's punch. Using Hybrid III dummies, Viano et al. 2005 have studied concussion due to football impacts and compared the outcome with that obtained from Walilko et al. 2005. From a blunt impact head trauma point of view, the performance of ATD is comparable with that of human cadaver surrogates. So far, no researcher has evaluated the ATD's for their usefulness in predicting blunt thoracic trauma due to ballistic impacts.

It is important to note that all ATDs were validated with the human response corridors developed by Kroell (Kroell et al. 1986; Kroell, Schneider & Nahum 1971, 1974) which were pertinent to the automotive impacts. The human response corridors developed ((Bir, Viano & King 2004) for test conditions germane to blunt ballistic impacts to the thorax could be useful for validation of any thorax surrogates. Therefore, using these latter human response corridors, three front impact dummies, and one side impact dummies were reviewed to find out their suitability for measurement of the blunt thoracic trauma of interest. If a correlation exists with the cadaver test data, ATDs can be utilized for the validation of non-lethal munitions, chest protectors for sports personnel and safe solid sports balls, etc.

1.1.1.2 Development and validation of the FE model for a thorax surrogate

In case the ATDs are found not to be suitable for the applications of interest, as there is a need for a human thorax surrogate, development of new concepts is essential. Biomechanical responses measured by Bir et al. 2004 by subjecting thoraces of human cadavers to the blunt impacts of interest, could be useful for the validation of the surrogate concepts. The process of validation of surrogates using human response corridors (Bir, Viano & King 2004) is very cumbersome, therefore, a pilot study to assess the feasibility of the concept considered for the validation of the thorax surrogate is required.

Once the feasibility confirmed, thorax surrogate concept needs to be correlated with the cadaver test data. Further validation of the thorax surrogate may be required to confirm the bio-fidelity as far as the impacts of interest are concerned.

1.2 Statement of the problem pertaining to the design and development of the vehicle front protection systems

Owing to the high prevalence of vehicle-animal collisions in the Australian outback, to protect the crucial vehicle front-end systems (such as radiator and headlamps), owners equip their vehicles with the front protection systems (popularly known as Bumper bar, Bullbar, Nudge bar and Roo-bar, etc.) so that they do not get stranded somewhere very far from help, in the event of such a collision with an animal.

Standards Australia has developed specifications for the VFPS concerning pedestrian safety. Fitment of the VFPS should not alter the vehicle's pedestrian safety characteristics. Similarly, Australian Federal Office of Road Safety (FORS) set up minimum safety requirements for the vehicle occupant in the form of regulation called ADR 69/00. From the year of its inception, it is mandatory for all vehicles sold in Australia (whether fitted with FPS or not) to comply with the ADR 69/00.

Fitment of the VFPS (whether it is as over the bumper type or a bumper replacement type) alters the vehicle crash characteristics. It is critical to note that all modern day passenger cars are designed and developed to meet two contradicting safety requirements. In the event of vehicle collision, the occupants should, on the one hand, not experience deceleration levels more than a specified tolerance limit by absorbing the crash energy through plastic deformation, while

on the other hand, vehicle crush should be controlled in such a way that it does not degrade the passenger compartment more than by a specified safe intrusion limit. Addition of the stiffer, massive and rigid structures may cause occupant to experience a deceleration more than the tolerance limit. Addition of the FPS loads the front axle adversely. If the FPS is massive, Gross axle weight (GAW) of the front axle may exceed the design limit and pose serious problems for the steering and braking systems and may lead to fatal accidents in some cases. In a similar way, softer and lighter structures may degrade the passenger compartment which in turn can cause serious injuries to the occupant. Mounting points used for the fitment of the FPS, if not properly selected, can cause more damage to the structures and systems in the front end of the vehicle. Therefore, adequate care in designing FPS is required, as only suitably designed FPS can offer an additional protection to the vehicle front end components.

Present day vehicles offer many safety features such as airbags, seat belts, ABS and traction control, etc. pertinent to the occupant safety and vehicle control. Various airbags, which became standard features of most of the modern passenger cars, offer additional protection to the occupants in the event of major accidents. During the crash, due to inertia effect, vehicle occupant moves forward as the vehicle decelerates, and can get injured by impacting with the vehicle interiors such as a steering wheel or dashboard depending upon the occupant's seating position. Seat belt and air bag together protects the vehicle occupant and reduces the level of injuries in the event of major accidents. Before the passenger hitting the hard interiors of the vehicle during the crash, a fully inflated airbag stops the moving passenger and slowly decelerates the passenger by getting deflated with the calculated rate. Crash severity sensing would require many sensors (mechanical and electrical). By analyzing the crash sensor data, an electronic control unit (ECU) decides whether the airbag should be deployed or not. Addition of the FPS, depending upon how stiff and massive it is, alters the vehicle crash characteristics which in turn can affect the airbag deployment characteristics. In a nutshell, if fitted with improperly designed FPS, an airbag may not fire in the event of severe crash or an airbag may fire even in the event of innocuous vehicle impacts. In the former case, occupants would hit the hard interiors without any cushioning effect offered by the airbags and in the latter case, deploying the airbag itself can inflict serious injuries to the occupants. Therefore, if fitted to vehicles with airbag, FPS should be airbag compatible and irrespective of the presence of the airbags, every vehicle must comply with the ADR 69/00 requirements.

1.2.1 Research goals

1.2.1.1 Development of VFPS for non-air bagged vehicles

Small scale industries with limited resources have been developing FPS for non-air bagged passenger vehicles by taking few measurements of the vehicle, with the misconception that massive and stiff FPS with channel type fascia would provide additional protection to the vehicle. These bars look fantastic and attract many buyers. In Australia, it is illegal to fit the FPS if it does not comply with AS 4876.1-2002 and ADR 69/00. Though these standards and design rules outline the FPS requirements, no development methodologies are mentioned. Therefore, many manufacturers perform pendulum tests to find out the compliance of the FPS with ADR 69/00. Verification of the vehicle's compliance with ADR 69/00 requires full

vehicle full frontal crash tests with belted and instrumented Hybrid III dummies in the driver and passenger seats. However, a very first design may not be ADR 69/00 compliant. As these crash tests are very expensive, any FPS development project becomes commercially non-viable. Such situations necessitate a systematic method based on engineering calculations and CAE simulations for the development of fully compliant FPS.

1.2.1.2 Development of VFPS for air bagged vehicles

It is important that airbags get deployed only at certain levels of crash severity. Therefore, manufacturer of the vehicle sets 'airbag no fire' and 'airbag must fire' velocity thresholds for every vehicle. Sensors mounted on the vehicle (minimum two sensors) will collect the vehicle kinematics (deceleration, velocity and deformation) during the crash and send the signals to the ECU where they will be analyzed using the airbag crash sensing algorithm. Based on the outcome of the analysis, ECU can send a signal to activate the airbag deployment.

Sredojevic et al. 1998, by carrying out pendulum dynamic impact tests, proposed that if the lowest deceleration is 12 g, the FPS can be considered airbag compatible. This postulation was vehicle specific and not applicable to all other vehicles. Sensor type, sensor location, front end vehicle structure, etc. significantly influence the airbag deployment characteristics. Without taking any of these into account, just by impacting the FPS with a pendulum, airbag compliance cannot be decided. An Australian researcher (Bignell 2004) has conducted quasi-static compression tests and pendulum dynamic impact tests on 100 FPS and concluded that if FPS (bumper replacement type) absorb less than 8 % of the total impact energy, no further testing is required for the airbag compliance. It is, however, not correct to determine the airbag compatibility based on the energy absorption alone, without taking the vehicle's front-end structure into account.

The only way to develop airbag compliant FPS is by barrier tests (full vehicle crash tests). As mentioned earlier, these tests are very costly, and development of the FPS may become non-viable, especially if the vehicle has got many variants and manufacturers want to develop multi-variant FPS. For instance, development of airbag compatible and ADR 69/00 compliant FPS (one variant only) for a single variant vehicle, a minimum of 3 physical whole vehicle crash tests (airbag no fire test, airbag must fire test and ADR 69/00 high speed crash test) would be required. Similarly, for the development of five variants of VFPS for a vehicle with 8 variants, the number of whole vehicle crash tests required would be 120. Such situations make the FPS development projects commercially non-viable and practically impossible in the case of a new vehicle development program due to scarcity of prototype vehicles. Such situations necessitate a design and development method that is systematic and minimizes the number of physical crash tests and make FPS projects commercially viable.

1.3 Specific aims of the research study

The explicit aims of the research study include the following

1. The review of finite element models of the anthropomorphic test devices (ATDs) for their usefulness for the evaluation of blunt thoracic trauma due to ballistic impacts.

2. The development of novel concept for the mechanical thorax surrogates and feasibility study
3. The development and validation of the **M**echanical **THO**rax for **T**rauma **A**ssessment (MTHOTA) for the applications involving blunt ballistic impacts.
4. The evaluation of blunt thoracic trauma due to solid sports ball impacts, using MTHOTA surrogate.
5. Quasi-static foam compression tests to develop the material data for non-linear FE analysis involving foam nosed projectiles for providing a solution for some defense industry problems by determining the blunt thoracic trauma using MTHOTA as thorax surrogate.
6. The review of Viscous Criterion and its relation with energy interactions of the projectile – thorax.
7. The development of a systematic engineering approach for the design and development of (AS 4876.1-2002 and ADR 69/00) a compliant vehicle front protection systems for non-air bagged vehicles.
8. The development of a systematic engineering approach for the design and development of airbag compatible, AS 4876.1-2002 and ADR 69/00 compliant vehicle front protection systems for non-air bagged vehicles with a minimum number of whole vehicle physical crash tests.
9. The development of a cost-effective way to improve the pedestrian safety of the VFPS.
10. The review on the impact of VFPS on the other road users in the side impact scenario to decide whether 'VFPS is a Foe or a Friend?'

1.4 Thesis structure

Study and the outcome pertaining to all specific research aims are presented in the thesis. Every chapter of the thesis is a summary of at least one journal or conference paper published by the author of the thesis.

Chapter–2 summarizes the historical background of non-lethal weapons, blunt ballistic impacts, blunt thoracic injury, injury criteria and human tolerance limits. It also presents the outcome of the review of ATDs for the evaluation of blunt thoracic trauma. A technical paper pertinent to the research work presented in this chapter has been accepted for publication in the proceedings of the Australasian Conference on Applied Mechanics 8 (ACAM8) and the details of the paper are given in the Appendix – I of the thesis.

Chapter–3 summarizes some novel concepts for the human thorax surrogate for blunt ballistic applications and also presents the feasibility study of one of the developed concepts. A technical paper was pubslished in the proceedings of the Australasian Conference on Applied Mechanics 7 (ACAM7). The details of the paper are given in the Appendix – I of the thesis.

Chapter–4 summarizes existing thorax surrogates and their limitations and also presents the development and validation of the Mechanical THOrax for Trauma Assessment (MTHOTA) for blunt trauma applications, while highlighting the efficacy of the MTHOTA by further case studies related to the latest non-lethal projectiles. Development and validation of MTHOTA has been published in the Journal of Biomechanical Science and Engineering (JBSE), and the details of the paper are given in the Appendix – I of the thesis.

Chapter–5 deals with the evaluation of the blunt thoracic trauma due to solid sports ball impacts and also presents the effect of spin, material and impact velocity of the solid sports ball on the blunt thoracic injury while making an emphasis on the commotio-cordis, ball kinematics and relation between the viscous injury and ball-thorax energy interactions. The research outcome of the study presented in this chapter has been under review for the publication in the Journal of Biomechanical Science and Engineering (JBSE). Details of the manuscript submitted to the JBSE is provided in the Appendix – I of the thesis.

Chapter–6 deals with the development of cheaper alternative munitions for the MK79 foam grenade launcher and also summarizes the effect of energy absorbing mechanisms on the blunt thoracic trauma, when embedded in the foam nosed projectiles. Details of the technical papers published in the WCFMAAE-2013 and the ACAM8 conference proceedings were provided in the Appendix –I of the thesis.

Chapter–7 deals with an engineering approach devised for the development of AS 4876.1-2002 and ADR 69/00 compliant VFPS that offer additional safety to the front-end of the vehicle and the occupants. This chapter also exemplifies the importance of styling and mass setting calculations for even a car without airbags, while highlighting the novel method based on the simplified crash simulations for the selection of FPS mounts.

Chapter–8 deals with the CAE based methodology useful for the design and development of airbag compatible, ADR 69/00 multi-variant VFPS for a vehicle with multi-variants. This chapter also highlights the various methods employed for deciding the airbag compatibility of the VFPS and their shortcomings, while making an emphasis on the detrimental effects of the VFPS on the pedestrian safety and adverse effects on the 'crash compatibility' between vehicles. Details of a technical paper published in the WCFMAAE-2013 conference proceedings and also a technical paper published in the 'International Journal of Vehicle Structures and Systems' were given in the Appendix – I of the thesis.

Chapter–9 summarizes the overall outcome of the research study and also highlights the future study prospects in the areas of thorax surrogates for blunt trauma evaluation and airbag compliant VFPS related aspects.

CHAPTER-2: SUITABILITY OF ANTHROPOMORPHIC TEST DUMMIES FOR THE EVALUATION OF THE BLUNT THORACIC TRAUMA DUE TO BALLISTIC IMPACTS – A CAE BASED SCHOLASTIC STUDY

This chapter introduces the non-lethal munitions and their importance, blunt thoracic trauma, injury criteria and human tolerance limits while summarizing the pivotal role of physical and finite element models of the thorax surrogates in the development of non-lethal ammunition and sports safety equipment. This chapter also deals with the determination of the suitability of the anthropomorphic test dummies (ATD) for the evaluation of the thoracic trauma caused by blunt ballistic impacts, which is a summary of a technical paper accepted for the publication in the ACAM8 conference proceedings, details of which are given in the Appendix – I of the thesis.

2.1 Introduction

2.1.1 Blunt ballistics

Until recently, law enforcement officers and military personnel involved in peacekeeping missions and riot control situations, often used lethal force whenever the situation was beyond control. Usage of lethal force though not warranted in such circumstances, the officers involved have had no other choice but taking resort to lethal force. Owing to the increased scrutiny over the law enforcement scenarios, there has been lot of research in the area of non-lethal weapons to provide many options to the military forces and the civil police, ranging from the negotiation – lethal force (Bir 2000; Koene, Id-Boufker & Papy 2008; Volokh 2009).

With the increase in peace-keeping missions and with the rise in situations where civil police is called upon to subdue emotionally disturbed civilians without application of lethal force, military research organizations and law enforcement agencies have invested more time and resources to develop a broad variety of non-lethal weapons. Though there are other non-lethal means of chemical irritants and sprays, tear gas shells and water jets, this chapter focuses on the projectiles (ranging from wooden/plastic baton over sophisticated foam grenades to TASER-XREP rounds) that are designed to cause blunt thoracic trauma sufficient to deter or subdue the subject of interest. Some of the non-lethal weapons and munitions are as shown in Figure 2.1 and Figure 2.2 respectively.

Figure 2.1: TASER gun, Pepper spray gun, M79 grenade launcher, M32 grenade launcher (from top left to the last photo, in order)

Figure 2.2: Rubber bullets, Foam baton, Rubber buck shot, Bean bag, DIRECT IMPACT foam nosed grenades (from top left to the bottom right photo, in order)

Although every weapon is designed to perform a particular level of damage, non-lethal weapons designed to specifications what a weapon should not do. Definition of non-lethal weapons as per the United Nations Institute for Disarmament Research (UNIDIR) as given below clearly states the damage and injuries a non-lethal weapon should not cause (Koene, Id-Boufker & Papy 2008; Widder, Butz & Milosh 1997).

> *Non-lethal weapons are specifically designed to incapacitate people or disable equipment, with minimal collateral damage to buildings and environment; they should be discriminate and not cause unnecessary suffering; their effect should be temporary and reversible; and they should provide alternatives to, or raise the threshold for, use of lethal force.*

Though the application of non-lethal munitions intended to incapacitate or deter the individual without causing injuries that require medical treatment more than the simple first aid, there have been many reported fatalities and serious injuries with the usage of these weapons. More than 55000 rubber bullets were fired to control the civilian riots in Northern Ireland during the 6 years period from 1970-75. After careful analysis of the medical professionals, it was estimated that rubber bullets caused 5 deaths, and seriously injured more than 500 persons, while many sustained injuries that required hospitalization. During most recent confrontations of the Israeli-Police to subdue the Israeli-Arab rioters, usage of rubber bullets has caused 13 deaths and many more serious injuries (Krausz & Mahajna 2002; Mahajna et al. 2002). Similarly, during the year 1996 in Northern Ireland, more than 8000 plastic baton rounds were fired to control the riots. More than 155 persons sustained serious injuries and of these 45 persons were hospitalized (Steele et al. 1999). Even in North America five deaths and many injuries caused by the non-lethal weapons were reported (Ijames Spring, 1997). Of these 5 deaths, 4 were dead due to a severe structural damage to the thorax and the other one died because of commotio-cordis.

Though sports are for entertainment and enjoyment, many sports personnel of contact-collision sports sustained serious thoracic injuries. Many young adult players have collapsed and died on the spot due to ventricular fibrillation (commotio-cordis) when they were hit by solid sports balls (baseball, golf ball, Lacrosse ball and Cricket ball) and hockey pucks on the thorax. None of the victims were reported to have any past history of heart illness (Blas & Caussade 2011; Madias, Christopher et al. 2007; Maron & Estes III 2010; Maron et al. 2002; Maron et al. 1995).

In order to design, develop and validate non-lethal weapons (to meet the definition given by UNIDIR), validation of the bullet proof vests and chest protectors, safety balls and other personnel protective equipment for the sports personnel, it is important to understand and be able to measure the blunt thoracic trauma caused by blunt ballistic impacts i.e., impacts with the blunt projectiles of low mass 20 – 200 grams with speed 20 – 250 m/s (Bir 2000). The difference between blunt ballistic impacts and automotive impacts is delineated in Figure 2.3. Therefore, three Hybrid III dummies and one side impact dummy were reviewed whether they can be useful for the evaluation of the trauma due to blunt ballistic impacts, and outcome was presented in this chapter.

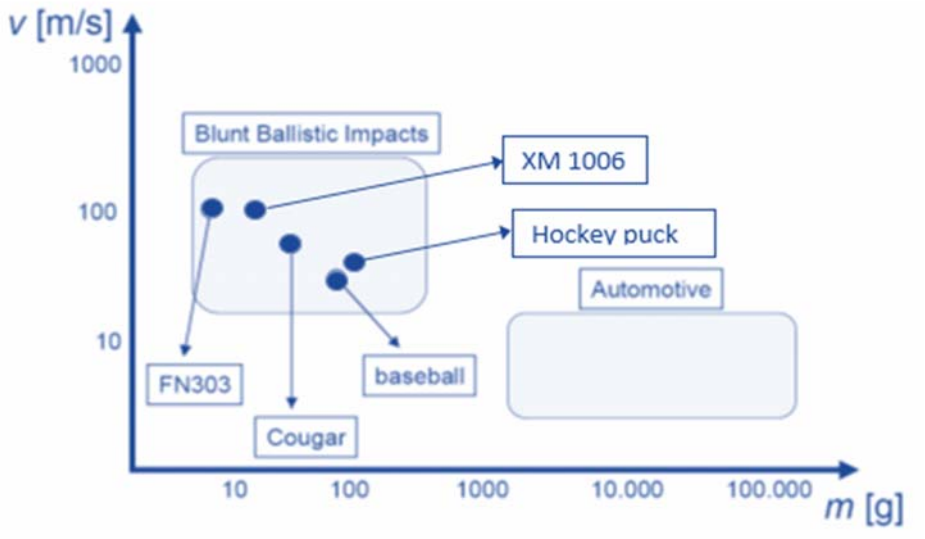

Figure 2.3: Difference between automotive collisions and the blunt ballistic impacts as far as the mass and speeds are concerned. Adapted from (Koene, Id-Boufker & Papy 2008) and with the addition of my own data

2.1.2 Thoracic injuries, injury criteria, human tolerance limits

When the thorax is subjected to a blunt impact force, ribs can deform and fracture if the amount of stress exceeds the tolerance of the ribs. Depending upon severity and location of the impact, fractured ribs can penetrate through the internal organs, leading to various injuries such as flail chest, hemothorax, pneumothorax, lacerated liver, punctured liver, heart contusion, ruptured aorta, ventricular septal defect, and so on (Mancini 2012). Therefore, non-penetrating thoracic trauma, depending upon the severity, can cause serious illnesses and can even lead to the death. More than 50% of the accidental deaths (automobile accidents, falls and street fights) are associated with chest trauma and of which 50% is directly due to blunt thoracic trauma (Vlessis & Trunkey 1997). As per the statistics published in the website of Centers for Disease Control and Prevention, unintentional injuries have been rated as the fifth among the leading causes of death. Such injuries were responsible for more than 120,000 deaths during the year 2011 in the United States. Approximately 25% of these deaths were caused by blunt thoracic trauma (Hoyert & Hu 2012). Evaluation of the blunt thoracic trauma and human tolerance limits plays a pivotal role in improving the vehicular occupant safety. Therefore, there has been extensive research in the automotive area leading to gaining greater insight into blunt thoracic trauma and human tolerance limits in terms of known measurable engineering parameters. As shown in Figure 2.3, blunt ballistic impacts differ from automotive collisions, and only very limited data is available for the case of blunt ballistic impacts.

Researchers have developed different criteria to evaluate the blunt thoracic trauma and also determined human tolerance limits in terms of whole body acceleration (Eiband 1959; Stapp 1970a), Average Spinal Acceleration (Cavanaugh et al. 1993), Force injury (Gadd & Patrick 1968), Thoracic Trauma Index (Morgan, Marcus & Eppinger 1986), and Viscous Criterion (Viano, David C. & Lau, Ian V. 1988;

Viano et al. 1989). Some of these researchers used human volunteers, and others used human cadavers and anesthetized animals in their experimental studies. In all cases, impacts were of heavy mass impacting with low speeds and were pertinent to the occupant in a vehicle crash scenario. The data developed from these experiments helped the scientists and engineers to develop safety restraint systems, both active and passive, for the automotive industry, which successfully reduced the fatalities due to blunt thoracic trauma. Thoracic injury criteria and human tolerance limits and the associated equations to evaluate the criteria, are treated more in detail in the following sections.

2.1.2.1 Force criterion

Stapp conducted rocket sled tests on passenger restraint systems volunteering himself as an occupant. He determined the human tolerance to whole body acceleration of long duration (Stapp 1951a, 1951b; Stapp 1955, 1970b). Though he sustained serious injuries during the experimentation, his experiments have inspired many researchers and organizations working on automotive safety. Eiband, 1959 has conducted similar experiments using cadavers as occupants. Other researchers (Gadd & Patrick 1968; Patrick, Kroell & Mertz 1965) have conducted sled crash experiments using cadavers mounted with load cells and have developed a force injury criterion according to which human tolerance for well distributed blunt chest loading is 8 kN.

2.1.2.2 Thoracic Trauma Index (TTI)

Another injury criterion, Thoracic Trauma Index (TTI), based on the rib and spinal acceleration was developed (Kallaieris et al. 1981; Kuppa et al. 2003; Morgan, Marcus & Eppinger 1986; Pintar et al. 2007).

Thoracic Trauma Index (TTI) can be evaluated using the equations given below.

$$TTI = 1.4\times AGE + 0.5(RIB_y + T12_y)\,(MASS/M_{std}) \quad (2.1)$$

TTI for 50^{th} percentile anthropomorphic test dummies is given by

$$TTI_{(d)} = 0.5(RIB_y + T12_y) \quad (2.2)$$

Where,

TTI = Thoracic Trauma Index in g

AGE = age of the subject in years

RIB_y = maximum absolute value of lateral acceleration in g's of the 4^{th} and 8^{th} ribs on struck side after signal filtering

$T12_y$ = maximum absolute lateral acceleration in g's of the 12 thoracic vertebra after signal filtering

MASS = mass of the subject in kg

M_{std} = Standard reference mass, 75 kg

Using TTI values in g's, the probability of p(AIS3+) and p(AIS4+) can be evaluated. For instance, TTI = 125 g corresponds to 50% probability for AIS3+

thoracic injuries and TTI = 170 g correlates to 50% of probability for AIS4+ thoracic injuries.

2.1.2.3 Average Spinal Acceleration (ASA)

Cavanaugh, 1993, from his experimental study, has defined ASA (Average Spinal Acceleration) which is an efficient acceleration injury criterion when compared to TTI. However, these researchers have ignored injury due to chest compression and considered only injury attributable to deceleration/acceleration.

2.1.2.4 Compression criterion

Kroell, 1971 had used unembalmed cadavers in blunt thoracic impact tests and proved that chest deformation is an important parameter for measuring the thoracic injury and also highlighted that acceleration and force are ineffective injury measuring criteria. He has expressed chest compression in percentage of Antero-posterior thickness of the body. Deflection tolerance was set at 88 mm which is equivalent to 39% of the chest compression which was, later on, reduced to 32%. A compression guide is given in Table 2.1 below.

Table 2.1: Relation between chest compression and thoracic injury

Chest compression in percentage of the antero-posterior thickness of the body	Details of the trauma
20%	Onset of the rib fracture
32%	Tolerance for rib stability
40%	Flail chest
45%	Sternum comes in contact with spinal vertebrae

2.1.2.5 Viscous Criterion (VC)

Clemedson et al. 1979, Lau, 1981 and Kroell, 1974 have conducted impact tests at 5- 20 m/s with human volunteers for lower impact speeds and cadavers, anesthetized rabbits and pigs as human surrogates for higher impact speeds. In all test cases, the liver was used as the target organ. It was found that the severity of injury increased with the rate of loading. From the autopsy of the surrogates, it was found that high-speed impacts caused serious mutilation of lobes of the lungs and major vessels. High-speed films of cadaver impacts also clearly revealed that chest compression causes the sternum to displace towards the spine as ribs bend and probably fracture (Cavanaugh et al. 1993).

Viano et al. 1989, based on their experimental investigation using anesthetized swine as human surrogates, have proposed viscous injury mechanism for soft biological tissues and devised viscous criteria (VC_{max}), which is a product of the maximum instantaneous velocity of deformation [V(t)] and compression [C(t)]. VC_{max} is the best known predictor of blunt thoracic trauma among all criteria discussed above.

VC_{max} can be calculated using the equation below.

$$VC_{max} = \max[\, V(t) \times C(t)] \qquad (2.3)$$

Where,

V(t) is the instantaneous velocity of deformation of the thorax

C(t) is the instantaneous chest compression

2.1.2.6 Blunt Criterion (BC)

The blunt criterion (Clare et al. 1975; Sturdivan, Viano & Champion 2004; Widder, Butz & Milosh 1997) has been in use for the design and validation of the non-lethal munitions. This criterion is based on the kinetic energy and the geometry of the projectile and some parameters of the thorax.

Blunt criterion can be evaluated using the equation given below.

$$BC = \log_n[\ (0.5 \times m \times v^2) / (M^{1/3} \times T \times d)] \quad (2.4)$$

Where,

m = mass of the projectile

v = velocity of the projectile

d = diameter of the projectile

M = Total mass of the torso

T = Thickness of the skin, muscle and fat layers of the torso at the location of the impact.

Though BC has been developed using non-lethal munitions and goats as surrogates, the correlations developed were proven to be applicable only to the munitions used in the impact experiments. For automotive, defense and sports applications, VC_{max} is the best predictor of the blunt thoracic trauma.

Post-mortem human subjects (PMHS) provide reliable data regarding the severity of injuries. Not only these are scarce in availability; there are many limitations on their usage for impact tests, as cadavers with a broken rib or lacerated or punctured internal organs cannot be useful for further trials. Most of the PMHS obtained from the fatal vehicle crashes are not useful as broken ribs and ruptured internal organs are most common in those cases. Animal surrogates could be used for such studies related to impact biomechanics. Due to ethical and religious reasons, there have always been restrictions on the utilization of animals in such experiments. Animal models also lead to erroneous correlations with the cadaveric test data, due to significant anatomical differences. These restrictions and limitations have been the driving force for the development of ATDs (both physical and finite element models) for the use of conducting automotive simulated crash tests. Cadaveric test data has been in use for the correlation of ATDs for decades. It is important to note that the cadaveric test data used for the correlation were relevant for typical automotive impacts. So far, no one correlated ATDs with the cadaveric test data or evaluated the usefulness of them for the determination of the blunt thoracic trauma due to blunt ballistic impacts, though researchers from Wayne State University have developed biomechanical human response corridors pertinent to the blunt ballistic impacts in the year 2000.

Though dummies lack the response of the bones and also lack internal organs, they have been widely used in the simulated vehicular crash tests in the laboratory, ranging from side impact tests to high speed frontal crash tests (Yang & King

2004). Finite element models of the ATDs (Hybrid III family of dummies for frontal impact and SID family of dummies for side impact tests) were developed by many commercial virtual testing software companies, in order to facilitate automotive companies to use them in the CAE based vehicular crash simulations. FE models of the ATDs, though evolving to become more biofidelic, initially correlated with some of or all of the thoracic injury criteria mentioned and most importantly with the human response corridors pertinent to the automotive impacts (Kroell et al. 1986; Kroell, Schneider & Nahum 1971, 1974). However, none of these ATDs (physical and FE models), developed for the vehicular occupant in simulated crash tests, were validated for the evaluation of blunt thoracic trauma caused by high speed blunt projectile impacts.

Human response corridors (force-time, deflection-time, force-deflection) were produced by impacting the thorax of human cadavers with wooden projectile of 140 grams with impact speeds of 20 m/s and 40 m/s and another wooden projectile of 30 grams with the speed of 60 m/s (Bir, Viano & King 2004; Bir 2000). These human response corridors could be useful for validating mechanical surrogates developed for evaluation of the blunt trauma due to high-speed ballistic impacts. In the research work presented here, thoraces of Finite Element model of 4 ATDs were subjected to similar impact cases as used by Wayne State University's researchers (Bir, Viano & King 2004; Bir 2000). For the sake of simplicity, these impacts were referred as LP_20, LP_40 and SP_60 respectively. For every impact case, force-time, deflection-time, and force-deflection responses were elicited. Details of the projectile and impact speed for all impact cases are given in Table 2.2.

Table 2.2 Impact cases and details of the projectile

Impact condition	Projectile details	Impact speed (m/s)
LP_20	Wooden baton, 140 g, 100 mm length, 37 mm diameter	20
LP_40	Wooden baton, 140 g, 100 mm length, 37 mm diameter	40
SP_60	Wooden baton, 30 g, 28.5 mm length, 37 mm diameter	60

By comparing the outcome of the simulations with the data obtained from the cadaveric experiments (human response corridors developed by Bir 2000) and suitability of the ATDs for quantifying the blunt thoracic trauma was evaluated and presented in this chapter.

2.2 Methodology

Finite element models of four ATDs were used in the study: 50th percentile male Hybrid III deformable dummy (LSTC), 50th percentile male Hybrid III rigid dummy (LSTC), NCAC Hybrid III deformable dummy (LSTC/NCAC) and ES-2re (LSTC). Material properties of the wood used in the simulations were collected from the published literature (Green 2001; Green, Winandy & Kretschmann 1999; Kretschmann et al. 2010; Murray et al. 2005). MAT_WOOD material model (available in LS-DYNA) was considered for the projectile in all impact

simulations. In the present study, no parameters, material models or components of the ATDs were altered. Simulations parameters such as ERODE in *CONTROL_TIME_STEP, DTMIN in CONTROL_TERMINATION, *CONTROL_HOURGLASS and element formulations were utilized from previously published work (Thota, Eepaarachchi & Lau 2012, 2013a, 2013c, 2013b). All impact simulations were carried out using LS-DYNA, which is a non-linear finite element solver developed by Livermore Software Technology Corporation, USA. LS-DYNA user manuals provide the details pertinent to the material models, control cards and many other input parameters (Hallquist 2007a, 2007b). The procedural steps for evaluation of the usefulness of the ATDs for blunt thoracic trauma caused by high-speed projectile impacts were as shown in Figure 2.4. The impact points selected for the four dummies were as illustrated in figure 2.5.

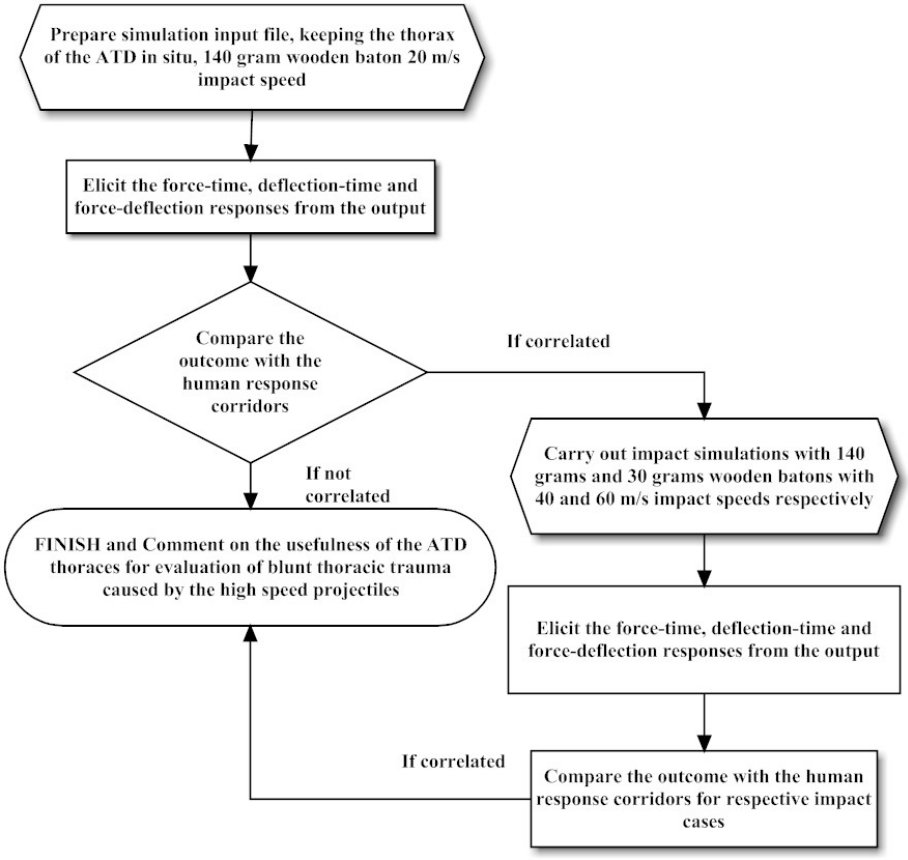

Figure 2.4: Procedural steps to evaluate the suitability of the ATDs for ballistic impacts

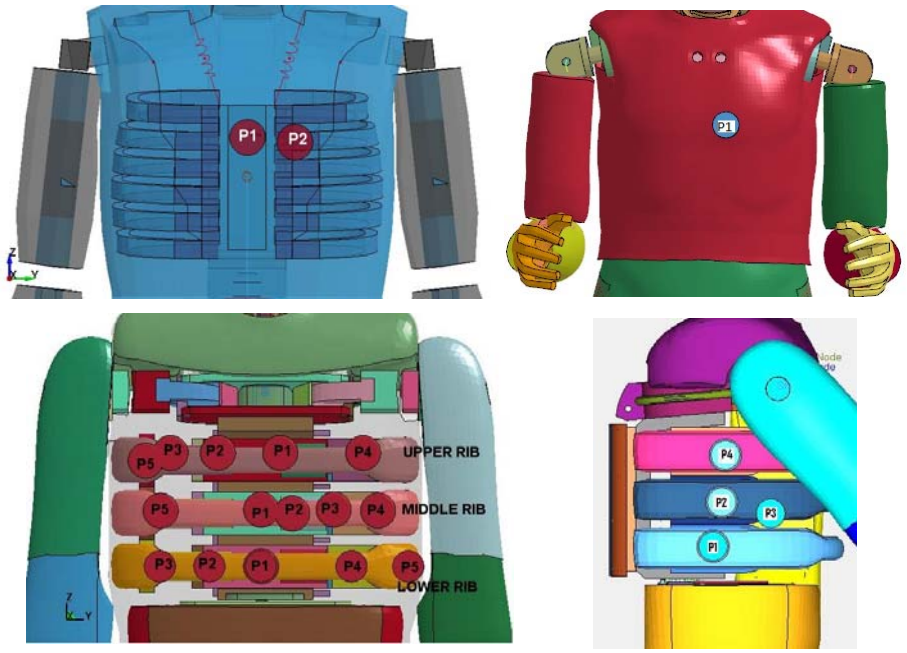

Figure 2.5: Impact points: deformable and rigid dummies of hybrid III LSTC dummies (top left), NCAC hybrid III dummy (top right), ES-2re dummy, frontal impact (bottom left), side impact (bottom, right). To show the rib cage, the jacket of the ATDs was either removed or made transparent.

The thoraces of the ATDs impacted at a number of selected points, with the wooden projectile of mass 140 g travelling at 20 m/s speed. By comparing the mechanical responses (force-time, deflection-time and force-deflection) and VC_{max} values elicited with those obtained from cadaveric tests for similar impact conditions, if the impact cases for which mechanical responses were appeared to be within the human response corridors, further two cases of (namely, 140 grams wooden projectile impacting with 40 m/s speed and 30 grams wooden projectile impacting with 60 m/s speed) impact simulations were carried out. It is important to note that for all cases, acceleration pulses were processed using SAE Class 600 filter and for processing deflection responses no filter was used.

Thoracic injury (in terms of VC_{max}) was quantified using the viscous criterion (Equation 2.3) which is a maximum value of the product of chest compression and velocity of chest compression. Values of VC_{max} provide the real means of validation of FE models, as it is an efficient predictor of thoracic trauma caused by blunt impacts. Viscous criterion or soft tissue criterion values can be calculated for an ATD using the formula given below.

$$VC = S.\ (Y/D).\ dY/dt \qquad (2.5)$$

Where,

VC= viscous criterion

S = scale factor (dimensionless multiplication factor)

Y= chest deformation or chest deflection

D= deformation constant in length units (based on the ATD used in the simulation or physical tests), and

dY/dt = rate of chest deformation

The guidelines laid down by SAE International (*Calculation Guidelines for Impact Testing* 2010) provide the scaling factors and deformation constants for all ATDs.

VC_{max} of 1 m/s indicates 25% of the risk of AIS3+ thoracic injury with Y/D equivalent to 33% (Viano, David C. & Lau, Ian V. 1988; Viano et al. 1989). $VC_{max} \leq 1$ has been included as a compliance requirement in various automotive safety standards such as FMVSS 214, ECE R94, and ECE R95, EuroNCAP (both frontal and side impacts)

For all relevant impact cases of ES-2re dummy, VC values were calculated using equation (2.5) above with the maximum rib deflections in lieu of thorax deformation. Probabilities for AIS3+ and AIS4+ injuries were calculated by using logistic regression model available in the literature (Kent & Patrick 2005).

$$p(AIS3+) = 1/(1+e^{(2.0975-0.0482\times \text{max.rib deflection})}) \quad (2.6)$$

$$p(AIS4+) = 1/(1+e^{(3.4335-0.0482\times \text{max.rib deflection})}) \quad (2.7)$$

Where,

p(AIS3+) = probability of injury greater or equal to score 3 on the abbreviated injury scale

p(AIS4+) = probability of injury greater or equal to score 4 on the abbreviated injury scale

max.rib.deflection = maximum rib deflection in mm

It is important to note that the equations (2.6) and (2.7) are applicable to only ES-2re dummy. By comparing the biomechanical responses and VC_{max} values obtained for all ATDs with the cadaveric test results, the suitability of ATDs for evaluation of blunt trauma was elicited and presented in the subsequent sections of this chapter.

2.3 Results and discussion

2.3.1 LP_20 impact condition

Thoraces of the 4 ATDs, namely, LSTC Hybrid III deformable, LSTC Hybrid III rigid, LSTC/NCAC Hybrid III and ES-2re were subjected to the LP_20 impact condition. From the simulation output, biomechanical responses (force-time and deflection-time) were elicited. Impact force was measured with an accelerometer mounted on the back face of the projectile and chest deflections were measured based on the impact location and also at the point where maximum deflection occurred. None of the impacts yielded any significant spinal acceleration and whole body movement. Therefore, the relative displacement of the chest wall with

respect to the spine was evaluated by measuring the nodal displacements on the jacket.

Frontal impacts of the former three dummies did not yield any realistic force-time response due to the high stiffness of those thoraces. Even after processing the force response with SAE class 600 filter, the magnitudes of the forces were very unrealistic. Therefore, only deflection-time responses of the thoraces were presented (Figure 2.6).

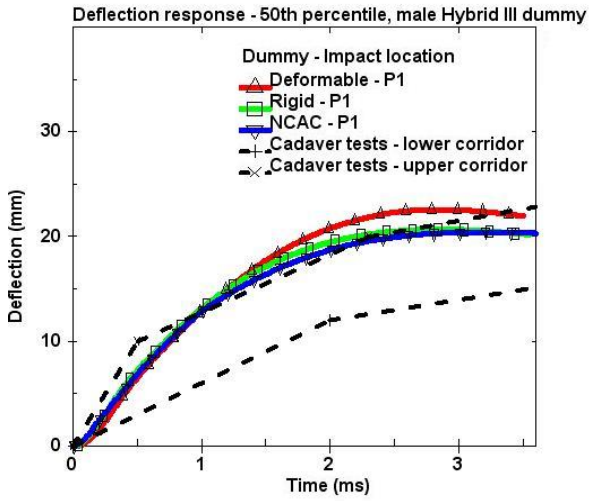

Figure 2.6: Dynamic chest deflection of the Hybrid III dummies' thoraces (LP_20 impact condition)

Euro SID dummy's finite element model and physical model are widely used in tests concerning the crashworthiness of vehicles. The ES-2re finite element model details, various calibration tests, carried out were given by (Stahlschmidt et al. 2010; Stahlschmidt et al. 2012) As shown in Figure 2.5, fifteen impact points were considered for the front impact. Only impact points P1, P2 on the lower rib, P1, P2 & P3 on the middle rib, P1& P2 on the top rib provided adequate loading surface to the projectile and yielded realistic force and deflection responses. For other frontal impact points, due to the skidding of the projectile, the mechanical responses were very less. Therefore, ignored for the study. Four impact points were considered for the side impact. Impact on the side surfaces did not yield any chest deflection as the stiffness offered by the thorax was very high. Different stages of projectile impacting at a point that provides adequate loading surface is shown in Figure 2.7.

Dynamic force and deflection response of the ES-2re to the LP_20 impact were shown in Figure 2.8 and Figure 2.9, respectively.

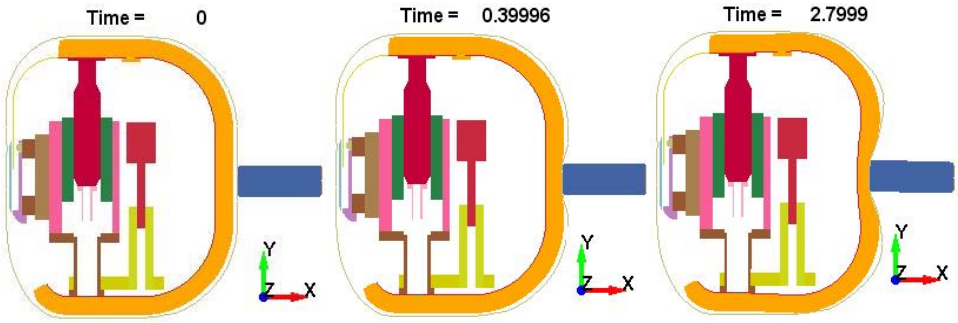

Figure 2.7: Stages of the impacting projectile and the cross section of the deflecting thorax of ES-2re.

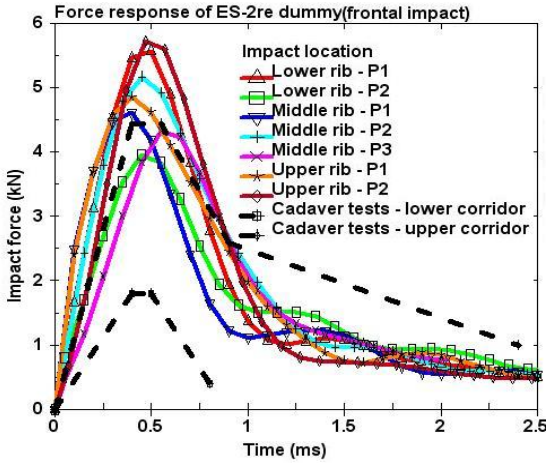

Figure 2.8: of the ES-2re dummy (LP_20)

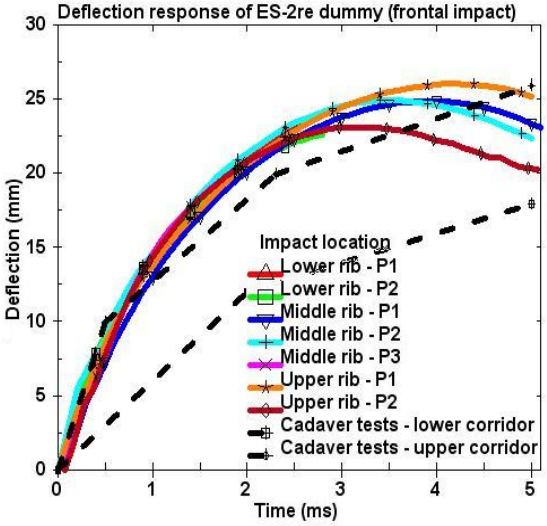

Figure 2.9: Dynamic deflection response of the ES-2re dummy (LP_20)

From the Figures 2.8 and 2.9, force response obtained for the impact point "Lower rib – P2" was within the human force response corridors and deflection response for the same point was not within the human deflection response corridors. Peak forces for all impact other points were 10-40% more than the upper limit of the force corridor. Peak deflections and rate of chest deformations for all other impact points were more than the upper boundary of the human deflection response corridor.

2.3.2 LP_40 impact condition

All Hybrid III dummies were not considered for the further analyses due to the high stiffness offered by their thoraces. Therefore, only the thorax of the ES-2re dummy was subjected to the LP_40 impact condition. Force-time responses obtained from the output of the analyses were as shown in the Figure 2.10.

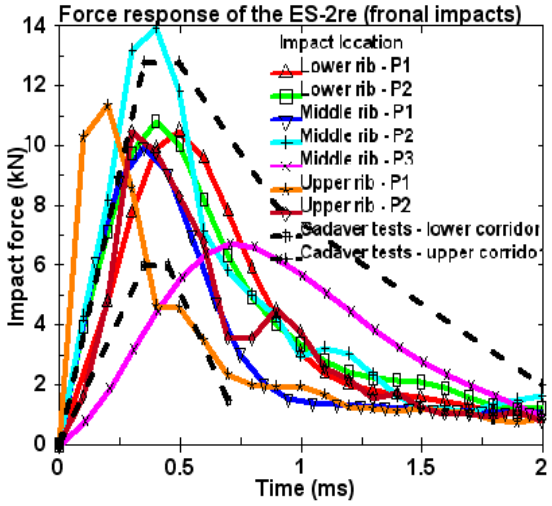

Figure 2.10: Dynamic force response of the ES-2re thorax when subjected to LP_40 impact condition

From the Figure 2.10, it was evident that dynamic force responses (Force-time responses) obtained for the midpoints (P1) of all 3 ribs were within the human response corridors developed from the cadaver tests. It is important to note that for the upper rib, though impact forces are out of the corridors, they are very close to the corridors. For the point P2, peak forces were more than the upper corridor, while for the point P3 the forces were low because of the inadequate loading surface. In the present simulation study, neither changes in orientation of the dummy nor impact direction of the projectiles were considered. It is important to note that this impact case (LP_40) is very close to the solid sports ball impacts. Therefore, deflection responses were elicited from the outcome of the simulations to review the suitability of the middle points of 3 ribs.

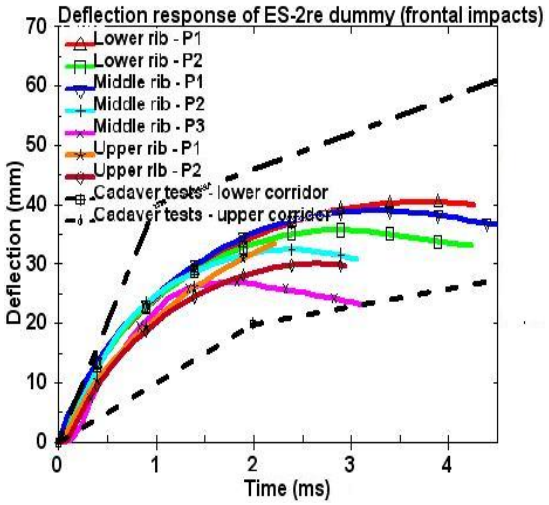

Figure 2.11: Dynamic deflection response of the ES-2re thorax when subjected to LP_40 impact condition

From the dynamic deflection plot (Figure 2.11) it was evident that the deflection-time responses obtained for all the points were within the human response corridors but the rate of chest deflection is very different from that obtained from the cadaver tests.

2.3.3 SP_60 impact condition

Impact with the short wooden baton of 30g mass, 28.5 mm length and 40 mm diameter is very relevant to the present day non-lethal ammunition.

From all 3 impact cases, it was evident that impacting with the projectile at the left or right end of the ribs would not provide an adequate loading surface and, therefore, would yield very minute or no chest deflection due to the skidding of the projectile. Only impact points P1 and P2 on all 3 ribs provided adequate loading surface to the projectile. In case of the ES-2Re, the approximate area that can provide adequate loading surface to the projectile impact is as shown in the Figure 2.12.

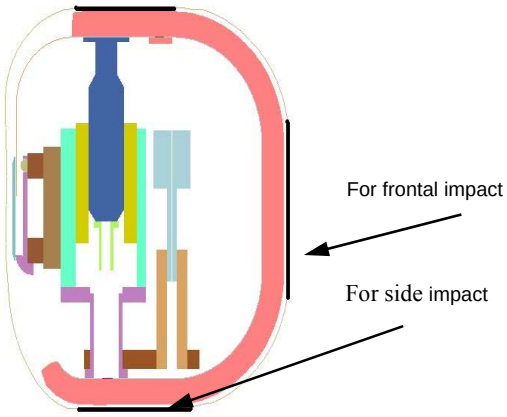

Figure 2.12: Thick black line shows the area that provide adequate loading surface for the projectile

Different stages for a skidding projectile at impact point P5 on the middle rib are shown in Figure 2.13, whereas the case for proper loading surface (for the impact point P1 of the lower rib) is presented in figure 2.14.

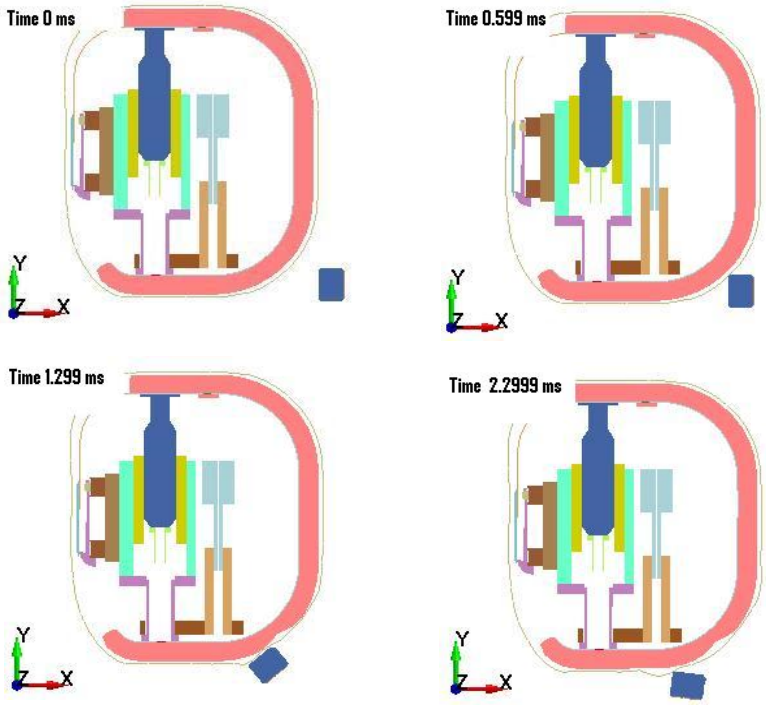

Figure 2.13: Different stages of skidding projectile due to inadequate loading surface of the ES-2re -thorax

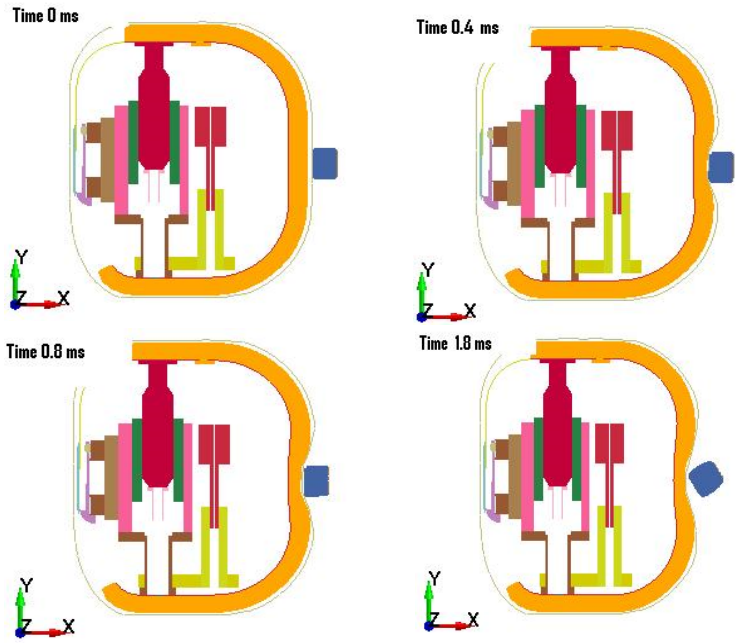

Figure 2.14: Stages of deflecting thorax – when adequate loading surface was available to the impacting projectile

Force-time and deflection-time responses elicited from the simulations' output of SP_60 impact case were as shown in the Figure 2.15 and Figure 2.16 respectively.

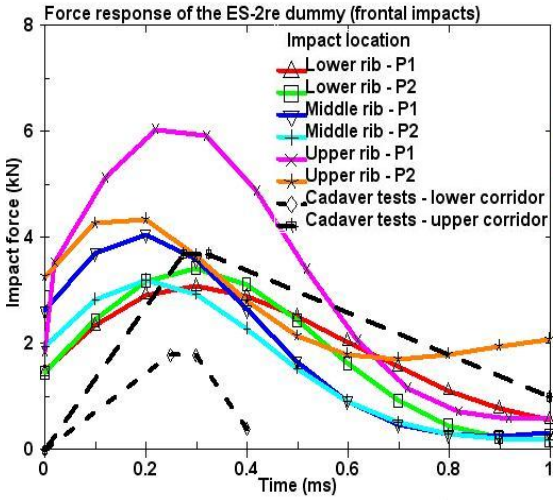

Figure 2.15: Dynamic force response of the ES-2re thorax when subjected to SP_60 impact condition

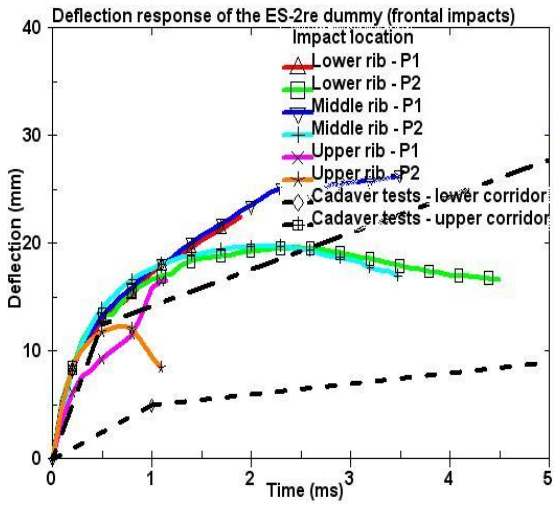

Figure 2.16: Dynamic deflection response of the ES-2re thorax (SP_60 impact condition)

The impact duration was much reduced for this case. In every impact case, the projectile lost the contact with the thorax within 1 ms. Peak forces (unfiltered deceleration pulse) were at 0.2 – 0.3 ms after impact. Filtered dynamic impact force responses were as shown in the Figure 2.15. The obtained mechanical responses (both force-time and deflection-time) were not in agreement with those obtained from cadaveric tests.

Though the mechanical responses, appeared to be very close to the human response corridors for some impact points, the rate of chest deflection influences the usefulness of the ATDs for quantifying the thoracic trauma due to blunt ballistic impacts. Therefore, for all impact cases the VC_{max} values were evaluated.

2.3.4 Evaluation of VC_{max}

VCmax values for all of the impact cases were calculated using the equation (2.5), and deflection responses (Figures 2.6, 2.9, 2.11, and 2.16) obtained from the simulations.

Scale factor (S) and Deformation constant (D) for all dummies and cadavers utilized for the evaluation of the VC_{max} (Bir, Viano & King 2004; Bir 2000; Chang 2001) were as presented in the Table 2.3. VC_{max} values were as given in Table 2.4.

Table 2.3: Scale factor and Deformation constant for all ATDs considered in the present study

ATD name	Scale factor (S)	Deformation constant (D) in mm
Hybrid III, male 95%	1.3	254
Hybrid III, male 50%	1.3	229
Hybrid III, female 5%	1.3	187
BioSID	1.0	175
EuroSID-1	1.0	140
ES-2re	1.0	140
SID-IIs	1.0	138
Cadavers as suggested by Viano et al. 1989	1.3	180

Table 2.4: VC_{max} values for all important cases of impacts

Impact condition	ATD-Impact location	Maximum chest deflection in mm	Impact duration @ Max chest deflection in mm
LP_20	Hybrid III, Deformable – P1	22.6	2.84
	Hybrid III, Rigid – P1	20.7	2.82
	Hybrid III, NCAC – P1	20.7	3.09
	ES2re-Middle rib – P1	24.9	4.1
	ES2re-Middle rib – P2	24.8	3.6
	ES2re-Upper rib – P1	26.1	4.3
	ES2re-Upper rib – P2	23.2	3.17
LP_40	ES2re-Lower rib – P1	40.5	3.8
	ES2re-Lower rib – P2	35.8	3
	ES2re-Middle rib – P1	39.1	3.3
	ES2re-Middle rib – P3	32.5	2.5
	ES2re-Upper rib – P2	30.1	2.7
SP_60	ES2re- Lower rib – P2	19.6	2.5
	ES2re- Middle rib – P1	26.4	3.5
	ES2re - Middle rib – P2	19.8	2.2
	ES2re- Upper rib – P2	12.9	0.7

VC_{max} values for all impact cases were as shown in the bar charts (Figures 2.17, 2.18 and 2.19). For comparison, VC_{max} values obtained from the cadaveric experiments (Bir 2000) were also shown in the charts.

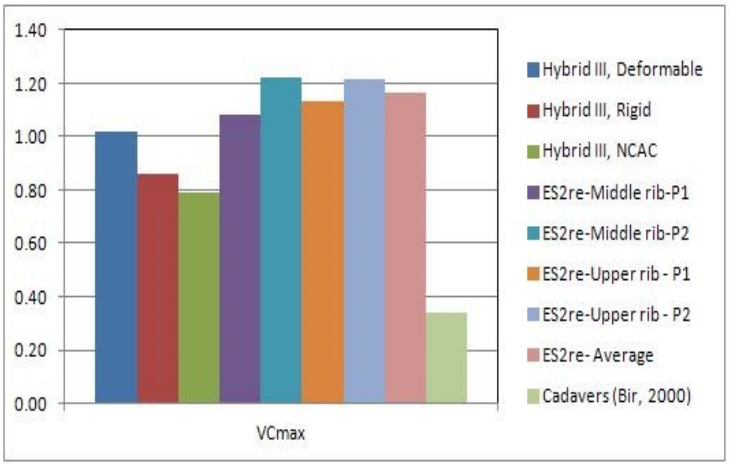

Figure 2.17: VCmax values for LP_20 impact condition

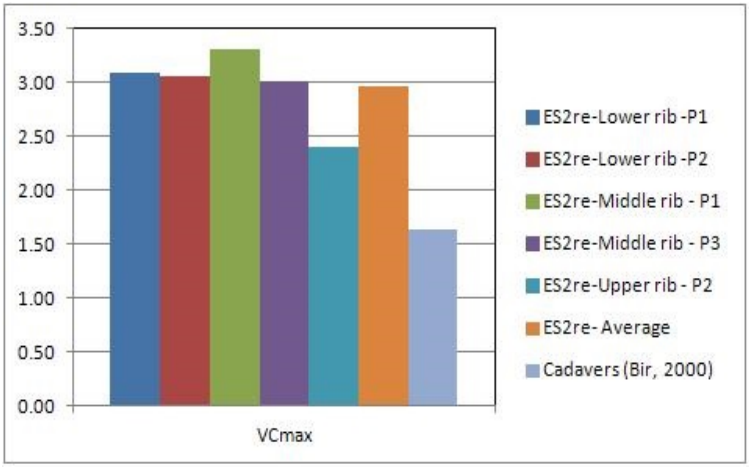

Figure 2.18: VCmax values for LP_40 impact condition

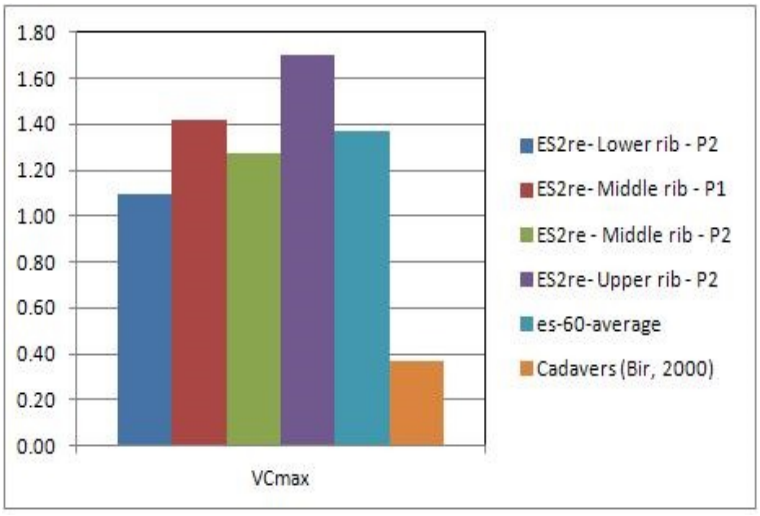

Figure 2.19: VCmax values for SP_60 impact condition

The VC_{max} values for all impact cases were not in correlation with those obtained from the cadaver tests of the respective cases. Therefore, dynamic chest deflection responses as a function of time obtained for ES-2Re were not useful for the evaluation of blunt thoracic trauma caused by ballistic impacts.

2.3.5 Evaluation of p(AIS3+) and p(AIS4+) using maximum rib deflections of ES-2re

In order to explore the last possibility whether ES-2re could be useful for the evaluation of the trauma due to high speed blunt ballistic impacts, maximum rib deflections were calculated from nodal displacements of the rib liners. To elucidate the thorax-projectile interaction, the rib liners and ribs in initial and final positions during the impact are shown in the Figure 2.20 (For the sake of clarity, the foam jacket was removed). Deflection of the ribs was measured using the nodes on the ribs. Mechanical responses of all three ribs were similar for similar impact points. Therefore, for assessing the deflections for each impact condition, only two points on one of the three ribs were evaluated and were as shown in the Figure 2.21. It is important to note that no electronic filter was used for processing of the displacement data obtained for the nodes of rib liners.

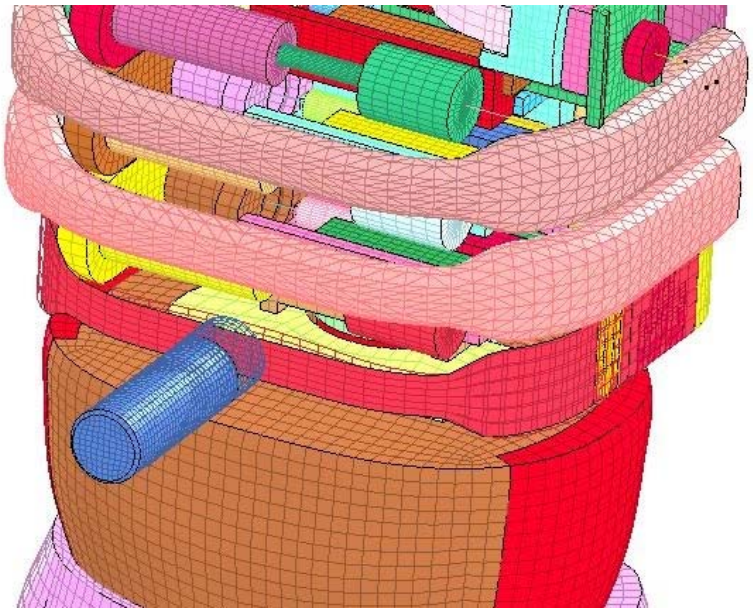

Figure 2.20: ES-2re subjected to the LP_40 impact condition. Impact point is P1 on the lower rib.

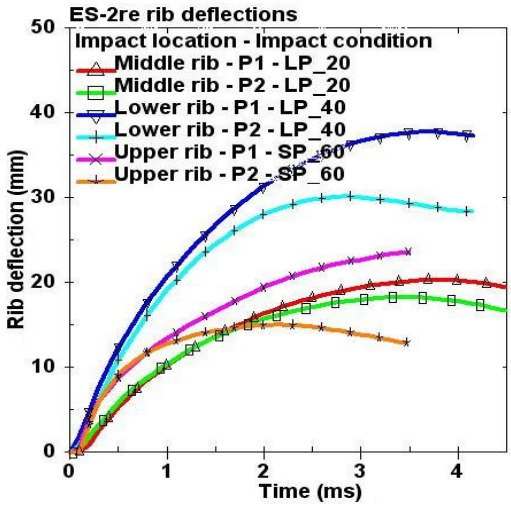

Figure 2.21: Deflection-time response for 3 impact conditions

Using the maximum rib deflections from the output of the impact simulations and Equations (2) and (3), probabilities for AIS3+ and AIS4+ injuries were evaluated and presented in Table 2.5.

Table 2.5: Probabilities of AIS3+ and AIS4+ injuries based on the rib deflections

Impact Location / Impact condition	p(AIS3+)	p(AIS4+)
Middle rib – P1 - LP_20	0.24	0.08
Middle rib – P2 – LP_20	0.23	0.07
Lower rib – P1 – LP_40	0.44	0.17
Lower rib – P2 – LP_40	0.35	0.12
Upper rib – P1 – SP_60	0.27	0.09
Upper rib – P2 – SP_60	0.20	0.06

Using the correlation between VC_{max} and AIS, probabilities for AIS3+ and AIS4+ injuries (Gennarelli & Scaling 1985; Scaling 1985; States 1969; States et al. 1971; Viano, D. C. & Lau, I. V. 1988) can be useful for the quantifying the blunt thoracic trauma. For instance, p(AIS3+) = 0.25 corresponds to VC_{max} of 1 m/s . From Table 2.5, VC_{max} values that correspond to p(AIS3+) and p(AIS4+) were not in correlation with the cadaver test results presented by Bir (2000).

2.4 Conclusion

The following conclusions were drawn from the mechanical responses obtained from the thoraces of 4 ATDs subjected to LP_20, LP_40 and SP_60 impact conditions,

- It was evident that three thoraces of the Hybrid III were very stiff and didn't yield any realistic force response.
- The thorax of the ES-2re dummy gave reasonable and realistic responses. However, VC_{max} values calculated from the dynamic deflection plots were much higher when compared to those obtained from the cadaveric experiments. In all impact cases pertaining to the ES-2Re side impact dummy, no measurable spinal deflections and accelerations were found, and this is an indication that the deformation is local and also that the thorax is too stiff.
- VC_{max} values evaluated using the probability for AIS3+, and AIS4+ injuries were also not in agreement with the cadaver tests data.
- In some impact cases, though the maximum rib deflections and maximum chest deflections were smaller in magnitude, velocity of maximum deformation was very high. In all instances projectile lost contact with the thorax within 2 ms time. In the case of SP_60 impact case, the contact time was less than 1 ms.
- None of the impact cases yielded any measurable spinal acceleration. Therefore, the force-time and deflection-time responses were only local, and not really responses of the thoraces of the ATDs.

None of the material data or design parameters pertaining to the ATDs were altered in the present study. By altering the material data or design parameters or attaching a thick soft, foam bib in front of the thorax might have made the thoraces emulate the cadavers.

In a nutshell, none of the thoraces of the ATDs under review that are useful for the simulated automotive crash applications can be used for the evaluation of the thoracic trauma caused by blunt ballistics (such as impacts of non-lethal projectiles, solid sports ball impacts, etc.). The same may be true for various other ATDs (both physical and numerical models) as every one of them got correlated with biomechanical response corridors developed for the impacts pertinent to the automotive crashes. Therefore, there is a necessity for the development of a fast solving and easy to use FE model thorax for the evaluation of blunt thoracic trauma.

CHAPTER-3: NOVEL CONCEPTS OF MECHANICAL THORAX FOR BLUNT TRAUMA MEASUREMENT – A FEASIBILITY STUDY

This chapter summarizes a feasibility study pertaining to a novel concept for a mechanical thorax discussed in a technical paper titled 'Develop and validate a biomechanical surrogate of the human thorax using corrugated sheets: A feasibility study' which was published in the proceedings of Australasian Conference on Applied Mechanics 7. The details of the paper is given in the Appendix –I of the thesis.

3.1 Introduction

In order to validate non-lethal projectiles or to design passive safety devices for the safety of vehicle occupant, it is essential to have an understanding of the mechanisms of trauma and injury criteria pertaining to the head, neck, thorax or whole body etc. Researchers involved in the development of non-lethal ammunition/projectiles, bullet proof vests, passive safety devices for vehicle occupant safety etc. have conducted experiments using human volunteers, Post-Mortem Human Subjects (PMHS), anesthetized swine and mechanical surrogates (both physical and mathematical) to gain insight into injury mechanisms and have developed injury criteria and human response tolerances, which were discussed in the Chapter 2.

Forbes, 2005 has theoretically studied the blunt thoracic trauma caused by automotive impacts using a finite element model. He refined the thorax of the FE model developed by Deng et al. 1999 and Chang, 2001, used it for various impact cases and compared the results with those obtained by other researchers. Viano (2011) has carried out thoracic blunt impact experiments using unembalmed cadavers. In his experiments, 24-34 kg impactors at velocities 8.6- 14.9 m/s were used and chest compression, and spinal accelerations were measured. After every impact test an autopsy was conducted on the cadavers to detect any rib fractures, internal organ injuries, heart contusion, etc. Most of the above-mentioned experiments are pertaining to automotive impacts where the area of contact for loading is much higher than that of a projectile. Though they are not directly useful for the validation of non-lethal projectiles, the outcome of those investigations (both theoretical and experimental) formed a great foundation for the development of various injury mechanisms and criteria.

Maron et al. 1995 has studied many cases of patients with thoracic trauma caused by blunt impacts resulting from sports activities. Serious injuries such as multiple rib fractures, lacerations to the liver and in some cases cardiac arrest was reported. Some researchers used PMHS as surrogates and gathered injury data with various impact conditions. Ijames, 1997 and Steele et al. 1999 have presented severe injuries (Multiple fractures of the rib cage, flail chest, lacerations of the lung, heart contusion, etc.) caused by blunt ballistic impacts. Data gathered by these researchers is limited due to the scarcity of the post mortem human subjects and limited number of case studies from the sports related injuries.

As far as the impact experiments with cadaver are concerned, they are not only scarcely availably and unpleasant to handle and but they also require a costly

experimental setup and cumbersome. Similarly, experiments with anesthetized animals have got ethical constraints, where as for human volunteers there are limitations on the impact speed and impactor mass. Especially for validating impact ammunitions, human volunteers are not suitable. Therefore, researchers realized the need for mechanical surrogates and using the cadaveric and other test data obtained from the experiments for correlation and validation, researchers made mechanical surrogates that emulate the responses of the human body. Though the usage of mechanical surrogates has started during the mid of the 20th century, the first human-like crash anthropomorphic test dummy (biomechanical surrogate) was Hybrid III. Hybrid III dummies are correlated to emulate the response of the thorax for frontal impacts. Response of the thorax to lateral impacts necessitated the development of side impact dummies. Viano et al. 1995 evaluated the performance of side impact dummies and correlated those with the cadaveric pendulum impact test data of Viano et al. 1989. EuroSID, BioSID, WorldSID, AUSMAN, 3-RCS, etc. are high-fidelity biomechanical surrogates developed for the study of the thoracic response to impact loads. The former three surrogates were developed for lateral impacts for automotive applications, and the latter two were developed for validating impact ammunitions and BABT related studies.

As described by Bir 2004, as far as non-lethal ballistics and solid sports ball impacts are concerned, injury criteria and human response corridors pertaining to the thorax are important for the cases involving low mass (20-200 grams) of the projectile and high impact velocity (20-250 m/s).

Many researchers and research organizations have made mathematical models of the Hybrid III and Side Impact Dummies to be used in theoretical analysis. FTSS has developed mathematical models of the ATDs with high biomechanical fidelity, and they are widely used in theoretical automatic crash and impact analyses. However, using FE models of the dummies not only require expertise in FEM and its application software and but also they were found to be not suitable for ballistic impact applications (as evaluated in the Chapter – 2).

Use of mechanical surrogates such as 3RCS and AUSMAN, or using cadavers, anesthetized animals for experiments is cumbersome and extremely expensive owing to the costly equipment. Though 3-RCS is widely used by the US military and weapons manufacturers, it has got so many limitations (Bir 2000; Dau 2012; Lyon 1997) such as only impacts on the centre of the middle rib in a very small area will give useful deflection–time response and impacts on other places yield either ineffective or erroneous responses. AUSMAN surrogate is developed for the Behind Armour Blunt Trauma (BABT) studies. Therefore, it can't be used for the blunt impacts of interest. Moreover, very limited published research is available on the AUSMAN. Most importantly, due to lack of knowledge and non-availability of the thorax surrogates, sometimes defence consultancies (suppliers to the defence research organizations) used "a block of Balsa wood", "a thick metal plate" as the thorax surrogates and ended up in getting very wrong results (author's own experience while working with a defence consultancy).

Therefore, there is a necessity for a simple to use finite element model of the thorax, for validating impact munitions that require less computational power and minimum working knowledge of non-linear finite element analysis. At the same time, design of the FE model should offer ease of making a reusable physical model (mechanical surrogate). Present author, having used a corrugated sheets for

making mounts of airbag compliant vehicle front protection systems and also as buffer stop in coal handling plants (unpublished technical work of the author), devised a methodology to develop and validate a FE model of the human thorax, conducted a pilot study to evaluate the feasibility of the methodology and presented the same in this chapter.

3.2 Novel concepts of thoracic surrogates

In order to accurately evaluate the thoracic trauma in known engineering parameters, two simple concepts were developed, and they were as shown in the Figures 3.1 (a) and (b). In both concepts thermo-plastic elastomer (TPE) foams used as the fascia for impact plate.

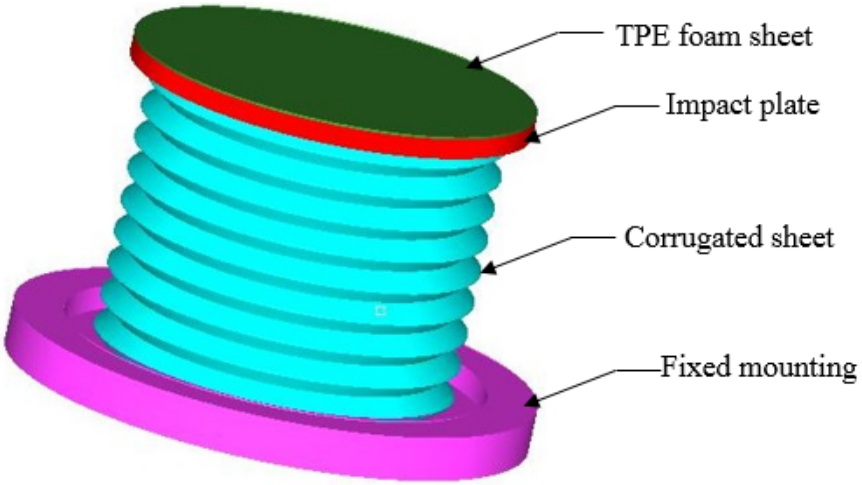

Figure 3.1 (a): Thorax surrogate made up of a hollow corrugated Aluminum cylinder

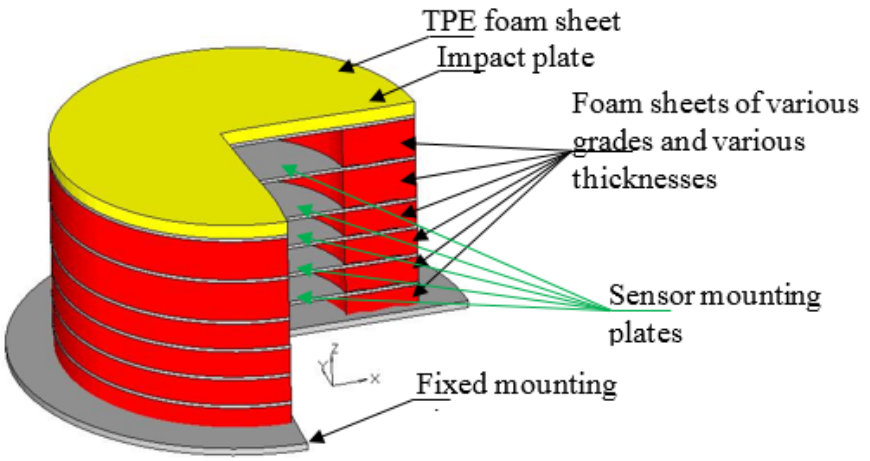

Figure 3.1 (b): Thorax made up stacked foam sheets

Though it is not manufacturable, the concept shown in Figure 3.1 (a) was considered for development due to the simple construction and well known correlated material data. Most importantly, the objective is to develop an FE model of the thorax surrogate that is accurate, easy to set up and fast solving. The potential of FE model is very high when compared to the physical model, because many things, which are practically impossible to measure with the physical surrogates, can be obtained from the output of the non-linear FE analysis. A methodology was devised (similar to the one used by Bir 2000) to correlate the baseline design of the thorax surrogate with the cadaveric test data (human response corridors developed by Bir 2000 and Bir et al. 2004).

3.3 Methodology devised for validation of the biomechanical surrogate of the thorax

Wayne State University researchers (Bir & Viano 2004; Bir 2000; Bir & Viano 1999) have conducted extensive experimental investigations to evaluate thoracic trauma caused by blunt ballistic impacts. They have developed the 3 Rib Chest Structure (popularly known as 3-RCS) with the components of Bio-SID ATD and correlated it with the results obtained from cadaver testing. She has developed human response corridors for the force-time, deflection-time and force-deflection. Using 3 RCS and various cadavers, gelatine and clay signature tests, non-lethal ammunition such as XM1006, M743 and MK Close (Lyon, Bir & Patton 1999) were validated.

Though the 3-RCS model is modified (Bir 2000) for better biomechanical fidelity for ballistic impacts and has been used as a standard experimental biomechanical surrogate of the thorax for evaluating blunt impact trauma caused by impact munitions, the model has some limitations: Impact with any projectile on the top and bottom rib yielded erroneous force-deflection response or less or negligible deflection values, and only impacting at specified small region on the middle rib yielded meaningful force-time and deflection-time responses.. Therefore, the present authors have devised a methodology, which is shown in the Figure 3.2, to design and develop a mechanical surrogate of the thorax (made up of corrugated sheets) which emulates cadaver test data and without the limitations of the 3-RCS.

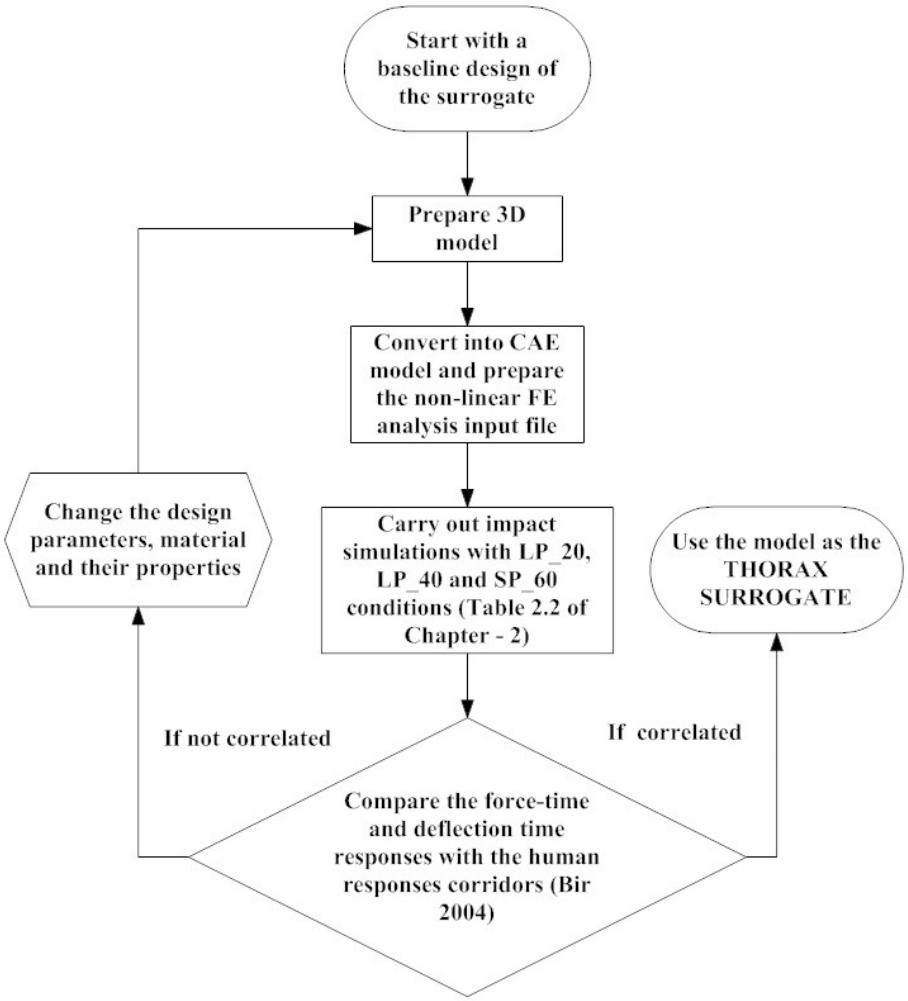

Figure 3.2: Methodology devised for theoretically validating the surrogate

The method of validating the collapsible cylinder made up of corrugated sheet mentioned in Figure 3.2 is straightforward but very cumbersome as correlation need to be achieved for all 3 impact cases used by Bir 2000. Therefore, a pilot study was carried out to evaluate the feasibility of the method in virtual testing environment. Feasibility study and the outcome presented in the following section.

3.4 Feasibility study

Due to complexities and challenges involved in the methodology shown in the Figure 3.2, in order to evaluate its feasibility, a pilot study was carried out in which a simple structure was correlated with the force-time response of the thorax of the Hybrid III rigid 50th percentile dummy (LSTC) under the high speed, low mass impact conditions. A foam nosed impactor was used in the pilot study simulations. In order to obtain meaningful simulation results without any errors and premature termination of the analysis runs, closed cell foam (polyolefin) was tested and calibrated material data suitable for the material model (available in LS-DYNA

software) MAT_057 (MAT_LOW_DENSITY_FOAM) was prepared. During the trial runs, as the foam is highly compressible, parameters such as DTMIN in the control cards *CONTROL_TERMINATION, ERODE in *CONTROL_TIMESTEP, DAMP etc. were set correctly so that severely distorted elements with negative volume gets deleted during the analysis. More details about these control cards and simulation parameters can be found in the LS-DYNA 971 manuals volume I & II. Though projectile design or foam data is not important in the pilot study, as the study was conducted only to evaluate the feasibility of the validation method, due care was given to material properties and the true stress versus true strain curve of the foam material was adjusted so that the nose material emulated a closed cell polyolefin foam.

Simulation iterations were carried out by impacting the thorax of the Hybrid III 50th percentile male rigid dummy (this FE model is freely available for LS-DYNA users) with the foam nosed impactor with 50-100 m/s (with an increment of 5 m/s) at point P0 (mid of the sternum, that is, approximately between 3rd left and right ribs of the ATD's thorax). By post-processing the results, force-time pulses (deceleration pulses) were obtained for all impact speed cases. Similarly, the analysis was repeated for 5 more impact points to find out the impact point that provides more loading surface to the projectile and for all simulation runs force-time responses were noted. Details of the impact points on the thorax are given in Table 3.2 and shown in Figure 3.3.

Table 3.1: Details of the impact points

Impact	Description
Po	Mid of the sternum (between 3rd left and right ribs)
P1	Junction of the sternum, 2nd and 3rd left ribs
P2	1st left rib and 55mm away from the center line
P3	Just above the 1st left rib, 90mm away from the center line
P4	In between 1st and 2nd left ribs and 90 mm away from the center
P5	Top of the sternum body, 65 mm below the superior thoracic

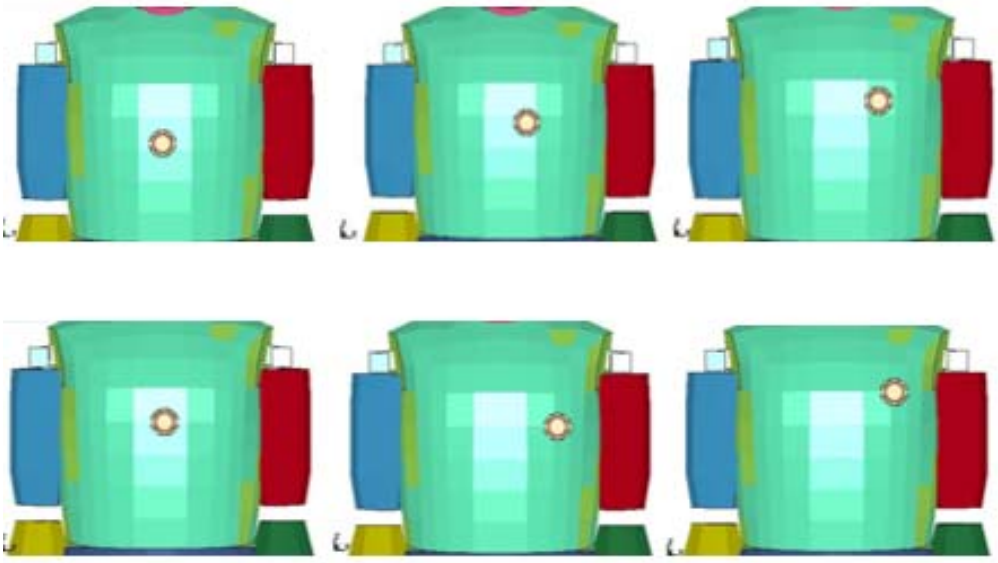

Figure 3.3: Impact points P0 to p5 (from top left to the bottom left in clock wise direction)

The baseline design of the target (surrogate of the Hybrid III dummy's thorax) used in the pilot study, along with the projectile are shown in Figure 3.4. Impact simulations were carried out with the projectile impacting the surrogate's rigid impact plate at 50 -100 m/s (with 5 m/s increment). For every analysis run, deceleration pulse (force-time response of the surrogate) and peak impact force were recorded and compared with those of the Hybrid III dummy's thorax. The force-time response of the surrogate (preliminary design) was nearly 38% less than that of the Hybrid III dummy's thorax. By changing the design parameters such as thickness, sheet material, radii of the corrugations, impact plate material etc., similar simulation iterations were repeated until the force-time response of the target was approximately equivalent to that of the thorax of the dummy.

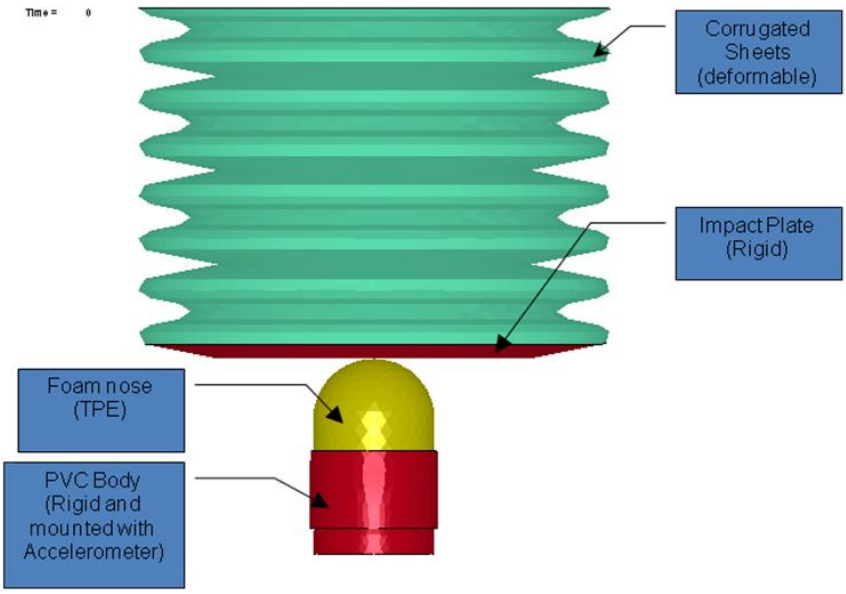

Figure 3.4: Thorax surrogate with the foam nosed projectile

3.5 Results and discussion

Force-time responses obtained for all impact speeds for the impact point and peak impact forces for all impact cases (12 impact speeds and 6 impact points) are shown in Figure 3.5 and Figure 3.6 respectively.

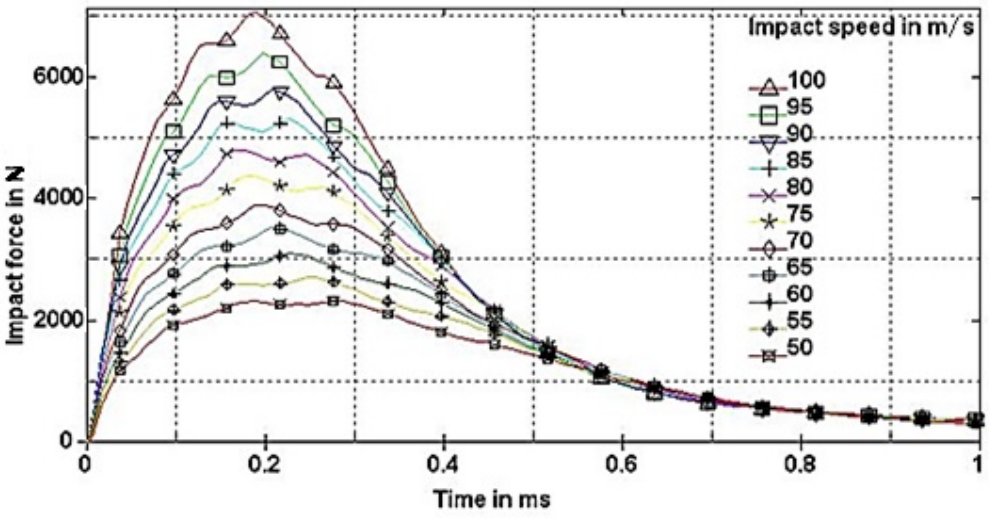

Figure 3.5: Force – time responses of the Hybrid III thorax when impacted at P1

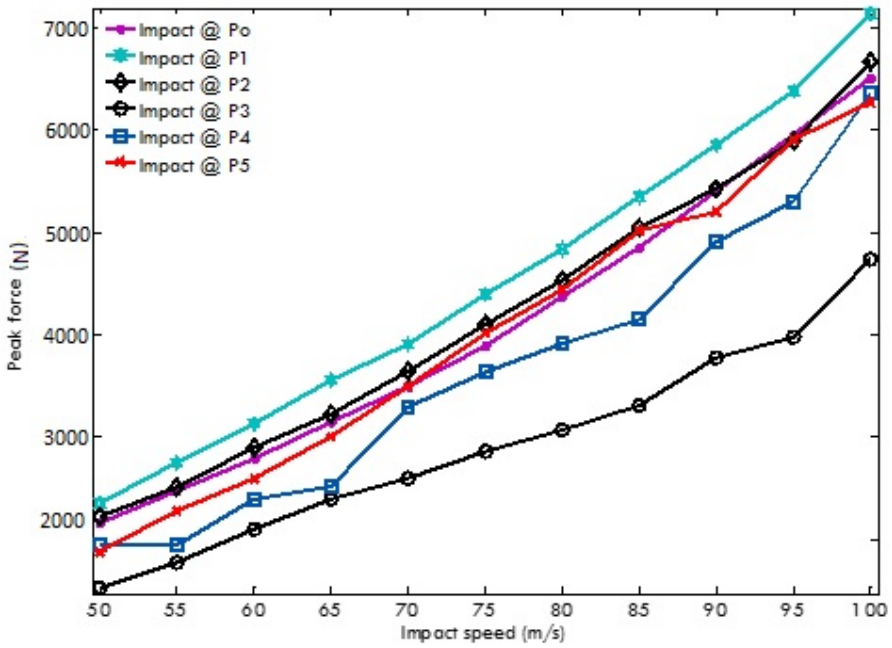

Figure 3.6: Peak impact forces for all impact cases

Stages of the projectile during the impact with the impact speed 100 m/s for the impact point P1 on the Hybrid III rigid dummy's thorax are shown in Figure 3.7. Impact stages at the impact time T = 0 ms, 0.13 ms, 0.68 ms, 1 ms, 1.5 ms and 2 ms are shown in the top row left, to the bottom row left, in the clockwise direction.

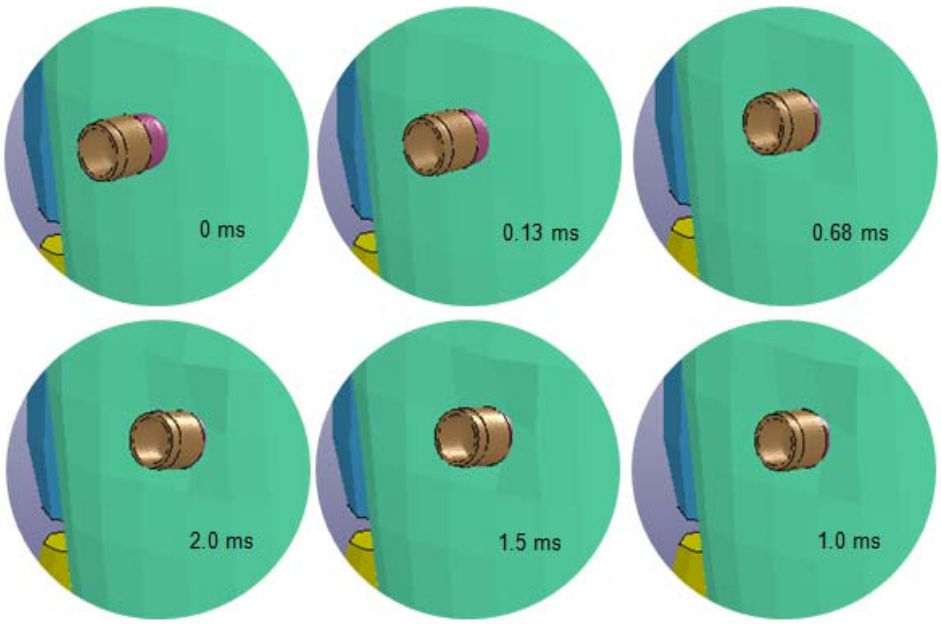

Figure 3.7: Stages of the projectile impacting with 100 m/s at P1 of the Hybrid III thorax

From the Figure 3.6 and post processing of the simulations results for all impact cases, it is evident that impact points P1 and P2 are providing proper loading surface to the projectile. For the feasibility study related correlation purposes only force–time responses obtained for P1 used.

Peak impact forces (in N) obtained by impacting with the projectile at the centre of the impact plate of the target for 15th design iteration and 25th design iteration of the surrogate model are shown in the Table 3.3 and graphically shown in the Figure 3.8. For comparison purpose, peak impact force (in N) obtained for impacting the projectile with the thorax of the Hybrid III dummy at P1 also given in the same table. Stages of the projectile impacting the target are shown in the Figure 3.9 and force–time responses obtained (after 25th design/simulation iterations) by impacting the surrogate (target with corrugated sheets) for all impact speeds are shown in the Figure 3.10.

Table 3.2: Peak impact forces obtained by impacting the Hybrid III and the surrogate

Impact speed (m/s)	**Peak impact force (N)**		
	Hybrid III thorax for the impact point P1	**Surrogate after 15th design iteration**	**Surrogate after 25th design iteration**
50	2314.37	2438.57	2356.07
55	2701.67	2829.50	2755.43
60	3076.80	3233.87	3055.52
65	3489.61	3612.73	3540.13
70	3835.91	4000.42	3903.49
75	4309.34	4532.22	4366.52
80	4746.96	5090.61	4803.46
85	5243.25	5621.72	5305.93
90	5741.50	6188.44	5812.81
95	6255.15	6759.78	6379.83
100	6994.33	7376.04	7116.66

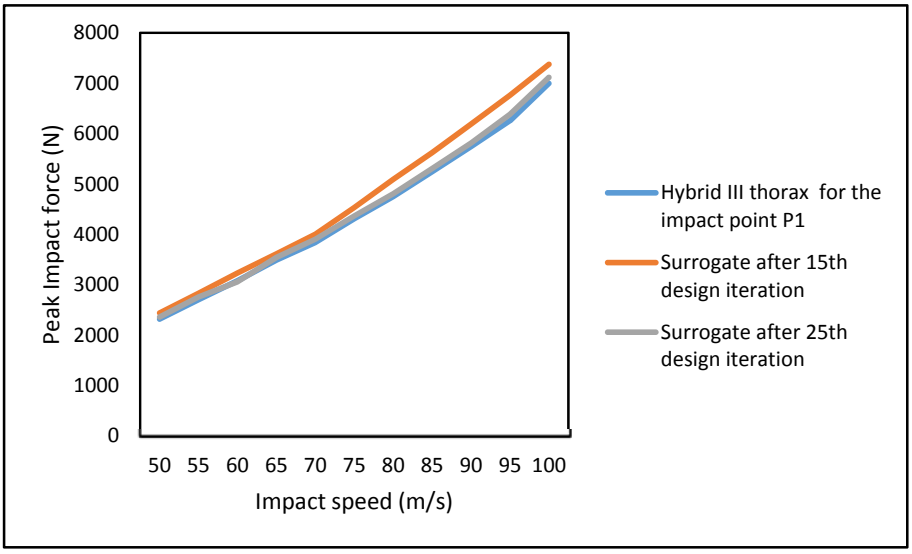

Figure 3.8: Comparison of peak impact forces obtained from Hybrid III thorax and the target

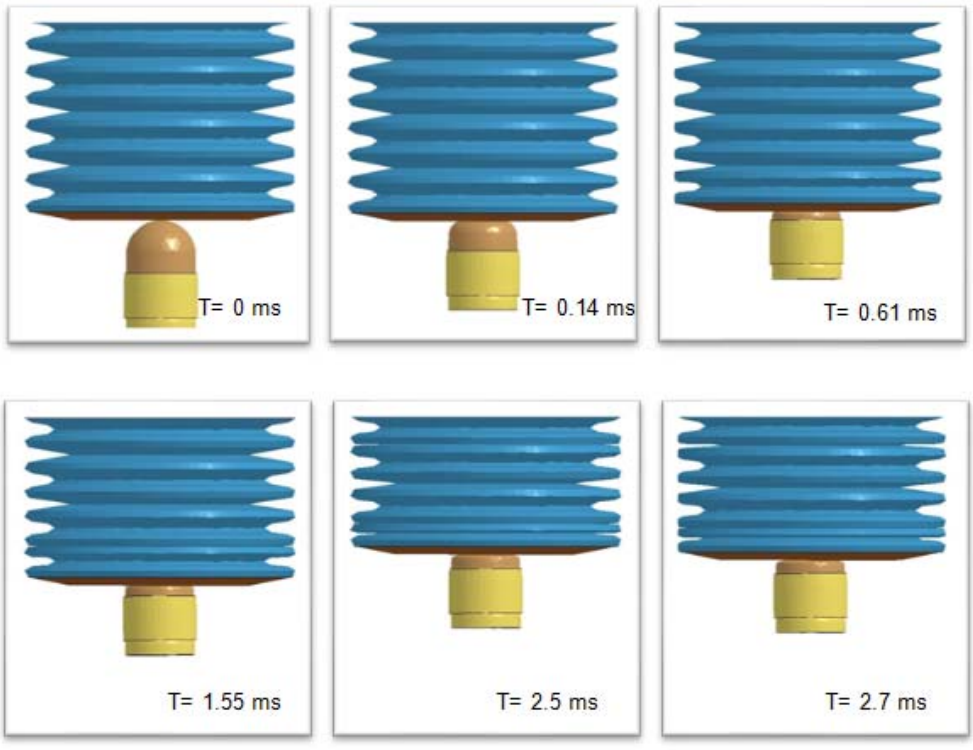

Figure 3.9: Projectile impacting the target at various impact times

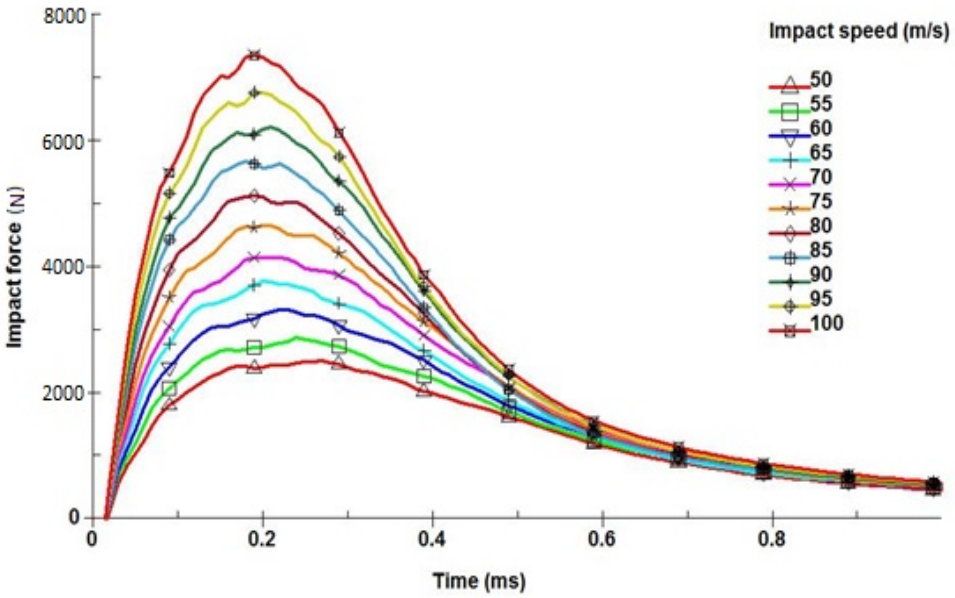

Figure 3.10: Force – time response of the target (surrogate) after 25th design iteration

From the similarities in the trend and values of the force–time response (Figures 3.5 and 3.10) obtained by impacting the thorax of the Hybrid III ATD and the target (made up of corrugated sheets), it is evident that as far as the force–time responses are concerned, the target is correlated with the thorax of the ATD.

3.6 Conclusion

In the feasibility study, deflection–time responses were not considered for correlation. The target was successfully correlated (as far as force–time response is concerned) with the thorax of the Hybrid III dummy. From the outcome of the study, it is evident that the methodology presented in Figure 3.2 is feasible, though cumbersome. Once developed and validated, the mechanical surrogate of the thorax made up of corrugated sheets offer significant advantages such as less solution time, accurate solution and also empowers the user with so much data which otherwise not measurable by the physical experiments of any kinds.

CHAPTER 4: DEVELOPMENT AND VALIDATION OF A THORAX SURROGATE FE MODEL FOR ASSESSMENT OF TRAUMA DUE TO BLUNT BALLISTIC IMPACTS

This chapter represents the full length paper titled " Development and validation of a thorax surrogate FE model for the assessment of trauma due to high speed blunt impacts" authored by Thota N, Eparaachchi J and Lau K-T, and published in the Journal of Biomechanical Science and Engineering. Details of the paper are given in the Appendix – I of the thesis.

4.1 Introduction

In order to develop and validate non-lethal weapons, bullet proof vests, chest protectors for sports personnel, it is essential to have greater insight into the response of the human thorax subjected to high speed blunt impacts by projectiles of low mass. Blunt projectiles with masses of 20–200 g and impact speeds of 20–250 m/s represent the ballistic impacts pertinent to the contact and collision sports activities and non-lethal ammunition (Bir, Viano & King 2004; Bir & Viano 2004; Bir 2000). In the past few decades, law enforcement agencies, military and defense forces have started using less-lethal weapons which were designed to temporarily incapacitate the subject in the situations where lethal force is not warranted. The very basic requirement of non-lethal weapons are that the projectile impact should give short duration pain, be sufficient to deter the subject and should not cause any serious injuries, which require hospitalization and medical treatment (Koene, Id-Boufker & Papy 2008; Widder, Perhala & Rascoe 2003; Widder, Butz & Milosh 1997). Depending upon the amount and the rate of chest deformation, ribs get deflected and compress the internal organs and vessels in their way. Ribs get fractured, when the deflection exceeds the tolerance limit. Compression of the rib cage without any fractured ribs can cause minor injuries, such as bruises and cuts which require only first aid. Depending upon the location and the number of ribs fractured, internal organs can get penetrated with the broken ribs, leading to serious thoracic injuries such as pneumothorax, hemothorax, flail chest, lungs contusion, punctured liver, sternal fractures, heart contusion, fractured aorta etc. Though the probability is very low, aftermath of the blunt trauma could be ventricular septal defect (VSD), which is fatal if untreated. Design of the non-lethal weapons should be such that they should not cause any of these serious injuries mentioned above to the subject. Validation of non-lethal projectiles is very challenging, as blunt thoracic trauma caused by impact ammunitions is greatly influenced by the location of the impact, projectile mass, speed and characteristics of the subject such as age, gender, built, race, clothes worn etc.(Hubbs & Klinger). Therefore, blunt projectiles such as stiff plastic baton, wood baton projectiles, plastic and rubber bullets etc. have been reported to cause serious injuries and fatalities (Hughes et al. 2005; Krausz & Mahajna 2002; Maguire et al. 2007; Mahajna et al. 2002; Rocke 1983; Sheridan, Sean M & Whitlock, Roy IH 1983). Therefore, it is essential to validate (confirm that the effect is non-lethal) the non-lethal weapons by measuring the blunt thoracic trauma in terms of known engineering parameters, well before putting them into the use. In this paper the authors have developed a novel concept of finite element (FE) model of a mechanical surrogate of the thorax, MTHOTA, to evaluate the blunt thoracic trauma in terms of a viscous criterion (VC_{max}).

Many research studies indicated that the blunt chest injuries involving motor vehicle accidents constituted more than 75% of overall such injuries and the blunt thoracic trauma alone was responsible for approximately 25% of overall accidental deaths (Hoyert & Hu 2012; Mancini 2012; Vlessis & Trunkey 1997). In the past few decades, numerous experimental studies (such as pendulum impact tests, drop tests, simulated crash with volunteers, human cadavers and anesthetized animals as test subjects) have been carried out by various researchers and by which greater insight was gained into the different aspects of impact biomechanics of the thorax. Thoracic injury mechanisms, responses of the thorax (elastic, viscous and inertial responses) to the impact in terms of known engineering parameters and human tolerance limits (injury criteria such as acceleration, force, average spinal acceleration, thoracic trauma index, chest compression, viscous criterion etc.) were developed. Therefore, impact biomechanics became synonymous with the study of the vehicular occupant in various crash situations. With the knowledge of the injury mechanisms and human tolerance limits, automotive occupant safety restraint systems (both active and passive) and various anthropomorphic test dummies (ATD) were developed. ATDs such as the Hybrid III family of dummies for frontal impact tests, side impact dummies for lateral impact tests, were designed and validated with the outcome of the various simulated vehicle crash tests using cadavers and animals as human surrogates. Due to the limitations such as scarcity of human cadavers, lack of internal organs in ATDs, erroneous scaling from animal tests to human model etc., researchers have started developing numerical (Finite Element) models of the human body to use as surrogates in vehicle crash tests in a virtual test environment (Crandall et al. 2011; King 1993, 2000; King, Yang & Hardy 2011; Yang & King 2004). Many researchers (Campbell & Tannous 2008; Chang 2001; Cıhalová 2006; Číhalová 2009, 2005; Forbes 2005; Lyon 1997; Shigeta, Kitagawa & Yasuki 2009; Song, Lecuyer & Trosseille 2011; Wang 1995; Zhao & Narwani 2005) have developed finite element models of the full human body with the internal organs. These FE models were validated with the human response corridors (Chen 1978; Kroell, Schneider & Nahum 1971, 1974; Nahum, Kroell & Schneider 1973) and other cadaver tests pertinent to the vehicular occupant in the crash scenarios. However, none of these ATDs (both physical and numerical models) and a full human body FE models were validated for blunt ballistic impacts. From the outcome of the review of ATDs (Chapter – 2), it was clear that none of the thoraces of common ATDs are suitable for the evaluation of the blunt thoracic trauma due to ballistic impacts.

4.2 Existing surrogates of the thorax for blunt trauma applications

Wayne State University's scientists (Bir & Viano 2004; Bir 2000) carried out impact tests by subjecting the thoraces of 13 cadavers to 3 impact cases pertinent to blunt ballistic impacts and developed the force-time, deflection-time, and force-deflection human response corridors. They also evaluated thoracic injury in terms of VC_{max}. These human response corridors and viscous criterion values are very handy in development of thoracic surrogates for determination of trauma caused by blunt ballistic impacts. Bir 2000 has constructed a thorax surrogate, which is popularly known as 3 Rib Chest Structure (3-RCS), by combining the advantages of Hybrid III dummy's loading surface and BIOSID's continuous rib structure. She validated the surrogate with the human response corridors. To construct 3-RCS, 3

ribs of the BIOSID were mounted to a heavy spine box and the impact surface was created with a polyurethane bib. Urethane bib on the impact side of the surrogate provided the response of the thoracic wall's muscle and the damping material inside the 3-RCS provided the viscous response of the internal organs (Figure 4.1)

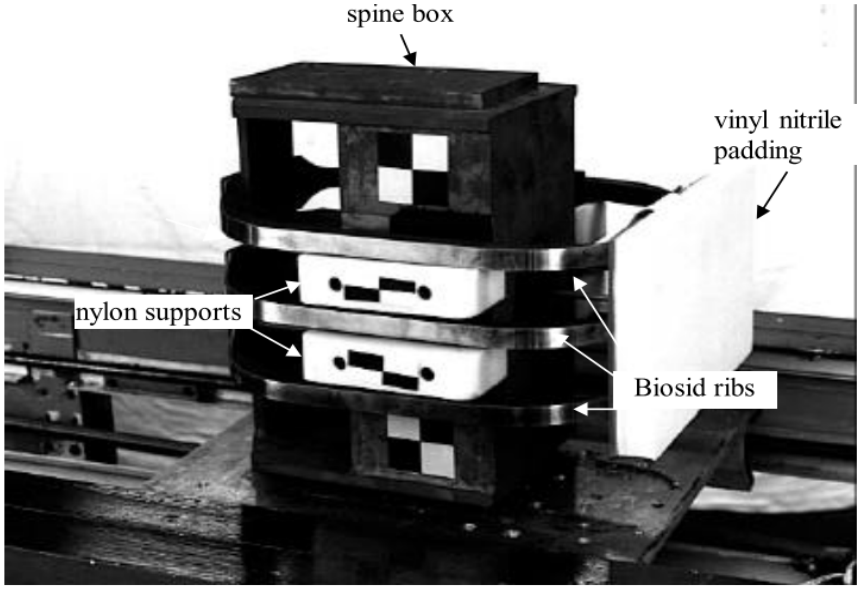

Figure 4.1: Reusable thorax surrogate 3-RCS. Adapted from Bir, 2000

However, 3-RCS is a physical surrogate and has got some limitations, such as only impact on a small area on the bib (2 inch by 3 inch area at the center of the bib) provided useful biomechanical responses for the correct evaluation of the VC_{max} correctly (DuBay & Bir 1998), lack of space for additional accelerometers, no provision to mount chest protectors or armors etc. Due to these limitations, the cumbersome test methodology and expensive test setup, usage of 3-RCS might not be attractive especially during the development stage of new non-lethal weapons or sports personnel's safety related products.

Researchers at the DSTO (Department of Science and Technology Organization) of Australia developed a reusable thoracic surrogate AUSMAN, but limited published data were available on the surrogate. From the limited published research, it was clear that AUSMAN was mainly developed for BABT studies (Bass et al. 2006). Cadaver test data pertinent to such impacts is very limited, and clay signature tests were used for the validation of a surrogate. Therefore, it can't be used for the blunt trauma caused by ballistic impacts of our interest. The AUSMAN is shown in Figure 4.2.

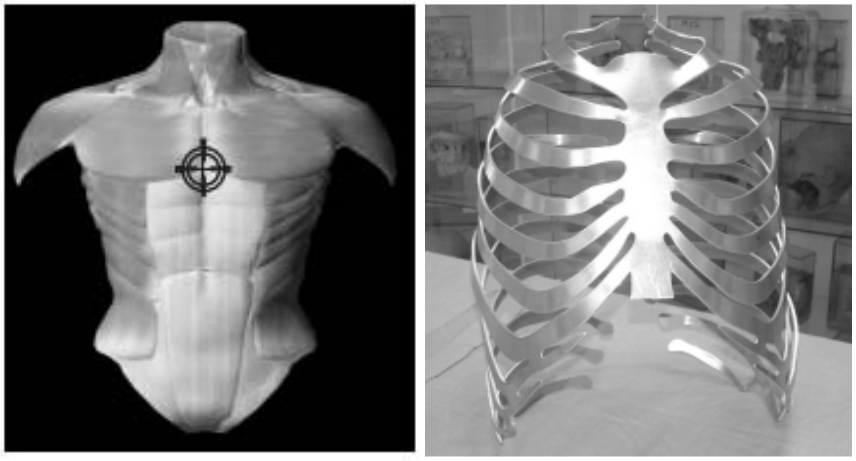

Figure 4.2: Reusable thorax AUSMAN (left) and the rib cage (right). Adapted from Bass et al. 2006

Similarly, both physical and FE human surrogate torso models (HSTM) have been developed (Roberts, O'Connor & Ward 2005; Roberts et al. 2007) and used for BABT studies.

As far as the numerical models of the thorax surrogates are concerned, only Nsiampa et al. 2011a, 2011b, 2012, validated their human thorax FE model with the human response corridors (Bir & Viano 2004) and subsequently evaluated the performance of two non-lethal projectiles, namely, a foam nosed projectile and a 140g PVC baton. Though impact location significantly influences the outcome, as their thorax FE surrogate is modeled with lungs, ribs and chest wall, they have presented results for only one impact point and have not validated that model for any subject specific responses.

In nutshell, from the published literature, it is evident that in spite of so many ATDs (both mathematical and physical models) and numerous detailed full human body FE models, only 4 (AUSMAN, 3-RCS, HSTM and FE model of the thorax by Nsiampa et al. 2011a and 2011b) surrogates were validated for the impacts of interest. However, they are very cumbersome and expensive to use, necessitating the development of an FE model surrogate of the thorax which is simple yet effective and accurate in predicting the thoracic trauma caused by blunt ballistic impacts.

In this chapter, the concept, development methodology, details of the FE model and impact simulations for the validation of MTHOTA are presented.

4.3 Methodology

A simple concept of MTHOTA was developed, and details of the concept are shown in Figure 4.3. A steel metal impact plate was added to one side of a corrugated collapsible structure, while the other end is fixed. Low density, highly compressible, stiff TPE closed cell foam sheet is added to the impacting side of the metal plate. 4 metal plates were attached to the collapsible corrugated structure.

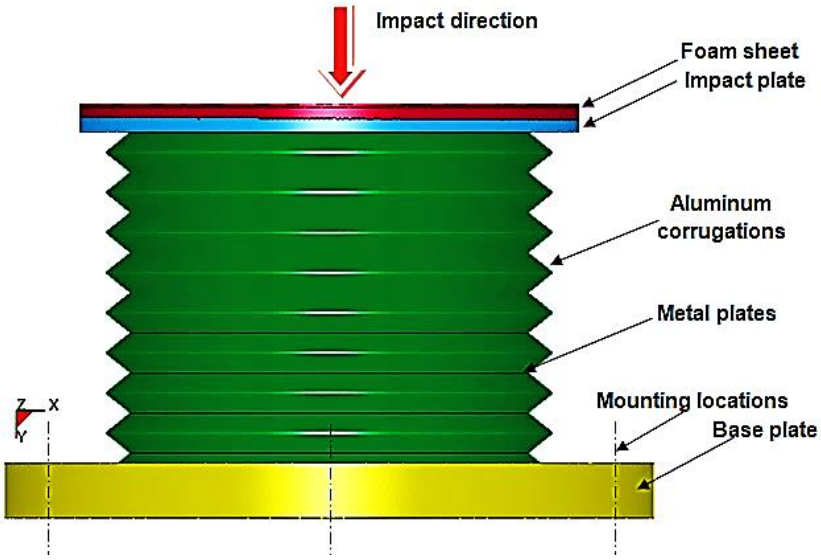

Figure 4.3: Details of the concept of MTHOTA

The purpose of the foam sheet is to provide muscle response upon the impact. The metal impact plate, and the corrugations along with 4 metal plates together are to provide the inertial, elastic and viscous responses of the rib cage, internal organs, etc.

The procedural steps involved in the validation method are shown in Figure 4.4. Details of the wooden baton projectiles and impact velocities used in the present study are given in Table 4.1.

Table 4.1: Impact conditions

Impact condition	Projectile details	Impact speed
LP_20	Wooden baton, 140 g, 100 mm length, 37 mm diameter	20 m/s
LP_40	Wooden baton, 140 g, 100 mm length, 37 mm diameter	40 m/s
SP_60	Wooden baton, 30 g, 28.5 mm length, 37 mm diameter	60 m/s

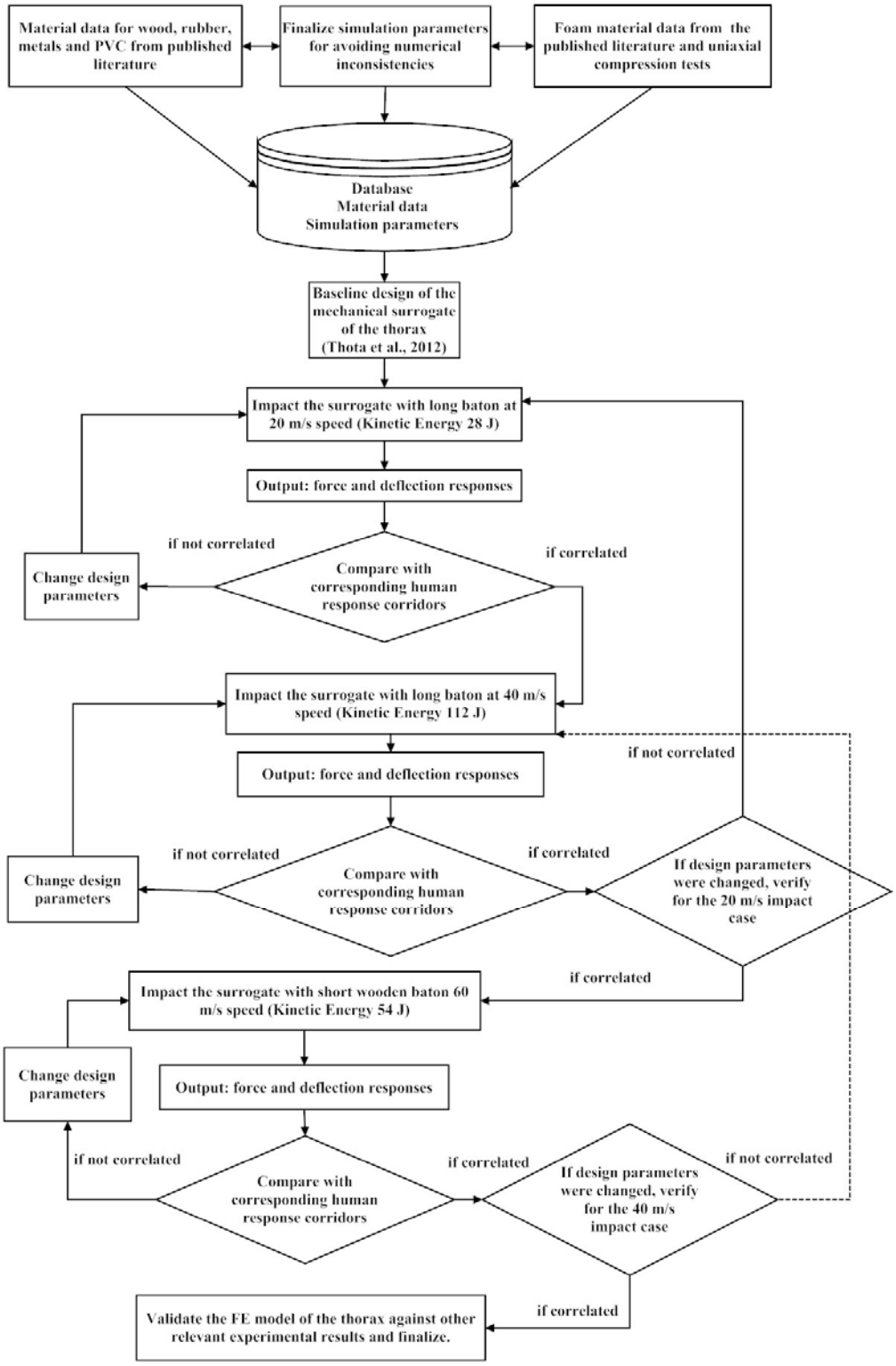

Figure 4.4: Process flow chart for validation the thorax surrogate using human response corridors

Aim of the study is to make the MTHOTA to emulate force-time and deflection-time responses, and VCmax values of the human thorax for all of the impact conditions mentioned in the Table 1, by suitably changing the design parameters such as thickness of the foam (T1), thickness of the impact plate (T2), thickness of the corrugated sheet (T3), thickness of the 4 metal plates (T4), inner and outer diameter of the collapsible structure (D and d), height of the corrugation (h), height of the collapsible structure (H), and the locations of the 4 metal plates. Cross section of the MTHOTA along with the design variables are shown in Figure 4.5.

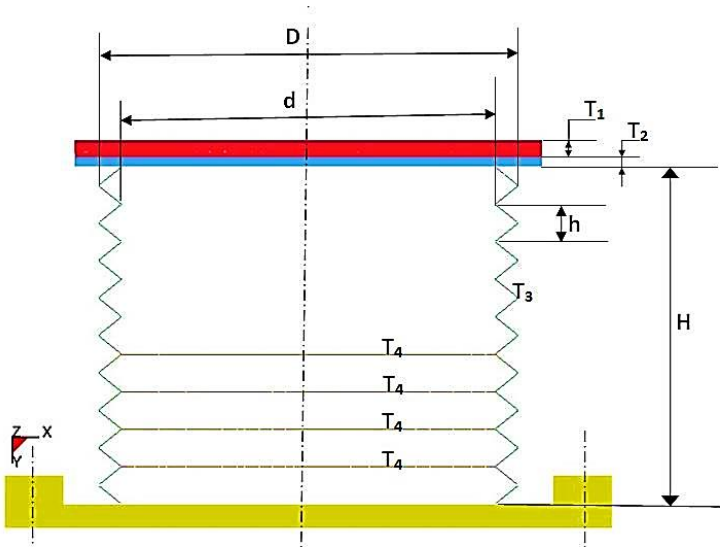

Figure 4.5: Cross section of the MTHOTA concept and design variables

In order to gain greater insight into the behaviour of MTHOTA to blunt ballistic impacts, the very first analysis was carried out with the dimensions of MTHOTA comparable with the human thorax and Anthropomorphic Test Dummies used in the automotive simulated crash tests (for instance, D = 300 mm, H = 180 mm, T_1 = 10 mm, T_2 = 3 mm, T_3 = 2 mm, T_4 = 2 mm. etc.,). In this analysis, the surrogate was subjected to LP_20 impact condition and didn't yield any measurable deflection-time response. In some cases, MTHOTA responded to LP_40 and didn't give any response to SP_60, due to the heavy impact plate and the high stiffness of the corrugated structure. Because of this, the profile of the corrugations was changed to a less stiff configuration and dimensions were reduced drastically to see the usefulness of the concept. With D = 160mm, H = 160 mm, T_1 = 8 mm, T_2 = 2mm, T_3 = 4 and T_4 = 3 mm, the thoracic surrogate gave measurable deflection-time responses to all 3 impact cases under consideration. By taking this configuration as the baseline design (ignoring all other configurations which didn't yield measurable deflection responses to all 3 impact cases), iterative analysis was carried out by varying the design parameters. For accomplishing the perfect correlation of MTHOTA with the cadaver test results (human response corridors), the methodology mentioned in Figure 4.4 was strictly followed.

Range of thicknesses (foam sheet, impact plate, Aluminium corrugations and 4 plates) chosen, material models, element types, and element formulations used in

the FE model of the MTHOTA are given in the Table 4.2. Cross-section and FE model of the baseline configuration of the surrogate under development is as shown in Figure 4.6. In all, nearly 850 simulation iterations were carried out by varying design parameters to achieve the correlation of the MTHOTA with the responses obtained from the cadaveric tests. Parameters of the final (validated) MTHOTA were given in Table 4.2 and enclosed in the parenthesis. To finalize the appropriate element size, the convergence study was performed. Suitable element sizes to achieve the solution convergence were given in Table 4.2. Responses of the validated MTHOTA are given in the subsequent sections.

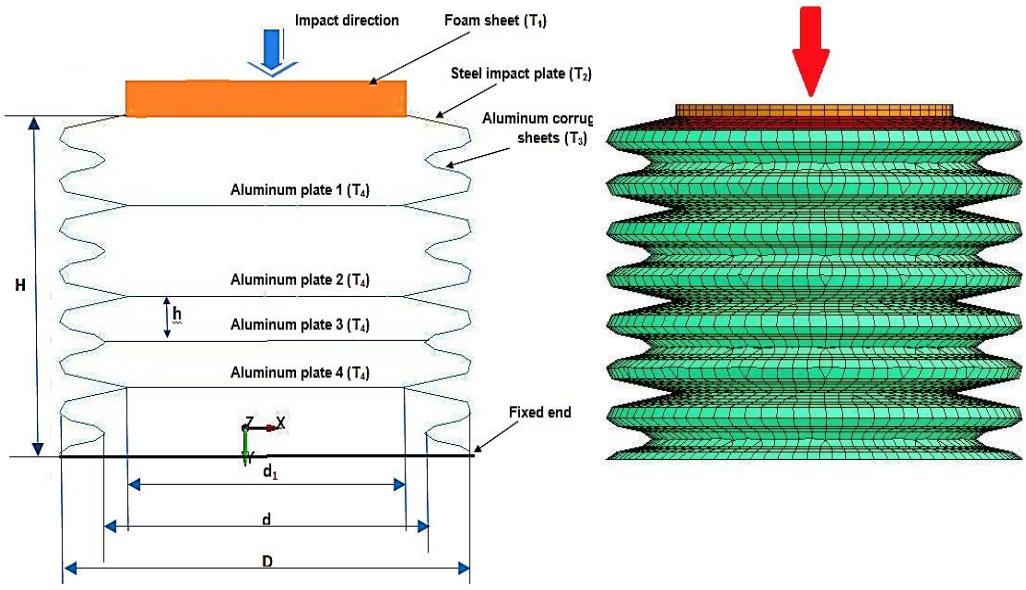

Figure 4.6 Cross section (left) and the FE model (right) of the baseline configuration of MTHOTA surrogate

Table 4.2: Details of the MTHOTA finite element mode

Component	**Range of the parameter in mm (final values)**	**Element Type**	**Material model**	**Element size (final MTHOTA configuration)**
Foam sheet	2.0 – 10.0 (4.0)	Brick (8 nodes)	MAT_LOW_DENSITY_FOAM or MAT_057 (Highly compressible closed cell foam)	Two layers in the thickness and 5 mm
Impact plate	0.5 – 4.0 (1.0)	Shell (3 and 4 noded)	MAT_ELASTIC or MAT_001 (Isotropic elastic material)	5 mm
Aluminum corrugations	0.5 – 3.0 (0.6)	Shell (3 and 4 noded)	MAT_PLASTIC_KINEMATIC or MAT_003 (Isotropic and kinematic hardening plasticity)	5 mm
Aluminum metal plates	0.5 – 4.0 (0.55)	Shell (3 and 4 noded)	Same as above	5 mm
Projectile	-	Brick (8 nodes)	MAT_WOOD or MAT_143 (transversely isotropic) /MAT_001 (isotropic elastic)	3 – 5 mm
D	140 – 160 (150)	-	-	-
d	110 – 130 (115)	-	-	-
d_1	85 – 110 (100)	-	-	-
H	90 – 160 (110)	-	-	-
h	10 – 20 (16.5)	-	-	-

In all impact cases, the projectile was a wooden baton and material properties for MAT_WOOD (MAT_143) were taken from the published literature (Green 2001; Green, Winandy & Kretschmann 1999; Kretschmann et al. 2010; Murray et al. 2005). PVC (with MAT_ELASTIC) as the projectile material yielded almost the same output as the wooden baton. Material data, experimentally obtained load curve data points of the TPE foam and details of the contact interfaces used in the present study are given in Table 4.3, Table 4.4 and Table 4.5 respectively. Details of the contact interfaces and material models used in the FE analysis can be found in the LS-DYNA keyword users' manual, Volume I and II (Bush & Challener 1988; Hallquist 2007a, 2007b) respectively.

Table 4.3: Mechanical properties of the materials used in the MTHOTA FE model

Material name	**Material properties used in the material data cards of LS-DYNA (v9.71 R7.0)**				
	Density (kg/mm^3)	Young's modulus (GPa)	Poisson's ratio	Yield Stress (GPa)	Comments
Aluminum	2.17E-06	75.0	0.34	0.179	Aluminum alloy 3XXX series
Steel	7.87E-06	210.0	0.30	-	Structural steel
PVC	1.38E-06	2.30	0.33	-	Low-density PVC
TPE foam	1.43E-07	0.04	Poisson's ratio input is not required. Load curve input (Engineering stress versus Engineering strain) is required. Experimentally obtained stress, and strain data is given in Table 4.4.		

Table 4.4: Load curve data of the TPE foam used in the MTHOTA construction

Engineering Strain	**Engineering Stress (GPa)**
0.000	0.00
0.027	5.00×10^{-5}
0.030	1.19×10^{-4}
0.040	1.60×10^{-4}
0.087	2.20×10^{-4}
0.100	2.30×10^{-4}
0.200	2.40×10^{-4}
0.500	3.81×10^{-4}
0.600	4.20×10^{-4}
0.800	5.81×10^{-4}
0.850	6.32×10^{-4}
0.900	9.02×10^{-4}
1.000	1.20×10^{-3}

Table 4.5: Contact interfaces in the FE model of the MTHOTA

Contact interface	Type of the contact
Impact plate – Foam sheet	AUTOMATIC_SURFACE_TO_SURFACE
Projectile – foam sheet	CONTACT_NODES_TO_SURFACE
Impact plate - corrugations	CONTACT_NODES_TO_SURFACE
Corrugated sheet	SINGLE_SURFACE_CONTACT

Problems associated with the FE modeling of low-density foams and precautions to be taken to avoid the error termination are described below.

Premature termination due to negative volume of the element is the most common error with FE analysis involving highly compressible foams (for instance TPE foam sheet in the present study). Due to the large deformations, elements may become so deformed that the volume of the element is evaluated as negative. Unless the severely deformed area is re-meshed, or elements are smoothened, a Lagrangian mesh can accommodate only limited amount of deformation. To avoid the termination error due to negative volume of the foam elements, the following precautions were taken:

- The variable "ERODE" in *CONTROL_TIMESTEP card was set to 1.
- The variable DTMIN in *CONTROL_TERMINATION was set to non-zero value.
- The variable TSSFAC (Time step scale factor) in the *CONTROL_TIMESTEP was reduced to 0.5 from the default 0.9.
- The variable DAMP in the MAT_LOW_DENSITY_FOAM data card was set to 0.5 (maximum recommended damping value) and the variables HU (hysteretic unloading factor) was set to 1.0 (no energy dissipation) and the variable SHAPE (shape factor for unloading) was set to 1.0.
- Load curve was stiffened up (Engineering stress versus Engineering Strain) at large strains. This is a very efficient measure to avoid the premature termination of the simulation run. The material data for the TPE foam used for the analysis is experimentally determined, but after 90% of the strain, the data was manipulated to stiffen the material.

With the above-mentioned precautions, premature termination of the simulation runs was entirely avoided. Details of the contact interface definitions and definition and importance of the control cards (*CONTROL_TIMESTEP and *CONTROL_TERMINATION) and all related variables (such as ERODE, DTMIN, DAMP, etc.) can be found in the theory manual and keyword user's manual, volume I and II (Hallquist 2006; Hallquist 2007a, 2007b)of LS-DYNA.

4.4 Results and discussion

4.4.1 Thorax surrogate (MTHOTA) impacted with a long baton of 140 grams with 20 m/s impact velocity (LP_20)

The dynamic force response of the MTHOTA for the LP_20 impact condition along with the force-time human response corridors for the respective impact case are as shown in Figure 4.7. The force response obtained for MTHOTA has been filtered using an SAE class 300 filter.

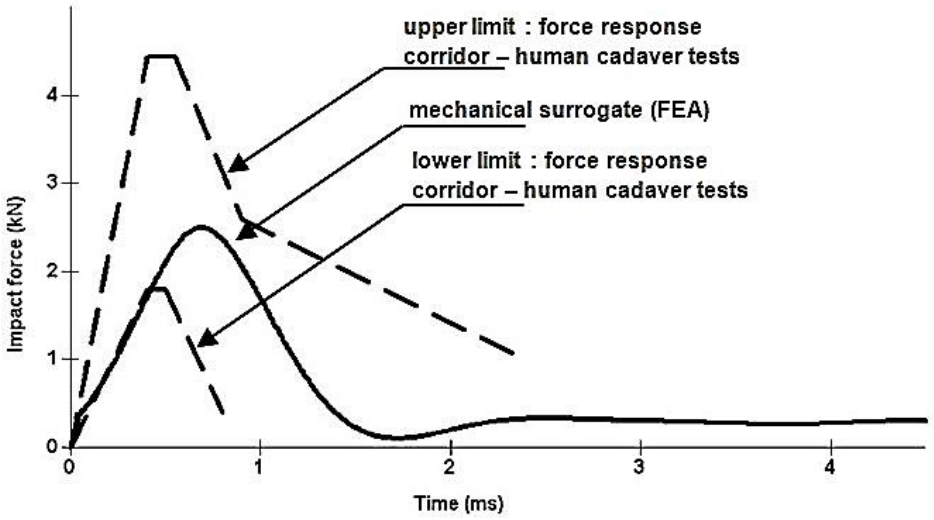

Figure 4.7: Force – time response of the thorax surrogate MTHOTA when subjected to LP_20 impact

Peak impact force was measured as 2509 N, which is within the range (3383 ± 761) of force-time response established for the condition A (Bir 2000).

Deflection of the impact plate (any nodal displacement serves the purpose as the impact plate has been modeled as rigid material) and deflection of the impact plate with respect to plate-3, both as a function of time were measured and both deflection-time curves are shown in the Figure 4.8 and Figure 4.9 respectively. No filter was used for processing the dynamic deflection data.

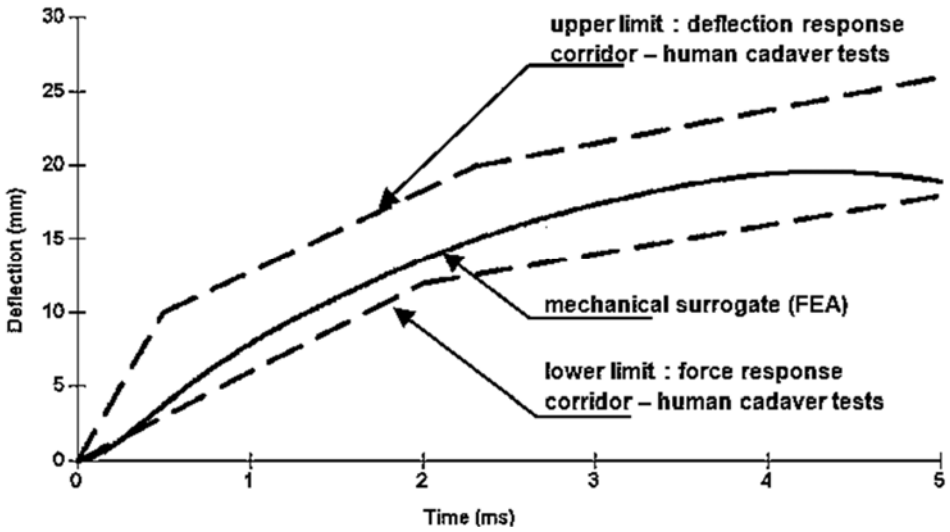

Figure 4.8: Deflection response of the MTHOTA when subjected to LP_20 impact (measured using the node on the impact plate

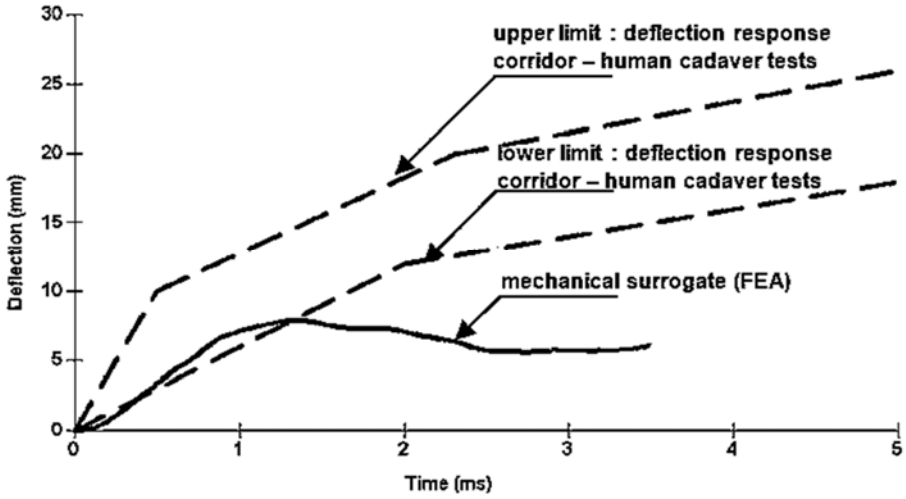

Figure 4.9: Deflection response of the MTHOTA when subjected to LP_20 impact (measured using the node on the impact plate with respect to the node on the plate-3)

4.4.2 Evaluation of blunt thoracic trauma in terms of VC_{max}

Wayne State University researchers (Lau & Viano 1986; Viano, David C. & Lau, Ian V. 1988) proposed Viscous Criterion (VC), which is a function in the time formed by the product of the velocity of chest deflection and the chest compression at that instance. Viano & Lau 1988; Viano et al. 1989 have conducted numerous experiments, in which thoraces of the cadavers were subjected to the lateral impact loads in simulated vehicle crashes. They found that VC value based on maximum chest deflection and rate of chest compression (VC_{max}) is better injury predictor than all other injury criteria. Values of VC_{max} can be expressed in terms of abbreviated injury scale (Gennarelli & Scaling 1985; Scaling 1985; States 1969; States et al. 1971).

For frontal loading on the thorax (Viano, et al., 1989, Viano, et al., 2000),

VC_{max}	= 1.0 m/s;	25% probability of AIS3+
	= 1.3 m/s;	50% probability of AIS3+

Similarly, for lateral/side impact of the thorax (Viano, et al., 1989, Viano, et al., 2000),

VC_{max}	< 1.0 m/s;	AIS 0-2
	>1.0 m/s;	AIS 4, 5
	= 1.47 m/s;	25% probability of AIS4

In case of occupant of the vehicle frontal and side impact scenarios, $VC_{max} \leq 1.0$ m/s was taken as specification in vehicle standards such as ECE-R94, ECE-R95, EuroNCAP (front and side impact) and FMVSS 214. Defense and military research organizations have also considered $VC_{max} \leq 1.0$ m/s as the specification for the non-lethal weapons.

In the case of the front and side impact dummies, viscous criterion can be calculated by using the formula given below.

Equation (2.3) provides the generic expression for VC_{max}, while the equation (2.5) provides the complete expression employed in the evaluation of the VC_{max} using surrogates (PMHS and ATDs).

Using MTHOTA surrogate, VCmax value can be evaluated by using the equation given below.

$$VC_{max} = S \,.\, (Y_{max}/D).\, (Y_{max}/T) \qquad (4.1)$$

Where,

VC_{max} = Max of Viscous Criterion (m/s)

S = Scaling factor (Dimensionless multiplication factor. S = 0.366 for method-1 and 1.3 for method-2)

Y_{max} = Peak chest deflection (mm) for method-1, and Peak chest deflection (mm) with respect to the plate-3 for method-2

D = Dummy constant in mm (110 mm for method-1 and 180 mm for method-2)

T = Time taken for the deflection to reach its peak (ms)

The two methods (method-1 and method-2) developed for the calculation of VC_{max} using MTHOTA were described below. VC_{max} values are good enough for validation of the non-lethal ammunition, chest protectors, etc.

4.4.2.1 Method-1

(i) Perform the FE simulation by impacting MTHOTA with the blunt projectile

(ii) Measure the dynamic deflection (deflection-time) response of the metal impact plate.

(iii) Measure the maximum deflection and time taken for attaining the maximum deflection

(iv) Evaluate VC_{max} using the Equation (4.1). Use scaling factor as 0.366 and 110 mm as the deformation constant. It is important to note that Bir (2000) has used 1.3 as scaling factor and 180 mm as the deformation constant for the calculation of VC for all her experiments involving cadavers and 3-RCS surrogate.

For the LP_20 impact condition of MTHOTA, it is evident from the Figure 4.8, that the impact plate's maximum displacement was 19.6 mm, and it took 4.16 ms to reach the maximum displacement. Maximum compression can be calculated by normalizing the maximum displacement with 110 mm which is the depth of the MTHOTA. Therefore,

$$VC_{max} = 0.366\ (19.6/4.16)\ (19.6/110) = 0.31$$

4.4.2.2 Method-2

(i) Perform the FE simulations by impacting MTHOTA with the blunt projectile.

(ii) Measure the dynamic deflection (deflection-time) response of the rigid impact plate with respect to the plate-3

(iii) Measure the maximum deflection and the time at which deflection attained maximum.

(iv) Evaluate maximum deformation velocity

(v) Evaluate VC_{max} using the Equation (4.1). Use 1.3 for the scale factor and 180 mm as the deformation constant.

Thorax surrogate MTHOTA subjected to the same LP_20 impact condition, from Figure 4.9; the maximum displacement (7.85 mm) of the impact plate with respect to plate-3 occurred at 1.3 ms. Therefore, VC_{max} was calculated as follows.

$$VC_{max} = 1.3\ (7.85/1.3)\ (7.85/180) = 0.34$$

Though VC_{max} calculated using both methods mentioned above was very well correlated with the VC_{max} measured from the cadaver tests, only method-2 has been used for the calculation of VC_{max} for remaining cases of impact simulations.

4.4.3 Thorax surrogate (MTHOTA) impacted with the long baton of 140 grams with 40 m/s impact velocity (LP_40)

The force response of the thorax surrogate MTHOTA, dynamic deflection of the impact plate and the dynamic deflection of the impact plate with respect to the plate-3

were calculated from the output of FE simulations in which thorax surrogate MTHOTA was subjected to the LP_40 impact condition and are shown in Figure 4.10, Figure 4.11 and Figure 4.12 respectively.

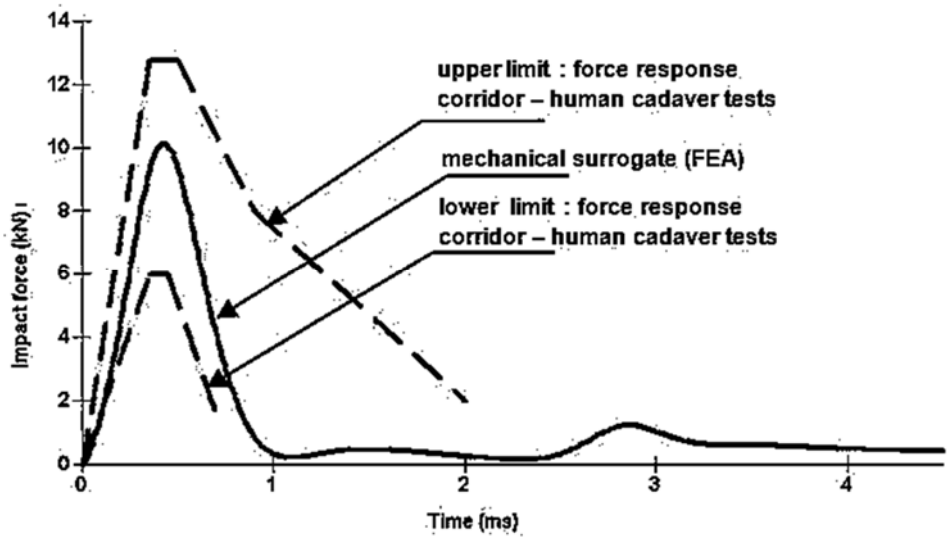

Figure 4.10: Force response of the MTHOTA when subjected to LP_40 impact (Measured using the accelerometer mounted on the back face of the projectile)

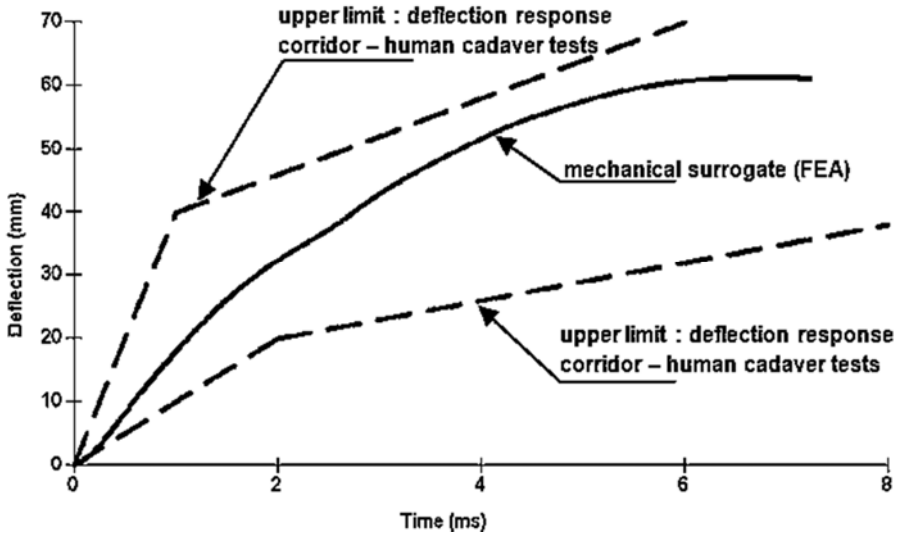

Figure 4.11: Deflection response of the MTHOTA when subjected to LP_40 impact (measured using the node on the impact plate)

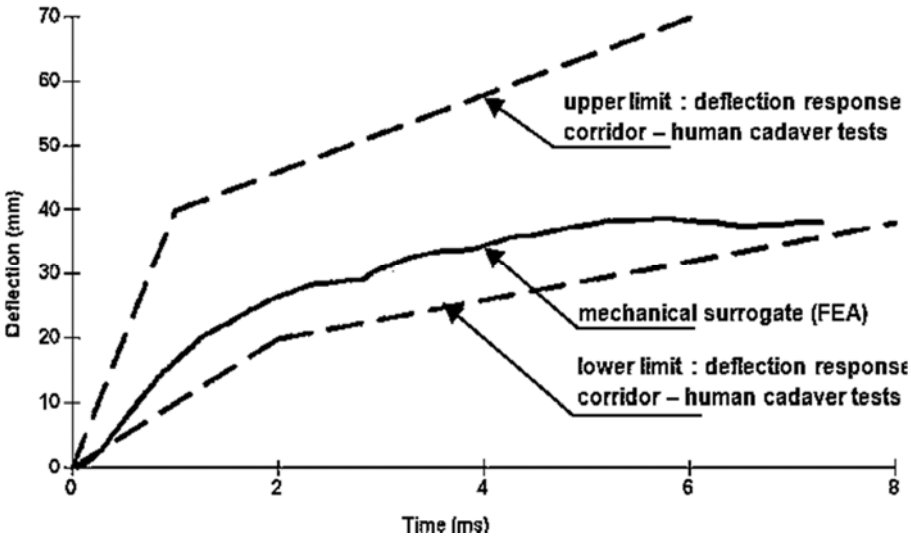

Figure 4.12: Deflection response of the MTHOTA when subjected to LP_40 impact (Measured using the node on the impact plate with respect to the node on the plate-3)

Peak impact force measured for this case was 10200 N at the impact duration 0.41 ms, which is very well correlated with human response corridor for the respective impact case as the peak force is within the range of 7400 – 12600 N.

From the Figure 4.12, maximum deflection was measured as 38.5 mm and the time taken for a maximum deflection was approximately 5.7 ms. Using method-2, VC_{max} was calculated as 1.87. For the case of MTHOTA subjected to LP_40 impact, variation in the total energy of the projectile and the surrogate as a function of time are shown in the Figure 4.13.

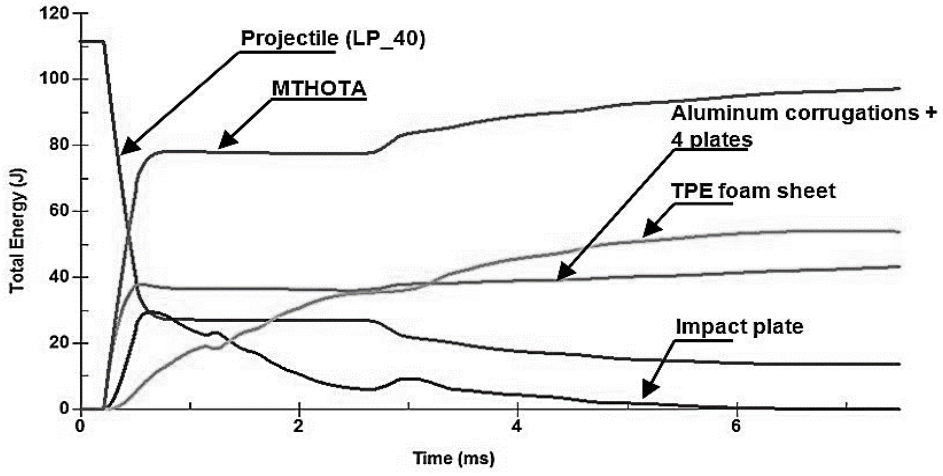

Figure 4.13: Variation in the total energy of the projectile and the surrogate during the impact

4.4.4 Thorax surrogate (MTHOTA) impacted with the short baton of 30 grams with 60 m/s impact velocity (SP_60)

Force-time, deflection-time responses of the impact plate and the same with respect to the plate-3 were elicited from the output of the FE impact analysis of MTHOTA for SP_60 impact condition. These responses are shown in Figure 4.14, Figure 4.15 and Figure 4.16 respectively.

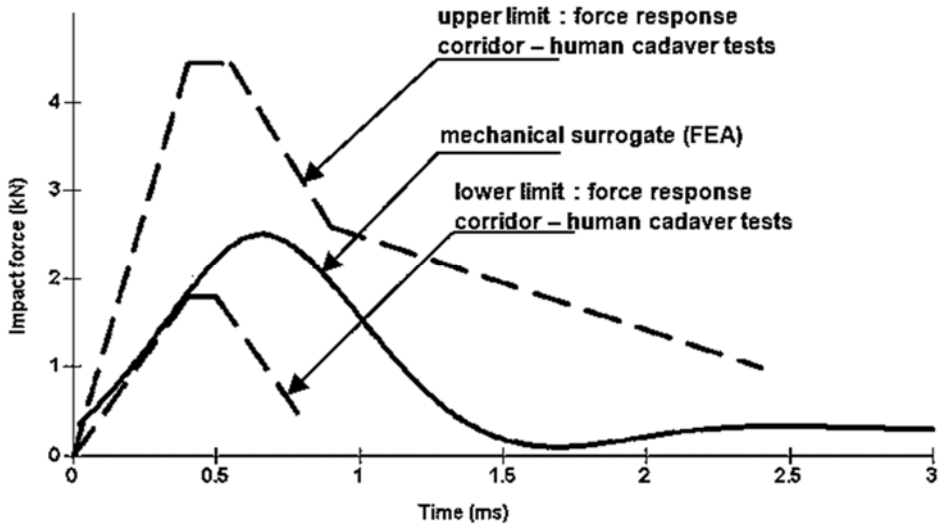

Figure 4.14: Force response of MTHOTA surrogate when subjected to the SP_60 impact

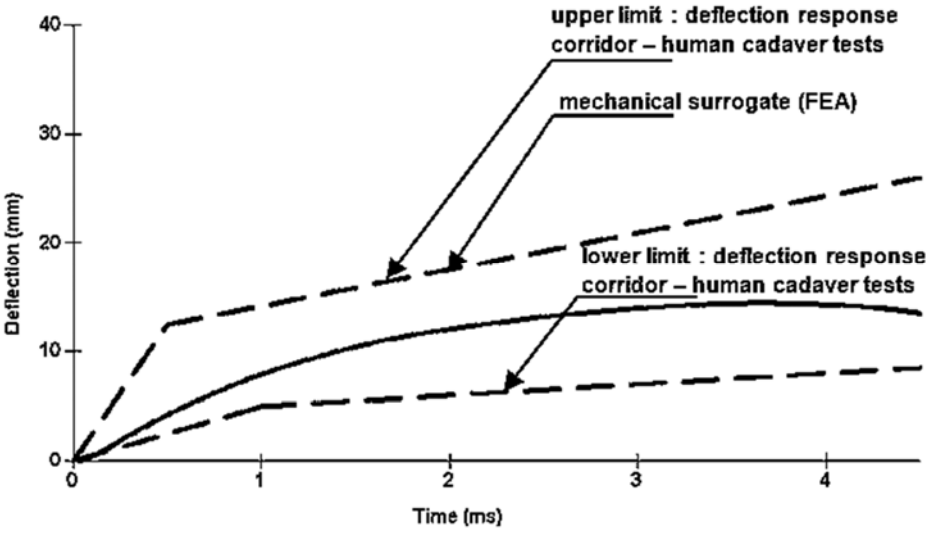

Figure 4.15: Deflection response of MTHOTA surrogate when subjected to the SP_60 impact (measured using the node on the impact plate)

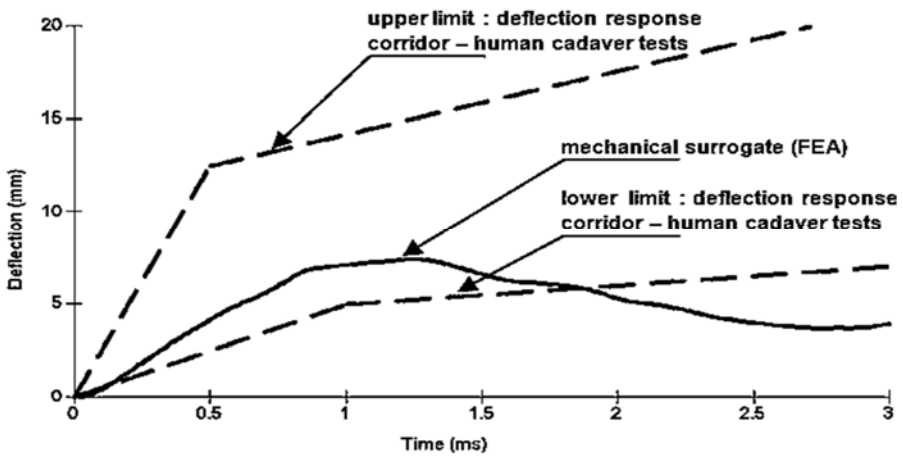

Figure 4.16: Deflection response of MTHOTA surrogate when subjected to the SP_60 impact (measured using the node on the impact plate with respect to the node on the plate-3)

A 30 gram wooden baton with 60 m/s impact velocity is very much relevant to latest impact munitions (non-lethal projectiles such as XM1006, Direct Impact-OC, Direct Impact-Inert and extended range versions of all these ammunitions), except for the impact velocity (muzzle velocity) is in the order of 100 m/s in the case of kinetic less lethal ammunition. Stress contour plots in the surrogate when subjected to the SP_60 impact are shown in the Figure 4.17.

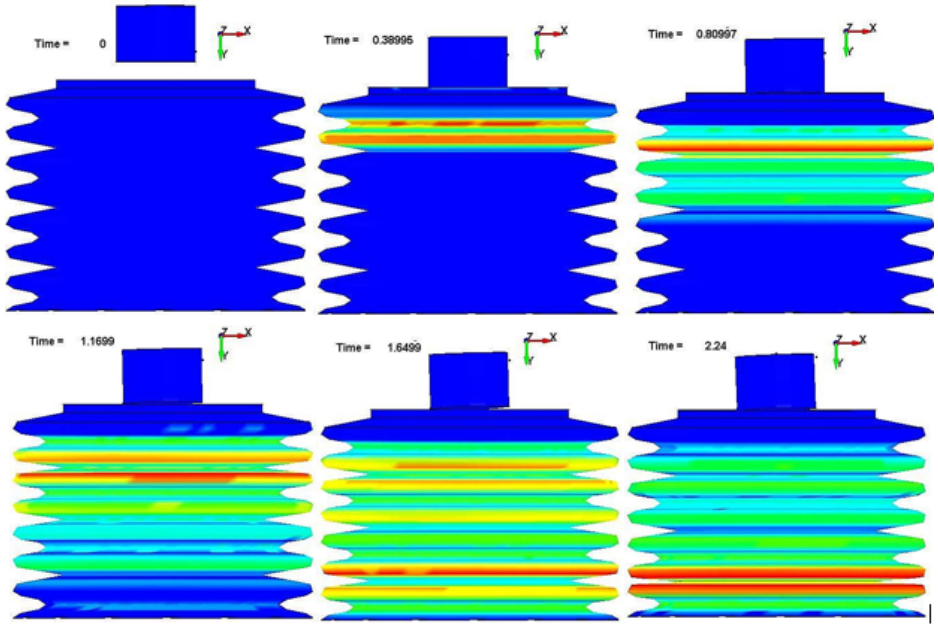

Figure 4.17: Stress contour plots in the thorax surrogate (MTHOTA) when subjected to SP_60 impact

From the dynamic force response as a function of time for this impact case, it is clear that peak impact force of 2510 N occurred at approximately 0.7 ms of impact time. Force response of MTHOTA for SP_60 impact case too was very well correlated with the human response corridors for the respective impact case.

The VC_{max} for this impact case was evaluated as 0.33, using the 7.55 mm of maximum deflection of the impact plate with respect to plate-3, which occurred at 1.22 ms time.

The VC_{max} values obtained for all 3 impact cases of MTHOTA and those obtained from respective impact cases of cadavers and 3-RCS surrogate are compared and are as shown in the Figure 4.18.

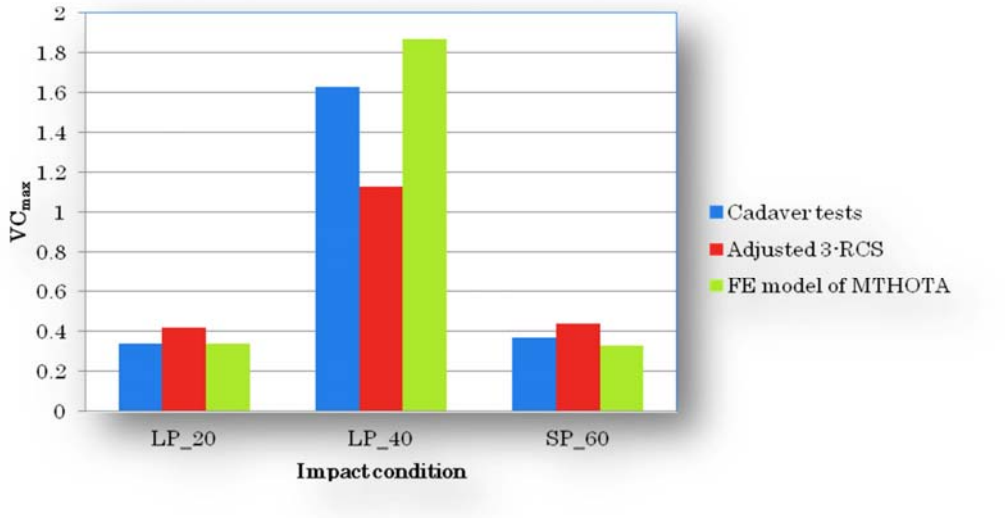

Figure 4.18: Comparison of VC_{max} values obtained from MTHOTA with cadaver tests and 3-RCS surrogate

From 3 impact cases, it is evident that the dynamic force response, dynamic deflection response and VC_{max} values of MTHOTA for all impact cases were very well correlated with the test data obtained from cadaveric experiments for the same impact cases. Being able to accurately measure the blunt thoracic trauma in terms of Viscous Criterion, the FE model of the thorax surrogate MTHOTA can be confidently used for validation of less-lethal ammunition and sports personal protective equipment.

4.5 Further validation of the FE model of MTHOTA surrogate

Though the FE model of the mechanical thorax surrogate MTHOTA has been validated, it was subjected to further corroborative tests to verify its robustness and reliability, using the data published by well-known researchers working on the design, development and validation of non-lethal projectiles.

4.5.1 Sponge nose PVC grenade of mass 41.9 gram and size of 40 mm diameter

Two cases of finite element simulations were carried out with MTHOTA subjected to the impact with a sponge nosed projectile with impact velocities 37 m/s and 73 m/s. Approximate dimensions and material properties of sponge nose were collected from the literature (Nsiampa et al. 2012).

Initial and final stages of MTHOTA subjected to the impact by a sponge nosed projectile with 73 m/s were as shown in the Figure 4.19, and cross sections of the same were as shown in the Figure 4.20.

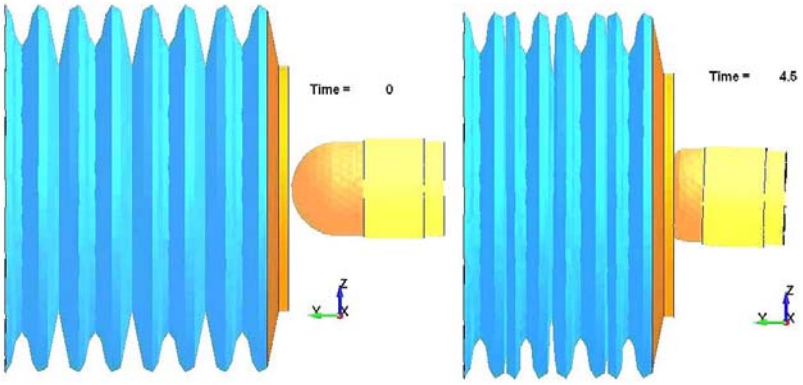

Figure 4.19: Sponge nosed projectile (mass of 41.9 g, 40 mm diameter) impacting the thorax surrogate (MTHOTA) at 73 m/s speed. Initial and final stages of the MTHOTA and the projectile

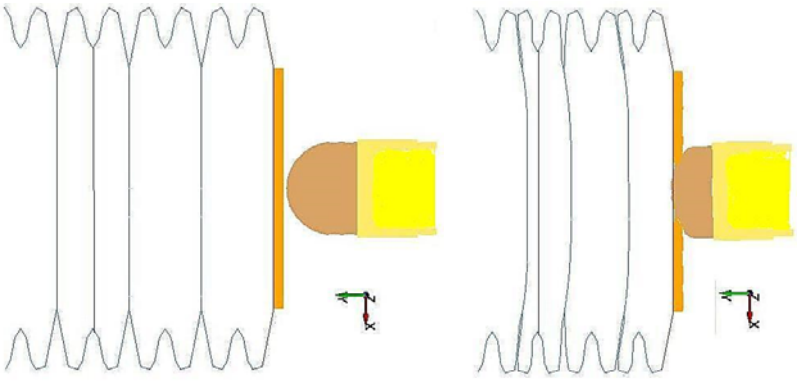

Figure 4.20: Sponge nosed projectile (mass of 41.9 g, 40 mm diameter) impacting the thorax surrogate (MTHOTA) at 73 m/s speed. Cross sectional view of the Initial and final stages of the MTHOTA and the projectile

Dynamic deflection (as a function of time) of the impact plate with respect to plate-3, was as shown in the Figure 4.21.

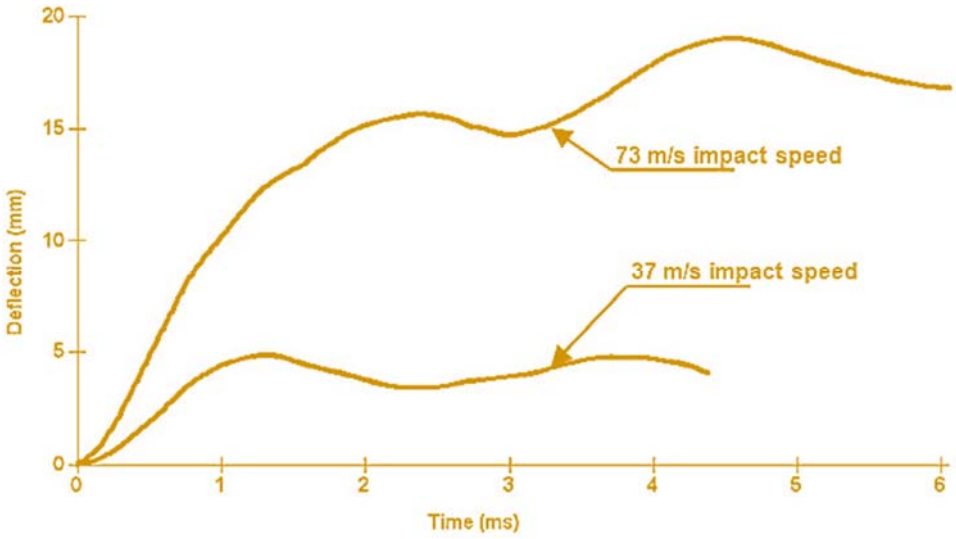

Figure 4.21: Dynamic deflection of the impact plate, with respect to plate-3 when MTHOTA is impacted with a sponge grenade at 37 m/s and 73 m/s.

VC_{max} for both impact cases were evaluated using the method-2 described in previous sections. These values were compared with the results presented in the literature (Bir & Viano 2004; Bir 2000; Nsiampa et al. 2012) and were as shown in the Figure 4.22.

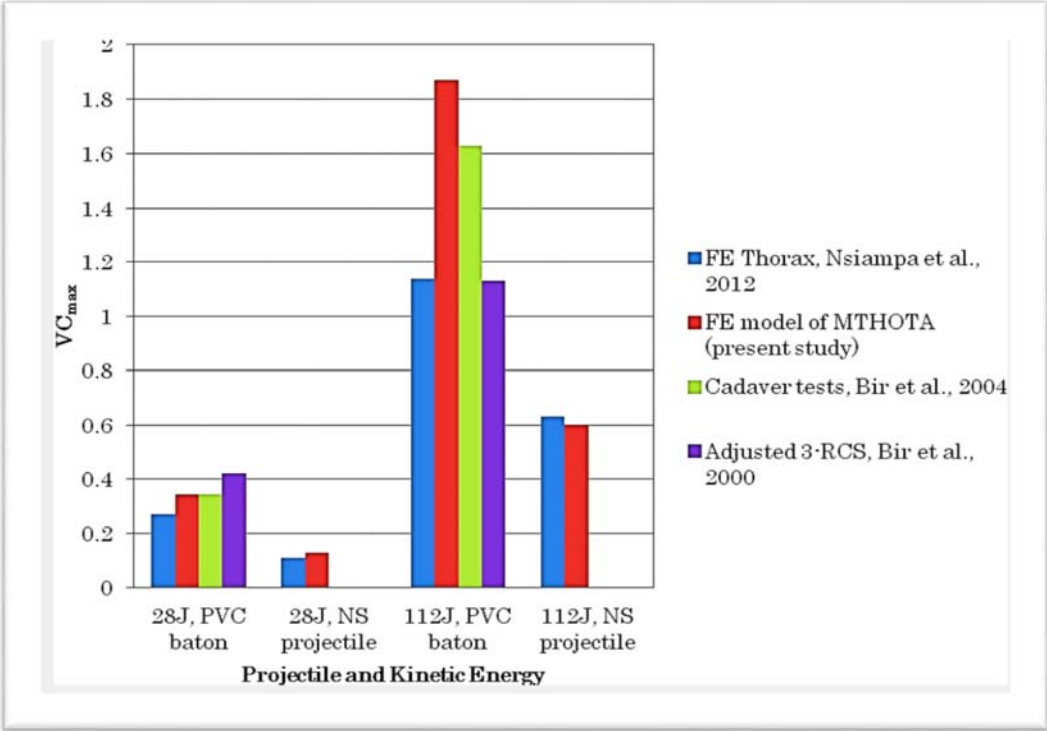

Figure 4.22: Comparison of the VC_{max} values obtained by using MTHOTA which those obtained from the cadaveric tests, adjusted 3-RCS (Bir 2000) and FE thorax model (Nsiampa et al. 2012; Widder, Perhala & Rascoe 2003; Widder, Butz & Milosh 1997)

4.5.2 Rubber ball of 60-cal, 15 mm diameter, 3.7 gram

As mentioned in the specification manual (titled ".60-CAL STINGER, 37 mm black powder, Rubber ball round," published by Defense Tech, USA in 2006), .60-cal stinger rubber ball round has been developed by modifying the designs of 28A and 28B and designs of Federal Laboratory's manufactured RB25 and RB40 rounds. DuBay and Bir 1998 have evaluated VC_{max} for the 60-cal, 15 mm diameter, 3.7 gram rubber ball by impacting it with 326 m/s and 346 m/s speeds using thorax surrogate 3-RCS. VC_{max} calculated for former and later impact cases were 0.20 and 0.09 respectively. High-speed rubber ball impact produced lesser chest displacement (consequently, lesser VC_{max}), when compared to lower speed impact with the same projectile. This discrepancy in the VC_{max} might be due to the limitations of 3-RCS (Bir & Viano 2004; Bir 2000; Dau 2012; DuBay & Bir 1998).

A dynamic transient impact analysis was carried out by impacting the MTHOTA with the 60-cal rubber ball at 326 m/s. Due to high impact speed of the projectile, MAT_057, and MAT_027 (MOONEY_RIVLIN_RUBBR material model) didn't give any useful results as the projectile got eroded within a very small time frame. Without ERODE option active, it is not possible to carry out impact simulations involving foam and thermoplastic elastomers. Therefore, PLASTIC_KINEMATIC material model was used for the projectile.

Various stages of the projectile impacting the MTHOTA are shown in the Figure 4.23.

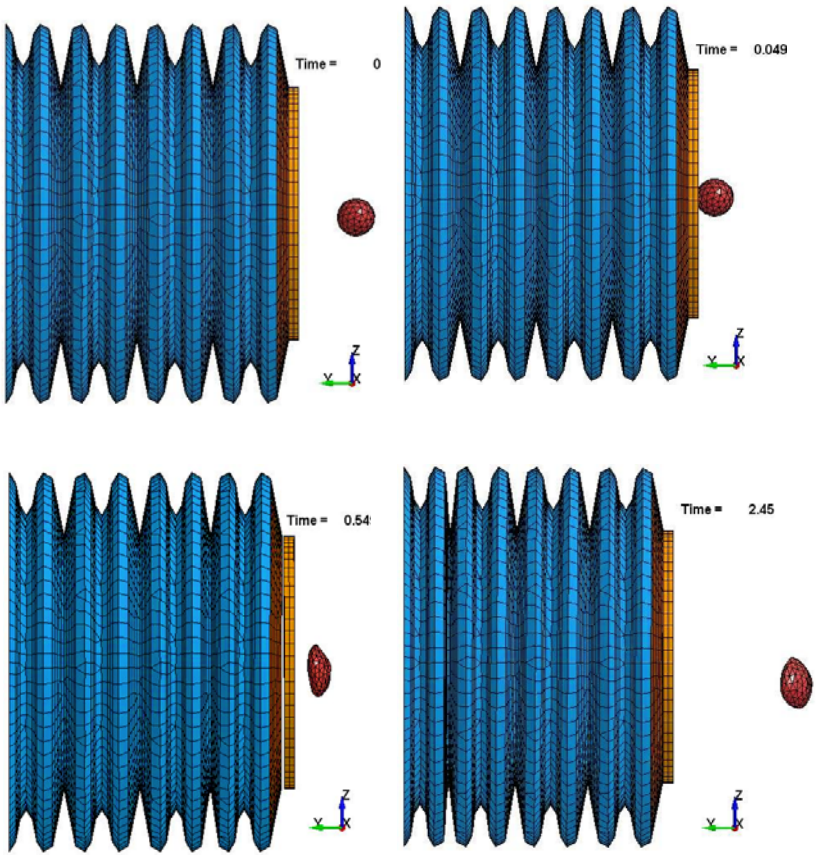

Figure 4.23: Stages of the thorax surrogate (MTHOTA) during the impact with 0.60 caliber rubber ball projectile impacting with the speed of 326 m/s

Relative displacement of the impact plate with respect to the plate-3, as a function of time, is shown in the Figure 4.24.

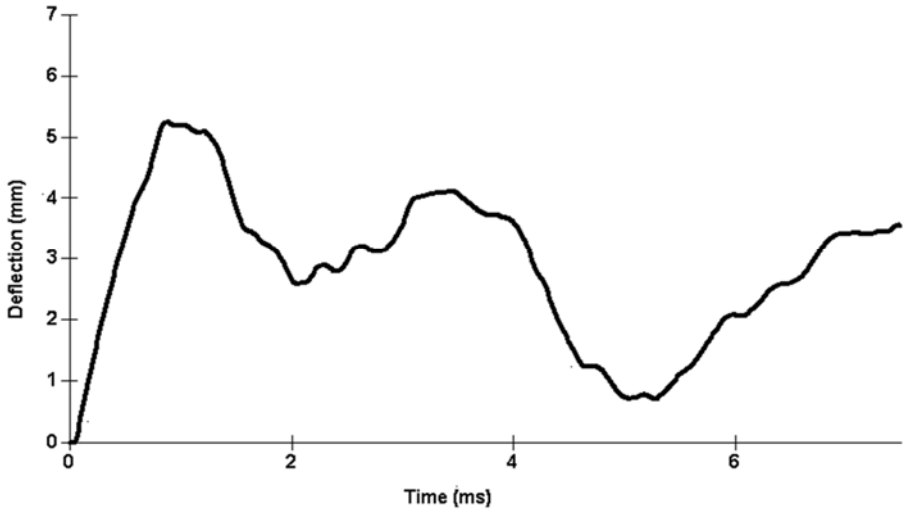

Figure 4.24: Dynamic deflection of the impact plate with respect to the plate-3 when MTHOTA subjected to the impact of rubber ball projectile (0.60 caliber with 326 m/s impact speed)

From the Figure 4.24, the maximum relative displacement of the impact plate with respect to the plate-3 was 5.25 mm at 0.849 ms impact duration. Method-2 of VC_{max} calculation described in previous sections yields 0.23, which is well correlated with the results presented in a technical report (DuBay & Bir 1998).

4.6 Conclusion

From the corroborative impact simulations carried out using MTHOTA as the surrogate, it is evident that MTHOTA emulates human thorax. Force response, deflection response, and VC_{max} values were in very good agreement with those obtained from the cadaver tests. MTHOTA is further validated for the two impact cases presented by Nsiampa using the full human thorax model. Though the FE model thorax of Nsiampa et al. (2011a, 2011b and 2012) has got some internal organs, it doesn't provide any organ-specific injuries and only provides VC_{max}. The major disadvantage with this model is the high computational time and also that VC_{max} depends on the impact point. Therefore, number of impact simulations need to be carried out so that average VC_{max} values can be used. MTHOTA facilitates the accurate calculation of the VC_{max} with only one simulation, without any ambiguity. As VC_{max} is well correlated with thoracic injuries on Abbreviated Injury Scale, MTHOTA serves the purpose of validating non-lethal ammunition, chest protectors, etc.

MTHOTA is not computationally demanding. The surrogate MTHOTA consists only of 7543 shell elements, 723 solid brick elements, 7 components (foam sheet, rigid impact plate, corrugated sheet, 4 plates) and 4 contact interfaces (including the interface between the projectile and MHTOTA's impacted surface). Therefore, the solution time is much reduced. Due to the simple model, MTHOTA also offers ease in setting up the simulation preprocessing files.

The physical surrogate (3-RCS), which is developed for the evaluation of the trauma caused by blunt ballistic impacts, requires a costly experimental setup and a cumbersome assessment process. Due to limitations of 3-RCS as mentioned in the

previous sections, a larger number of impacts would be required either to get the proper deflection response or to perform sampling or averaging to obtain the values of VC_{max}. Major disadvantage with physical surrogates is the requirement of the prototypes of the products of interest, which is another costly and cumbersome affair. MTHOTA requires only one impact simulation as there is no ambiguity in the impact point and doesn't require any prototypes.

Though the material data used in the FE model of the surrogate MTHOTA were real, due to the shape of the corrugated sheet, MTHOTA is not manufacturable. At the same time, it is not difficult to make a new manufacturable design based on the same concept.

Development and validation of MTHOTA, therefore, undoubtedly paves a way for developing application-specific, easy to use, unsophisticated surrogates (both FE and physical models), which will be very handy during the development stage of products such as non-lethal munitions, safe solid sports balls, chest protectors for sports personnel, and bullet proof vests.

CHAPTER 5: EVALUATION OF THE BLUNT THORACIC TRAUMA CAUSED BY SOLID SPORTS BALL IMPACTS

This chapter represents the full length paper titled "Evaluation of the blunt thoracic trauma caused by solid sports ball impacts" authored by Thota N, Eparaachchi J and Lau K.T, and published in the Journal of Biomechanical Science and Engineering. The details of the paper are provided in the Appendix – I of the thesis.

5.1 Introduction

Injuries are very common during sports activities such as cricket, baseball, hockey, rugby, and footy (Bell 1992; Corrigan 1984; Davids & Morgan 1988; Elliott et al. 1995; Finch, Elliott & McGrath 1999; McGrath & Finch 1996; Walker et al. 2010) . Injuries can be due to a collision between the players, a collision with the barricades along the boundary, due to solid sports ball impacts and due to movements of the athletes during the sports activity. Solid sports ball impacts can cause injuries ranging from minor sprains and bruises to chest wall injury including rib fractures. The latter, depending upon the location and number, may be further complicated by secondary phenomena like flail chest, pulmonary contusion, hemothorax, pneumothorax, rupture of the aorta, among others. Although a variety of recreational and competitive sporting activities may lead to thoracic wall injuries and its sequelae, this chapter evaluates thoracic injuries caused only by solid sports ball impact.

5.1.1 Commotio-cordis

Blunt chest impact, depending upon the location and time of the impact, can also cause commotio-cordis; the term is a translation from its original Latin "agitation of the heart", and is a fatal cardiac arrhythmia caused by functional re-entry and ventricular fibrillation (Doerer et al. 2007; Madias, ChristopherMaron, Barry J, et al. 2007; Madias, ChristopherMaron, Barry J., et al. 2007; Maron et al. 2006; Maron et al. 2009; Maron & Estes III 2010). Now increasingly recognized, in a 15 year period (1995-2010), 224 cases of commotio-cordis were reported in the USA alone. Of these, 99 cases were pertaining to the recreational sports and other circumstances (fights, friendly ball throws and falls). 125 cases were pertaining to the competitive sports, out of which nearly 50% were victims of baseball impacts (Abrunzo 1991; Classie, Distel & Borchers 2010; Link 2003; Madias, C. et al. 2007; Maron & Estes III 2010). Although young male athletes have been reported to be more susceptible to commotio-cordis owing to a relatively thin, underdeveloped and compliant chest cage with less capability to withstand potentially arrhythmogenic precordial blows, older athletes are not immune (Douglas 2011; Maron & Estes III 2010). Work from several researchers (Abrunzo 1991; Link 2003; Link & Estes Iii 2007; Link et al. 2001; Link, M. S. et al. 2003; Link et al. 1998; Link et al. 1999), has now translated into a better understanding of the aetiopathogenesis and pathophysiology of the commotio-cordis. It is now established that commotio-cordis is caused by blunt impacts on the cardiac silhouette (para-sternal area Figure 5.1(a) and (b)). The second pre-condition for commotio-cordis relates to the timing of the impact in relation to the cardiac cycle which must occur during a window in the cardiac cycle when the myocardium is particularly electrically vulnerable for inhomogeneous dispersion of repolarization triggering ventricular fibrillation. This period of the cardiac cycle is during the upslope of the T wave, just before it reaches its peak (Figure 5.1 (c)). Stated simply, such low-frequency

impacts, although innocuous in causing structural myocardial damage, lead to commotio-cordis because they happen at the wrong place and wrong time, leading to an abnormal cardiac rhythm instead of the normal period of relaxation preceding the next contraction.

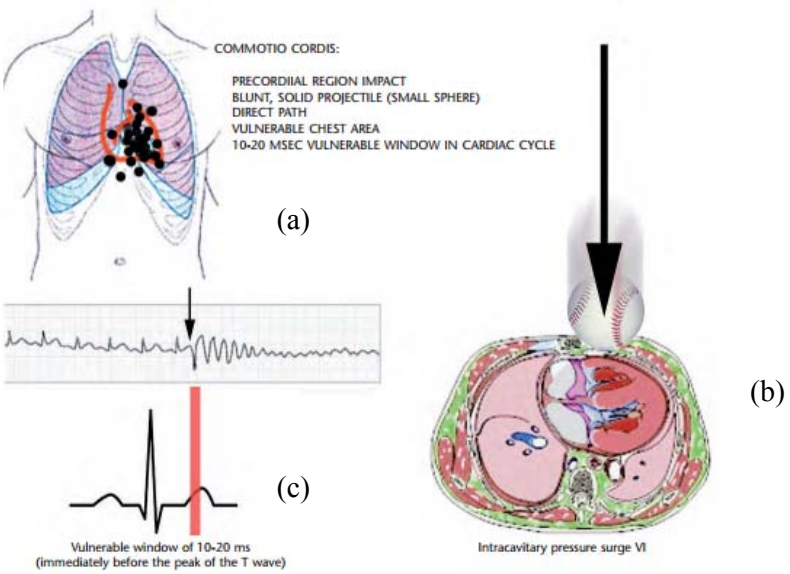

Figure 5.1: Location and time of impact for the occurrence of commotio-cordis. Adapted from (BLAS & CAUSSADE 2011) with written permission

Cardiac repolarization related various abnormalities were obtained by impacting the para-sternal area of the porcine models in different phases of the cardiac cycle and the heart rhythms obtained were as shown in the Figure 5.2 (BLAS & CAUSSADE 2011; Link 2003; Link et al. 2001).

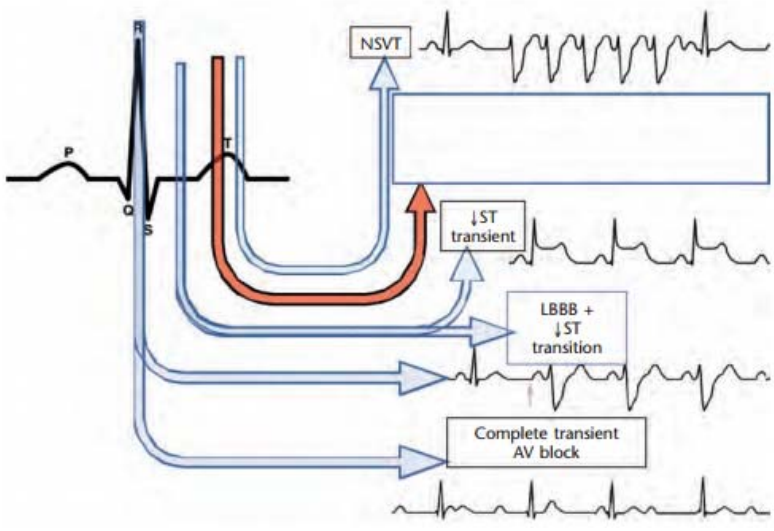

Figure 5.2: Heart rhythms obtained by impacting the porcine models with the projectile at difference phases of the cardiac cycle. Adapted from (BLAS & CAUSSADE 2011) with written permission

Pathophysiological sequence that is responsible for commotio-cordis (Link et al. 1999) is as shown in Figure 5.3.

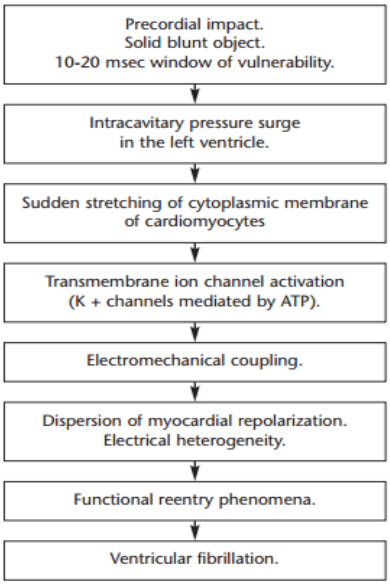

Figure 5.3: Pathophysiology of the commotio-cordis. Adapted from (BLAS & CAUSSADE 2011) with written permission

Due to its peculiarly specific nature, commotio-cordis has to be dealt with separately from the structural damage related aspects. Therefore, structural damage related thoracic injuries caused by the solid sports ball impacts were evaluated and presented. The viscous criterion, which is the product of the chest deformation velocity and chest compression, is the best predictor of structural damage to the thorax and is used throughout the chapter. Commotio-cordis related evaluations were carried out using the force-time response of the thorax surrogate and discussed in detail in the subsequent sections.

5.1.2 Historical background

So far, many researchers (Cheng 2009; Cheng, Takla & Subic 2011; James et al. 2012; Munroe & Sherwood 2012; Mustone & Sherwood 1998; Nicholls, Miller & Elliott 2005, 2006; Pang, Subic & Takla 2011) have developed an FE model of the solid sports balls (baseball, cricket ball and golf ball) with various material models and tried to fine tune the model with experimental testing such as having the ball impacting a rigid wooden block or ball impacting cantilever beam etc. With the developed FE model of a ball, researchers have studied the ball-bat interactions to a greater extent. Ignoring the layered structure of the solid sports ball and the hyperelasticity of the leather cover, experimentally developed and theoretically optimized material data (Cheng 2009; Cheng, Subic & Takla 2008; Cheng, Takla & Subic 2011; Smith 2001; Smith, Shenoy & Axtell 2000) and a viscoelastic material model were used for the FE model of all solid sports balls (baseball and cricket ball) considered for the evaluation of blunt thoracic trauma.

Very limited research has been carried out in the area of evaluation of the thoracic injuries due to solid sports ball impacts. Janda et al. 1992 have impacted the thoraces

of a child crash test dummy and a 5th percentile female Hybrid III with baseballs (both soft core and standard) and evaluated the viscous responses. They have extended the experiments to assess the effectiveness of the chest protectors (generic closed cell foam and various other materials) available on the market. Closed cell foam sheet protectors of any thickness, definitely to a certain extent, can attenuate impact force. Surprisingly, based on results obtained from the experiments, they have concluded that chest-protectors are not only ineffective in reducing the viscous response of the thorax also increased the risk of chest injury and fatal cardiac arrhythmia as they exacerbated the impact force. Thoraces of the crash test dummies used for automotive simulated crash tests are very stiff and are not suitable for obtaining the force and displacement responses due to impacts by blunt ballistic impacts. Therefore, the study conducted by (Janda et al. 1992) is neither accurate nor useful for the comparison with the results presented in this study.

Janda et al. 1992 have also experimentally investigated the relative risk of fatal cardiac injury by impacting the 3-RCS surrogate of the thorax designed for the evaluation of viscous injury due to blunt ballistic impacts with various soft-core baseballs at impact speeds of 17.9, 22.4 and 26.8 m/s. From the results obtained, they have concluded that as far as the commotio-cordis concerned, soft-core balls offer no benefit when compared with the standard baseballs. Though 3-RCS has got some limitations (for example, very less effective impact area which is only 2inch by 3 inch at the centre of the middle rib, smaller in size, not validated for cardiac loads etc.), the experiments are relevant to the study. However, the impacts considered for the study are well below the normal speeds encountered by baseball players. (Viano et al. 2000) have evaluated the effectiveness of the chest protectors by impacting the 3-RCS surrogate with and without chest protectors for a standard baseball at 17.9, 22.4, 26.8 and 31.2 m/s. By comparing the viscous injury in both cases, they have concluded that chest protectors offer no significant benefit. Due to the limitations of the 3-RCS and since there is no provision to attach the chest protector to the 3-RCS to simulate the real life situation, only the viscous injury results obtained for the unprotected 3-RCS can be used for comparative purposes. Usual pitching speeds of the baseball in the youth sports (9 – 18 years) goes beyond 95 mph (i.e., > 42.5 m/s). Therefore, in the present analysis, in order to estimate the injuries caused by baseball impacts with the realistic pitching speeds, a wider range of impact speeds (10 – 45 m/s, with an increment of the 5 m/s) was considered and results obtained are presented in the paper.

(Dau 2012) carried out experiments to study the commotio-cordis by impacting PHMS and anesthetized swine, on the cardiac silhouette with the lacrosse balls with impact speeds of 13.4 – 26.8 m/s (with increments of 4.5 m/s). From these results, a sports specific thoracic surrogate and injury risk curve (percent risk of commotio-cordis versus surrogate cardiac load) were developed. Impact speeds considered for the analysis were not realistic, and also the surrogate only exhibited bio-fidelity at lower impact speeds. From the experimental results obtained by researchers (Link 2003; Link, Mark S. et al. 2003), the highest incidences of commotio-cordis were observed for impacts with baseball at 17.9 m/s. This impact corresponds to cardiac load of 2368N. The probability of ventricular fibrillation (VF) due to commotio cordis in relation to the maximum left ventricle (LV) pressure followed a Gaussian distribution. From the injury risk curve developed (Dau 2012), cardiac load of 2368N corresponds to only 28% risk of commotio-cordis (as per the results of Dau 2012, probability of VF due to commotio cordis increased with the cardiac load). Similarly, owing to the

complex nature of the commotio-cordis, many contradictions can be found in the published literature.

The baseball kinematics, MTHOTA's displacement-time responses, MTHOTA-solid sports ball interactions, VC_{max} values and their relation with energy interactions of MTHOTA-projectile, due to direct impact (with and without ball spin) were presented in this chapter. Commotio-cordis related calculations were also presented in this chapter to highlight the importance of MTHOTA's development concept in making thoracic surrogates for any particular industrial application.

5.2 Methodology

5.2.1 Details of the impact tests

In order to evaluate the blunt thoracic injury caused by solid baseball impacts, a series of impact analyses were carried out, in a virtual testing environment, by impacting an FE model surrogate MTHOTA with the following solid sports balls.

a) A soft-core baseball of 75 mm diameter and 146 grams weight.

b) A synthetic baseball of 75 mm diameter and 146 grams weight.

c) A cricket ball of 75 mm diameter and 160 grams weight.

Realistic pitching speeds were considered as impact speeds and for every sports ball, 8 impacts speeds (10 – 45 m/s with an increment of 5 m/s) were considered. So far no researchers have examined the spin of the impacting ball. Therefore, Spin of the ball with respect to the impact direction (y-axis) and perpendicular to the impact direction (both x and z –axes) are taken into consideration (1000 – 8000 rpm with an increment of 1000 rpm, 8 cases of ball spin). In order to evaluate the effect of the spin of the ball on the structural damage of the thorax, only for one velocity case (30.7 m/s) with 8 cases of ball spin in each direction (x, y and z – axes) were carried out and results are presented in this chapter.

5.2.2 Details of the thorax surrogate

For all impact cases mentioned in the previous section, FE model of MTHOTA was used as the thoracic surrogate. Though there are two methods to evaluate VCmax using the equation (4.1) by employing MTHOTA surrogate, in this chapter only method-1 was used.

5.2.3 Finite element model of the solid sports ball

Though many leagues introduced strict regulations on the baseball bats, there are several types of baseballs as they are selected purely based on their size, weight and coefficient of restitution (COR) at 26.8 m/s (Drane & Sherwood 2004). A typical league baseball is made up of a small cork center within two rubber layers, covered with a thick wool winding layer and a stitched synthetic leather cover. Many researchers carried out finite element simulations of a baseball for a performance evaluation, using LS-DYNA software. For the FE model of the baseball, a homogeneous linear elastic sphere (Crisco et al. 2002; Crisco, Hendee & Greenwald 1997), a linear viscoelastic model (Nicholls et al. 2003; Nicholls, Miller & Elliott 2005, 2006; Smith 2001), a hyperelastic model (Mustone & Sherwood 1998), viscoelastic and hyperelastic models (Munroe & Sherwood 2012) have been used.

From the published work (Smith 2001), the performance related parameters of the baseball obtained from the numerical simulations were very well correlated with those from the experiments. Therefore, a linear viscoelastic model, which is a simplest approximation to represent the time-dependent, non-Hookean deformation, was considered for the baseball modeling.

The material data and material model (MAT_006, MAT_VISCOELASTIC of LS-DYNA non-linear finite element software) are given in Table 5.1.

Table 5.1: Material data and material model for baseballs (soft core & synthetic) used in the present study

S.No.	**Parameter**	**Description**	**Soft-core baseball**	**Synthetic baseball**
1	Material model	Linear Viscoelastic	MAT_006 (LS-DYNA)	
2	Shear relaxation behavior of the baseball material is described by:	$G(t) = G_\infty + (G_0 - G_\infty) e^{-\beta t}$	From the published research (Hallquist 2007b; Herrmann & Peterson 1968; Nicholls et al. 2003; Nicholls, Miller & Elliott 2006; Smith 2001)	
3	RO in kg/mm^3	Mass density	6.325×10^{-7}	
4	BULK in GPa	Elastic bulk modulus	0.069	0.019
5	G_0 in GPa	Short-time shear modulus	0.041	0.002
6	G_∞ in GPa	Long-time shear modulus	0.011	0.001
7	β in Hz or s^{-1}	Decay constant	9000	1250
8	Weight of the baseball in grams		140 (both soft-core and synthetic)	

Some convergence studies related to the baseball and other solid sports balls are available in the literature. As the impact cases are not relevant, convergence studies were performed to finalize the FE model of the baseball used in the present study. The baseball FE model details are given in Table 5.2, and the ball FE models (cross section, and full) are shown in the Figure 5.4.

Table 5.2: Details of the FE model of the solid sports ball

FE entity	comments
Nodes	17589
Elements	Hex8 brick elements – 16360; Penta6 (wedge elements) – 200;
Element size	Smallest 3 mm , longest side 5 mm
Element formulations	ELFORM = 1 and AET = 2 were used
Ball-MTHOTA interface	CONTACT_SURFACE_TO_SURFACE

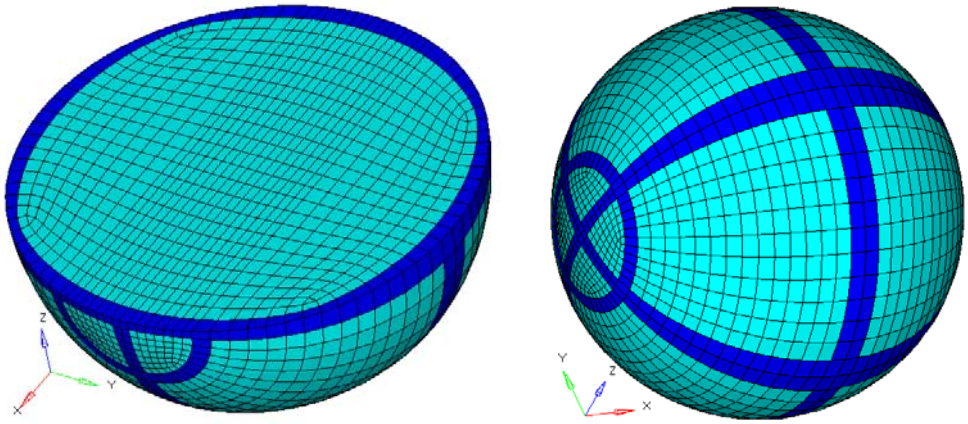

Figure 5.4: Finite element model of the solid sports ball used in the simulations

As the ball used in the cricket game is almost of the same size as a baseball, the FE model shown in Figure 5.4 was used for all simulations related to cricket ball impacts. MOONEY_RIVLIN_RUBBER material model (MAT_027 of LS-DYNA software) was used for the cricket ball and material properties were taken from the published literature (Cheng 2009; Cheng, Subic & Takla 2008; Cheng, Takla & Subic 2011). Material data used for a cricket ball FE model and details of the MOONEY_RIVLIN_RUBER material model are given in Table 5.3.

Table 5.3: MOONEY_RIVLIN_RUBBER material data

Material parameter	**Details**	**Comments**
Strain energy density function	$W = A(I - 3) + B(II - 3) + C(III^{-2} - 1) + D(III - 1)^2$ I, II and III are invariants of right Cauchy-Green Tensor $C = 0.5\ A + B$ $D = [A(5\mu - 2) + B(11\mu - 5)] / (2 - 4\mu)$	From the published literature (Cheng, Takla & Subic 2011; Hallquist 2007b; Tanaka et al. 2006)
Shear modulus of linear elasticity	$2\ (A + B)$	
μ (Poisson's ratio)	Value between 0.49 and 0.5 recommended	
ρ (mass density)	7.8×10^{-7} kg/mm^3	
A	0.00402	
B	-4.1×10^{-4}	
Weight of the ball	165 gram	

It is important to note that synthetic baseball and cricket ball simulations were carried out exclusively to show the influence of the material and weight of the solid sports ball on the blunt thoracic trauma.

5.3 Results and discussion

5.3.1 Viscous injury due to solid sports ball impacts and its calculation

In order to evaluate dynamic force response as a function of impact time, dynamic deflection response as a function of impact time, and thoracic injury due to the baseball impact in terms of VC_{max}, MTHOTA's foam sheet was impacted with the soft-core baseball at speeds of 10 – 45 m/s, with an increment of 5 m/s. Various stages of the MTHOTA during baseball impact (for 30 m/s impact speed) are shown in Figure 5.5. By post-processing the simulation results, the deflection-time response of the MTHOTA for all impact cases was elicited and shown in Figure 5.6.

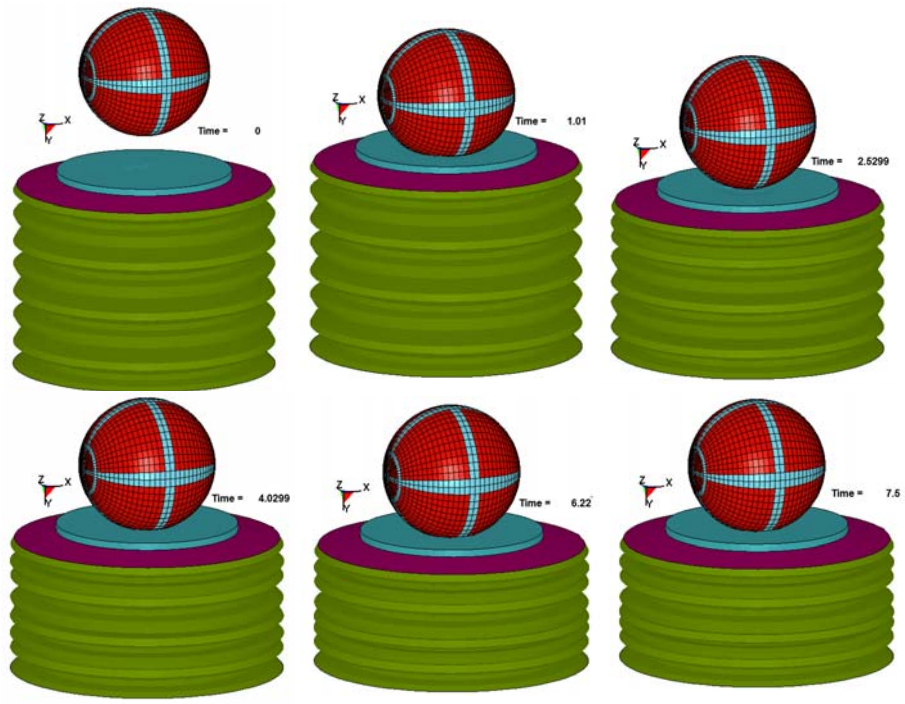

Figure 5.5: Stages of the MTHOTA when subjected to the soft core baseball impact with 30 m/s speed

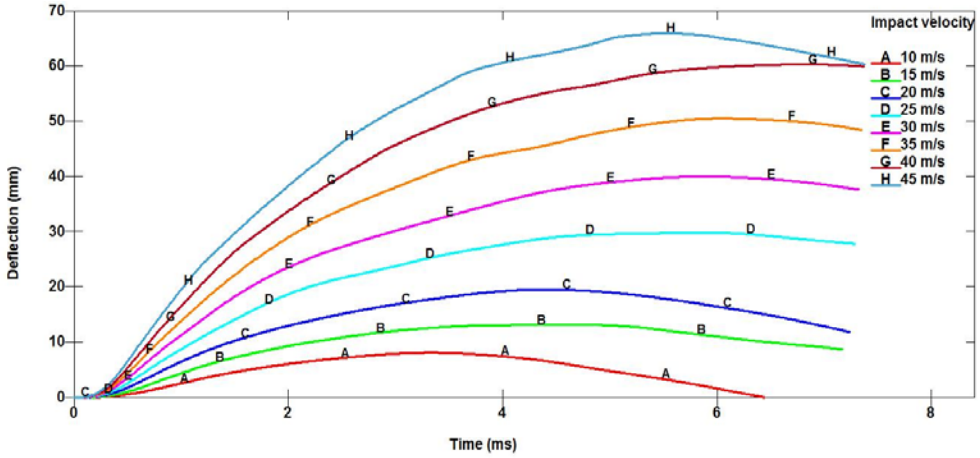

Figure 5.6: Deflection – time response of the MTHOTA when subjected to impacts of soft core baseball (dynamic deflection with respect to the time measured using the nodal time histories of the impact plate

Similarly, deflection-time responses of the MTHOTA surrogate were obtained by impacting it with the synthetic baseball and cricket ball with the 8 impact speeds considered for the present study. VC_{max} values were calculated for all impact cases (3 sports balls and 8 impact speeds for each ball) by substituting the maximum deflection

of the impact plate and the time at which deflection is highest, in the Equation 4.1 and were as shown the Figure 5.7.

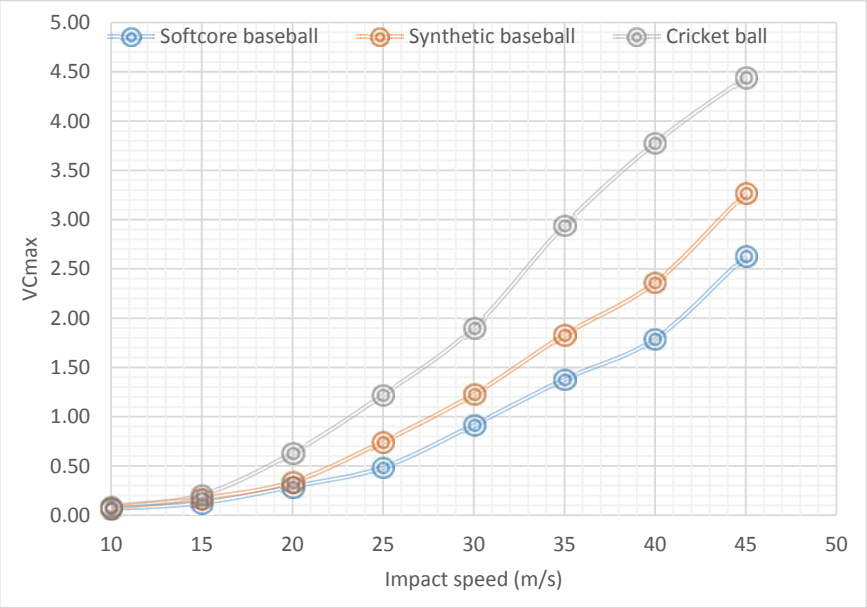

Figure 5.7: Influence of the material, weight and the impact speed of the solid sports ball on the VC_{max}

Soft-core baseball, synthetic baseball and cricket ball impacting at 30.7 m/s, 27.9 m/s and 23.2 m/s respectively, have caused injuries equivalent to VC_{max} = 1 m/s (i.e., 25% percent probability for AIS3+ injuries). This clearly shows that material and weight of the solid sports balls have got significant effect on the thoracic injuries. Though soft-core baseball has better injury performance when compared to the other two balls considered, the injuries caused are fatal at usual pitching speeds.

Only soft-core baseball impacts were envisaged for the study of kinematics, energy interactions and influence of the rate of change in maximum kinetic energy, rate of change in maximum total energy and ball spin on the VC_{max}.

5.3.2 Energy interactions of the solid sports ball and the MTHOTA surrogate

For the study of energy interactions (during the impact) between the MTHOTA with the solid sports ball, only soft-core baseball was considered. These interactions for the impact speed of 30 m/s were as shown in Figure 5.8.

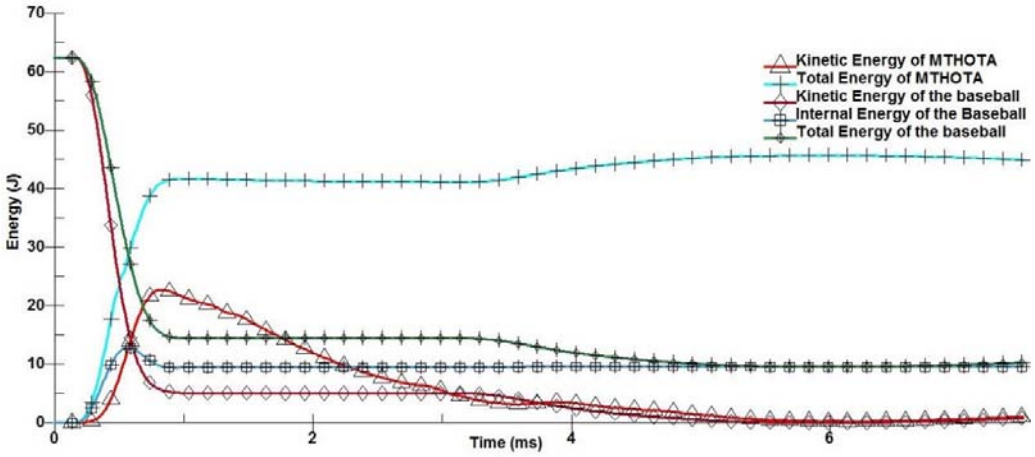

Figure 5.8: Energy interactions of the soft core baseball and the MTHOTA surrogate (Impact speed 30 m/s)

During the impact of MTHOTA with the baseball, let us say,

$KE_{ini.baseball}$ = Initial kinetic energy of the baseball

$KE_{t.baseball}$ = Kinetic energy of a baseball at given instance "t"

$IE_{t.baseball}$ = Internal energy of a baseball at given instance "t"

$TE_{t.baseball}$ = Total energy of a baseball at given instance "t"

$KE_{t.MTHOTA}$ = Kinetic energy of the surrogate at given instance "t"

$IE_{t.MTHOTA}$ = Internal energy of the surrogate at given instance "t"

$TE_{t.MTHOTA}$ = Total energy of the surrogate at given instance "t"

From the law of conservation of energy,

$$KE_{ini.baseball} - TE_{t.baseball} = TE_{t.MTHOTA} \quad (5.1)$$

$$TE_{t.MTHOTA} = KE_{t.MTHOTA} + IE_{t.MTHOTA} \quad (5.2)$$

Using Equations 5.1 and 5.2 & the Figure 5.8, energy transactions between MTHOTA and the baseball (blunt projectile) can be evaluated for any instance of the impact duration. From the analytical studies performed on Lobdell lumped mass model of the thorax, it was clear that VC_{max} is significantly influenced by rate of the maximum kinetic energy of the thorax and rate of the deformation of the thorax (Wang 1989). Therefore, from the output, Maximum of total Energy (TE_{max}), maximum of kinetic energy of MTHOTA (KE_{max}) were evaluated from the output. VC_{max} values (from the Equation 4.1 and Figure 5.6) were plotted against the rate of change in TE_{max} and rate of change in KE_{max}. The plots were as shown in the Figures 5.9 and 5.10 respectively.

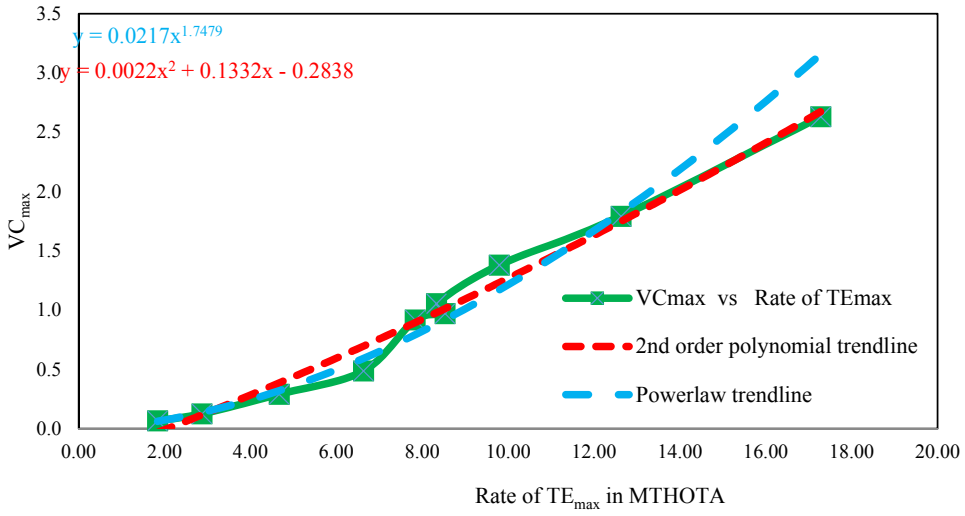

Figure 5.9: Influence of the rate of maximum total energy of MTHOTA on the VCmax

A linear curve gave a good correlation for the VCmax vs. Rate of maximum total energy of the MTHOTA, and the trend line is provided below.

$$VC_{max} = 0.0022(TE_{max}/t)^2 + 0.1332(TE_{max}/t) - 0.2838 \quad (5.3)$$

Where,

TE_{max} = Maximum total energy of the MTHOTA (in J)

t = Impact duration at which total energy is maximum (in ms)

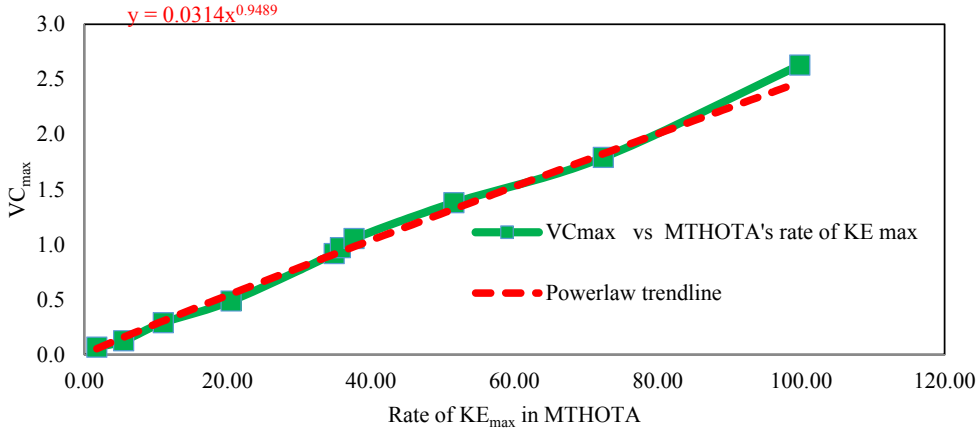

Figure 5.10: Influence of the rate of maximum kinetic energy of MTHOTA on the VCmax

The relation obtained by power-law curve fitting is given below.

$$VC_{max} = 0.0314\ (KE_{max}/t)^{0.9489} \quad (5.4)$$

Where,

VC_{max} = viscous criterion (in m/s)

KE_{max} = Maximum kinetic energy of the MTHOTA surrogate (in J)

t = impact duration at which kinetic energy is maximum (in ms)

The Equation 5.4, due to the good match between the trend line and the plot showing the variation of the VC_{max} with the rate of change in KE_{max}, it can be used for evaluating VC_{max} for other impact cases

5.3.3 Influence of the deformation velocity of the MTHOTA on the injury

VC_{max} values calculated were plotted against the maximum deformation velocity obtained from the output of the impact simulations (Figure 5.11).

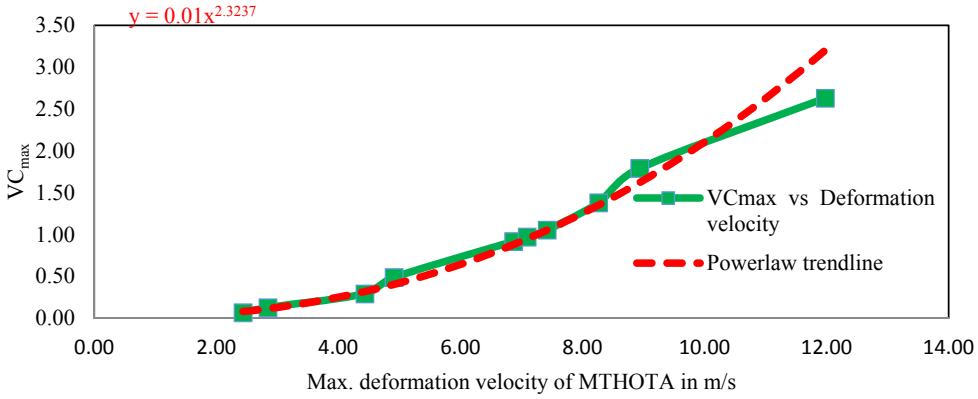

Figure 5.11: Influence of the deformation velocity of MTHOTA on the VCmax

From the plot of VC_{max} versus maximum deformation velocity of MTHOTA, power-law curve fitting yielded the following relation.

$$VC_{max} = 0.01\ (Y_{max}/t)^{2.3237} \quad (5.5)$$

Where,

Y_{max} = Maximum deformation of the impact plate of the MTHOTA, in mm

t = Impact duration at which the deformation is maximum, in ms

5.3.4 Effect of the impact velocity on the thoracic injury

VC_{max} values obtained for the soft-core baseball impacts were plotted against the impact speed and shown in the Figure 5.12.

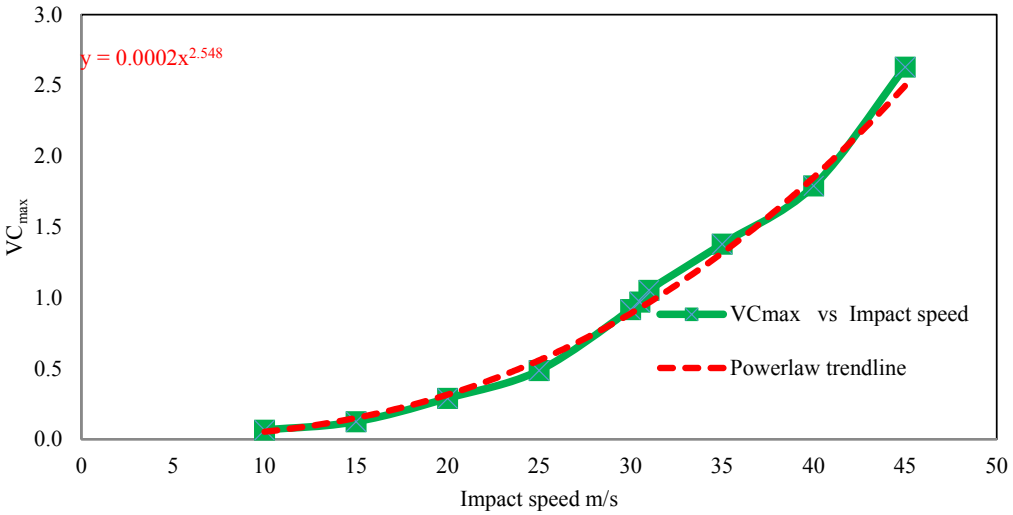

Figure 5.12: Influence of the impact speed of the soft core baseball on the VCmax

The relation between baseball impact speed and the thoracic injury (VC_{max}) is given below.

$$VC_{max} = 0.0002\ (v)^{2.548} \qquad (5.6)$$

Where,

v = baseball impact speed in m/s

As the injury is greatly influenced with the projectile diameter and material, the Equation 5.6 can be used only for the baseball considered in the analysis, for extrapolation or interpolation of the VC_{max} for various impact speeds.

5.3.5 Effect of the ball spin on the thoracic injury

Effect of ball spin on the thoracic injury is unknown as no one has conducted experiments or analytical study. In the case of baseball, during the game, depending upon the ball-bat interaction, baseball spins ranging from 1000 – 8000 rpm. Therefore, to elucidate the effect of the baseball spin on the blunt trauma, a series of simulations were carried out for the following impact conditions.

Baseball impact speed = 30.5 mm/ms and

Baseball spin about X, Y and Z axes = 1000 -8000 rpm, with an increment of 1000 rpm.

In all, 24 simulation runs were carried out to evaluate the effect of the baseball spin on the injury (blunt thoracic trauma). From each output, rate of change in KE_{max} and TE_{max} were evaluated (Table 5.4). Maximum deflection of the impact plate could not be

calculated due to the eccentric collapse of the corrugated structure. Various stages of the MTHOTA during the impact with a baseball (30.7 m/s impact speed and 8000 rpm anti-clockwise spin about Z-axis) were as shown in the Figure 5.13.

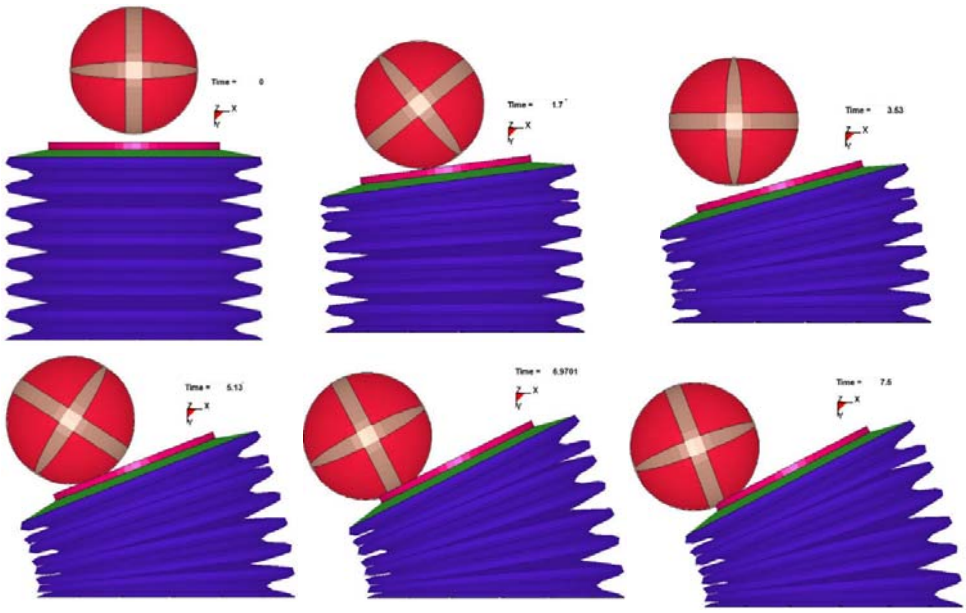

Figure 5.13: Stages of the MTHOTA surrogate when impacted with a soft core baseball with 30.7 impact speed and 8000 rpm spin about the Z-axis, anti-clockwise direction

Table 5.4: Rate of change in Kinetic Energy and the Total Energy of the surrogate

Anticlockwise spin		**Kinetic energy**	**MTHOTA surrogate**					
Baseball			Spin about X-axis		Spin about Y-axis		Spin about Z-axis	
Impact speed in mm/ms	Spin in rpm	Total initial energy (J)	Rate of KEmax (J/ms)	Rate of TE_{max} (J/ms)	Rate of KEmax (J/ms)	Rate of TE_{max} (J/ms)	Rate of KEmax (J/ms)	Rate of TE_{max} (J/ms)
30.7	1000	64.94	35.80	7.80	35.80	8.20	36.38	7.62
30.7	2000	66.24	36.11	7.73	35.80	8.15	36.41	8.70
30.7	3000	68.37	36.15	7.78	35.55	8.14	36.88	7.77
30.7	4000	71.36	36.94	7.74	35.21	8.10	37.03	7.73
30.7	5000	75.21	37.33	7.64	35.49	8.12	37.46	7.67
30.7	6000	80	37.99	7.66	35.53	8.10	37.61	7.59
30.7	7000	85.55	38.40	8.07	35.37	8.08	37.78	7.92
30.7	8000	92.08	38.81	9.11	35.34	7.98	38.50	8.36

Due to the eccentric collapse of the MTHOTA for the baseball spin about X and Z axes, it is not possible for evaluating the unique maximum deflection of the impact plate. For the case of baseball spin about Y-axis, the collapse was normal without any

imbalance. Equations 5.3 and 5.4 can be used to evaluate the VCmax based on the MTHOTA's rate of maximum TE and rate of maximum KE. Due to projectile non-specificity of the Equation 5.4, it was considered for the evaluation of the VC_{max} for all 24 cases of baseball spins, using the rate of maximum KE of MTHOTA obtained from the simulation outcome and tabulated (Table 5.5). For comparison purposes, VC_{max} values calculated by using the rate of maximum deflection of the impact plate (for only the baseball spinning about Y-axis) were given in the same Table 5.5.

Table 5.5: Effect of the baseball spin on the VC_{max}

	Anti-clock wise	**VC_{max} = $0.0314(KE_{max})^{0.9489}$ Equation (5.4)**			**For Y-spin, $VC_{max} = S.(Y_{max}/D).(dY_{max}/dt)$ Equation (4.1)**		
Ball impact speed in m/s	**Ball spin in rpm**	**X-spin**	**Y-Spin**	**Z-spin**	**Max. deflection**	**Time at Maximum deflection**	**VC_{max} m/s**
30.7	1000	0.94	0.94	0.95	41.06	5.85	0.96
30.7	2000	0.95	0.94	0.96	41.20	5.90	0.96
30.7	3000	0.95	0.93	0.97	41.21	5.90	0.96
30.7	4000	0.97	0.93	0.97	41.20	5.90	0.96
30.7	5000	0.98	0.93	0.98	41.12	5.86	0.96
30.7	6000	0.99	0.93	0.99	41.12	5.86	0.96
30.7	7000	1.00	0.93	0.99	41.12	5.86	0.96
30.7	8000	1.01	0.93	1.01	41.14	5.88	0.96

From the Table. 5, it is clear that the spin of the baseball has got no significant effect on the injury. In the case of X and Z spins the VC_{max} values 0.98±0.03 and for the Y-spin it is 0.93 which is approximately 3% less than the value calculated using Equation 4.1. For the cases of Y-spin, the VC_{max} values calculated based on the Equation 4.1 are exactly as same as the baseball without spin. From these calculations, it is evident that the Equation 5.4 (due to projectile non-specificity) is applicable to all impact cases of the baseball considered and apparently spin of the baseball about the axis parallel to the impact direction has got no influence on the blunt thoracic trauma.

5.3.6 Kinematics of the impacting ball and evaluation of the risk of commotio-cordis

Ball kinematics are very important in the evaluation of the impact force. The product of the mass of the ball and deceleration of the center node of the ball during any instance gives the impact force at that particular instant. Force – time response of MTHOTA subjected to soft-core baseball impacts is shown in the Figure 5.14.

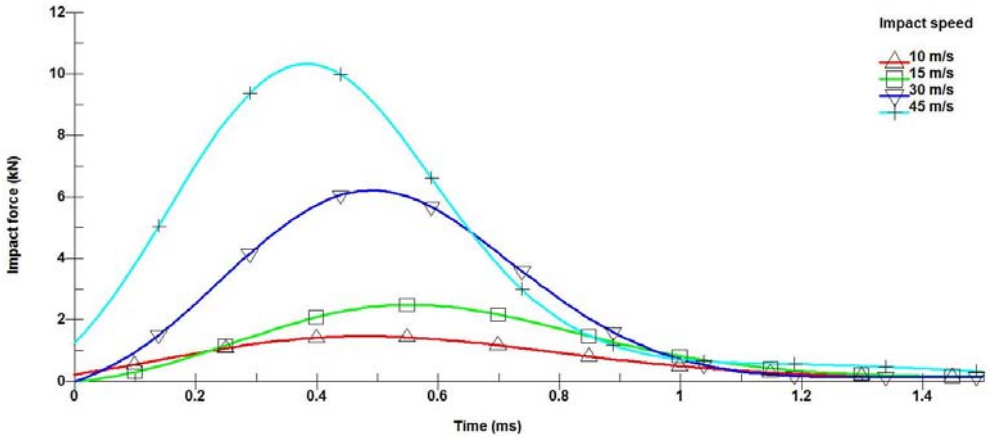

Figure 5.14: Dynamic force response of the MTHOTA when subjected to the soft core baseball impacts

Using the correlations "Internal cardiac load = 0.8 × External load on the sternum" and percent risk of commotio-cordis with the internal cardiac load (Figure 5.15), the percent risk of commotio-cordis due to baseball impacts can be evaluated and is presented in the Table 5.6.

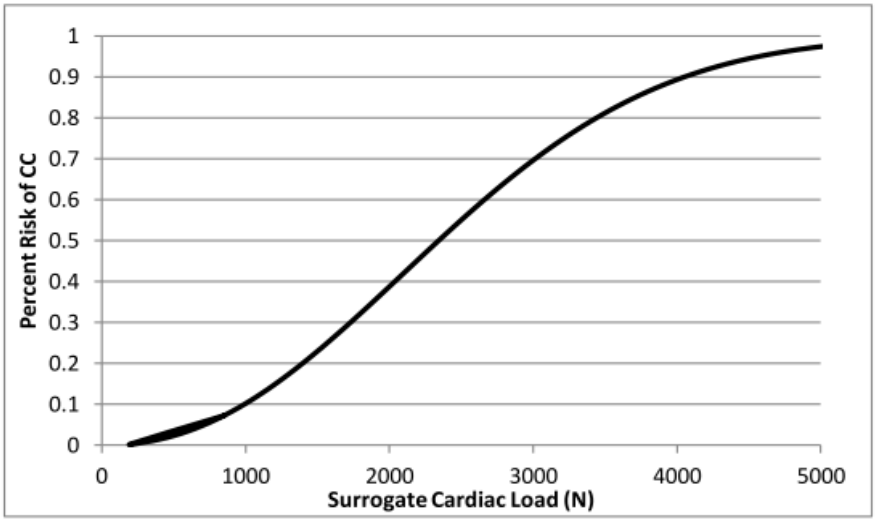

Figure 5.15: Correlation of commotio-cordis with the cardiac load (Dau 2012)

Table 5.6: Percent risk of the commotio cordis due to baseball impacts evaluated from MTHOTA force-time response

Baseball impact speed (m/s)	Average impact force (N)	Cardiac load (N)	Percent risk of commotio-cordis
10	490	392	< 2
15	1035	828	<8
30	3040	2432	Approximately 50
45	5129	4100	90

45 m/s baseball impacts in the para-sternal area might cause serious structural damage (such as heart contusion or heart wall rupture, ruptured aorta, flail chest, and punctured lungs, etc.) to the thorax. Such serious injuries can be fatal. At the same time, it is important to note that the death is not due to commotio-cordis. From the autopsy reports of commotio-cordis victims (Maron et al. 2006), it was clear that only mild impacts which were not enough to cause any structural damage to the thoracic wall and internal organs resulted in the sudden death due to commotio-cordis. From the most notable experimental study using the porcine model, probability of the commotio-cordis with the pressure in the left ventricle yielded Gaussian distribution as shown in the Figure 5.16. Therefore, though MTHOTA surrogate can provide the force-time response, it is not advisable to use the correlations mentioned above, due to the complex nature of commotio-cordis.

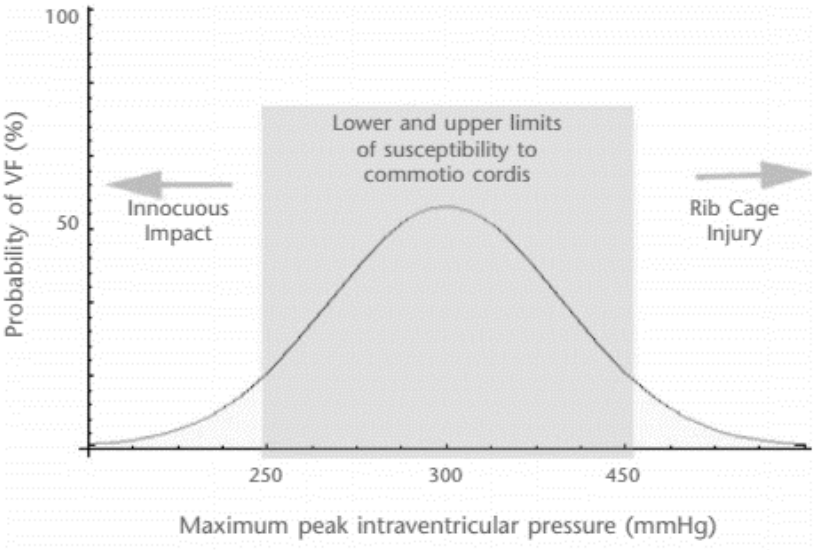

Figure 5.16: Correlation of probability of commotio-cordis with the maximum peak LV pressure follows Gaussian distribution. Courtesy of Blas & Caussade (2011)

5.4. Conclusion

The following conclusions were drawn from the outcome of the impact experiments carried out in virtual testing environment, in which thorax surrogate MTHOTA was impacted with baseballs (both soft-core and synthetic) and the cricket ball.

- Direct baseball impacts with > 30.7 m/s speed can cause structural damage to the thorax as the VC_{max} is 1 m/s (approximately) for the impact speed 30.7 m/s. In the

case of young athletes, the injury may be more as the MTHOTA or any surrogate (for instance, 3-RCS) used by other researchers were not validated for the underdeveloped thorax. Synthetic baseball and cricket ball impacts can cause more damage when compared to the soft-core baseball. Therefore, it is important to provide the appropriate training to the athletes (especially young) not to use their chest against the pitched or batted solid sports balls of any kind. It is also important to develop effective chest protectors so that fatal thoracic injuries during the sports are completely mitigated.

- Material of the solid sports ball has got great influence on the severity of the thoracic injuries. At any given speed, both balls possess the same amount of kinetic energy as they are equal in weight. Effect of size is also same as they are equal in shape and size. At 30.7 m/s impact speed, measured VC_{max} is 1 m/s and 1.27 m/s for soft-core baseball and synthetic baseball respectively. Means, probability for AIS3+ thoracic injuries with the synthetic baseball has become doubled. At the same time, it is important to note that at usual pitching speeds, soft-core baseballs are not offering any safety to the players.
- Though the size of a cricket ball is almost same as a baseball, weight is approximately 20 grams more. From the results, it is evident that the weight of the ball has got great influence on the blunt thoracic trauma.
- $VC_{max} \propto (v)^{2.548}$ trend line is very well fitted with the curve. Therefore, it can be used for evaluating blunt thoracic trauma caused by the baseball impacting with other speeds.
- $VC_{max} = 0.0314\ (KE_{max}/t)^{0.9489}$ is very handy as it provided the VC_{max} values with only ≤ 3 % error. Therefore, it can be used for evaluation of the blunt thoracic trauma caused by impacts with spinning baseball.
- Spin of the baseball about the impact direction has got no influence on the injury.
- Spin of the baseball about axes perpendicular to the impact direction has got very little influence (only ± 4 %) on the VC_{max}. From the collapse of the corrugated sheet of MTHOTA upon the impact of a spinning ball, it is clear that depending upon the spin direction, it may reduce or increase the load on the cardiac region. Therefore, spin of the ball can have an influence on the heart related injuries.
- Though MTHOTA facilitates accurate evaluation of the force-time responses, due to the complexity of the commotio-cordis, it is not advisable to evaluate commotio-cordis related parameters using the correlations found in the literature.

Measurements of the blunt thoracic trauma (viscous injury or VC_{max} values) caused by solid sports ball impacts using the FE model surrogate MTHOTA, are fairly accurate and results are well correlated with the published results in which 3-RCS was used as the thoracic surrogate. In the present study, viscous injuries are evaluated by taking the wide range of ball impact speeds (i.e., 10 – 45 m/s with an increment of 5 m/s) into consideration. MTHOTA being an FE model surrogate offers many advantages such as a fast solution, ease in setting up the simulation run, no ambiguity in impact location, etc. In case of solid ball sports, like any other activity, primary objective is to avoid injuries, for which a tool to estimate the injury is very important. With the current shape, size and working principle of the MTHOTA surrogate, it can also be used for evaluation of the attenuating effect of a cushioning material on the blunt trauma caused

by the ballistic impacts of all kinds. The authors would further work on the development of MTHOTA to study ball-thorax interactions more effectively so that it can be used for the development and validation of chest protectors.

CHAPTER 6: DEVELOPMENT AND VALIDATION OF A NON-LETHAL PROJECTILE USING MTHOTA FE MODEL SURROGATE – A CASE STUDY

This chapter summarizes the process of developing a cheaper alternative non-lethal ammunition for the M79 grenade launchers and also presents the outcome of a scholastic study to improve the performance of the foam nosed projectiles (i.e., reducing the probability for serious injuries). It also deals with the study of a viscous criterion relation with the projectile-thorax interactions. This chapter also makes an emphasis on the quasi-static compression tests of the poly-olefinic elastomers (closed cell foams) and their calibration methodology for developing the material database for non-linear FE analysis, evaluation of blunt thoracic trauma of foam nosed projectiles using MTHOTA surrogate and effectiveness of the foam nosed projectiles when embedded with energy absorbing mechanisms by summarizing three conference papers, of which two papers were published in the proceedings of WCFMAAE-2013 and the other published in the proceedings of the ACAM8. Full details of the papers are given in the Appendix – 1 of the thesis.

6.1 Introduction

Of the latest non-lethal impact munitions, projectiles made up of hard PVC body that fitted with a poly-olefinic foam nose and projectiles with the breakable tips, perform better with a low probability of permanent injury. One of effective kinetic energy non-lethal impact munitions (KENLW) is XM 1006 (eXact iMpact 1006) which was designed and developed by Army Research Laboratory of USA. Penn Arms GL-1 gun was used for testing the XM 1006. The M79 grenade launcher has been used for firing 3 types of non-lethal munitions, one of which is XM 1006.

Though there are no definitive test specifications for the validation of such munitions, Def-Tec (USA) validated these sponge rounds using 3-RCS thorax surrogate and NIJ body armour tests, such as ballistic clay signature tests (Lyon 1997).

3-RCS facilitates the evaluation of blunt thoracic trauma due to blunt ballistic impacts, in terms of VC_{max}. Values of VC_{max} between 0.0 and 1.0 indicates low probability and 25% probability for serious thoracic trauma respectively. Further increase in VC_{max} value indicates a greater risk of serious thoracic injuries.

As per weapon manufacturers test protocols and NIJ standard 0101.04 (published by National Institute of Justice, USA), in case of the body armor back face ballistic clay test, cavity depth less than 44 mm indicates the low probability for severe thoracic trauma (Bass et al. 2006). Similarly, in case of ballistic gelatine impact tests, penetration depth less than 3 inches indicates the low probability for serious thoracic injury. In reality, such tests which were not properly correlated and using them for the validation of body armours stirred much controversy and in some occasions many body armours were recalled (Erwin 2009, an article published by National Defense magazine).

Non-lethal munitions, though made up of foam and PVC, are very expensive (cost of each round of XM 1006 is approximately 70 USD, and the cost of TASER-XREP round is more than 130 USD). Therefore, a scholastic study was carried out to produce cheaper alternatives to XM 1006 which can be fired using the same M79 grenade launcher. The scholastic study furthered to find out the effect of energy absorbing

mechanisms on the blunt thoracic trauma caused by such sponge nosed projectiles. The scholastic study carried out was, in fact, the original motivation to review ATDs and develop a novel thorax surrogate FE model, etc. which as presented in the chapters 2, 3 and 4.

Though the main focus of the research study has been the development of a thorax surrogate for the evaluation of blunt thoracic trauma, the study was extended to develop an alternative to XM 1006 foam grenade. The projectile, once developed, to be considered as an alternative to XM 1006, impact should cause blunt trauma equivalent to that of XM 1006 at specific speeds, and also possess equal or lesser head trauma when it hit unintentionally hit the head of the human subject due to the effect of ballistic dispersion. Therefore, head damage characteristics were also assessed using the 'force wall method' (Jacquet 2010; Oukura 2013) for the new projectile without any additional 'energy absorbing (EA)' mechanisms. The results (force-time responses) obtained from the analysis were compared with those obtained for XM1006 and other recent foam nosed projectiles. Complete results and comparative studies are presented in this chapter.

6.2 Requirements for the scholastic study

The projectile of interest XM 1006, in the laboratory tests using 3-RCS, has produced a VC_{max} of 0.21 at an impact velocity of 91.5 m/s. It has produced depth of 36.4 mm with back face ballistic clay signature tests at an impact velocity of 99 m/s and caused 63.5 mm penetration in the ballistic gelatine block at 100 m/s impact velocity.

Though the design (only dimensions) of the XM1006 is available in the technical documents published by Def-Tec, without knowledge of the materials used in the construction of the XM 1006, the development of an XM 1006 equivalent foam grenade becomes an arduous task. As a preparation of the prototypes, procuring grenade launchers and conducting physical tryouts were beyond the scope of the study, non-linear FE analysis was used for the scholastic study that necessitated the following:

1) Quasi-static compression tests of a number of closed cell, thermoplastic elastomers (foams) to develop the material database for the non-linear impact simulations using LS-DYNA.
2) An FE model thorax surrogate for the evaluation of the blunt trauma.
3) Carry out impact simulations with PVC base and nose with various foams to select the candidate foam.
4) Develop concepts of energy absorbing mechanisms and perform factorial study to accentuate the effect on the blunt thoracic trauma.
5) Assess the head trauma caused by the impacts of the developed projectile (with and without EA mechanism) to prove that the development projectile would match the benchmark projectile (XM 1006).

All of these activities were carried out (only the first foremost step was experimental, all of the latter activities were carried out in virtual testing environment using LS-DYNA) and outcome of the study is presented in this chapter.

6.3 Methodology

6.3.1 Quasi-static compression tests for the foam material data preparation

Material data requirements dependent on the material model suitable for FE modeling of the impact problem. The foam material model available in LS-DYNA software (MAT_057 and MAT_083) assume that the poison ratio as zero, because of which coupling between the material's axes does not exist. Therefore, a simple uniaxial compression test is sufficient for obtaining the required load curves. Due to its simplicity and suitability MAT_57 (MAT_LOW_DENSITY_FOAM) material model was selected, though MAT_53 and MAT_83 models available. MAT_053 material model used in FE analysis of impact limiters used in automotive applications. The MAT_83 material model of LS-DYNA is incorporated with rate effects and therefore requires more than one load curve. For this model, density will also be interpolated using the load curves, depending upon the strain rate in the simulation (LS-DYNA Theory manual V970). Therefore, for simplicity MAT_057 material model was used for modelling the TPE foam nose of the projectile.

The load curve obtained from the foam compression test varies with the size, shape of the test specimen and also varied with the strain rate (Todd et al. 1998). To suit the foam nose of the projectile shape and size, test specimen of 50 mm long, cylindrical in shape with 40 mm diameter were prepared by milling the frozen foam blocks. Uniaxial compression test was conducted as per ASTM–D3574 test specifications. Due to limitations of the machine used for testing and also size of the foam specimen, a square plate of side 300 mm and thickness 20 mm was joined to the original mounting plate of the machine. A 10 mm thick square plate with a side of 50 mm was used as an indenter as heavy plate can cause large initial deformations. The indenter size was also more than the specimen size as suggested by Chung, 1987. Procedural steps given below followed for testing of foam specimens.

1) Pre-flex the foam specimen by compressing it two times to 80% of its original thickness at indenter speed of 0.42 mm/s.
2) Allow the specimen to rest for 7 min prior to the commencement of the test. This rest is to avoid possible viscoelastic effects.
3) Compress the foam specimen to 25% of its original thickness at an indenter speed of 50 mm/min, before allowing the specimen to rest for about 1 minute.
4) Compress the foam specimen to 65% of its original thickness at the same strain rate of 50 mm/min.
5) Allow the specimen to rest for about 1 minute, before raising the indenter at a speed of 50 mm/min until the indenter plate is not in contact anymore with the foam specimen.
6) Store the obtained data points (force and deflection) for further processing.

Due to the high sampling rate of the electronic data acquisition system, data points were more than 6000 sets of stress and strain. A visual basic application was written using B-Spline algorithm for post-processing of the data points obtained from the uniaxial foam compression test. Block diagram of the foam specimen in test condition

is shown in Figure 6.1, and complete procedural steps for the above-mentioned research study were as shown in the self-explanatory Figure 6.2.

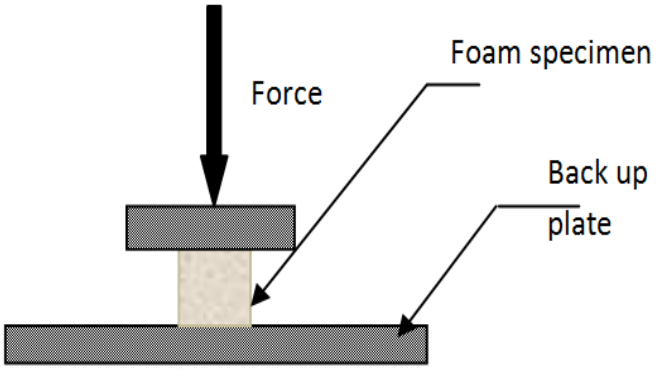

Figure 6.1: Schematic of the foam specimen in the test

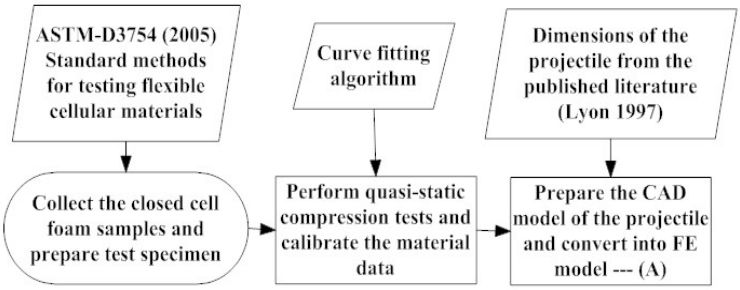

Figure 6.2: Preparation of foam material data and the FE model of the projectile

Though 16 foams were considered for the testing, only one foam material data found suitable (few materials tested were rubber like materials with higher density with lower compressibility and some other foam material tests were not successful) for non-linear FEA simulations presented here. Material data input for the MAT_057 is presented in Table 6.1, and the load curve is as shown in the Figure 6.3. More details of the definitions of the mechanical properties can be obtained from the LS-DYNA manuals (Hallquist 2006; Hallquist 2007a, 2007b).

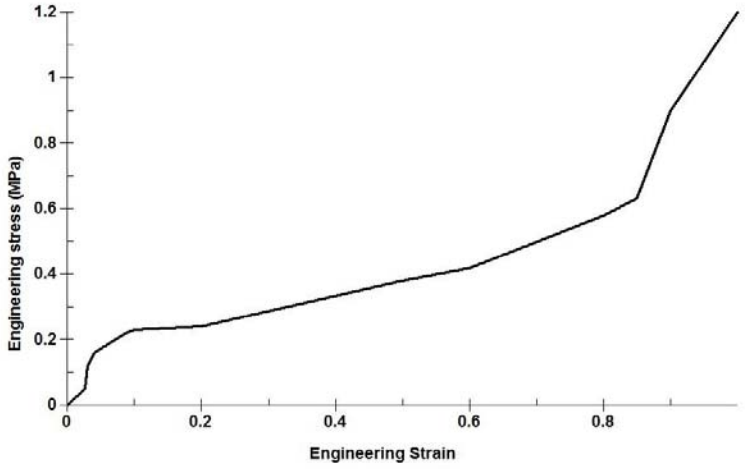

Figure 6.3: Load curve obtained for one of the foams tested (mechanical properties of the same foam were as given in the Table. 6.1)

Table 6.1: Foam material data obtained from the experimental tests and laboratory measurements

Mechanical property	Material data
RO – Mass density in kg/mm^3	1.43×10^{-7}
E – Young's modulus in GPa	0.04
LCID – Load curve data points	Figure 6.3
TC – Tension cut-off stress	0.0
HU – Hysteretic unloading factor (as no energy dissipation condition is assumed to simplify the energy interactions of the projectile and the Thorax)	1.0
BETA – Decay constant to model creep	0.0
DAMP – Viscous coefficient	0.35
SHAPE – Shape factor for unloading	1.0

6.3.2 Selection of the suitable foam for the projectile

Projectile dimensions were taken from the published literature (Lyon 1997). Complete procedural steps to select the most suitable foam (among the foams tested) for the construction of the projectiles for M79 grenade launchers, were as shown in Figure 6.4. The solid model of the projectile along with the thorax surrogate (MTHOTA) are shown in Figure 6.5.

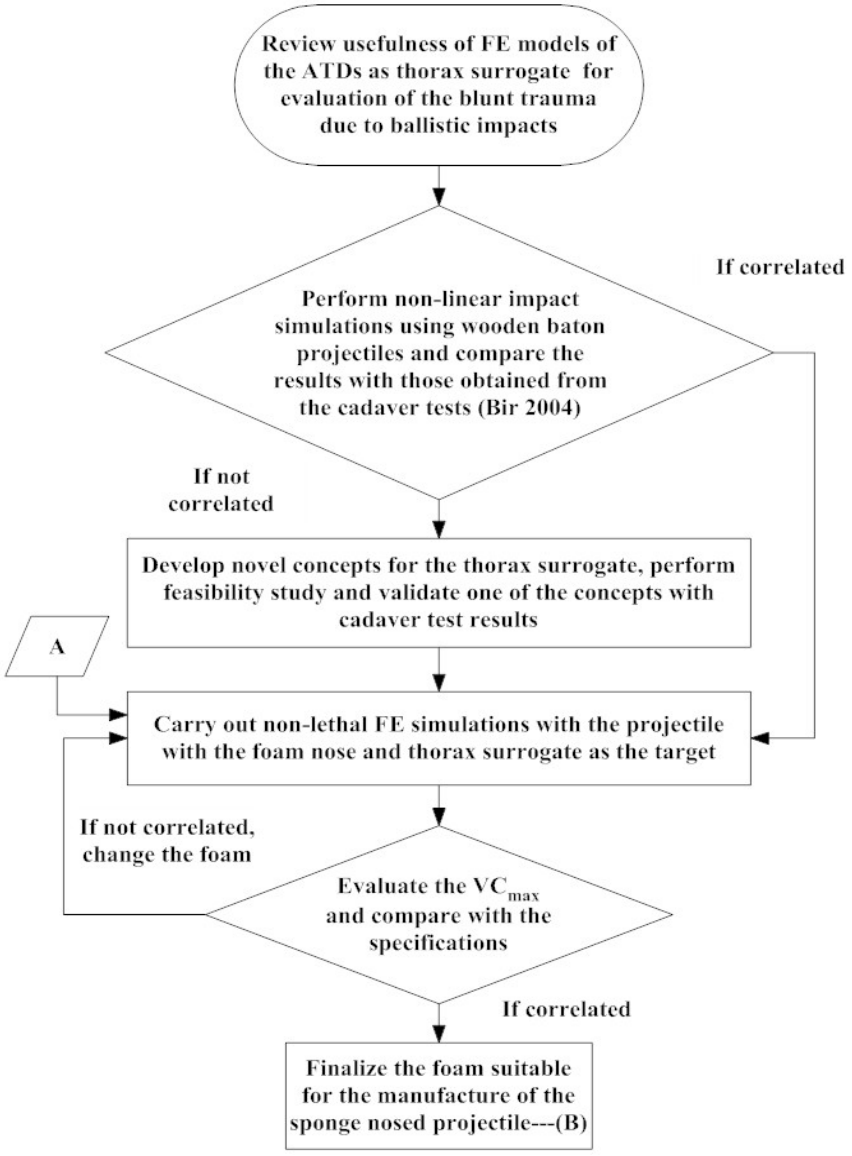

Figure 6.4: Selection of the candidate foam for the projectile (For input A, refer the Figure 6.2)

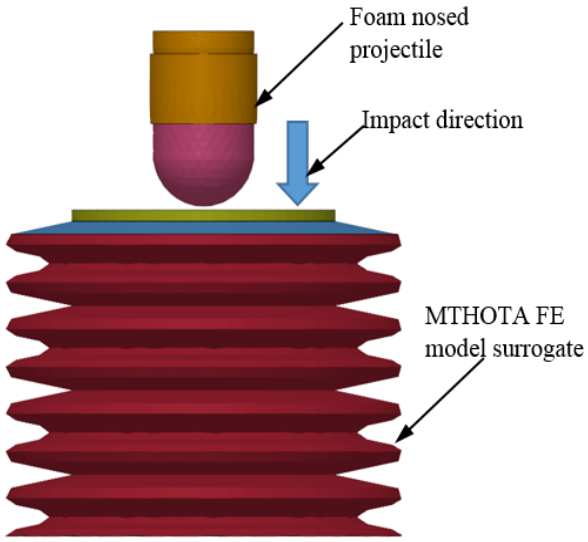

Figure 6.5: Foam projectile and MTHOTA surrogate used in the non-linear FEA simulations carried out for the selection of the candidate foam

6.3.3 Concepts of the energy absorbing mechanisms for the foam nosed projectiles

Three configurations of energy absorbing (EA) mechanisms were conceptualized and were as shown in Figure 6.6.

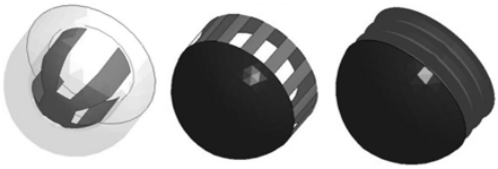

Figure 6.6: EA mechanisms conceptualized for the scholastic study (from left to right: collapsible alloy foil in the hollow foam nose, Collapsible alloy cylinder and corrugated alloy cylinder between the PVC body and the nose

Design for the manufacture study was performed for all three EA concepts and due to the manufacturability constraints, only first concept pursued. Complete procedural steps of the study were as shown in Figure 6.7.

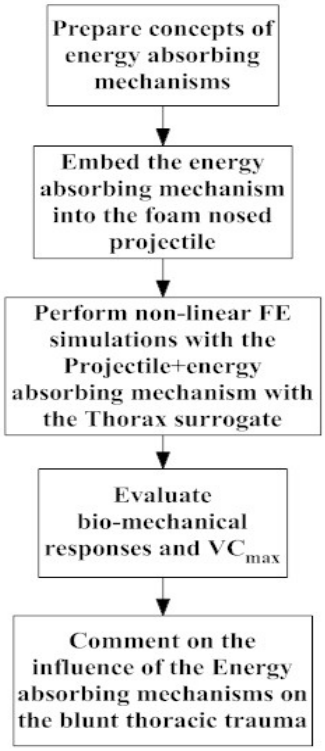

Figure 6.7: Procedural steps to evaluate the effect of energy absorbing mechanisms on the blunt thoracic trauma due to foam nosed projectiles

6.4 Results and discussion

6.4.1 Development of foam nosed projectile equivalent to XM 1006

Due to criticalities of the test, though advanced data collection systems were employed, only two foam materials were considered for the study. Others were discarded either due to high density or due to lack of availability of more foam specimen to repeat the tests in case of failure. It is important to note that XM 1006 weighs less than 30 grams. Therefore, the research study focussed on the development of the projectile with overall weight 30 grams or less.

Non-linear FEA simulations were carried out by impacting the MTHOTA with the foam nosed projectile at 30 – 100 m/s (with an increment of 5 m/s). Using the method -2 described in the section 4.4.2.2 of the chapter-4, VC_{max} values were evaluated for every impact case. Stages of the impacting projectile and MTHOTA were as shown in the Figure 6.8 and maximum deflection of the thorax (maximum deflection of the impact plate with respect to the deflection of the plate-3) measured for the 100 m/s impact case was as shown in the Figure 6.9.

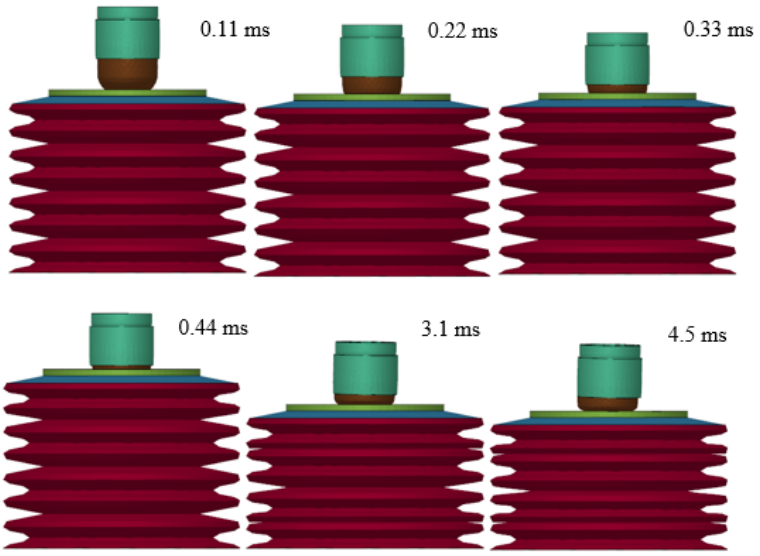

Figure 6.8: Stages of the projectile and MTHOTA surrogate during the impact (impact case 100 m/s)

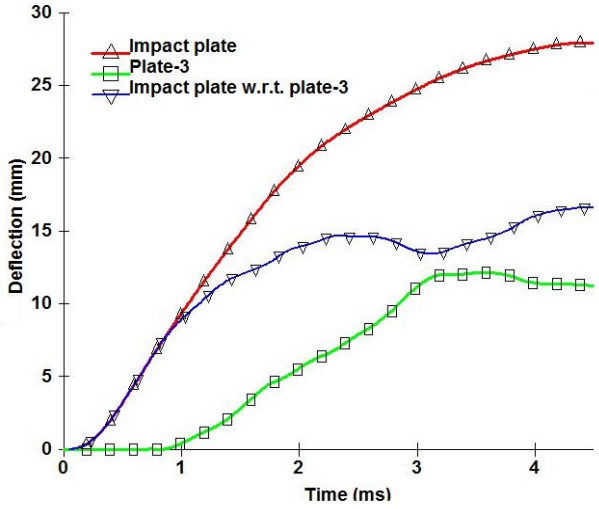

Figure 6.9: Dynamic deflection plots useful for the evaluation of the VC_{max}

From the Figure 6.9, maximum deflection of the impact plate with respect to the plate-3 is 16.7 mm at 4.48 ms impact duration. Therefore,

$$VC_{max} = 1.3\ (16.7/4.48)\ (16.7/180) = 0.449$$

Similarly VC_{max} values elicited for all impact cases are given in the Table 6.2.

Table 6.2: VC_{max} values evaluated for all impact cases of the candidate foam

Impact speed m/s	Time ms	Max. Deflection mm	VC_{max} m/s
30	3.29	3.65	0.029
35	3.28	4.26	0.039
40	3.52	4.8267	0.047
45	3.5	5.2543	0.057
50	3.63	5.27	0.055
55	1.44	5.011	0.126
60	1.44	5.5814	0.156
65	1.44	6.18	0.191
70	1.44	6.845	0.235
75	1.4499	7.557	0.284
80	1.47	8.311	0.339
85	1.4999	9.14	0.402
90	1.99	10.332	0.387
95	2.67	13.28	0.477
100	4.48	16.7	0.449

The force-time response elicited by using the nodal time histories of the back face of the PVC body were as shown in the Figure 6.10. SAE class 600 filter was used for processing of the dynamic force response.

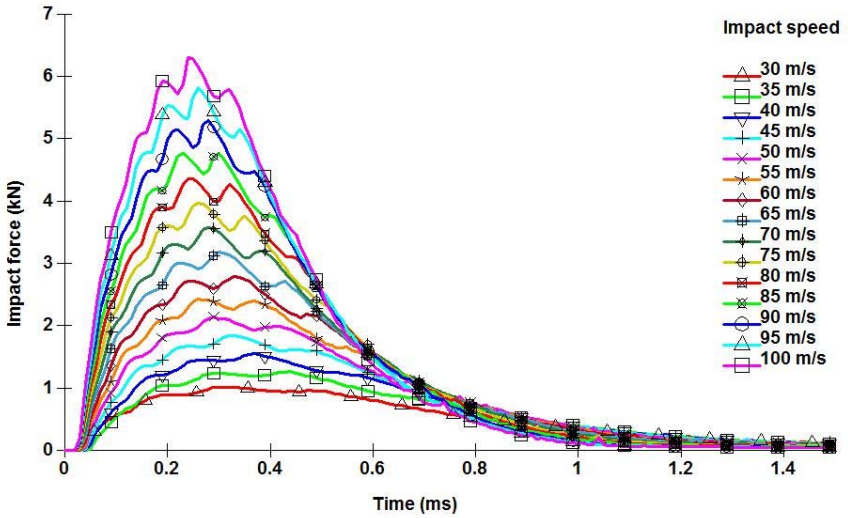

Figure 6.10: Dynamic force response plots for all impact cases

From the Table 6.2, it is evident that the projectile with the nose made up of the candidate foam is suitable for usage as a non-lethal ammunition. As the design intent is not altered, it can be fired using an M79 grenade launcher. For lowering the risk of

severe thoracic injuries (as MTHOTA is very accurate in predicting the VC_{max} comparable with the average value of VC_{max} obtained from the cadaver tests), speed of impact (accordingly muzzle velocity) may be selected from the Table 6.2 depending upon the VC_{max} requirements.

6.4.2 Effect of EA mechanism on the blunt thoracic trauma

To study the effect of an EA mechanism on the blunt thoracic trauma caused by the foam nosed projectiles impacts, a collapsible Aluminium foil (with thickness from 0 – 4.0 mm with an increment of 0.5 mm) was embedded into the hollow foam nose. In the simulations, full foam nosed projectile impacting the MTHOTA at 90 m/s was considered as a reference. An increase in the thickness of the foil can proportionately increase the projectile mass and also initial kinetic energy, if the same impact speed is used. In order to maintain the initial kinetic energy same for the projectile with all EA foil thicknesses, impact velocities were altered accordingly. Various foil thicknesses of EA mechanism and corresponding impact velocities are as given in Table 6.3.

Table 6.3: EA mechanism foil thickness and corresponding impact velocity to keep the kinetic energy constant

Aluminum foil thickness	Projectile weight in grams	Velocity in m/s	Energy in J
No foil	27.31	90	110.61
0.5 mm	27.66	89.43	110.61
1	28.51	88.09	110.61
1.5	29.35	86.82	110.61
2	30.2	85.59	110.61
2.5	31.04	84.42	110.61
3	31.9	83.28	110.61
3.5	32.73	82.21	110.61
4	33.58	81.17	110.61

The dynamic deflection responses of the impact plate for all cases of impacts and dynamic force responses for all impact cases are as shown in the Figure 6.11 and Figure 6.12 respectively.

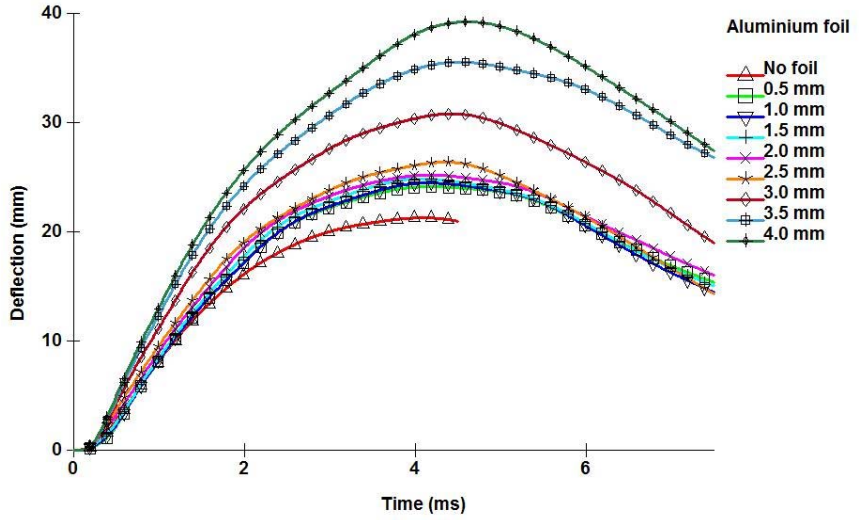

Figure 6.11: Dynamic deflection response of the impact plate for the evaluation of the VC_{max} using the method-1)

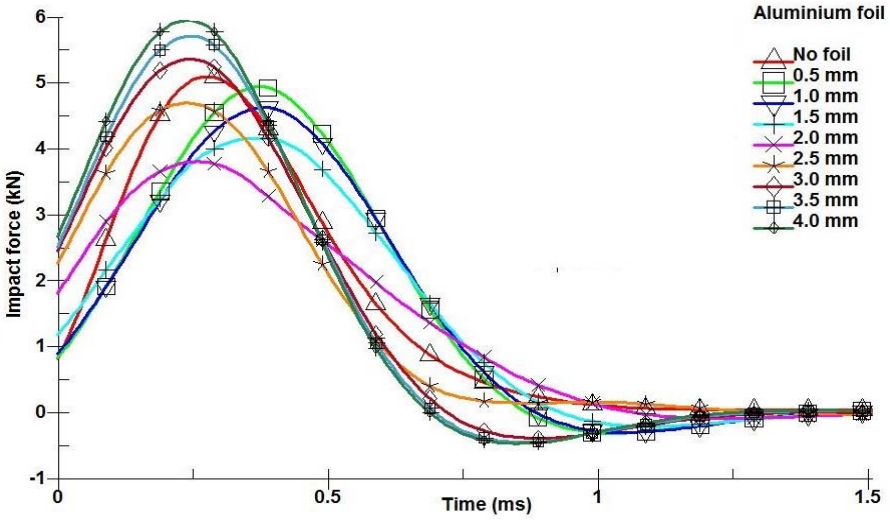

Figure 6.12: Dynamic force response plots for all impact cases (constant kinetic energy and variable thickness of the foil)

From the dynamic force response (Figure 6.12), it is clear that the peak force got lowered with the increase in the thickness up to 2.5 mm thick plate. Afterward the peak force increased with the increase in the thickness of the foil. This is due to the fact that above 2.5 mm, the foils didn't collapse and also added to the mass and stiffness of the projectile, therefore, more peak impact force. Collapse of EA mechanism (Aluminium foil) at 1.2 ms duration of the impact for two cases of foil thicknesses (2.5 mm and 4.0 mm) are shown in the Figure 6.13.

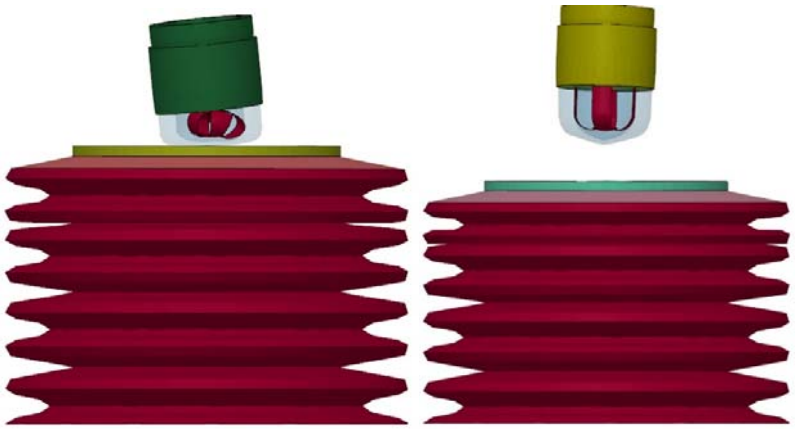

Figure 6.13: Projectiles of same initial kinetic energy with Aluminum foils of 2.5 mm and 4.0 mm (left and right respectively). For the sake clarity, foam nose is made transparent

VC_{max} values calculated using the method-1 described in the section 4.4.2.1 of the chapter-4 were provided in Table 6.4.

Table 6.4: VCmax values evaluated for the projectile impacts

Aluminum foil thickness (mm)	**Time (ms)**	**Deflection of the impact plate (mm)**	**VC_{max} in m/s**
0.0	3.8	22.00	0.35
0.5	4.16	24.11	0.38
1.0	4.1	24.52	0.40
1.5	4.04	25.00	0.42
2.0	4.16	25.54	0.43
2.5	4.34	26.00	0.43
3.0	4.39	30.80	0.59
3.5	4.54	35.50	0.76
4.0	4.56	39.20	0.92

Though the peak impact force was reduced due to the collapsing alloy foil that absorbed more impact energy, from a VC_{max} point of view (Table 6.4), it increased gradually with the increase in the foil thickness. In a nutshell, it is not beneficial to use the EA mechanism considered in the foam nose. By suitably reducing the muzzle velocity or exploring better elastomers, the risk on serious thoracic injuries may be minimized, while maintaining the ability to temporarily incapacitate the subjects of interest.

6.4.3 Head damage characteristics of the projectile

As presented by Oukura et al. 2013, researchers of the Direction Generale de l'Armement of the French Ministry of Defense have developed tolerance limits for human head subjected to blunt ballistic impacts by using human biological models and

animal biological models of the head. The outcome of their research work (types of damage and tolerance limits in terms of intracranial pressure and peak impact force) are given in Table 6.5.

Table 6.5: Human head tolerance limits when head subjected to blunt ballistic impacts (Oukura et al. 2013)

Type of head damage	**Intracranial Pressure (ICP) kPa**	**Peak impact force (PIF) kN**
Insignificant	≤ 2.5	≤ 2.5
Unconsciousness	$2.5 \leq ICP \leq 45$	$2.5 \leq PIF \leq 5$
Meningeal	$45 \leq ICP \leq 150$	$5 \leq PIF \leq 7.5$
Bone fracture and coma	≥ 150	≥ 7.5

The DGA researchers have developed head damage curves for non-lethal munitions using both human and animal head biological models. The head damage curve developed for the XM 1006 (Equation 6.1)) is of paramount importance as the projectile is the benchmark projectile in the study presented here.

$$(F_{XM})_{head} = K*(V_{XM}/10)^N \quad (6.1)$$

K = experimentally obtained coefficient = 0.083

N = experimentally obtained coefficient = 2.585

$(F_{XM})_{head}$ = Maximum force of XM 1006 projectile on the head (kN)

V_{XM} = Impact velocity of XM1006 projectile (m/s)

Oukura et al. 2013 have presented force wall method that is used in the defense industry to assess the head injury caused by the blunt projectile impact. The basis of this method is that if blunt impacts by two different projectiles causes the same amount of force on a rigid wall, then would cause equivalent head injuries. Oukara et al. 2013 have presented the peak force values obtained by impacting the rigid wall with XM 1006, NS Spartan LE-40, NP and B&T latest foam nosed KENLW. To assess the performance of the projectile under development, nonlinear transient dynamic simulations, in which rigid plate is subjected to impacts of the projectile (PVC base and nose with the candidate foam), were carried out. From the output of each impact case, dynamic force response and peak force values were elicited. Dynamic force responses obtained for the different impact cases are as shown in the Figure 6.14.

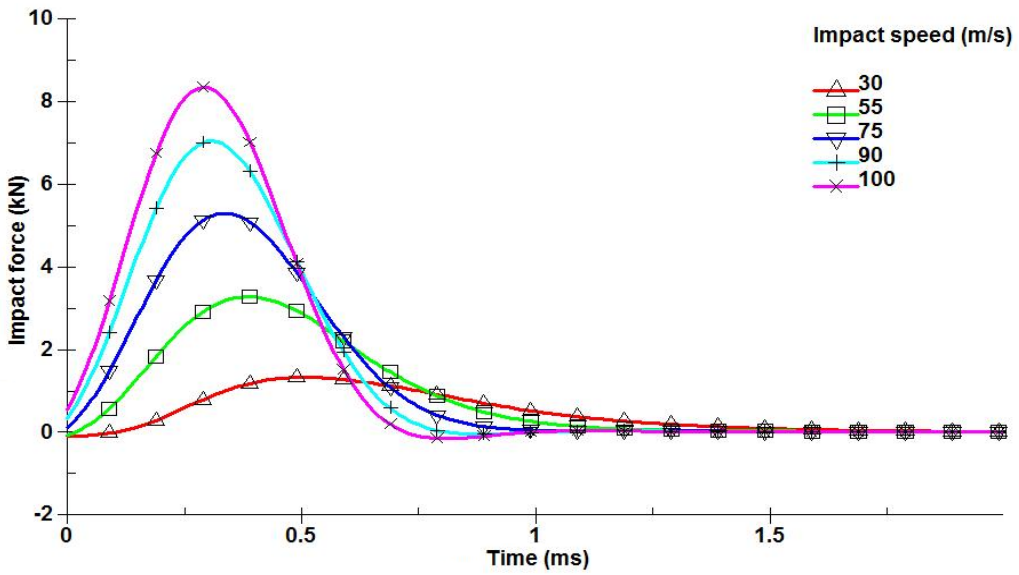

Figure 6.14 Force-time response obtained by impacting the fixed rigid plate with the projectile under development (PVC base and nose with the candidate foam)

From the Figure 6.14, it is evident that the projectile under development has performed far better than the foam nosed projectiles evaluated by Oukura et al. 2013, using the rigid wall impact method. For instance, 90 mps impact by the projectile under development produced peak impact force of 7.29 kN. For the same impact speed, the NS projectile produced 20 kN, the NP projectile produced nearly 45 kN, and the B&T projectile produced approximately 40 kN. The benchmark projectile XM 1006 has produced nearly 24 kN at an impact speed of 55 m/s. Therefore, without any doubts, the projectile under development would cause far lesser head damage when compared with the benchmark projectile. The head damage curve for the new projectile was developed by plotting peak impact forces against the impact speeds (Figure 6.15) and compared with the results presented for the benchmark projectile (XM 1006) by Oukura et al. 2013.

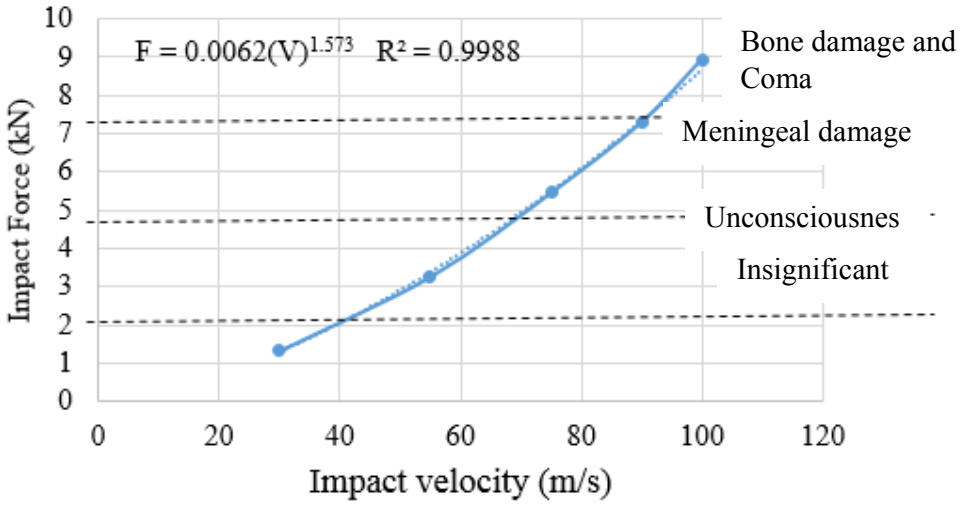

Figure 6.15: Head damage curve obtained for the new projectile being developed for M79 grenade launcher

The damage curve developed for the new projectile was rewritten in the form of that developed by researchers of the DGA of the French Ministry of Defense.

$$F = 0.213 * (V/10)^{1.573} \quad (6.2)$$

Rigid wall results obtained for the new projectile through CAE simulations were compared with those obtained experimentally for the benchmark projectile and other novel non-lethal projectiles.

Table 6.6: Rigid wall impact test results

Projectile	K	N	Comments
Projectile with new foam nose	0.213	1.573	Nonlinear simulations of rigid wall impacts (present study)
XM 1006	0.314	2.543	Rigid wall impact results presented by Oukura et al. 2013
NS	0.281	1.986	
NP	1.1	1.801	
B&T	0.087	2.881	

From the Figure 6.15 and the Table 6.6, it is clear that projectile with the new foam nose would emulate the benchmark projectile in non-lethal characteristics while performing better as far as the head damage concerned for the case of accidental head impacts. The proposed energy absorbing mechanisms were found to be not ineffective. The study shows the importance of the nose material properties in controlling the damage and lethal effects of the blunt ballistic impacts. This study shows the importance of thoracic surrogates and demonstrates how thoracic surrogates can be used for development and validation of new non-lethal projectiles.

6.5 Conclusion

Scholastic studies performed accentuate the efficacy of the MTHOTA FE model thorax surrogate for the development and validation of non-lethal projectiles or for validation of new materials to suitably alter the injury characteristics of the KENLW.

From the blunt thoracic trauma calculations using the MTHOTA surrogate, it was evident that VCmax values for the new projectile (new foam as the nose) well below the specified limits. The risk of serious thoracic injuries is reduced with the new projectile below 90 m/s impact speeds. From the rigid wall impact tests of the new projectile, peak force at 90 m/s is less than 7.5 kN, while benchmark projectile impacts at 55 m/s caused approximately 23 kN. At impact speeds of 90 m/s, NS, NP and B&T projectiles gave 20, 45 and40 kN respectively. Therefore, as far as the head damage is concerned (damage due to the unintentional hits to the head due to the dispersion effect), the new projectile with new foam material performed very better when compared to the benchmark projectile XM 1006 and the other latest foam nosed projectiles (NS, NP and B&T).

Though 14 out of 16 foams tested were discarded after the preliminary investigation (due to high density, unsuccessful material tests and lack of availability of the samples), one of the two foams proved very effective to be used as the nose in the KENLW.

EA mechanisms proved to be ineffective due to the limitations on the size. In the case of collapsible aluminium foil in the foam nose of the new projectile, up to 2.5 mm thickness, it collapsed foil and absorbed some energy. Further increase in the thickness however increased blunt thoracic trauma (VC_{max}) due to the added mass and increased stiffness. Therefore, adequate caution needs to be exercised to use EA mechanisms in the non-lethal projectiles.

CHAPTER-7: DESIGN AND DEVELOPMENT OF FRONT PROTECTION SYSTEMS FOR NON-AIR BAGGED PASSENGER VEHICLES – A SYSTEMATIC METHOD

This chapter discusses all necessary requirements for the design and development of the front protection systems (FPS) for the passenger vehicles that are not equipped with airbags. This chapter also summarizes the journal article titled 'Vehicle front protection systems: CAE based approach to achieving airbag compatibility' that is under review for publication in the 'International Journal of Vehicle Structures and Systems'. Complete details of the paper are given in the Appendix – I of the thesis.

7.1 Introduction

Vehicle front protection systems (VFPS) are one of the common accessories for all passenger vehicles, though most commonly designed for 4WD recreational vehicles. VFPS have been in the market with the names such as 'Bull bar, Kangaroo bar, Nudge bar and Loop bar (Bignell 2004). Depending upon the design and the way they mounted, VFPS are mainly classified into two categories; 1 – Bumper replacement type and 2 – Over the bumper type or additional front protection system. The former one is very sturdy and stiff with metal fascia and tubular sections and can be fitted to the vehicle after removing the bumper and some of its supporting parts. The latter one is usually an inverted U-SHAPED shaped tubular section and sometimes with additional loops to offer added protection to the headlamps. Additional FPS can be fitted to the vehicles without removal of the bumper and related components. Some typical VFPS of both categories were as shown in Figure 7.1.

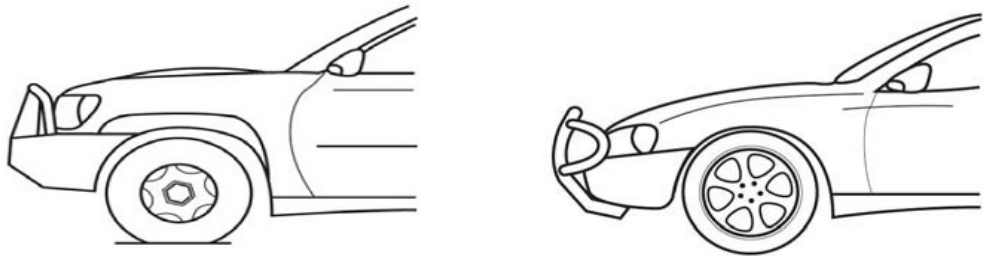

Figure 7.1: Bumper replacement FPS (left), and 'Over the bumper type' FPS (right)

It is important to note that automotive engineers and researchers worldwide have been working on the methods of improving the pedestrian safety characteristics of the passenger vehicles to minimize the pedestrian fatalities. There are 100s of innovative designs ranging from the spoilers to outward opening airbags on the bumper, though the latter one is with so many additional crash sensing devices (Schuster 2006). On the contrary, manufacturers of the aftermarket accessories have been developing VFPS that are sturdier and stiffer than the bumper and leading edge of the bonnet. Because of the pedestrian safety issues, many countries in the Europe banned the VFPS and in Australia, the topic "Is bulbar a friend or foe" has always been debatable.

In Australian outback, road users often exposed to animals in their path. Every year, few hundreds of vehicle crashes involving animals are being reported. As official 'database for vehicle accidents' records only the accidents reported to the police, there was very limited data available on the vehicle-animal collision scenarios (Attewell & Glase 2000). After analysis of the crash report database, it was reported that a total of 11636 vehicle crashes involving animals have occurred in Australia during the period from 2001 to 2005. Of these 61 were fatal, and 1049 were hospitalization crashes (Rowden, Steinhardt & Sheehan 2008). Owing to the high prevalence of vehicle-animal collisions, many vehicles, not limited to recreational 4WD vehicles, are fitted with the wide variety of vehicle front protection systems (VFPS) to protect not only the systems under the bonnet but also occupants of the vehicle. VFPS also provides additional protection to the occupants and systems in the engine bay, when involved in low-speed crashes.

Though fitment of the VFPS is justifiable in Australia, improperly designed FPS poses increased injury risk of vehicle occupants and also instead of offering the protection, causes more damage to the vehicle components and systems. In the subsequent sections of this chapter, various design aspects of FPS, ranging from the weight to styling will be discussed with a real example of that deals with the development of the FPS for a typical Ute.

7.2 Specifications for the design and development of the vehicle front protection systems

Many researchers have, so far, analyzed the accident databases, studied the prevalence of bull bars and their detrimental effects on the pedestrian safety (Anderson et al. 2009; Anderson, Ponte & Doecke 2008; Attewell & Glase 2000; Chiam & Tomas 1980; Doecke, Anderson & Ponte 2008; Hardy 1996; Lawrence & Hardy 1992; Rowden, Steinhardt & Sheehan 2008; Thota, Eepaarachchi & Lau 2013c). Australian standard AS 4876.1-2002 published by Standards Australia made a great emphasis on minimizing the pedestrian injury risk due to colliding with a vehicle equipped with a VFPS (Australia 2002). Every bull bar sold in Australia must comply with AS 4876.1-2002 (i.e., for the pedestrian safety, Head Injury Criterion $\leq$ 1000) and the ADR69 (vehicular occupant safety). Though these standards and design rules highlight the requirements of the FPS, there is no mention of the methods for accomplishing the design to the specifications. Lack of information on the development methodologies will lead to the production of unsafe FPS.

The following aspects are very critical in design and development to of the front protection systems that meet the requirements of AS4876.1-2002, ADR 69 and other warranty related specifications.

- Fitment of the FPS should not cause overloading of the vehicle front axle. Therefore, maximum allowable weight of the FPS by performing mass setting calculations.
- Mounting points, and mounting brackets should be such a way that FPS produces the desired effect.
- Styling of the FPS should be such a way that, it should conform to the contours and profiles of the vehicle so that it enhances the aesthetics of the vehicle, should not adversely affect the visibility of the driver, should not reduce the effectiveness of the headlamps and cooling characteristics of the engine while maintaining the accessibility of the vehicle recovery points.

- Pedestrian safety (Head Injury Criterion ≤ 1500)
- Endurance life (FPS should last for at least the warranty period, without any cracks, rust, and bolt failures, during the ordinary course of usage)
- ADR 69/00 compliance: After inception of ADR 69/00 in the year 1995, all MA vehicles (passenger cars), MB vehicles (forward control passenger vehicles), MC vehicles (off-road vehicles) and NA1 vehicles (light goods vehicles) sold in Australia must meet the minimum levels of occupant protection set by the ADR69/00.

Many of the FPS manufacturers worldwide are small scale industries with very limited resources. Of these, more than 50% of manufacturers do not even use CAD/CAM for producing great looking (sometimes, very aggressive) FPS. These manufacturers only take necessary measurements of the vehicle and go ahead with the look and feel. Though they are exquisite at the claim of having a 'black art', their non-engineering approach and misconceptions makes the FPS produced by them detrimental to the vehicle, vehicle users, and pedestrians. Some of the such aggressive FPS were as shown in Figure 7.2.

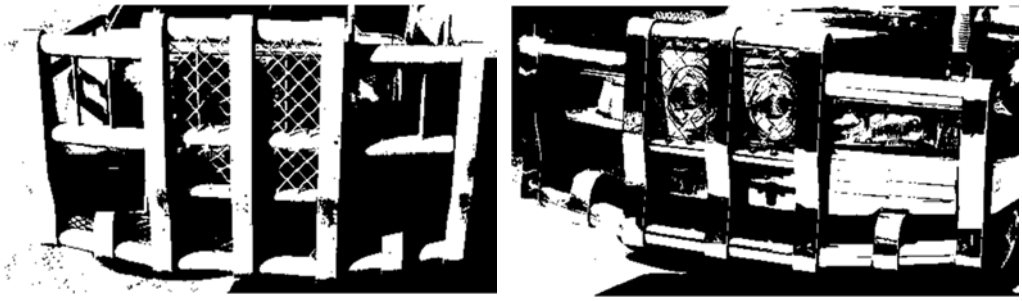

Figure 7.2: Bumper replacement FPS. Visibility of the driver, vehicle cooling characteristics, effectiveness of the headlamps, occupant safety, pedestrian safety and front axle load bearing capacity etc. are greatly compromised

Heavier and stiffer FPS provides more safety to the vehicle and vehicular occupant and FPS with any weight, any mounts and any mounting points can be equally effective for non-air bagged vehicles, etc. have been major misconceptions which lead to the development of the aggressive FPS.

7.3 Methodology for the development of VFPS

A systematic methodology was devised to design and development of the VFPS that meet all specifications and requirements mentioned in section 7.2. Major procedural steps or stages in the development procedure were as given here.

1. Styling of the FPS fascia and tubular sections
2. Selection of the mounting points
3. Development of various concepts of FPS mounts
4. Selection of the FPS mounts based using simplified crash simulations
5. Manufacture of the production representative samples
6. Perform ADR 69/00 crash tests
7. Endurance tests
8. Release the FPS as an accessory

In this chapter, only aspects related to the design development (former 6 steps) were discussed. Input data required for the development of FPS for non-air bagged vehicles is as shown in Figure 7.3. Though in the current day cars, airbags (both driver and front passenger) are standard features, FPS development for non-air bagged vehicles is considered for the study, to highlight the importance of engineering approach.

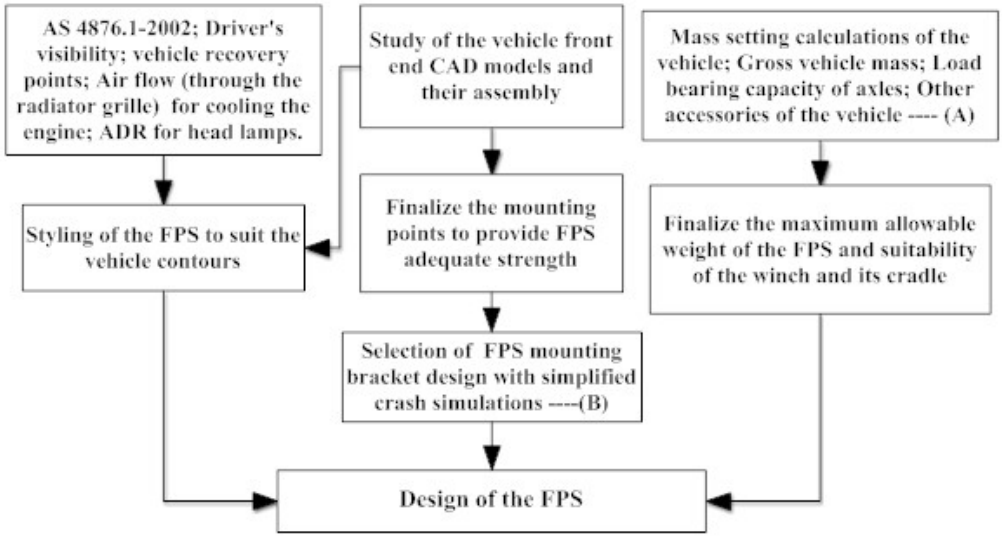

Figure 7.3: Inputs and procedural steps required for the development of AS 4876.1-2002 compliant FPS for non-air bagged vehicles

Modern day passenger cars are not only occupant safe, also esthetically very appealing. Therefore, styling of the FPS should be such a way that contours of the FPS must conform to the profile of the vehicle. During the concept stage of the FPS design itself, stylist and designers must consider all the guidelines provided by the AS 4876.1-2002 so that FPS does not adversely affect the driver's visibility, engine cooling, accessibility of vehicle recovery points and performance of the headlamps. Stylists and designers should also incorporate semi-rigid foam embellishments (such as, bumperettes and tubular covers) for the fascia and tubular sections, to not only ameliorate the aesthetics, but also to improve energy absorbing characteristics and pedestrian safety performance of the VFPS.

Mounting points provide the rigidity to the VFPS. For some vehicles in the market, "over the bumper" FPS fitted utilizing the sheet metal components such as headlamp support and radiator support. In some cases, holes available on the plastic parts were also used for mounting. Such mountings of the FPS, even during the low-speed collisions, can cause considerable damage to the radiator and headlamps. It is important to remember that the primary function of the VFPS is to protect the engine systems (under the bonnet) and headlamps in the event of low-speed vehicle impacts and vehicle-animal collisions. Therefore, adequate caution must be exercised in the selection of mounting points. Front end of the chassis (in the single-hat or double-hat crush-can) is one of the best locations to mount the FPS.

After selecting the mounting points, development of the concept for FPS mounts become an easy task. Design configurations such as plate with a fold, corrugated box and box section with weak points are suitable for mounting bracket design. Flat plate

mounts, plate with a fold mounts and mounts with box sections were as shown in the Figures 7.4 (a), (b) and (c) respectively.

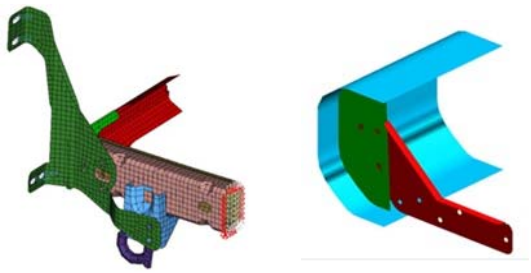

Figure 7.4(a): Flat plate mount configurations along with their mounting points

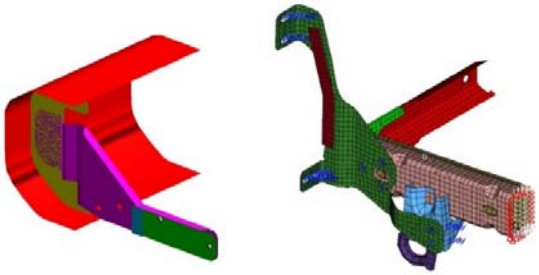

Figure 7.4(b): Folded plate mount configurations and their mounting locations

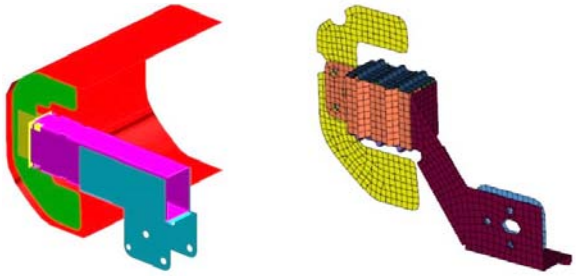

Figure 7.4(c): Box section mounts with their mounting locations

Crash simulations involving whole vehicle model is computationally very demanding. Therefore, selection of the concept FPS and finalizing the design entails numerous vehicle crash simulation iterations, and the process becomes tedious. A novel method of using simplified crash simulations would be very useful to select the design of the FPS mounts. The procedural steps were as shown in Figure 7.5.

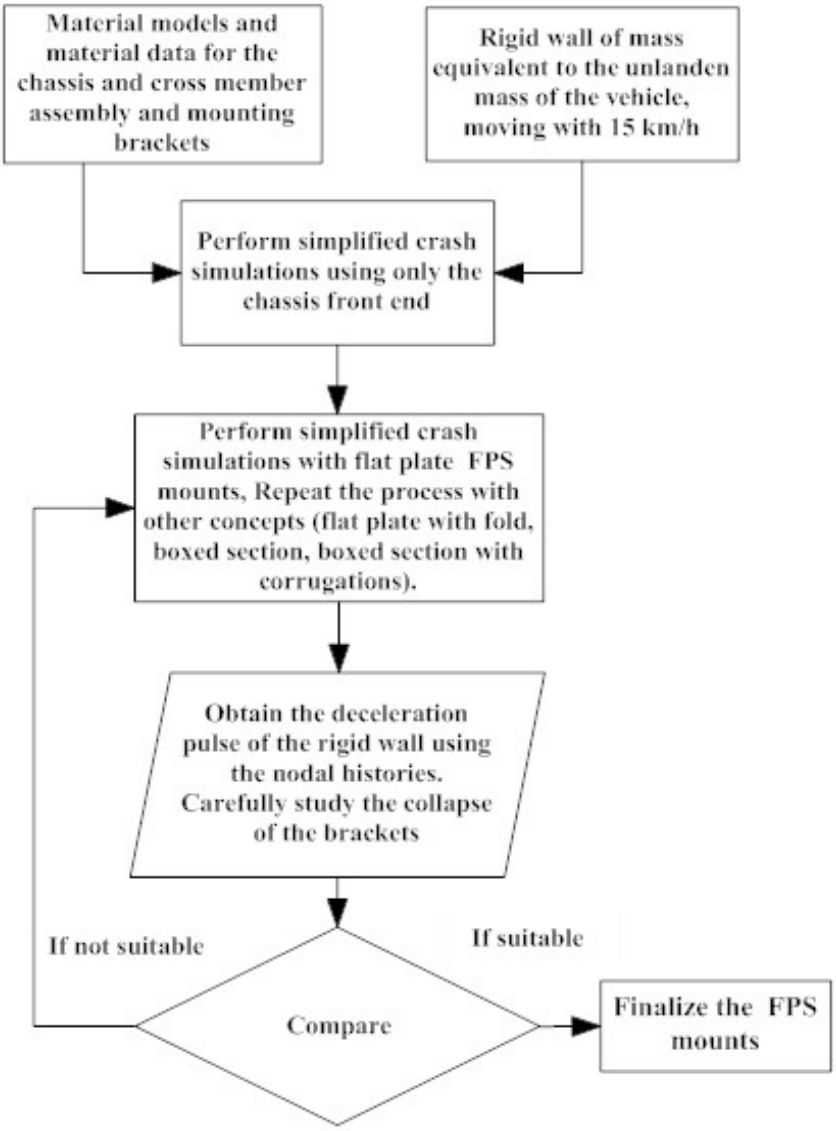

Figure 7.5: Procedural steps to select the suitable FPS mounts

Procedural steps to achieve the ADR 69/00 compliance were as given in Figure 7.6.

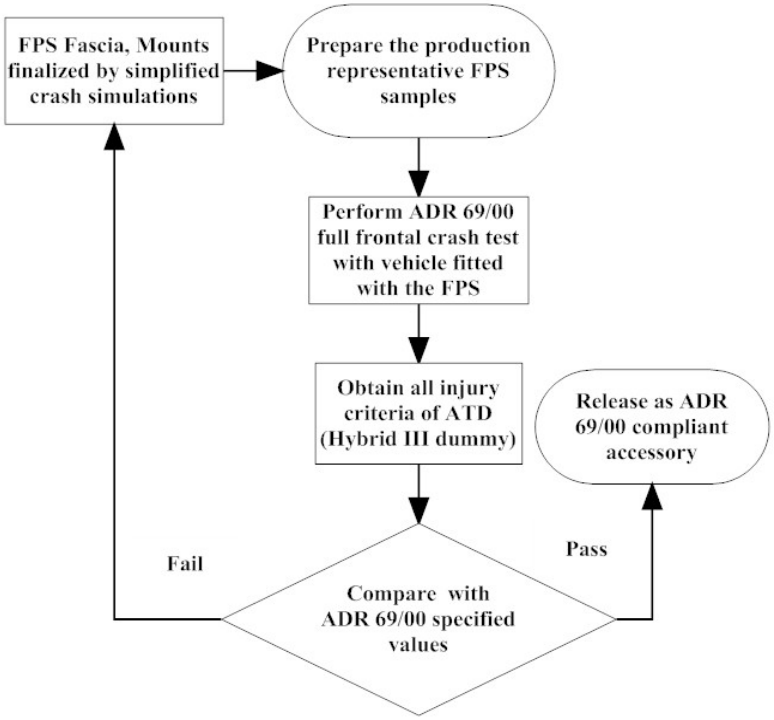

Figure 7.6: ADR 69/00 test protocol

Full vehicle crash tests are very expensive, therefore, to avoid the failures and avoid the physical crash test iterations, one can take resort to full vehicle crash simulations. With the mounts finalized by simplified crash simulations, so far no FPS failed the ADR 69/00 compliance tests. Full vehicle crash simulations, ADR 69/00 test specifications, and related aspects will be discussed in great details in the subsequent chapters.

7.4 Results and discussions

Efficacy of the devised method was demonstrated with a real life project of design and development of the bumper replacement FPS for a typical Ute, which has got 8 variants in the same model.

7.4.1 Mass setting calculations of the Ute under consideration

Every passenger vehicle is developed to meet two contradicting requirements; 1 – In the event of impact, vehicle structure must crumple to absorb the energy of the impact so that deceleration levels of the passenger would be tolerable and 2 – In the event of collision or vehicle crash, degradation of the passenger compartment (intrusion) space would be such a way that occupant sustain minimum injuries. Therefore, fitment of the FPS that are sturdy and stiffer than the required to even non-airbag equipped vehicles pose serious injury risk as occupants experience high levels of decelerations. Therefore, vehicle owners should exercise great caution in selecting the FPS for their vehicles.

Determination of the maximum allowable weight of the FPS has got paramount importance during the concept stage of the FPS as every vehicle is designed with Gross Axle Weight Rating (GAWR) for both front and rear axles. Options offered by the vehicle manufacturers and other accessories significantly influence the GAWR. Therefore, based on the allowance available on the front axle load bearing capacity, maximum allowable weight of the FPS should be finalized. Enough caution should be exercised so that the weight of the FPS kept well below the evaluated maximum allowable weight.

Fitment of the FPS to any vehicle increases the load on the front axle and causes an uplifting force on the rear axle. If the front axle is overloaded because of the massive bull bar–winch assembly, it will have detrimental effects on the steering system, the braking and the control over the vehicle.

A systematic method to accomplish all requirements of FPS was devised and developed the bumper replacement type FPS to a typical utility vehicle that has got 8 variants. Importance of the vehicle's GAW calculations in the development of the FPS is highlighted with the same vehicle as an example.

The Ute, which is a compact pick-up utility van that has got 8 variants. Though all looked same as far as the front-end of the vehicle is concerned, they had differences in GAW ratings, owing to the differences in the type of drive, standard items, accessories, etc. Most importantly, all variants of the vehicle of got the GVM of 2720 kg. Looking at the front-end shape and size and knowing the fact that all variants have got the same GVM, FPS makers may feel that FPS manufactured for one variant can be sold for remaining variants of the car.

In order to highlight the factors influencing the front axle GAWR by performing mass setting calculations, an Excel macro was developed. For this purpose, whole vehicle CAD model was used. In the case of some options, equivalent masses were added in the appropriate locations. Utilizing the 'method of moments,' reaction forces at axles due to each component were evaluated to finalize the designed GAWR of both front and rear axles. Similarly, loads on the axles due to fitment of the all accessories were also evaluated. To simplify the process of the whole calculation, an excel macro was developed that provide the required output in the form of easily understandable graphs.

GVM allowance for accessories and load on the axles due to the fitment of accessories to the vehicle were extracted from the output of the macro and given in Table 7.1 and Table 7.2 respectively. For the sake of simplicity, only relevant output obtained from the macro for only two variants (Variant-1 and Variant-2 of the Ute) were considered for the presentation. GAW-Front axle for all accessories for 1 and 2 variants of the vehicle was as shown in Figure 7.7.

Table 7.1: GVM allowance for all accessories (only for 1 and 2 variants of the vehicle were given)

Ref	Specifications of the Vehicle	1	2
1	Gross Vehicle Mass(GVM)	2720	2720
2	Unladen Mass	1780	1880
3	Allowance for Passengers + Cargo + Options + Accessories	940	840
4	5 Passengers (5X68Kg)	340	340
5	Payload (as per MMC specs)	500	430
6	Options	75	55
7	**GVM Allowance for Accessories = [3-(4+5+6)]**	**25**	**15**

Table 7.2: Loads on the front and rear axles due to all accessories

Accessory	Weight in kg	Front Axle Load	Rear Axle Load
Bull bar (bumper replace)	45	52.5	-7.5
Winch	35	40.8	-5.8
Sports Bar	0	0.0	0.0
Canopy OR Tipper Tray	50	-6.9	56.9
Hard Tannaou Cover	0	0.0	0.0
Tub Liner	10	-1.4	11.4
Rear Glass Protector	0	0.0	0.0
Rear Protection Bar	7	-2.6	9.6
Roof Racks	5	2.5	2.5
Max Load. Roof racks	0	0.0	0.0
Front Skid Plate	5	5.8	-0.8
Rear Skid Plate	5	-1.8	6.8
Underbody Protection	5	2.5	2.5
Tow bar	30	-11.0	41.0
Trailer with Electronic brakes (2300Kg)	0	0.0	0.0
TOTAL	**197**	**80.5**	**116.5**

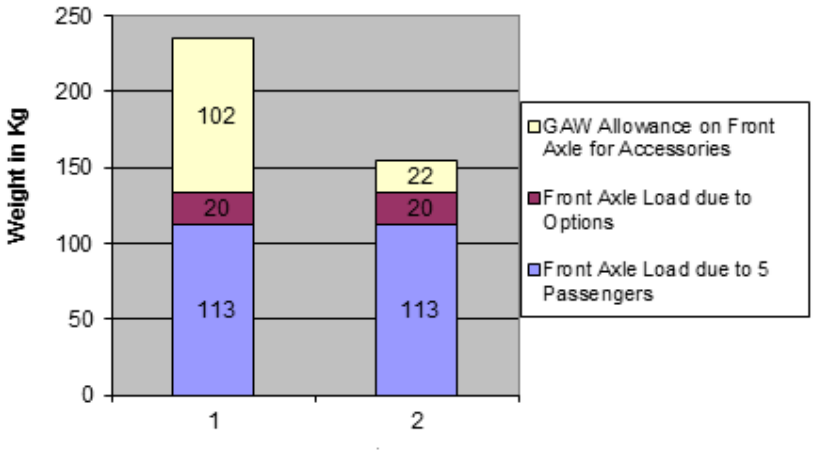

Figure 7.7: GAW-FRONT AXLE allowance for all accessories of 1 and 2 variants

Depending upon the mass setting calculations outcome (that is, using the GAW-FRONT AXLE allowance), suitability and maximum allowable weight of FPS were evaluated for all variants of the vehicle and were as given in the Table 7.3.

Table 7.3: Suitability and maximum allowable weights of the FPS for all vehicle variants (Y = YES, N = NO)

Variant	**1**	**2**	**4**	**5**	**6**	**6**	**7**	**8**
Allowable Front Axle Loads in kg	102	22	82	37	87	138	73	37
Allowable Additional Mass on the Front(Over Bumper) in kg	87	19	70	32	75	108	62	32
Allowable Additional Mass on the Front (Bumper Removed) in kg	97	29	80	42	85	118	72	42
Target weights for FPBs are given below								
Steel bull bar of 40-45 kg	Y	Y	Y	N	N	Y	Y	N
Winch and its cradle 40-50	Y	N	N	N	N	Y	N	N
Acceptability of Winch with steel bull bar	Y	N	N	N	N	Y	N	N
Alloy Bull bar without winch cradle up to 40Kg	Y	Y	Y	Y	N	Y	Y	N
Acceptability of Winch with alloy bull bar	Y	Y	N	N	N	Y	N	N
Alloy Nudge (inverted U shape) 5-7Kg	Y	Y	Y	Y	Y	Y	Y	Y
Alloy Loop Type (Tubular FPB) 10kg	Y	Y	Y	Y	Y	Y	Y	Y
Plastic FPB Over the bumper 20 Kg	Y	Y	Y	Y	Y	Y	Y	Y

From Figure 7.7, it is clear that though both variants of the vehicle look alike in size and shape with the same GVM and also with no significant differences in the front end structures, variant-1 can be fitted with bumper replacement type FPS, Winch and its cradle as it has got 102 kg allowance on the GAW-FRONT-AXLE. Whereas vehicle variant-2 can be equipped with the FPS with weight less than 20 kg (probably with an 'over the bumper type' nudge bar, loop bar or plastic bar).

There are many vehicles of other makes and models similar to variant-2 as far as the GAW-FRONT AXLE allowance for accessories is concerned. Therefore, fitment of the FPS that were developed without taking the mass setting calculations into account would be detrimental to the vehicle's life and performance and potentially could lead to fatal accidents.

By summarizing mass setting calculations, maximum weight allocated for the bumper replacement type Steel and Alloy FPS (including mounting brackets) was ≤ 37 kg.

The design of the fascia and tubular sections of the bull bar developed by utilizing all inputs were as shown in Figure 7.8.

Figure 7.8: Baseline design concept of the bumper replacement type of FPS

The design of the VFPS has met the specifications for the engine cooling (as there was no difference in the grille size and position). Accessibility of the vehicle recovery hooks was maintained, and weights of the VFPS were also found to be well below the available GAW-FRONT AXLE allowance for all variants of the vehicle.

7.4.2 Selection of the mounting points for the fitment of the FPS

In order to demonstrate the efficacy of the method presented in this chapter, a typical recreational utility vehicle was considered for development of the VFPS. The vehicle has got both driver and front passenger airbags. Taking GVM, unladen weight, load capacity of the axles and other options & accessories into consideration, it was found that front axle has got 45 kg allowance for the FPS (refer the mass setting calculations). Therefore, aimed at developing VFPS (Steel and alloy bumper replacement FPS) with a maximum weight 45 kg. As the winch adds at least 45 kg weight on the front axle, it was not considered in the design and development. After careful study of the front end vehicle structure, 5 mounting points were selected (Figure 7.9) symmetrically on each side of the vehicle (3 on the FRAME_OUTER and 2 on the BRACKET_HOOK) for the fitment of the FPS.

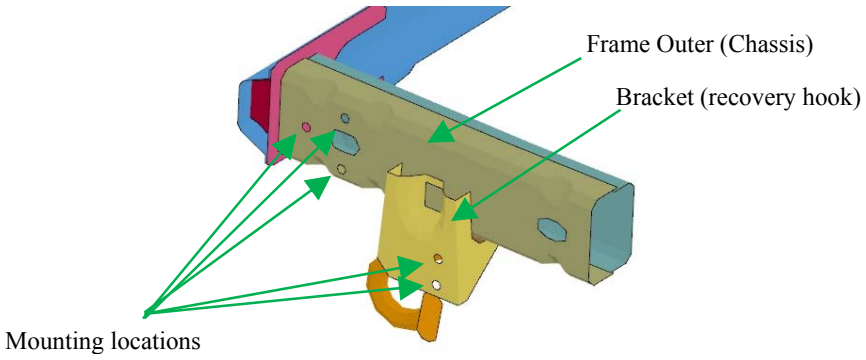

Figure 7.9: Mounting locations selected for the fitment of the VFPS

Though there were so many sheet metal parts in the front end structure, taking mounting points from them transfers the impact energy directly to the components (Radiator, Headlamps, and etc.) supported them. Aim of the VFPS is itself to protect these components in the event of vehicle collision with animals or low-speed impacts in other scenarios. Therefore, it is highly recommendable for the mounting points to be on the crushcan region of the chassis. Mounting points away from the crushcan could be very detrimental as the impact force directly gets transferred to the chassis and crushcan would become a dummy.

7.4.3 Simplified crash simulations to finalize the FPS mounts for the Ute

Mounting points, and mounting brackets together significantly influence the airbag compatibility and energy absorbing characteristics of the VFPS. With the mounting points on the chassis, it is possible to develop many configurations of the mounting brackets. With simplified crash simulations which are equivalent to dynamic pendulum tests were performed. With the proper analysis of the deceleration pulse, a suitable design concept for the mounts was selected and utilized for the development of baseline FPS design.

In simplified CAE crash analysis,

- Only crash-can of chassis (front-end of the chassis) and cross beam assembly considered
- Mid-surfaces of the components were utilized for the FE model
- SURFACE_TO_SURFACE contact interface definition was used for all contract interfaces
- Simplified vehicle assembly was impacted with a rigid wall of mass 1736 kg (unladen weight of the utility vehicle under consideration), moving with the speed of 15 km/h.
- Deceleration pulse obtained from the time histories of the node created on the rigid wall was extracted

Material models and material data used in the analysis (including FPS fascia, tubular sections and mounting brackets etc.) were as given in Table 7.4. Simplified crash

simulation set-up and various stages of crumpling of the chassis – cross beam assembly were shown in the Figure 7.10 and Figure 7.11 respectively. Using the nodal histories of the node on the 'Rigid Plane', deceleration of the vehicle was obtained. In the comparative studies, this deceleration pulse used as a reference.

Table 7.4: Material data and material models used in the crash simulations (both simplified and full vehicle crash)

Component	**Material model**	**Young's modulus GPa**	**Density kg/mm^3**	**Poisson's ratio**	**Yield Stress GPa**
Chassis (crash can)	MAT_PIECEWISE_LINEAR_PLASTICITY (MAT_024 in LS-DYNA)	206.0	7.85×10^{-6}	0.3	0.24
FPS mounts, Fascia of the steel bulbar and tubular sections		215.0	7.85×10^{-6}	0.3	0.225
Bumperettes (Semi-rigid polyurethane)		0.39	9.27×10^{-7}	0.35	-
Alloy fascia and tubular sections		70.0	2.6×10^{-6}	0.27	-

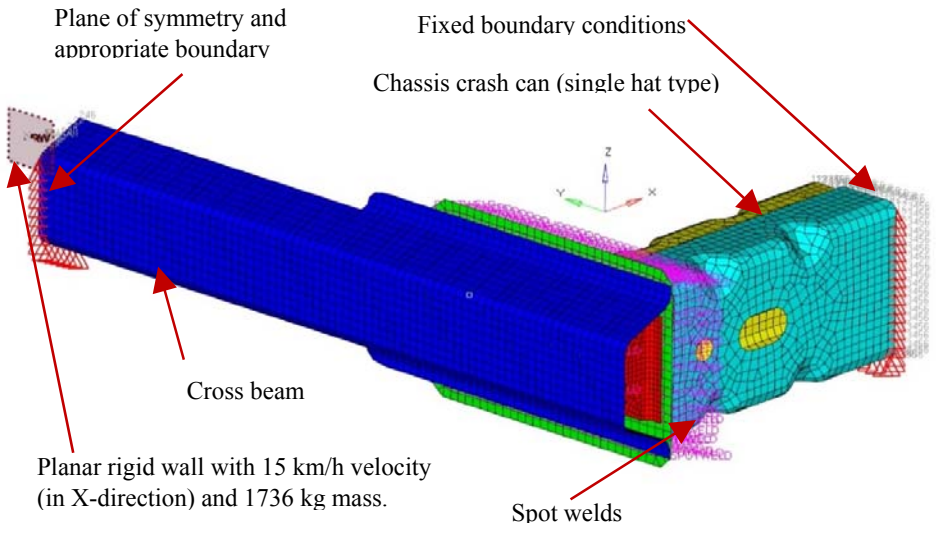

Figure 7.10: Set up of the simplified crash analysis, which is equivalent to dynamic pendulum test

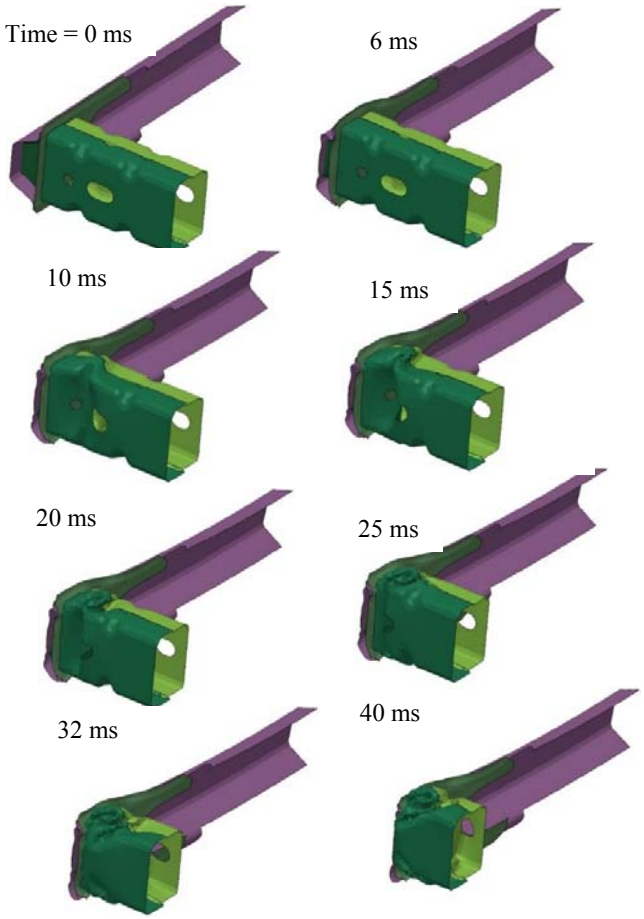

Figure 7.11: Stages of crumpling crash can and cross member assembly (when impacted with a rigid wall of 1736kg, moving with 15 km/h velocity). Due to symmetry of the assembly, for the sake of clarify, only LH side of the assembly was shown.

If any VPFS is mounted to the chassis, crush characteristics of the crushcan will be entirely different, and it may be detrimental to the occupants of the vehicle as it alters the crash characteristics of the vehicle front end. Therefore, similar simplified analysis were carried out with three configurations of the FPS mounts (Flat plate, plate with a fold and corrugated box) attached to the crushcan –CROSS_MEMBER assembly.

This exercise is for the selection of an appropriate FPS mount configuration that nullifies the effect of stiffening the crushcan. From the simulation output, deceleration pulses were obtained and compared with that obtained for the only chassis and cross-member assembly. All configurations of the FPS mount were shown in the Figure 7.12.

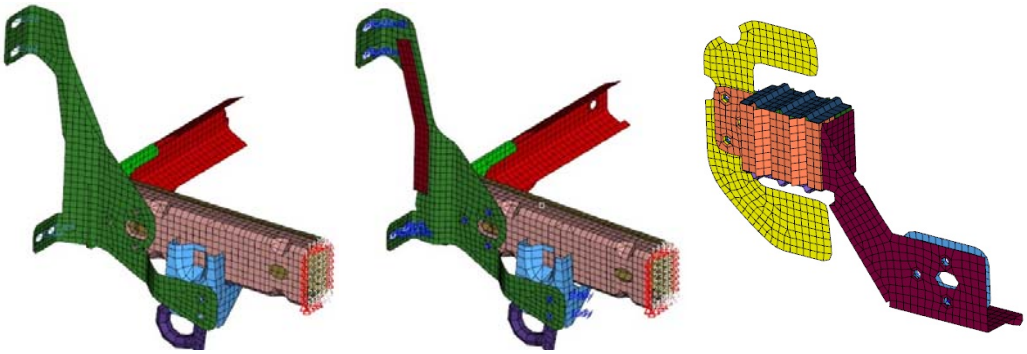

Figure 7.12: Configurations of the FPS mounts (from left to right: Flat plate, Plate with a fold, Plate with a corrugated box). Due to symmetry of the FPS and chassis assembly, for the sake of improving clarity, only LH mounts were shown.

After few simulation iterations, though results were promising, FPS mount with box section was not considered for the further study, owing to the higher weight, complexity in design and many design variables.

In the case of flat plate (even with 6 mm thickness), the deceleration pulse obtained had peaks higher than the reference pulse. The peak deceleration increased with the increasing thickness. Flat plate either provided weak or stiff mounts for the FPS, and both were not desirable. It is important to note that in simplified crash simulations of the mounts, steel bumper replacement FPS was considered.

Stages of crash of steel bulbar with ‘plate with a fold’ FPS mounts during the simplified crash analysis were as shown in the Figure 7.13. For the sake of clarity and also due to the symmetry, only LH portion is considered for the presentation.

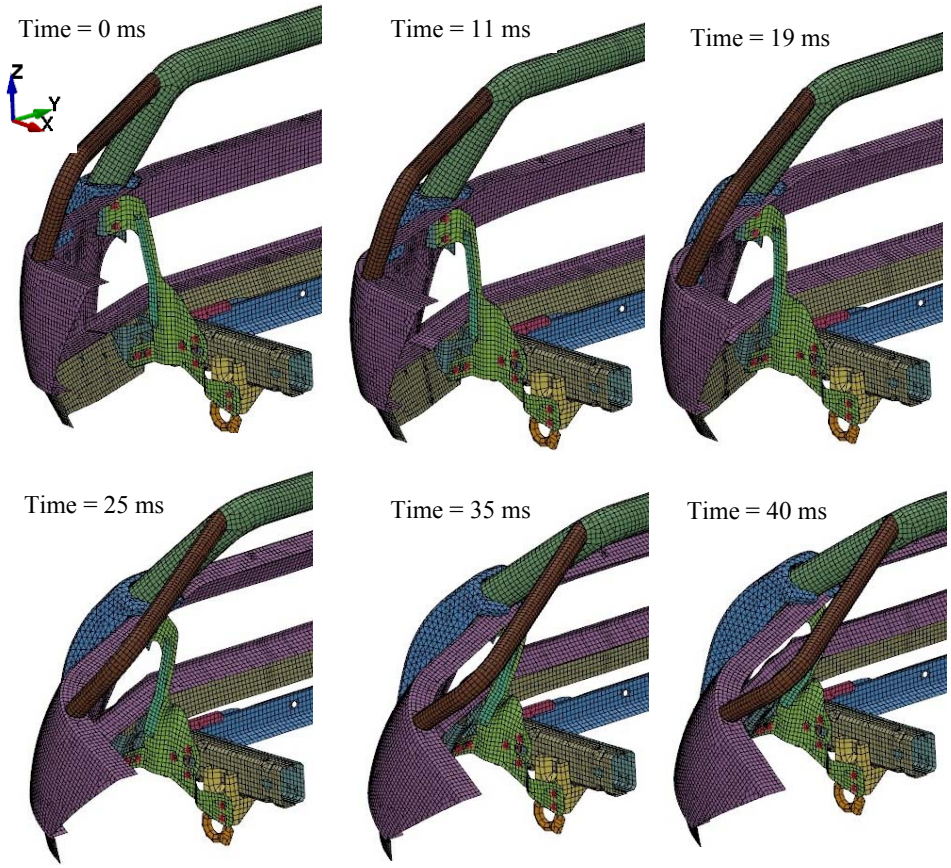

Figure 7.13: Stages of crushing steel bull bar with 'plate with a fold' mounts (15 km/h, full frontal simplified crash simulations)

Deceleration pulses obtained for two FPS mounts ('flat plate' and 'flat plate with a fold') were shown in the Figure 7.14. For the sake of comparison, deceleration pulse obtained for 'chassis cross-member' assembly was also displayed in the same plot.

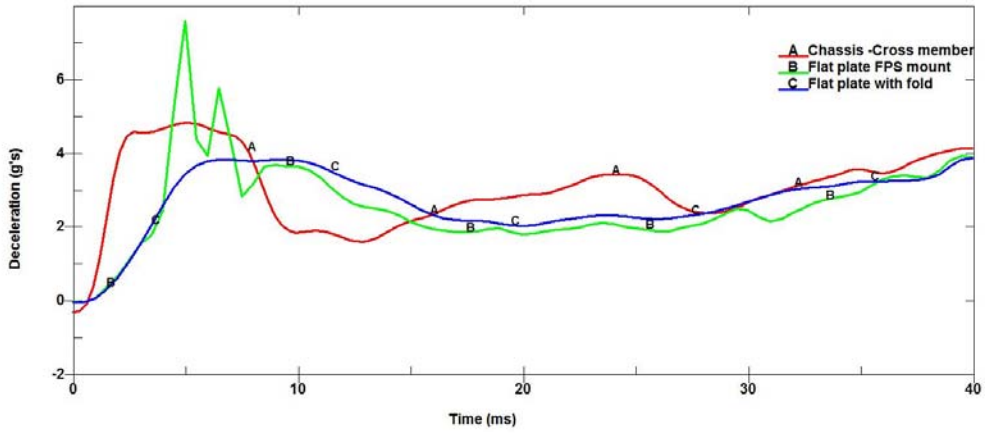

Figure 7.14: Deceleration pulses elicited from the simplified CAE simulations

Deceleration pulse obtained with the 'plate with a fold' FPS mounts was smooth and varied with the position of the fold and dimensions of the fold. With the plate thickness 8 mm and a fold, deceleration pulse obtained was smooth and comparable with the reference pulse.

Addition of the brackets to the 'crushcan' alters (by increasing its stiffness) its crush characteristics. It is clear from the Figure 7.14 that the fold is working to rebuild the crush characteristics of FPS mount – chassis assembly. Owing to the simplicity of design, ability to fine tune the deceleration pulse, 'plate with a fold' mount was considered and finalized the bumper replacement type of FPS design for the Ute under consideration. By varying the fold dimensions, location of the fold and other design parameters such as the thickness of the mounts and material grade, etc. deceleration pulse obtained with the FPS, mounts, chassis assembly can be made similar to the reference deceleration pulse.

It is important to mention that all of the bolts considered for the FPS mount in the CAE simulations were 12.9 grade. Bolts of lesser strength failed well before 12 ms after the impact. Material model *MAT_SPOTWELD_DAMAGE_FAILUE. *SECTION_BEAM were used for the bolt modeling.

7.4.4 ADR 69/00 full frontal vehicle crash tests

Production representative samples were made with the finalized steel FPS design and full frontal vehicle crash test was conducted and very first test vehicle fitted with the Steel FPS achieved the ADR 69/00 compliance by performing well enough to meet the minimum set occupant safety requirements.

7.5 Conclusion

From the application of devised systematic method to develop baseline design of the FPS, the following conclusions were drawn.

Even for the vehicles equipped with no airbags, mass setting calculations are necessary as every vehicle axles are designed to withstand only certain amount of loads. Two or more variants of a vehicle having same GVM and same in size and shape does not necessarily mean that they have got the same GAW-FRONT AXLE. This was very evident from the mass setting calculations of the 1 and 2 variants of the Ute.

Evaluation of the loads due to all accessories would help the project engineering personnel to make executive decisions. For instance, for the variant-2 of the vehicle, allowance on the GAW-FRONT AXLE was 22 kg. With this allowance, steel bull bar of 37 kg is not suitable for the fitment. Bumper removal would provide 10 kg more allowance. Fitment of the tow-bar and 'rear protection bar' would provide an additional 13.6 kg (refer the Table 7.2 and 7.3), which makes the total GAW-FRONT AXLE 45.6 kg and makes the vehicle variant suitable for the fitment of the above said FPS.

Complete knowledge and awareness of the methodology resolves many design issues during the concept stage itself.

Baseline designs developed using a systematic procedure and mass setting calculations not only makes the further steps easy but also improves the vehicle's performance and life with increased occupant safety.

The technique of using simplified crash simulations were proven very handy for the selection of the suitable mounts, bolt design and achieving the ADR 69/00 compliance with the very first crash test.

Therefore, with the systematic engineering approach based methodology can make vehicle front protection systems compliant with AS 4876.1-2002 and ADR 69/00 compliant. So far, this method was successfully implemented and developed 11 bull bars for various vehicles for aftermarket accessory developers in Australia and Thailand.

CHAPTER-8: VEHICLE FRONT PROTECTION SYSTEMS: A SYSTEMATIC CAE BASED METHOD TO ACHIEVE AIR BAG COMPATIBILITY

This chapter represents the summary of the technical article titled 'Vehicle front protection systems: CAE based methodology to achieve airbag compliance' published in the International Journal of vehicle structures and systems. This chapter also discusses Head Injury Criterion (HIC) related aspects and effect of the FPS fitted vehicles on 'crash compatibility' with other vehicles. Details of the technical papers those published and under consideration for publication were given in the Appendix – I of the thesis.

8.1 Introduction

Due to the high prevalence of vehicle-animal collisions in Australian rural areas, many vehicles, not limited to recreational 4WD vehicles, are fitted with the variety of vehicle front protection systems (VFPS) to protect not only the components under the bonnet but also occupants of the vehicle. VFPS also provides additional protection to the occupants and systems in the engine bay, when involved in low-speed crashes. VFPS are categorized mainly into two types: 1 – Over the bumper (such as nudge bar and loop bar) and 2 – Bumper replacement type (Steel, Alloy and Plastic bull bars). VFPS (depending upon the type, design of the mounting brackets and mounting points) significantly influences the crush characteristics of the vehicle. Changes in the vehicle crash signature (crush pulse or deceleration pulse) affect the airbag deployment characteristics. With the altered crash pulse, airbag may not get deployed when required, and it may get deployed when not necessary (very low speed impacts). In the former case, passenger safety is compromised as airbag did not get deployed during the serious accident and in the latter case, premature or delayed deployment of the airbag (punch out loading and membrane forces) itself may inflict serious injuries to the driver and passenger (Lau et al. 1993). In a nutshell, if the VFPS is not compliant with airbags, it can make the vehicle that is otherwise compliant with all safety standards and local design rules), not roadworthy. Therefore, airbag compatibility is very crucial and mandatory requirement for all VFPS. A systematic CAE based method was devised for accomplishment of the airbag compatibility of the VFPS and applied to many real life projects. In this chapter, devised method and a case study (development of 5 variants of FPS to a vehicle with 8 variants) to demonstrate the efficacy of the method were presented.

8.2 Various other methods in use and their limitations

Many researchers have, so far, analyzed accident databases, studied the prevalence of bull bars and their detrimental effects on the pedestrian safety (Anderson et al. 2009; Anderson, Ponte & Doecke 2008; Attewell & Glase 2000; Chiam & Tomas 1980; Doecke, Anderson & Ponte 2008; Hardy 1996; Lawrence & Hardy 1992; Rowden, Steinhardt & Sheehan 2008; Thota, Eepaarachchi & Lau 2013c). Australian standard AS 4876.1-2002 published by Standards Australia made a great emphasis on minimizing the pedestrian injury risk due to colliding with a vehicle equipped with a VFPS (Australia 2002). Every bull bar sold in Australia must comply with AS 4876.1-2002 (i.e., for the pedestrian safety, Head Injury Criterion $\leq$ 1000 and the occupant safety, compliance with the ADR 69/00). Only few have studied and published the

research related to the airbag compliance of the vehicle front protection systems. There are few methods in use for achieving the Airbag compatibility and ADR 69/00 compliance. These methods, their limitations, and advantages discussed below.

8.2.1 Pendulum test

Pendulum test is commonly used by VFPS manufacturers for the ADR 69/00 compliance and also for airbag compatibility. One of the famous pendulum test facility of the bull bars is shown in Figure 8.1.

Figure 8.1: Pendulum test rig for the dynamic testing of the bull bar (Adapted from the website of Automotive Safety Engineering

In this test, FPS being tested will be subjected to the pendulum impact by adjusting the mass of the pendulum so such a way that it represents a vehicle for which FPS is designed. Deceleration pulse, deformation, velocity and energy absorption by the FPS are the outcome of the pendulum tests. This is low cost test as only FPS being tested will get damaged. There are many bull bars (aftermarket) with the claim that they are airbag compliant, and most of the manufacturers perform pendulum test. Though the deceleration pulse obtained from the pendulum test provides some clue on the performance of the bull bar, that test is not enough to determine the airbag compatibility as the test does not take vehicle structure, sensors and their mounting points into consideration.

A researcher (Bignell 2004) has conducted quasi-static and dynamic pendulum impact tests on 100 VFPS of various kinds, and concluded that VFPS require no further testing if the energy absorbed by 'over the bumper' type loop bar is less than 4% of the total impact energy. In the case of 'bumper replacement' type, the energy absorbed should be less than 8% of the total impact energy. In both quasi-static and dynamic pendulum tests, vehicle structure was not taken into consideration and VFPS was fitted to a rigid fixture. Vehicle front end structures were developed to meet the stringent occupant safety requirements. Airbag trigger algorithms are very complicated due to many airbags in the current day passenger cars and also due to many sensors mounted on desired critical locations on the car. Therefore, just energy absorption of the VFPS is not helpful to decide whether it is the airbag compliant or not. Sredojevic et al. (Sredojevic & Zivkovic 1998) has conducted experiments and recommended that lowest deceleration to trigger the airbag as 12g for 4WD recreational vehicles and 3.5g for sedan passenger vehicles. Sredojevic et al. has not mentioned any information

about the vehicle structure, sensor type and location, etc. Therefore, the outcome is vehicle specific (only applicable to the vehicle used in the study) and can't be applicable to decide whether VFPS have got the airbag compliance for other vehicles.

8.2.2 Barrier crash test

In the barrier test full vehicle fitted with the FPS impacts either a rigid wall or deformable barrier with the velocity specified (both barrier and impact velocity selected as per the 'airbag no fire', 'airbag must fire' and 'ADR 69/00 test protocols). Though this is a mandatory test before releasing the FPS into the market, commercially it is not viable as it may require few physical crash tests to achieve the ADR 69/00 compliance of the FPS.

Some vehicle manufacturers develop FPS as the part of the vehicle development program. Means, they perform complete regime of crash tests with the vehicle fitted with the FPS and develop new ECU with airbag crash sensing algorithm. Though this is very efficient method, it is very expensive. Buyer of the vehicle need to replace the original ECU with that designed for the vehicle with the FPS. Therefore, additional expenses for the purchaser.

Though many vehicle manufacturers provide VFPS as genuine accessories with airbag compatibility, there is no published research on the methodology and test specifications related to the airbag compliance. It is illegal to fit the bull bar to any passenger vehicles unless the vehicle with the bull bar is crash tested to meet the safety standards. Though most of the 4WD vehicle owners tend to go for some bull bar, revenue generated by the sale of VFPS, physical tests are not commercially viable, especially when bull bar manufacturers want to produce 5 – 6 types of vehicle front protection systems for every vehicle. Due to the variation in the material, design of the fascia and tubular sections, mounting bracket design and mounting locations, to accomplish the airbag compatibility, for every variation of the bull bar would require many physical crash tests. Most importantly, the development process is iterative, as the first design itself may not be airbag compliant. Therefore, physical tests are commercially not viable. Another problem that poses great hindrance to the development of airbag compliant VFPS is vehicle manufacturers' secrecy pertaining to the airbag triggering algorithm. In this chapter, authors have presented the systematic method devised that is based on the virtual testing, to produce all variance of the VFPS with the airbag compatibility, for any vehicle with a minimum number of physical crash tests. Authors have also presented a real-life case in which 5 variants of FPS were developed for a utility vehicle that has got 8 variants.

8.3 Airbag compatibility

All passenger cars undergo rigorous crash tests to achieve the compliance with Australian standards and Australian design rules pertaining to the safety (occupant and pedestrian) and performance. Though NCAP safety ratings vary based on the performance of the vehicles, only those comply with the safety standards released to the market.

Though initial days, premature deployment of the airbags have caused serious injuries, in conjunction with seatbelt restraints, they evolved to be most important safety features of the modern day passenger cars due to the robustness of the frontal crash

sensing algorithms. These airbag triggering algorithms developed using the crash pulses obtained from the wide variety of physical crash tests in a simulated environment and also the pre-crash and post-crash data from the event data recorders of the vehicle (Chidester, Hinch & Roston 2001; Correia et al. 2001; Ueyama et al. 1998).

For every vehicle equipped with airbags, manufacturers would define velocity thresholds for 'airbag no fire' and 'airbag must fire' scenarios (Chan 2000; Chan 2002b, 2002a). For the utility vehicle under consideration, these velocity thresholds are given in Figure 8.2.

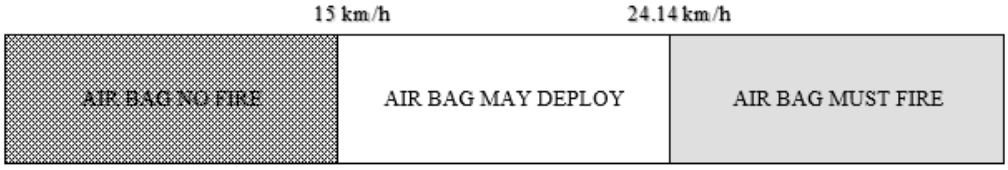

Figure 8.2: Details of the velocity thresholds for the airbag deployment (Adapted from Bignell 2004)

Irrespective of the type of the VFPS and whether any parts need to be removed from the front-end structure of the vehicle to fit the VFPS, the vehicle equipped with the FPS must pass the following tests in order to consider the VFPS as airbag compatible.

Airbag no fire test: This test is a low speed crash test in which vehicle fitted with the FPS impacts a 40% offset rigid barrier at 15 km/h speed. During the impact, air bag should not fire and also the deceleration pulses obtained from two airbag sensors must pass the air bag triggering algorithm's requirements. In some cases, authors have witnessed that deceleration pulses obtained from the G-sensors did not meet the requirements of the air bag algorithm, though the airbag did not get deployed.

Airbag must fire test: This is moderate speed crash test in which vehicle fitted with FPS impacts a 40% offset rigid barrier at 24.14 km/h speed. During the impact, not only airbag must fire, but also the deceleration pulses obtained from two G-sensors must pass the air bag triggering algorithm.

Australian Design Rule 69: During the high speed impact, severity of the injuries solely depends on intrusion of the passenger compartment and deceleration levels experienced by the occupants. In order to improve the passenger safety, Australian Federal Office of Road Safety has developed Australian Design Rule 69 and every vehicle (whether or not equipped with airbags) sold in Australia must meet the specific injury criteria (Hollowell et al. 1999; Morris et al. 2001). Test specification and performance standards are as given in Table 8.1. Therefore, irrespective of the type of the FPS, it is mandatory to prove that fitment of the FPS did not degrade the ADR69 test performance of the original vehicle.

Table 8.1: ADR69 test specifications and performance criteria

Crash barrier	Full frontal rigid barrier to conform the SAE document J850 (1963) or FMVSS 208 rigid barrier
Speed of impact	48.3 km/h
Occupants	Belted Hybrid III dummies
Head injury	HIC ≤ 1000
Chest deflection	Sternal deflection must not exceed 76.2 mm
Chest deceleration	Must not exceed 60g
Femur load	Axial force must not exceed 10 kN

From the specifications, it is evident that airbag compatible FPS development would require many vehicles for the crash tests. Authors have witnessed VFPS development program which took three crash tests for visual pass of the “airbag no fire” test and, unfortunately, the vehicle deceleration pulse did not pass the “airbag deployment related crash sensing algorithm." Because of the exorbitantly expensive crash test and vehicle costs, non-availability of prototype vehicles and cost of making production representative samples for every design iteration, development of airbag compliant VFPS becomes commercially non-viable. The development process becomes practically impossible, if multi-variant FPS systems are required for multi-variants of the same vehicle. A CAE based novel methodology to develop airbag compatible VFPS (all variants of FPS to all variants of a vehicle) with only minimum physical crash tests was devised and presented in the subsequent sections of this chapter.

8.4 Methodology

The CAE based method consists of the following major phases.

Phase–1: Development of the baseline design of VFPS

Phase–2: Simplified crash simulations for the selection of the proper design for VFPS mounts.

Phase–3: Development of correlated FE model of the whole vehicle

Phase–4: Finalization of the FPS design with full vehicle CAE crash simulations.

Phase–5: Full vehicle physical crash tests as per the specifications

8.4.1 Baseline design of the VFPS

Mass setting calculations to evaluate the allowable maximum weight of the FPS, selection of the mounting points, conceptualization of the mounts, styling to conform the vehicle contours and fascia design not to alter the cooling characteristics and accessibility of the recovery hooks, etc. were discussed in the Chapter – 7. Therefore, only process flow chart to suit the present context is given in Figure 8.3.

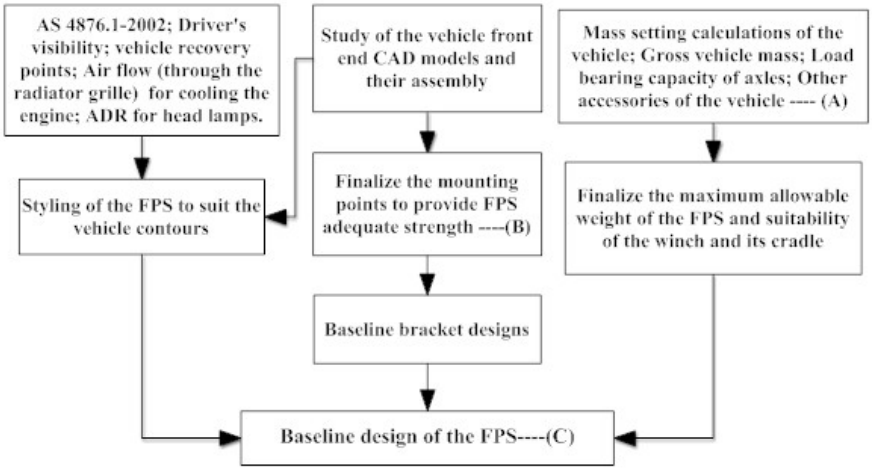

Figure 8.3: Procedural steps and input data requirements for the baseline design of the FPS

8.4.2 Simplified crash simulations for finalization of the baseline design of the FPS mounts

After selection of the mounting points, development of the FPS mounting brackets becomes an easy task. Design configurations such as plate with a fold, corrugated box and box section with weak points are suitable for mounting bracket design. Crash simulations involving whole vehicle model is computationally very demanding. Therefore, selection of the concept FPS and finalizing the design entails numerous vehicle crash simulation iterations, and the process becomes tedious.

A novel method of using simplified crash simulations equivalent to dynamic pendulum tests would be very useful to select the baseline design of the FPS mounts. The procedural steps were as shown in Figure 8.4

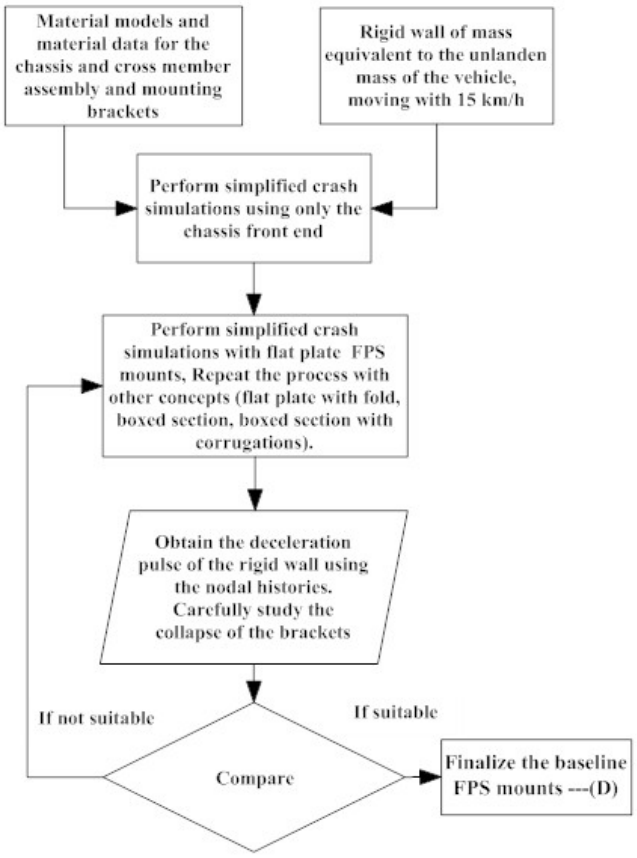

Figure 8.4: Procedural steps and input data requirements for the simplified crash simulations

This process of selecting the proper configuration of the FPS mounts, through the dynamic tests through virtual simulations, is very beneficial, and there would be a considerable reduction in the number of full vehicle crash simulations required

8.4.3 Development of the correlated FE model of the vehicle

Most of the vehicle manufacturers do develop correlated FE model of the vehicle for various compliance tests in a virtual environment to exploit the benefits offered by the CAE technology. Correlated full vehicle models for crashworthiness related simulations can be directly utilized for the full vehicle crash simulations pertaining to the airbag compatibility (Airbag no fire, airbag must fire and ADR 69 test). If not available, correlated FE model of the vehicle can be developed, and procedural steps for the same were as shown in Figure 8.5

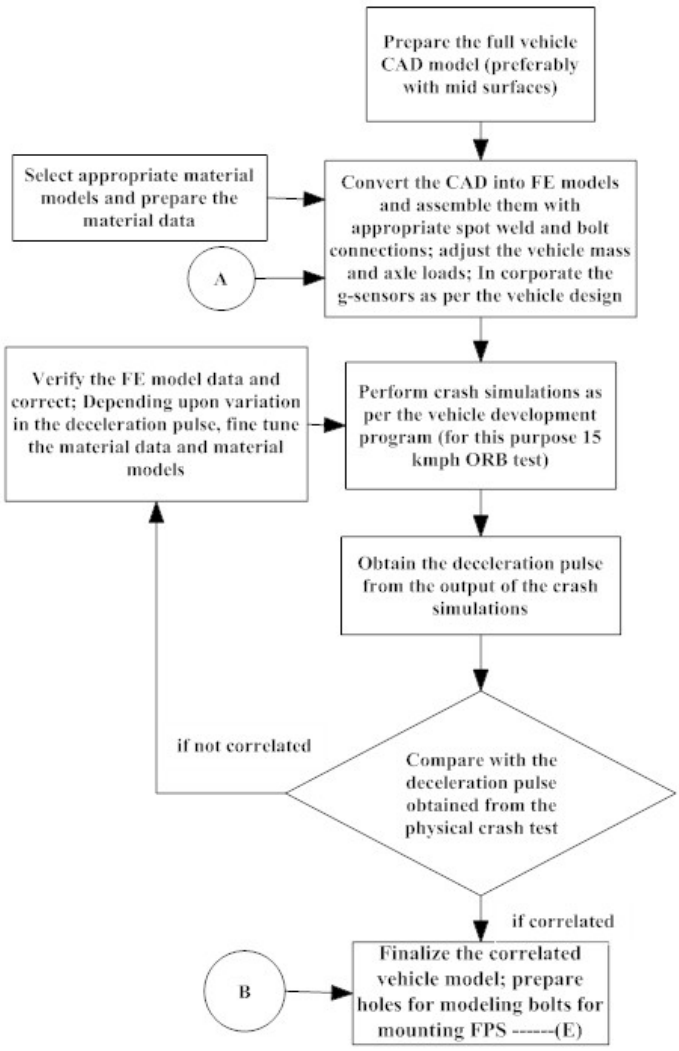

Figure 8.5: Procedural steps for the development of whole vehicle model correlation

8.4.4 Whole vehicle crash simulations for finalization of the FPS design

With the availability of correlated FE model of the entire vehicle, the baseline design of FPS fascia and tubular sections, mounting locations and baseline design of the mounts, the next step is performing full vehicle crash simulations. As it is very crucial step in the airbag compatible VFPS development, procedural steps shown in Figure 8.6 must be followed strictly. From the output of the every crash simulation, using the nodal time histories, deceleration pulses obtained for the nodes representing the front sensor and ECU sensor must be sent to vehicle manufacturer or airbag developers to review the airbag compliance of the VPFS. Using the airbag deployment crash sensing algorithm, vehicle manufacturers analyze the crash pulse and would confirm the airbag compliance of the FPS.

As already dynamic tests were carried out to select the appropriate design of the FPS mounts, with very minimum (3-5) full vehicle CAE simulation iterations, airbag compatible FPS mounts can be developed. Though theoretically these mounts are airbag compatible, and ADR69 compliant, physical crash tests are mandatory to release the FPS into the market as airbag compliant. Simplified crash simulations would reduce the number of whole vehicle crash simulations and together would reduce the number of physical crash required to 3. In case, multi-variant FPS for multi-variants of the same vehicle, complete vehicle crash simulations would play a vital role in reducing the physical crash tests.

8.4.5 Full vehicle physical crash tests for the development of ADR 69 compliant VFPS

Virtual tests are only useful to gain confidence in the design and results obtained from these simulations are not helpful to release the VFPS as an airbag compliant accessory into the market. Therefore, the final step is to carry out physical crash tests to attain the ADR 69 or airbag compliance. The crash test protocol is as shown in Figure 8.7.

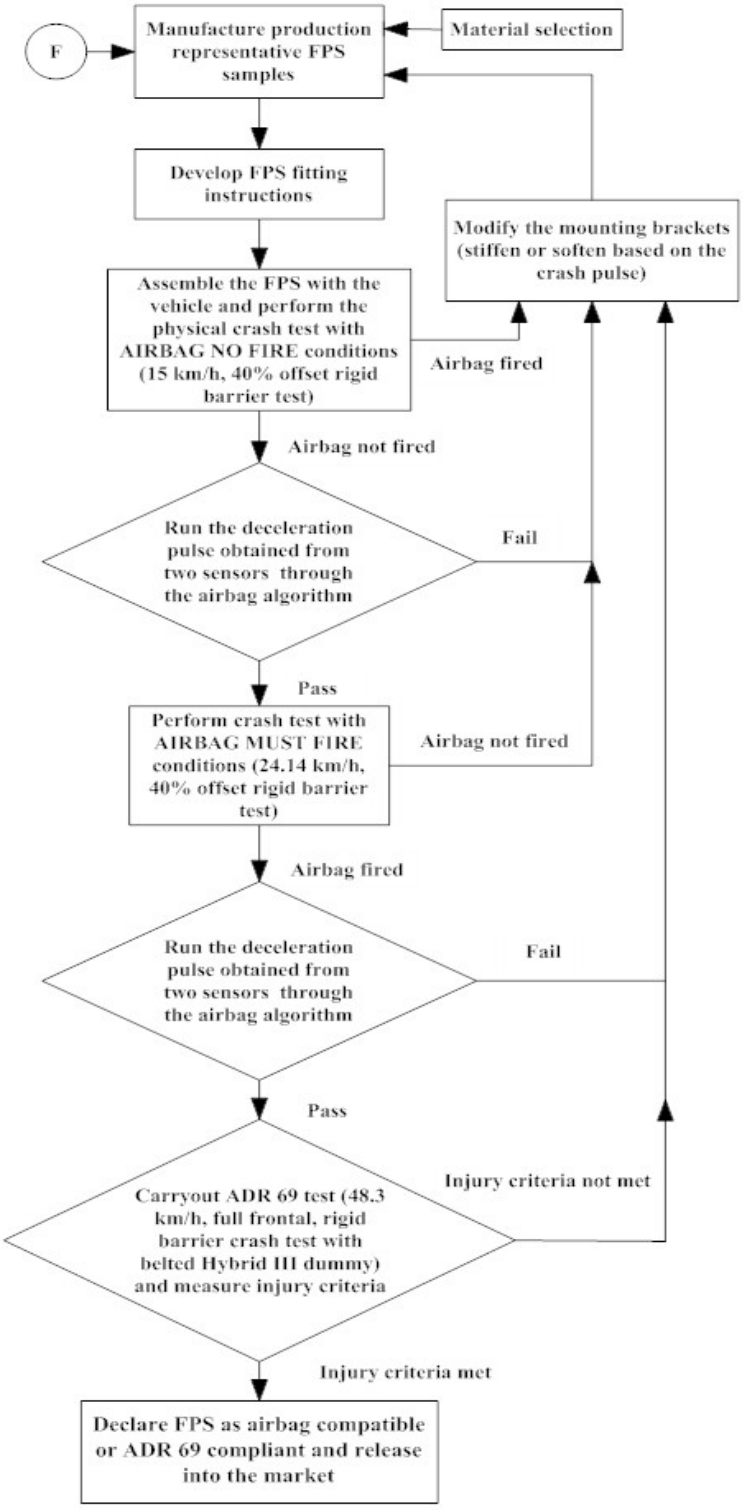

Figure 8.6: Protocol of the whole vehicle crash simulations to accomplish the airbag compatibility and ADR 69 compliance

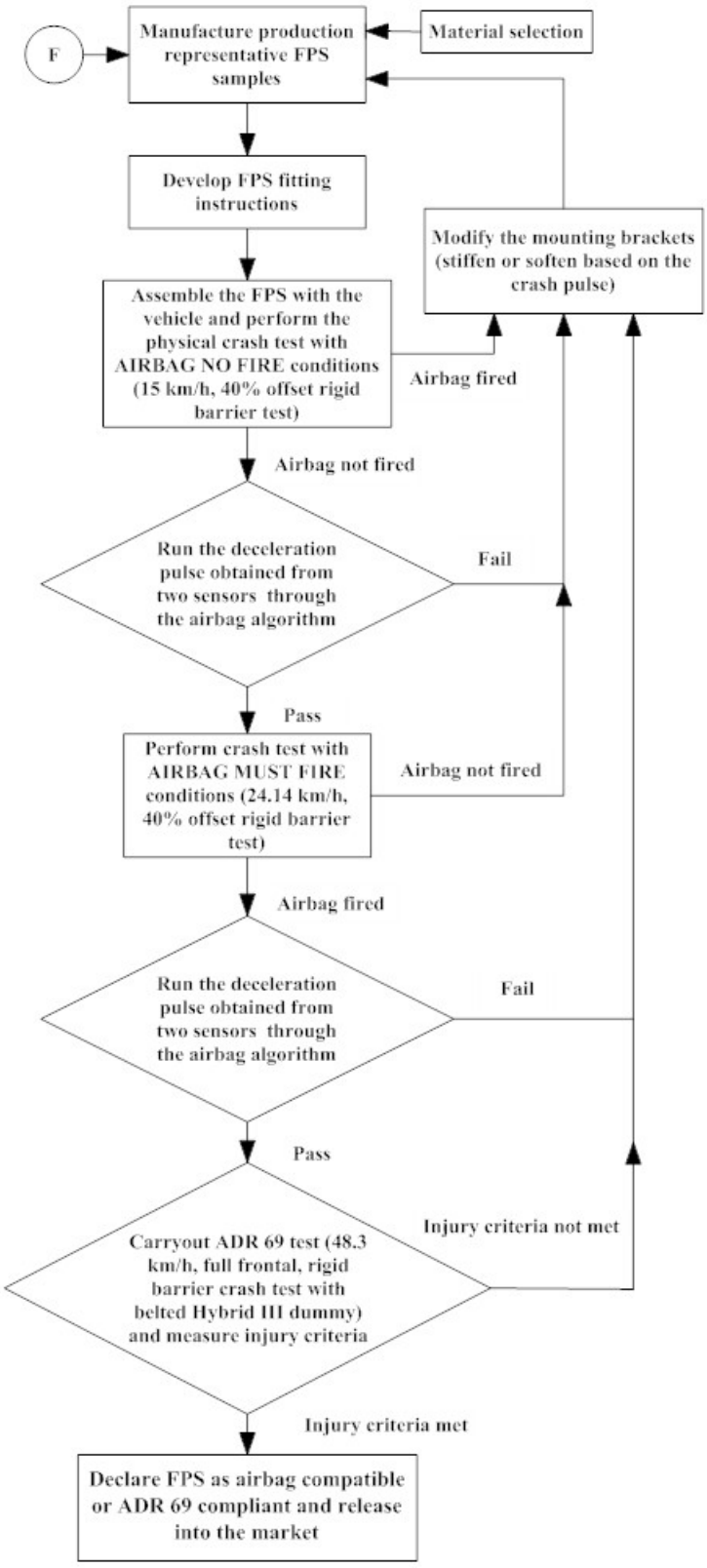

Figure 8.7: Protocol of the physical crash tests of the vehicle fitted with FPS to accomplish the airbag compatibility and ADR 60 compliance.

Authors have not only devised the above technique, also developed ADR 69 compliant or airbag compatible VFPS for many passenger vehicles. Following the same method, irrespective of the number of variants of vehicle, all variants of ADR compliant FPS (Steel bull bar, Alloy bull bar, Alloy nudge bar, Alloy loop bar and plastic loop bar) were developed with the minimum number of physical crash tests. The case study demonstrates the significance of the devised method.

8.5 Results and discussion

The design of the VFPS that is finalized in the Chapter-7 for the same Ute can be considered as the baseline model for the development of the airbag compatible and ADR 69/00 compliant FPS. Because every step mentioned in the sections 8.4.1 and 8.4.2 were systematically executed to achieve the final design of the VFPS in the Chapter-7.

8.5.1 Whole vehicle (Ute) FE model correlation

Partly build FE model of the vehicle (a typical compact Ute) under consideration was supplied by the vehicle manufacturer. Hypermesh – a general purpose pre-post processor was used for meshing the missing parts of the vehicle. Mass setting calculations outcome was used to fine tune the model so that axle loads match with the designed GAWR for both front and rear axles. 15 km/h physical crash test data (deceleration pulses obtained from the front sensor and ECU sensor during the prototype vehicle physical crash test) was provided for the correlation of the FE model.

Stages of crashing car during the impact, Deceleration pulse of the ECU sensor, velocity – time plot obtained from the front sensors for one of the simulation iterations to achieve correlation were as shown in the Figure 8.8. In all only 3 iterations were carried out to achieve the correlation of the FE model of the whole vehicle with the physical crash tests of the prototype vehicle.

Vehicle manufacturers removed the plastic bumper, bumper stay, hood, hood reinforcement, left and right fenders and their reinforcements while doing the 15 km/h, 40% offset rigid barrier test (air bag no fire test specifications). Therefore, in the correlation CAE model, all these parts were removed.

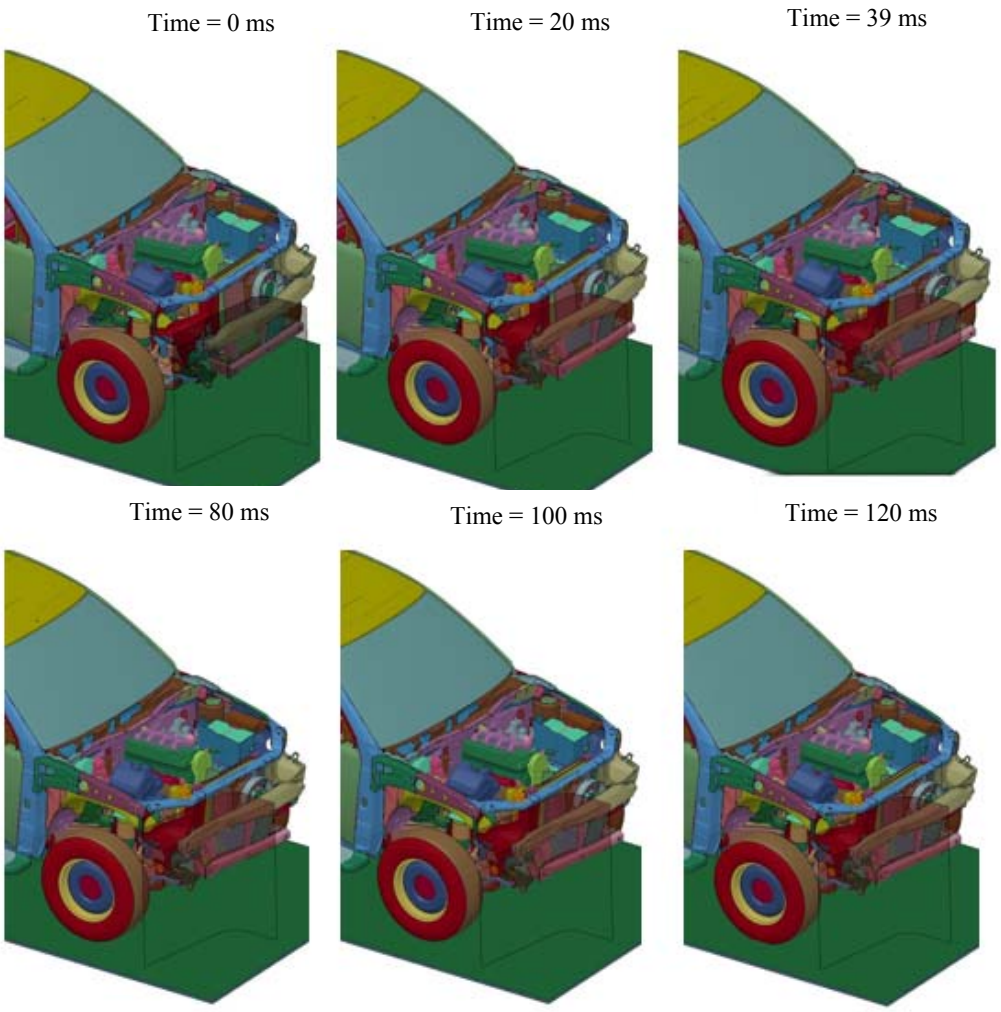

Figure 8.8: Stages of the vehicle during the crash (Correlated CAE vehicle with 15 km/h ORB test)

8.5.2 Full vehicle crash simulations

Full vehicle CAE crash simulations were carried out with 'airbag no fire' test conditions by integrating the FE model of the baseline steel bull bar with correlated vehicle model. Rigid barrier FE model freely available to LS-DYNA users was used in the simulations with 40% offset. Bolts were modeled with beam and spider connections. Stages of the vehicle during the impact were as shown in Figure 8.9.

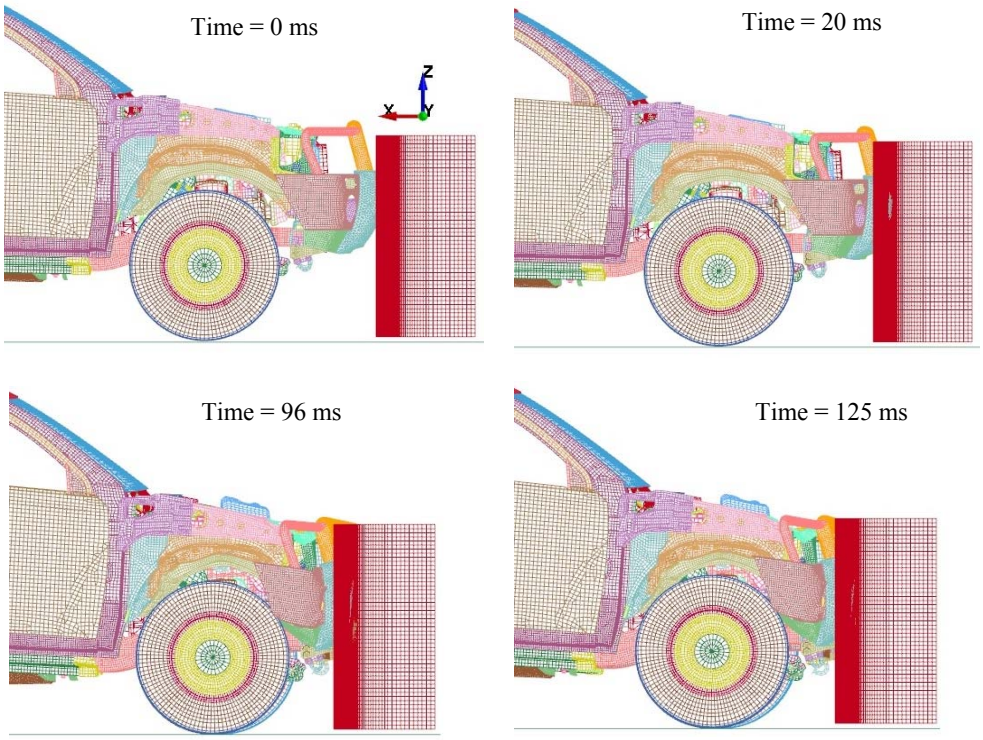

Figure 8.9: Stages of the impacting vehicle fitted with bumper replacement type of steel bull bar (40 % offset rigid barrier, impact velocity 15 km/h, 'airbag no fire' test condition)

Deceleration pulses obtained from the sensors (both front sensor and ECU sensor) were sent to the vehicle manufacturer for review of airbag compatibility. As the first design of mounts were found to be "non-compatible" with airbag, by varying the design parameters of the FPS mount (size and location of the fold), airbag no fire test CAE simulations were carried out. Deceleration pulses obtained from every simulation were sent for a review of airbag compatibility. Airbag 'no fire' test specification compliant FPS mounts were evolved with four iterations of CAE simulation. Four variations of the FPS mounts and outcome from the 'airbag crash sensing algorithm' were as shown in the Figure 8.10. The deceleration pulse from the front sensor and ECU sensor, velocity – time plot from the front sensor for all relevant cases will be presented in the subsequent sections.

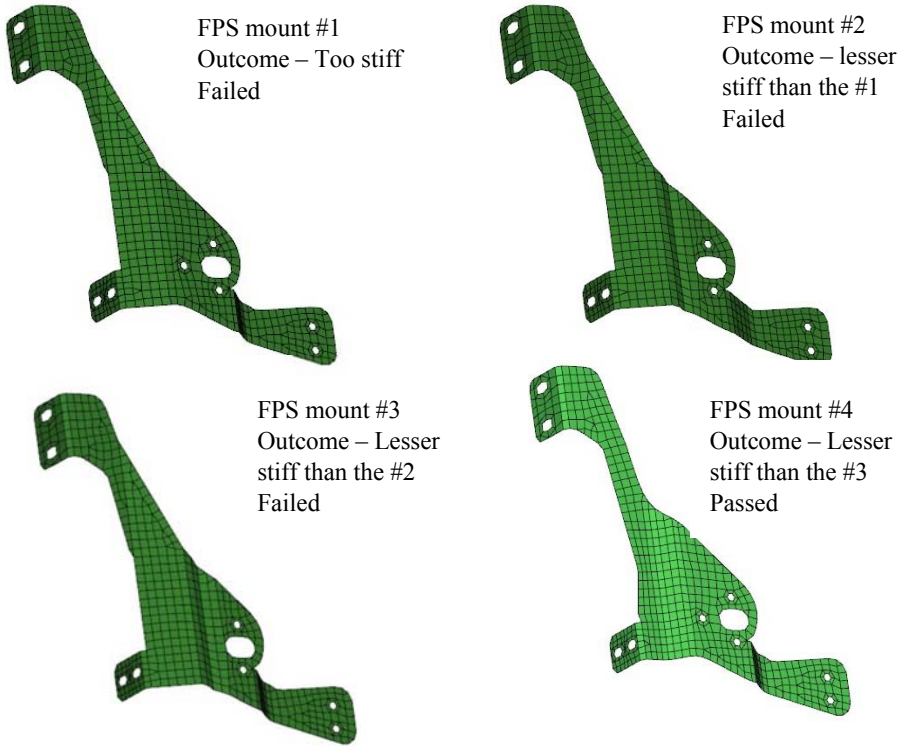

Figure 8.10: FPS mounts used in 4 CAE simulation iterations carried out with 'airbag no fire' test conditions (outcome from the airbag crash sensing algorithm is also mentioned in the picture along with the comment on the stiffness)

Using the finalized FPS mounts, CAE simulation with 'airbag must fire' test conditions (40% offset rigid barrier, 24.14 km/h impact speed) was carried out. Deceleration pulses obtained from the analysis were analyzed by using 'airbag crash sensor triggering algorithm.' The very first iteration, FPS mounts have accomplished the 'airbag must deploy' requirements. Similarly, deceleration pulses obtained from the CAE simulation iteration carried out (with ADR 69 test specifications), were analyzed and found that FPS mounts were ADR 69 compatible. The developed bumper replacement type of steel bull bar is, therefore, theoretically airbag compatible and ADR 69 compliant.

It is crucial to note that the airbag compliant and ADR 69 compliant FPS mount # 4 has got very little differences when compared to the FPS mount finalized through the simplified crash simulations. Due to the involvement of the airbag manufacturer, four designs of mounts were used in the full vehicle crash simulations so that deceleration pulses can be analyzed for the airbag compatibility at the same time. In the case all four were found to be non-compatible with the airbag, outcome on the four variations would have been very helpful to develop potentially suitable design for the airbag compliance.

8.5.3 Problem associated with the development of multi-variants of FPS for multi-variants of the vehicle model

The vehicle considered for the case study has got eight variants (vehicle unladen weight ranging from 1736 kg – 1880 kg), and goal was to produce 5 variants of the FPS (2 bumper replacement type and 3 over the bumper type) for each vehicle. Even with CAE based methodology too, at least 8×5×3 = 120 vehicles for physical crash tests are required to obtain 'airbag no fire,' 'airbag must fire' and 'ADR 69' compliance. To minimize the physical crash tests, authors have decided to use the same brackets and mounting points to all variance of the FPS for all variance of the vehicles. A new FPS mount design was developed using the FPS mount #4, without altering its crash characteristics (Figure 8.11).

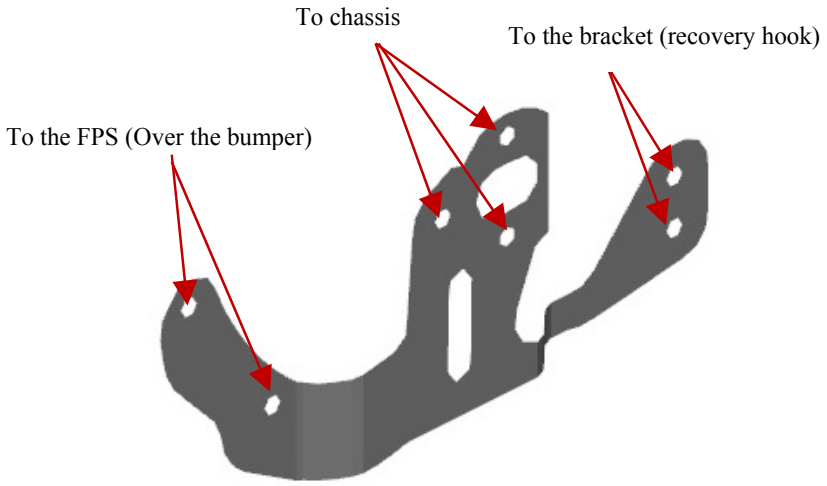

Figure 8.11: Mounts designed for over the bumper type of FPS using the finalized brackets for steel bumper replacement type bull bar). For the sake of clarify, only RH side of the bracket is shown along with the mating parts

As there were no differences in the vehicle front-end structures of all variances and also utilizing the same mounting points and mounts with the same crash characteristics, following tests (both CAE simulations and physical crash tests) would suffice to prove the airbag compliance of all FPS for all variance of the vehicle.

a) 'Airbag no fire' test
    1. Vehicle with lowest unladen mass fitted with lightest variant FPS (already carried out and the airbag compliance was achieved)
    2. Vehicle with highest unladen mass fitted with the heaviest variant FPS

b) 'Airbag must fire' test
    1. Vehicle with highest unladen mass fitted with the heaviest variant FPS

c) 'ADR69' test
    1. Vehicle with highest unladen mass fitted with the heaviest variant FPS

Correlated model was adjusted to emulate the heaviest variant of the vehicle and remaining CAE simulations were carried out. For every simulation nodal time histories, deceleration pulses were elicited and sent for the review. All five variants have passed the airbag crash sensing algorithm and theoretically qualified as airbag compatible or ADR69 compliant.

Though CAE simulations were performed by integrating all variants of FPS with the two vehicle variants with highest and lowest unladen mass, stages of vehicle fitted only with the alloy nudge bar during the crash (15 km/h, ORB 'airbag no fire' test) were as shown in the Figure 8.12.

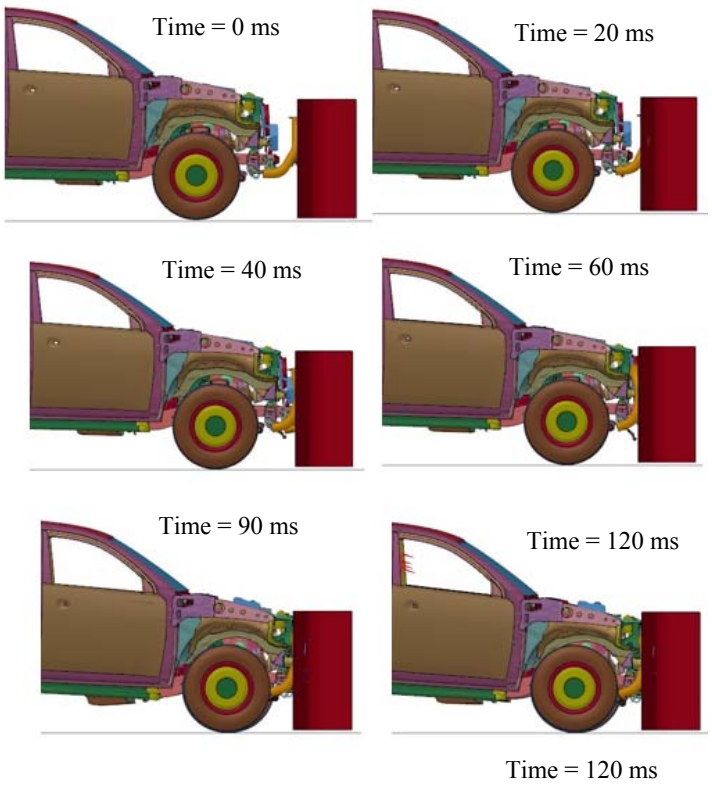

Figure 8.12: Stages of the impacting vehicle fitted with over the bumper type of alloy nudge bar (40 % offset rigid barrier, impact velocity 15 km/h, 'airbag no fire' test condition)

8.5.4 Physical vehicle crash tests

Firstly ‘airbag no fire’ test with lightest variance of the vehicle fitted with alloy nudge bar was carried out. Alloy nudge bar was equipped with the FPS mounts shown in the Figure 8.18 in the previous section. Airbag did not get deploy and also the deceleration pulse was analyzed and found that compatible with airbag crash sensing algorithm. Similarly, remaining physical crash tests (‘airbag no fire,' ‘airbag must fire’ and ADR 69 tests with heaviest vehicle fitted with steel bulbar). Deceleration pulses obtained from all these tests found to be in compliance with the airbag crash sensing algorithm. For the sake clarity, all relevant output from the CAE crash simulations and corresponding physical crash tests were shown in the Figures 8.13 to 8.18. Injury criteria measured using the ADR 69 crash test data clearly indicated that vehicle fitted with steel bulbar providing additional safety to the vehicular occupants Data obtained from the ADR 69 physical crash tests for the worst case (vehicle equipped with the steel bull bar) is given in the Table 8.2.

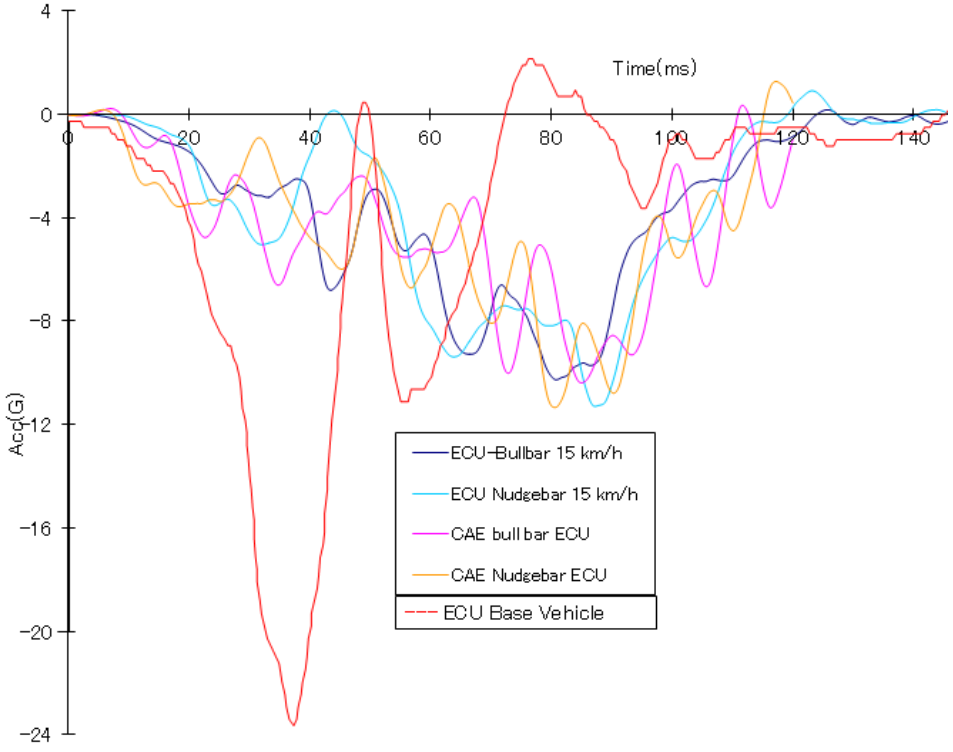

Figure 8.13: Deceleration pulse obtained from the ECU sensor for steel bull bar and alloy nudge bar (both CAE and physical crash tests). Base vehicle data also shown for convenience

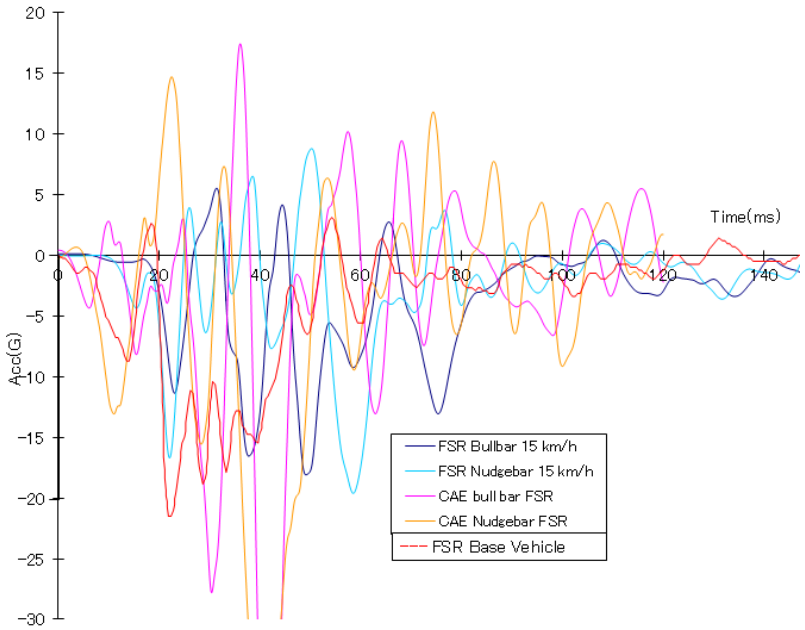

Figure 8.14: Deceleration pulse obtained from the front sensor (FSR) for steel bull bar and alloy nudge bar (both CAE and physical crash tests). Base vehicle data also shown for convenience

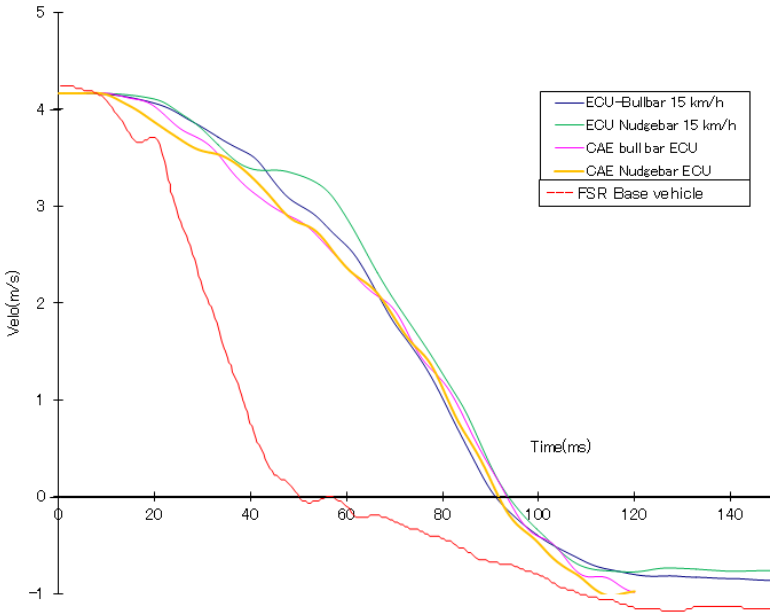

Figure 8.15: Velocity – time plot obtained from the ECU sensor for steel bull bar and alloy nudge bar (both CAE and physical crash tests). Base vehicle data also shown for convenience

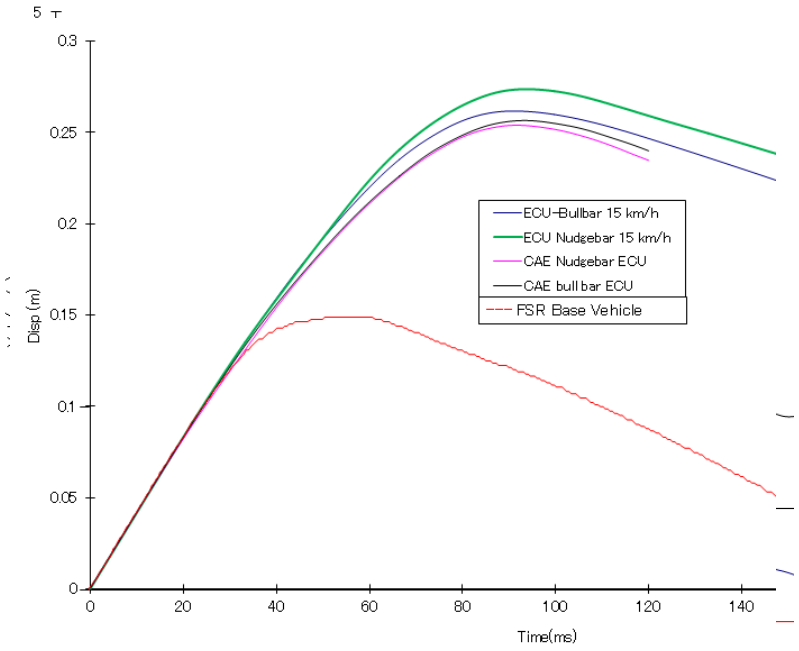

Figure 8.16: Velocity – time plot obtained from the Front sensor (FSR) for steel bull bar and alloy nudge bar (both CAE and physical crash tests). Base vehicle data also shown for convenience

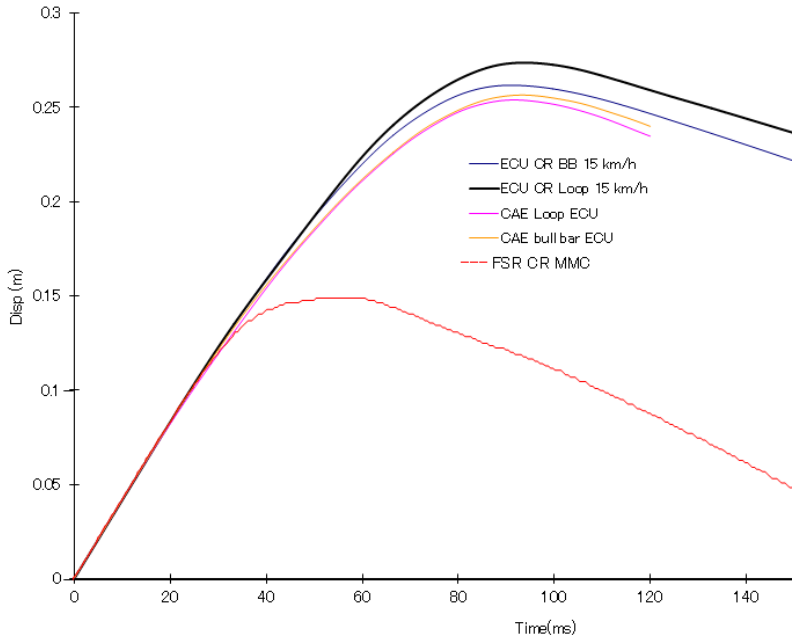

Figure 8.17: Displacement – time plot obtained from the ECU sensor for steel bull bar and alloy nudge bar (both CAE and physical crash tests). Base vehicle data also shown for convenience

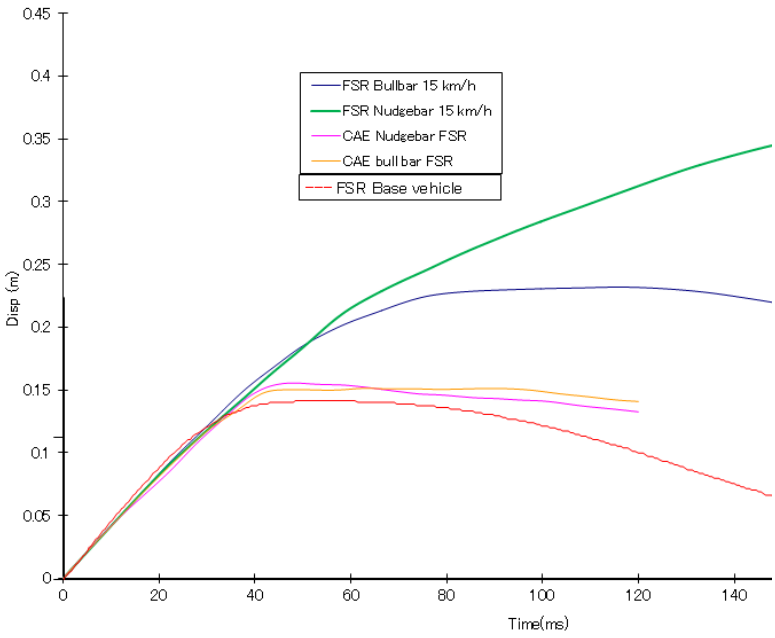

Figure 8.18: Displacement – time plot obtained from the Front sensor (FSR) for steel bull bar and alloy nudge bar (both CAE and physical crash tests). Base vehicle data also shown for convenience

Table 8.2: ADR 69/00 test results (vehicle without and with the FPS)

			Base vehicle without any Front Protection Systems		**Base vehicle fitted with the steel bull bar**	
Performance criterion		**Specification**	**Driver**	**Passenger**	**Driver**	**Passenger**
HIC		≤ 800	447	413	400	390
Chest deceleration		≤ 49G	53	53	47	45
Sternal deflection		≤60mm	53	58	51	58
Load on the knee	Left	≤8.0 kN	1.2	3.4	0.8	2.7
	Right		1.4	2.3	0.9	2.4

From the vehicle displacement plots (Figures 8.19 and 8.20) and the Table 8.2, it is clear that, as far as the occupant safety is concerned, the vehicle fitted with the steel bulbar performed better than that is not fitted with any FPS.

8.6 Energy absorption of the VFPS from the non-linear FEA simulations

As discussed in the previous sections, well before whole vehicle crash tests, non-linear FEA simulations were carried out in order to finalize the FPS mounts and theoretically achieve the airbag compatibility and ADR 69/00 compliance for all 5 variants of VFPS. Non-linear FEA simulations using commercial software packages (for instance, LS-DYNA developed by Livermore Software Technology Corporation, USA) facilitate the user to obtain various stresses, strains, kinetic energy and internal energy etc. from the nodal histories of the FE model, with an adequate ease.

Kinetic energy and Internal energy of the Steel bumper replacement FPS (complete assembly of fascia, tubular sections and bumperettes with the FPS mounts#1 shown in the Figure 8.10) was evaluated and plotted with reference to the duration of the impact (Figure 8.19).

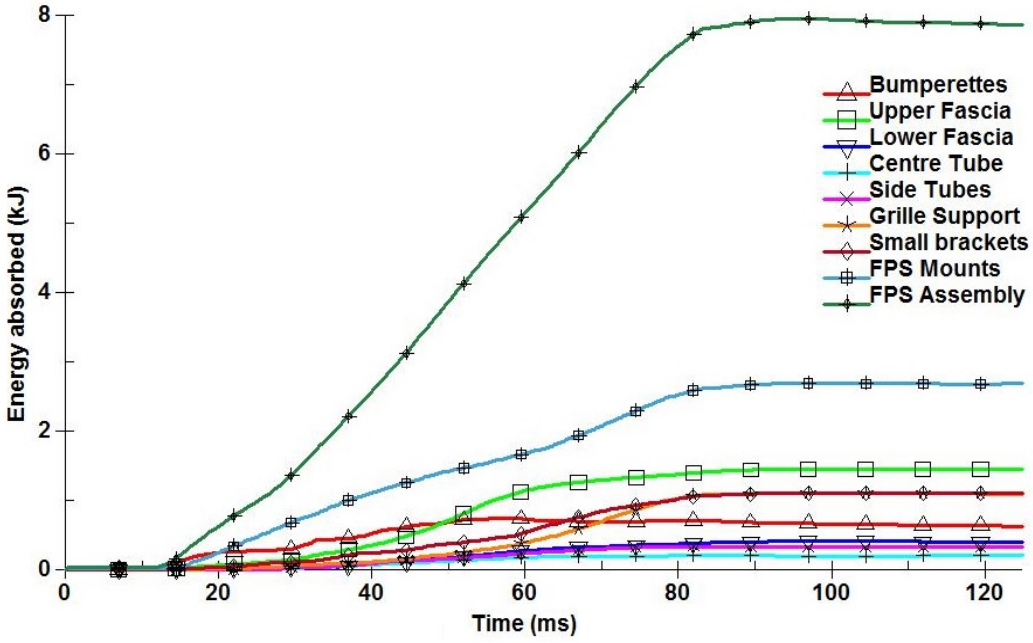

Figure 8.19: Energy absorbed by the bumper replacement type Steel FPS (for clarity energy absorbed by individual components of the FPS also shown in the picture) obtained from the whole vehicle crash simulations with the 'airbag no fire' test condition

Similarly, for all FPS mounts shown in the Figure 8.10, energy absorbed by the FPS assembly were calculated by using both simplified crash simulations (equivalent to dynamic pendulum tests) and whole vehicle crash simulations. The energy absorbed by the FPS and in terms of percentage of total impact energy obtained from the simulation output were as given in Table 8.3.

Table 8.3: Crash energy absorbed by the FPS assembly with various mounts

FPS mount #	Energy absorbed by the FPS		Energy absorbed by the FPS	
	kJ	in terms of the percentage of total impact energy	kJ	In terms of the percentage of total impact energy
1	7.87	5.62	5.2	3.45
2	7.29	5.20	5.17	3.42
3	7.70	5.49	5.29	3.50
4	7.59	5.41	5.49	3.64

Results presented in the Table 8.3 are very important to highlight how crucial it is to conduct whole vehicle crash tests (whole vehicle crash simulations to minimize the number of crash tests) for finalization of the FPS design that is airbag compatible and ADR 69/00 compliant. As per results presented by Bignell 2004, all FPS with all 4 mounts did absorb energy less than 12% of the total impact energy. Therefore, all should be airbag and ADR 69/00 compliant. In reality, FPS with former 3 mounts didn't pass the airbag crash sensing algorithm and only the FPS with mount #4 passed the algorithm and also passed all physical crash tests. Therefore, it is important to note that based on the results from the pendulum tests, FPS compliance requirements should not be finalized.

8.7 Pedestrian safety and crash compatibility aspects of the VFPS

8.7.1 Pedestrian safety – Head Injury Criterion

Traumatic brain injuries (TBI) are the leading cause of death and disability. In USA alone 1.7 million people, of which at least 125,000 permanently disabled and over 50,000 people die as a result of the TBI. At least 50% of the TBI related deaths involve automotive accidents. Therefore, researchers and engineers of the automotive industry have been working on improving not only the safety of the vehicular occupants but also other road users (pedestrians, cyclists, and motorbike riders). As the topic of interest is VFPS, only pedestrian safety aspects discussed here. Pedestrians were involved in 14% of all vehicle accidents in Victoria (Australian state) during 1973-78 and pedestrian deaths were 23% of overall fatalities (Chiam & Tomas 1980). According to the ATSB Fatality Crash Database, 1287 pedestrian fatalities occurred during the period from 1990 – 1997. Of these, 145 deaths were due to the impacts with vehicles fitted with FPS. Though it is not fair to attribute pedestrian fatalities to the FPS, there is scientific evidence to prove that bumper replacement type metallic FPS would increase the severity of head injuries, in the event of vehicle –pedestrian collisions. To ensure the pedestrian safety, vehicles sold in Australia and New Zealand must comply with safety standards such as 4876.1-2002, AS/NZS 4422 and AS/NZS 2512.3.1. These safety standards often include specifications in terms of head injury criterion (HIC) which can be obtained from head form testing. According to the AS 4876.1-2002, most vulnerable portions of the VPFS (above a height of 1 m from the ground when fitted to the vehicle) hit with a child head form of 2.5 kg with a speed of

30 km/h. The standard specifies that HIC value should be less than 1500. From the deceleration pulse obtained from the head form test, HIC is measured using the formula given below.

$$\text{HIC} = \max(t2 - t1)\left(\left[\frac{1}{t2-t1}\right]\int_{t1}^{t2}[a]\ dt\right)^{2.5} \qquad (8.1)$$

Where, $(t2 - t1)$ = 36 ms.

As far as the AS 4876.1-2002 concerned, most of the vehicle frontend structures would perform poor or may marginally pass. Bumper replacement type of Steel, Alloy and even polymer FPS reported having performed very poorly. When compared to the vehicle frontend, performance of the bumper replacement type FPS is very poor. For instance, Steel FPS yielded HIC values in the order of 5000. FPS made up of polymers relatively better than the metallic FPS and in some cases even better than the vehicle frontend. It is important to note that HIC score of 1500 indicates 70% probability of a skull fracture (Hertz 1993). Therefore, instead of making the FPS dimensions to keep them below 1 m from the ground level, an effort to should be done to improve the headform test performance of the FPS.

Effect of foam embellishments on the pedestrian safety was studied using non-linear FEA simulations. FPS and head-form, poly-urethane foam embellishment in the form of tube were as shown in the Figure 8.20 and Figure 8.21 respectively.

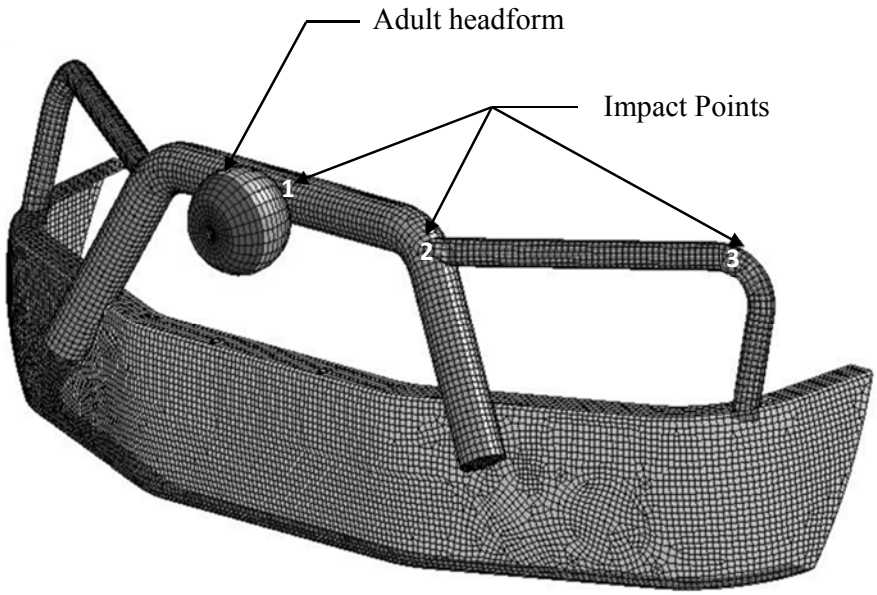

Figure 8.20 Adult headform impacting the Steel FPS at vulnerability points 1, 2 and 3.

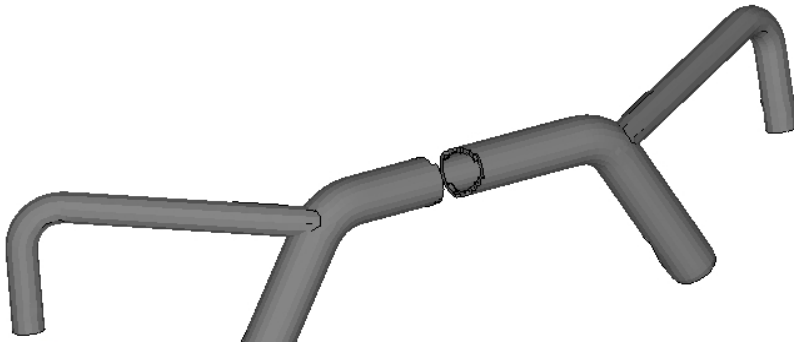

Figure 8.21 Foam tubing to cover the tubular sections of the FPS

Due to non-availability of the child head form, an adult head form of 4.5 kg weight was used in the non-linear impact simulations. HIC scaling law (Chou & Nyquist 1974) given below was used to obtain the HIC values which corresponds to the 2.5 kg child head form.

$$\frac{HIC_1}{HIC_2} = \left(\frac{m_1}{m_2}\right)^{\frac{-3}{4}} \left(\frac{v_1}{v_2}\right)^{\frac{5}{2}} \qquad (8.2)$$

Results obtained from the impact simulations and experimental tests for the FPS without any foam tubing were as given in Table 8.4.

Table 8.4: HIC values obtained from the simulations and experiments

Impact point	**HIC Scores obtained from CAE simulations using 4.5 kg adult headform @ 30**	**HIC Scores obtained by using Scaling law for 2.5 kg child headform @ 30 km/h impact**	**HIC scores obtained from experiments using 2.5 kg child headform @ 30 km/h**
1	2106	1378	1440
2	2200	1439	1360
3	1901	1244	1320

Table 8.4 reveals perfect correlation of the HIC values obtained from the non-linear FEA simulations with the 2.5 kg head form impact experiments. Therefore, similar impact simulations were carried out FPS with 12 mm thick foam (semi-rigid) cover to the tubular sections of the FPS. From the deceleration pulses, HIC values were elicited as 1570, 1505 and 1358 for the impact points 1, 2 and 3 respectively. This shows nearly 25% reduction in the HIC values which in turn indicates the great reduction in the TBI, therefore, higher level of pedestrian safety. Foam embellishments not only ameliorate the aesthetics of the FPS (vehicle fitted with the FPS) but also improve the performance of the head form test.

8.7.2 Crash compatibility

Automotive engineers worldwide have been working to improve not only the crashworthiness, but also crash compatibility of the vehicles to minimize the severity of the injuries to the vehicular occupants in vehicle-vehicle collision scenarios. Vehicles sold in Australia (as a matter of fact, sold anywhere in the world) must comply with the minimum safety requirements in the event of side impact. Therefore, all new vehicles before their release into the market would undergo side-impact crash test in the simulated environment in which vehicle under development will be impacted with a trolley fitted with deformable barrier at 50 km/h. Though many small cars perform poor, they meet the minimum safety requirements in terms of various performance criteria. This is due to the crash compatibility between vehicles. Fitment of the FPS (irrespective whether FPS is airbag compatible and ADR 69/00 compliant or not), would reduce the crash compatibility due to which struck vehicle occupants may experience more injuries.

In order to study the effect of the bumper replacement type of Steel FPS on the crash compatibility of the vehicle, non-linear simulation were performed in which a small car seated with USSID (side impact dummy) was laterally impacted (as per the side impact specifications) with a FPS fitted Ute, as shown in the Figure 8.22. Definitions of interfaces used were also displayed in the same illustration.

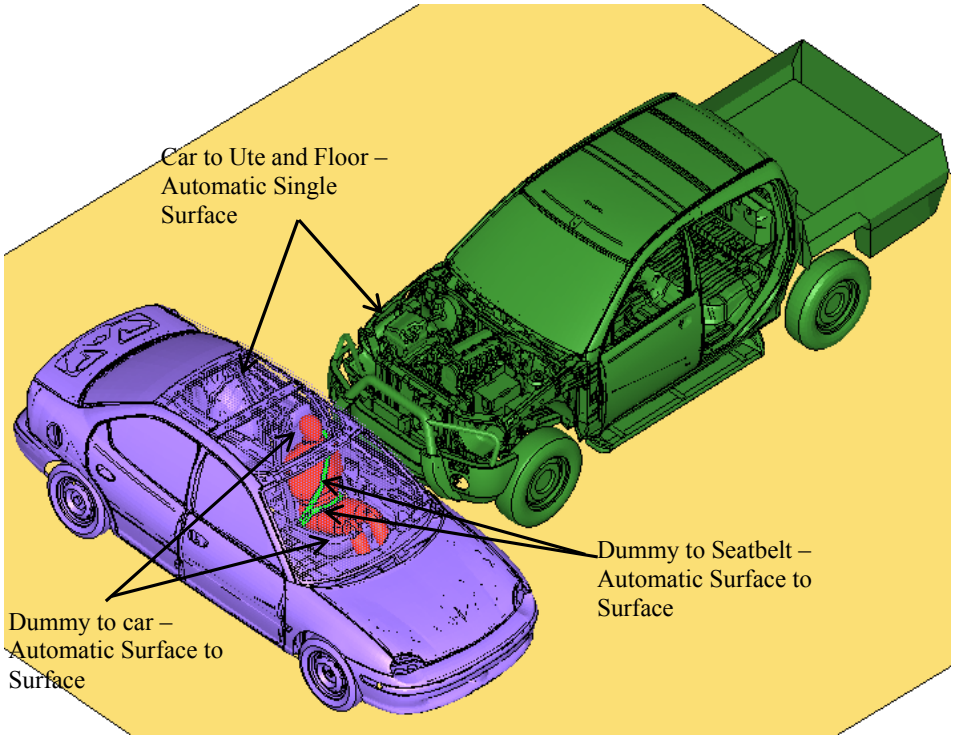

Figure 8.22: Small car seated with USSID impacted with the Ute fitted with Steel FPS

It is important to note that bio-fidelity of the USSID is less than the ES-2Re. Simulations with ES-2Re dummy got terminated with unknown errors. Therefore, USSID/LSTC was used in the research study. Using the time histories of the nodes at specific locations, HIC_{36}, pelvic force, abdominal reaction force and Chest deflection were evaluated as 1660, 10.25 kN, 4.9 kN and 58.4 mm respectively.

The stages of impact were as shown in the Figure 8.23.

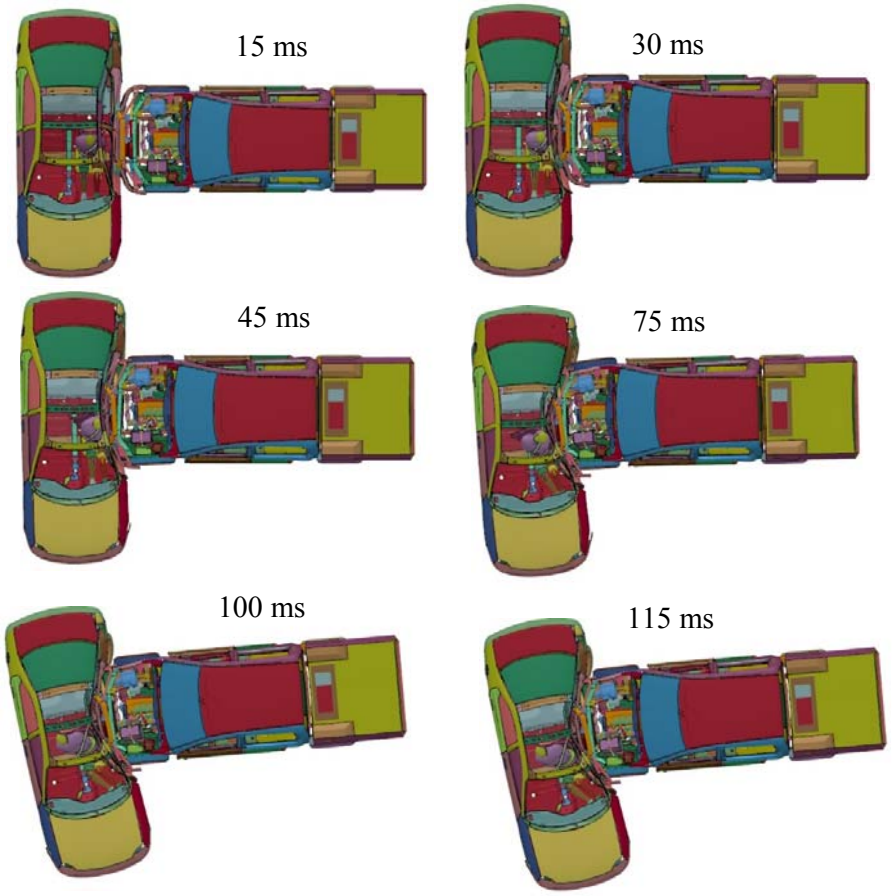

Figure 8.23: Stages of small car crash during the side impact with a Ute fitted with a compliant FPS

Figure 8.23 and the measured injury parameters elucidate the crash compatibility issues of FPS fitted vehicles. At the same time, FPS fitted vehicle shows considerably small damage and in real life situation, the vehicle may be drivable. This shows that FPS is offering additional protection to the vehicle to which it is fitted with.

Similarly, impact simulations were carried out by replacing the Steel FPS with the over the bumper Alloy Nudge bar. Damage to the small car and injury parameters measured were lesser than the previous case. Final stage of the crash (small car and the Ute with the Nudge bar) was as shown in the Figure 8.24.

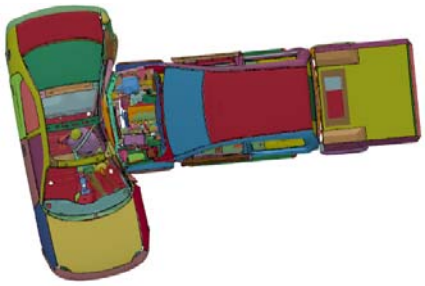

Figure 8.24: Stages of small car crash during the side impact with a Ute fitted with a compliant Nudge barFigure

For the impact case in which Ute equipped with over the bumper type Alloy Nudge bar impacted a small car, HIC_{36}, pelvic force, abdominal reaction force and Chest deflection were evaluated as 1150, 6.25 kN, 3.29 kN and 40.24 mm respectively. It is important to note that the Nudge bar offered equally good protection to the front end components of the striking vehicle. Due to the prevalence of the vehicle-animal collisions, fitment of the FPS is justifiable in rural areas. At the same time, due to FPS' detrimental effects on the pedestrians and crash compatibility between the vehicles, vehicle owners those drive only in the cities should limit themselves with Nudge bars or polymer bars.

8.8 Conclusion

CAE based simulations proved very beneficial in the development of the airbag compatible and ADR 69/00 compliant front protection systems. Irrespective whether the VFPS is 'over the bumper' type or 'bumper replacement' type, fitment to the vehicle can undoubtedly alter the vehicle crush characteristics. Therefore, full vehicle crash tests are mandatory for proving the airbag compliance of the VFPS.

Dynamic tests (pendulum impact tests) do not take the vehicle parts (onto which FPS mounted) into consideration. Therefore, it is not okay to judge the airbag compliance based on the deceleration pulse obtained from the pendulum test. Simplified crash simulation method devised by the author addresses the shortcomings of dynamic pendulum test. These simulations are simple and not computationally demanding too. Most importantly, airbag compatible and ADR 69 compliant FPS were successfully developed using the CAE based method. Development of 5 variants of FPS to a vehicle with 8 variants took only 4 vehicle crash tests to achieve the Airbag compatibility and ADR 69 compliance. With the conventional trial and error, minimum 120 physical crash tests are required. Of course, communizing the mounts for all variants of the FPS itself has reduced the number of crash tests required.

The fashion with which crush-can crumples play paramount role in the energy absorption. Crush-can in the laboratory condition (quasi-static compression test or dynamic pendulum test) without vehicle, crush-can in the whole vehicle crash tests, crush-can with vehicle fitted with FPS would crumple differently and provide different deceleration pulses and different energy absorption rates. Because of the same reason, though all 4 FPS mounts satisfies the airbag compatibility criterion developed by Bignell 2004, only mount#4 passed all compliance tests (both CAE and physical crash tests). Therefore, results obtained from any tests without reference to the vehicle front

end structures should not be used for the design and development of the FPS for modern passenger vehicles equipped with airbags of various kind.

Physical crash tests not only revealed the airbag compliance also elucidated that VFPS developed offered more protection to the vehicle and its occupants.

In a nutshell, the CAE simulations (both simplified and full vehicle crash simulations together) based method devised and presented in this chapter, made a commercially non-viable, unrealistically cumbersome project into reality.

Though not much scientific data is available on the effect of the VFPS on the crash compatibility of the VFPS fitted car that is striking the car in the lateral direction, vehicle crash databases provide some clue on the detrimental effect of the VFPS on the increase in fatalities or severity of the injuries of occupants of the struck car, while offering additional protection to the striking vehicle with FPS and its occupants. As per the ATSB Fatality Crash Database for years 1990 – 1997, 16% and 6% of the crashes with occupant fatalities for the striking vehicles without FPS with FPS respectively. This shows 10% reduction in the fatalities because of the FPS. Simulation results show good correlation with accident data base analysis results. Owing to the benefits and detrimental effects such as pedestrian safety and crash compatibility issues, it is not easy to decide whether FPS is a Foe or a Friend. As it is very difficult to make a legislation or law that refrains a vehicle owner from fitting the FPS, the best method is to increase the awareness of the pros and cons of the FPS, so that vehicle owners can make a proper choice.

CHAPTER-9: CONCLUSION AND FUTURE WORK

The research work presented in this thesis has been concerned with two major innovations. They are:

1. Development and validation of an FE model thorax for the evaluation of the blunt thoracic trauma due to ballistic impacts.
2. Development of a CAE based method for the design, development and validation of AS 4876.1-2002 compliant, airbag compatible and ADR 69/00 compliant multi-variant FPS for multi-variant vehicle with a minimum number of physical crash tests.

9.1 Thesis summary

Anthropomorphic Test Dummies (ATD), though widely used as human surrogates in the automotive industry for simulated vehicle crash tests, from the outcome of the systematic review presented in the Chapter – 2, it was clear that none of the biomechanical responses of the thoraces of the ATDs have shown correlation with the human cadaver test data pertinent to the similar impact cases. Therefore, ATDs can't be used for the evaluation of the blunt thoracic trauma relevant to the non-lethal projectile impacts, solid sports ball impacts, and related applications. Therefore, novel concepts of the thorax surrogate have been developed and presented at first in Chapter – 3. A concept was selected for the further development and pilot study was carried out whether validation of such novel concepts is feasible or not.

As the development and validation of the novel concept for the FE model thorax surrogate was found to be feasible, a systematic CAE based approach was devised and successfully validated (as presented in the Chapter – 4) the FE model thorax which was named as MTHOTA (Mechanical THOrax for Trauma Assessment). Force-time, deflection-time and force-deflection biomechanical responses and VC_{max} values obtained for blunt ballistic impacts have shown perfect correlation with the respective cadaveric test data. MTHOTA showed correlation with many case studies published by defense and military research organizations. In last 7 years, MTHOTA has been successfully used for solving many engineering problems pertaining to the defense and sports industries.

Defense industries have been using Blunt Criterion (BC) for the evaluation of thoracic trauma due to ballistic impacts. If BC is the correct predictor of the chest trauma, both soft core baseball and synthetic baseball (both of these solid sports balls have the same size and same mass) should have produced equal (or approximately equal) values of blunt thoracic trauma or VC_{max}. Measurements using MTHOTA clearly revealed the detrimental effects of the synthetic baseball when compared to soft cored baseball. Using MTHOTA, blunt thoracic trauma due to solid sports ball impacts was measured and presented first in the Chapter – 5. Using MHTOTA as the thorax surrogate, effect of material, impact speed and spin of the solid sports ball were studied and presented in the later sections of the Chapter – 5. With the ability to facilitate the accurate measurement of the blunt thoracic trauma, a cheaper alternative for XM 1006 (latest and very popular non-lethal projectile) was developed and presented in the Chapter – 6.

Justification for the fitment of the front protection systems, misconceptions prevailing in the VFPS manufacturing industry and detrimental effects of the poorly designed VFPS and related aspects were first presented in the Chapter – 7. A systematic engineering approach was devised for the development of VFPS for non-air bagged vehicles and presented the efficacy of the devised method with a real life case study of developing a FPS to Ute. Method to finalize the maximum allowable weight for the FPS, scientific selection of the mounting points and FPS mounts were also presented. The method of simplified CAE crash simulations proved to be very effective in not only selection of the FPS mounts, but also in reducing number of whole vehicle crash simulations, which in turn reduced the physical crash tests to a very minimum. The method was extended for the development of VFPS for the air bagged vehicles. It was demonstrated that with only 4 physical crash tests (minimum required tests for were 4) 5 variants of airbag compatible, ADR 69/00 compliant VFPS for a vehicle that has 8 variants, were developed. Without using the CAE based method, the same project would have been commercially non-viable and practically impossible.

9.2 Recommendations for the future work

Concept of MTHOTA can be used for the development of various thorax surrogates (both physical and FE models) for specific industry applications.

Although the MTHOTA FE model surrogate presented in the thesis has demonstrated very good correlation with the cadaver tests data, it could be further developed into application specific surrogates. For instance, MTHOTA's ability to measure dynamic force response, it can be used for the measurement of the percent risk of Commotio-Cordis (sudden death due to ventricular fibrillation) due to blunt ballistic impacts. Owing to the size and shape of the MTHOTA, it may not be useful as it is for the development and validation of the chest protectors for the sports personnel. Therefore, modification to the shape and size are required such a way that it can accommodate chest protectors. Due to changes in the form and size, revalidation would be necessary. The methodology used for the validation of MTHOTA would be suitable for validation of any such thoracic surrogates. Development and validation of the thorax surrogate that is useful for the evaluation of the chest protectors for the protection against the CC would become an excellent research project.

Another aspect that requires further investigation is ATDs for the evaluation of the blunt ballistic trauma. In the research work presented in the thesis, no changes were made to the ATDs. By changing material properties or adding a cushion in front of the thorax, it may be possible to validate them for the use of evaluation of the chest trauma due to blunt ballistic impacts.

Concerning VFPS design and development, no further study was carried out on the corrugated box type FPS mounts. It could be further developed into a generic FPS mounts suitable for all vehicles of the same category. By performing simplified crash simulations on few vehicles of a similar class, a global crash pulse for the chassis cross member and crush-can assembly could be developed and used for the validation of the generic FPS mounts.

REFERENCES

Abrunzo, TJ 1991, 'Commotio cordis: the single, most common cause of traumatic death in youth baseball', *Archives of Pediatrics & Adolescent Medicine*, vol. 145, no. 11, p. 1279.

Anderson, RWG, Ponte, G & Doecke, SD 2008, *A survey of bullbar prevalence at pedestrian crash sites in Adelaide, South Australia*, Centre for Automotive Safety Research.

Anderson, RWG, Doecke, SD, van den Berg, AL, Searson, DJ & Ponte, G 2009, *The effect of bull bars on head impact kinematics in pedestrian crashes*, Centre for Automotive Safety Research.

Attewell, R & Glase, K 2000, *Bull Bars and Road Trauma*.

Australia, S 2002, *Motor Vehicle Frontal Protection Systems, Part 1: Road user protection*, Australian Standard AS 4876.1.2002, Australia.

Bass, CR, Salzar, RS, Lucas, SR, Davis, M, Donnellan, L, Folk, B, Sanderson, E & Waclawik, S 2006, 'Injury risk in behind armor blunt thoracic trauma', *Int J Occup Saf Ergon*, vol. 12, no. 4, pp. 429-42, Nlm, item: 17156618.

Bell, P 1992, 'Spondylolysis in fast bowlers: principles of prevention and a survey of awareness among cricket coaches', *Br J Sports Med*, vol. 26, no. 4, pp. 273-5.

Bignell, P 2004, 'Evaluation of the performance and testing techniques of Vehicle Frontal Protection Systems'.

Bir, C & Viano, DC 2004, 'Design and injury assessment criteria for blunt ballistic impacts', *J Trauma*, vol. 57, no. 6, pp. 1218-24, Nlm, item: 15625452.

Bir, C, Viano, D & King, A 2004, 'Development of biomechanical response corridors of the thorax to blunt ballistic impacts', *J Biomech*, vol. 37, no. 1, pp. 73-9, Nlm, item: 14672570.

Bir, CA 2000, 'The evaluation of blunt ballistic impacts of the thorax', Wayne State University, Detroit, Michigan, USA.

Bir, CA & Viano, DC 1999, 'Biomechanical predictor of commotio cordis in high-speed chest impact', *J Trauma Acute Care Surg*, vol. 47, no. 3, pp. 468-73.

BLAS, CA & CAUSSADE, FM 2011, 'Commotio cordis as a cause of sudden cardiac death', *Emergencias*, vol. 23, pp. 471-8.

Bush, I & Challener, S 1988, 'Finite element modelling of non-penetrating thoracic impact', in INTERNATIONAL IRCOBI CONFERENCE ON THE: *proceedings of theINTERNATIONAL IRCOBI CONFERENCE ON THE*.

Calculation Guidelines for Impact Testing, 2010, SAE J1727, 02/2010, Safety Test Instrumentation Stds Comm, USA

Campbell, JQ & Tannous, R 2008, 'Using a finite element model to predict thoracic injuries', in IV Latin American Congress on Biomedical Engineering 2007, Bioengineering Solutions for Latin America Health: *proceedings of theIV Latin American Congress on Biomedical Engineering 2007, Bioengineering Solutions for Latin America Health* Springer, pp. 690-2.

Cavanaugh, JM, Zhu, Y, Huang, Y & king, AI 1993, 'Injury response o fthe throax in side impact cadaveric tests', in 37th annual Stapp car crash conference: *proceedings of the37th annual Stapp car crash conference* SAE paper no. 933127, Warrendalte, PA, USA, pp. 199-222.

Chan, CY 2000, *Fundamentals of crash sensing in automotive air bag systems*, Socity of Automotive Engineers, USA.

Chan, CY 2002a, 'A treatise on crash sensing for automotive air bag systems', *IEEE/ASME Transaction on Mechatronics*, vol. 7, no. 5, pp. 220-34.

Chan, CY 2002b, 'On the detection of vehicular crashes - System characteristics and architechture', *IEEE transaction on Vehicular Technology*, vol. 51, no. 1, pp. 80-193.

Chang, F 2001, 'The development and validation of a finite element human thorax model for automotive impact injury studies', *ASME APPLIED MECHANICS DIVISION-PUBLICATIONS-AMD*, vol. 251, pp. 103-12.

Chen, PH 1978, 'Finite element dynamic structural model of the human thorax for chest impact response and injury studies', *Aviat Space Environ Med*, vol. 49, no. 1 Pt. 2, pp. 143-9, Nlm, item: 623577.

Cheng, N 2009, 'Development of a universal FE model of a cricket ball'.

Cheng, N, Subic, A & Takla, M 2008, 'Development of a fast-solving numerical model for the structural analysis of cricket balls', *Sports Technology*, vol. 1, no. 2-3, pp. 132-44.

Cheng, N, Takla, M & Subic, A 2011, 'Development of an FE model of a cricket ball', *Procedia Engineering*, vol. 13, pp. 238-45.

Chiam, H & Tomas, J 1980, *Investigation of the effect of bull-bars on vehicle-pedestrian collision dynamics*, 0810-770X.

Chidester, A, Hinch, J & Roston, TA 2001, 'Real world experience with event data recorders', in Proceedings of the Seventeenth International Technical Conference on the Enhanced Safety of Vehicles, Amsterdam, Netherlands (June 2001): *proceedings of theProceedings of the Seventeenth International Technical Conference on the Enhanced Safety of Vehicles, Amsterdam, Netherlands (June 2001)*.

Chou, CC & Nyquist, GW 1974, *Analytical studies of the head injury criterion (HIC)*, SAE Technical Paper.

Chowaniec, C, Kobek, M, Jabłoński, C, Kabiesz-Neniczka, S & Karczewska, W 2008, 'Case-study of fatal gunshot wounds from non-lethal projectiles', *Forensic Sci Int*, vol. 178, no. 2, pp. 213-7.

Cıhalová, L 2006, 'Development of biomechanical deformable thoracic model', *Journal Engineering mechanics*, vol. 13, no. 6, pp. 453-65.

Číhalová, L 2009, 'Analysis of Thoracic Impact Responses and Injury Prediction by using FE Thoracic Model', *Engineering Mechanics*, vol. 16, no. 1, pp. 49-63.

ČÍHALOVÁ, L 2005, 'DEVELOPMENT OF BIOMECHANICAL MODEL OF THE THORAX', *Computational Mechanics, 21st conference with International participation, Pislen*, pp. 119-26.

Clare, VR, Lewis, JH, Mickiewicz, AP & Sturdivan, LM 1975, *Blunt trauma data correlation*, DTIC Document.

Classie, JA, Distel, LM & Borchers, JR 2010, 'Safety baseballs and chest protectors: a systematic review on the prevention of commotio cordis', *Phys Sportsmed*, vol. 38, no. 1, pp. 83-90, NLM, item: 20424405.

Correia, JT, Iliadis, KA, McCarron, ES, Smolej, MA, Hastings, B & Engineers, CC 2001, 'Utilizing data from automotive event data recorders', in Proceedings of the Canadian Multidisciplinary Road Safety Conference XII, London Ontario: *proceedings of theProceedings of the Canadian Multidisciplinary Road Safety Conference XII, London Ontario*.

Corrigan, A 1984, 'Cricket injuries', *Australian Family Physician*, vol. 13, no. 8, pp. 558-9, 62.

Crandall, JR, Bose, D, Forman, J, Untaroiu, CD, Arregui-Dalmases, C, Shaw, CG & Kerrigan, JR 2011, 'Human surrogates for injury biomechanics research', *Clin Anat*, vol. 24, no. 3, pp. 362-71, Nlm, item: 21433083.

Crisco, JJ, Hendee, SP & Greenwald, RM 1997, 'The influence of baseball modulus and mass on head and chest impacts: a theoretical study', *Medicine and science in sports and exercise*, vol. 29, no. 1, pp. 26-36.

Crisco, JJ, Greenwald, RM, Blume, JD & Penna, LH 2002, 'Batting performance of wood and metal baseball bats', *Medicine and science in sports and exercise*, vol. 34, no. 10, pp. 1675-84.

Dau, N 2012, 'Development of a biomechanical surrogate for the evaluation of commotio cordis protection'.

Davids, K & Morgan, M 1988, 'The effects of helmet design and bowling speed on indices of stress in cricket batting', *Ergonomics*, vol. 31, no. 11, pp. 1665-71.

Doecke, SD, Anderson, RWG & Ponte, G 2008, 'Bull bar prevalence among types of vehicle in metropolitan Adelaide', in Australasian Road Safety Research, Policing and Education Conference (2008: Adelaide, Australia): *proceedings of theAustralasian Road Safety Research, Policing and Education Conference (2008: Adelaide, Australia)*.

Doerer, JJ, Haas, TS, Estes, NAM, Link, MS & Maron, BJ 2007, 'Evaluation of Chest Barriers for Protection Against Sudden Death Due to Commotio Cordis', *The American journal of cardiology*, vol. 99, no. 6, pp. 857-9.

Douglas, RJ 2011, 'Sudden cardiac death following blunt chest trauma: commotio cordis', *World Journal ofEmergency Medicine*, vol. 2, no. 3, pp. 234-6.

Drane, P & Sherwood, J 2004, 'Characterization of the effect of temperature on baseball COR performance', *Engineering of sport*, vol. 5, no. 2.

DuBay, DK & Bir, CA 1998, *Injury risk assessment of single target and area fire less lethal ammunitions*, DTIC-OCA-19980820-063.

Eiband, AM 1959, *Human tolerance to rapidly applied accelerations: a summary of the literature*, National Aeronautics and Space Administration, Washington, DC, USA,<.

Elliott, B, Burnett, A, Stockill, N & Bartlett, R 1995, 'The fast bowler in cricket: A sports medicine perspective', *Sports Exercise and Injury*, vol. 1, no. 4, pp. 201-6.

Erwin, SI 2009, 'Army's Procedures for Testing Body Armor Stir Controversy', *National Defense Magazine*, October, 2009.

Finch, CF, Elliott, BC & McGrath, AC 1999, 'Measures to prevent cricket injuries', *Sports medicine*, vol. 28, no. 4, pp. 263-72.

Forbes, PA 2005, 'Development of a Human Body Model for the Analysis of Side Impact Automotive Thoracic Trauma', University of Waterloo.

Gadd, CW & Patrick, LM 1968, 'System versus Laboratory Impact Tests for Estimating Injury Hazard', SAE paper no. 680053, Warrendalte, PA, USA, pp. 8-12.

Gennarelli, TA & Scaling, AAfAMCoI 1985, *Abbreviated injury scale*, American Association for Automotive Medicine.

Green, D 2001, 'Wood: strength and stiffness', *Encyclopedia of Materials: Science and Technology*, pp. 9732-6.

Green, DW, Winandy, JE & Kretschmann, DE 1999, 'Mechanical properties of wood', *Wood handbook: wood as an engineering material*.

Hallquist, JO 2006, *LS-DYNA Theory Manual*, Livermore Software Technology Corporation, USA,<.

Hallquist, JO 2007a, *LS-DYNA Keyword User's Manual - Volume I*, Livermore Software Technology Corporation, USA,<.

Hallquist, JO 2007b, *LS-DYNA Keyword User's Manual, Volume II*, Livermore Software Technology Corporation, USA. ,<.

Hardy, B 1996, 'A study of accidents involving bull bar equipped vehicles', *TRL REPORT 243*.

Herrmann, L & Peterson, F 1968, 'A numerical procedure for viscoelastic stress analysis', in Seventh Meeting of ICRPG Mechanical Behavior Working Group, Orlando, FL, CPIA Publication: *proceedings of theSeventh Meeting of ICRPG Mechanical Behavior Working Group, Orlando, FL, CPIA Publication* pp. 60-9.

Hertz, E 1993, 'A note on the head injury criterion (HIC) as a predictor of the risk of skull fracture', in Proceedings: Association for the Advancement of Automotive

Medicine Annual Conference: *proceedings of theProceedings: Association for the Advancement of Automotive Medicine Annual Conference* Association for the Advancement of Automotive Medicine, pp. 303-12.

Hollowell, WT, Gabler, HC, Stucki, SL, Summers, S & Hackney, J 1999, 'Updated review of potential test procedures for FMVSS No. 208', *NHTSA's Office of Vehicle Safety Research*.

Hoyert, DL & Hu, J 2012, *Deaths: Preliminary Data for 2011*.

Hubbs, K & Klinger, D *IMPACT MUNITIONS: Database of use and effects*.

Hughes, D, Maguire, K, Dunn, F, Fitzpatrick, S & Rocke, LG 2005, 'Plastic baton round injuries', *Emergency Medicine Journal*, vol. 22, no. 2, pp. 111-2.

Ijames, S Spring, 1997, 'Testing and evaluation of less-lethal projectiles', *The tactical edge*, pp. 12-5.

Jacquet, JF 2010, 'Seuils de concussion, coma et endommagements irréversibles lors d'un impact crânien par projectiles cinétiques à létalité réduite', in 3rd congress of wound ballistics -2010: *proceedings of the3rd congress of wound ballistics -2010* Ecully, France.

James, D, Curtis, D, Allen, T & Rippin, T 2012, 'The validity of a rigid body model of a cricket ball-bat impact', *Procedia Engineering*, vol. 34, no. 0, pp. 682-7.

Janda, DH, Viano, DC, Andrzejak, DV & Hensinger, RN 1992, 'An Analysis of Preventive Methods for Baseball-Induced, Chest Impact Injuries', *Clinical Journal of Sport Medicine*, vol. 2, no. 3, pp. 172-9.

Kallaieris, D, Mattern, R, Schmidt, G & Eppinger, RH 1981, 'Quantification of Side Impact Responses and Injuries', in 25th Stapp Car Crash Conference: *proceedings of the25th Stapp Car Crash Conference* Society of Automotive Engineers, Warrendale, USA, pp. 329-66.

Kent, R & Patrick, LM 2005, 'Chest deflection tolerance to blunt anterior loading is sensitive to age but not load distribution', *Forensic Sci Int*, vol. 149, no. 2-3, pp. 121-8, Nlm, item: 15749351.

King, AI 1993, 'Progress of research on impact biomechanics', *J Biomech Eng*, vol. 115, no. 4b, pp. 582-7, Nlm, item: 8302045.

King, AI 2000, 'Fundamentals of impact biomechanics: Part I--Biomechanics of the head, neck, and thorax', *Annu Rev Biomed Eng*, vol. 2, pp. 55-81, Nlm, item: 11701507.

King, AI, Yang, KH & Hardy, WN 2011, 'Recent firsts in cadaveric impact biomechanics research', *Clin Anat*, vol. 24, no. 3, pp. 294-308, Nlm, item: 21433079.

Koene, B, Id-Boufker, F & Papy, A 2008, 'Kinetic non-lethal weapons', *Netherlands annual review of military studies*, pp. 9-24.

Krausz, MM & Mahajna, A 2002, 'Traumatic effects of rubber bullets', *The Lancet*, vol. 360, no. 9345, p. 1607.

Kretschmann, D, Green, W, TenWolde, S, Murphy, R, Carll, CG, Bendtsen, B, Gjovik, L, Verrill, S, Glass, SV & Zelinka, SL 2010, 'Wood Handbook, Chapter 05: Mechanical Properties of Wood', *General Technical Report FPL-GTR-190. Madison, WI: US Department of Agriculture, Forest Service, Forest Products Laboratory*.

Kroell, CK, Schneider, DC & Nahum, AM 1971, 'Impact tolerance and response to the human thorax', in Proceedings of the 15th Stapp Car Crash Conference, : *proceedings of theProceedings of the 15th Stapp Car Crash Conference,* Society of Automotive Engineers, Warrendale, USA, pp. 84-134.

Kroell, CK, Schneider, DC & Nahum, AM 1974, 'Impact tolerance and response to the human thorax II', in Proceedings of the 18th Stapp Car Crash Conference, : *proceedings of theProceedings of the 18th Stapp Car Crash Conference,* Society of Automotive Engineers, Warrendale, USA, pp. 383-457.

Kroell, CK, Allen, SD, Warner, CY & Perl, TR 1986, 'Interrelationship of velocity and chest compression in blunt thoracic impact to swine II', in Proceedings of the 30th Stapp Car Crash Conference, : *proceedings of theProceedings of the 30th Stapp Car Crash Conference,* Warrendale, USA, pp. 99-121.

Kuppa, S, Eppinger, RH, McKoy, F, Nguyen, T, Pintar, FA & Yoganandan, N 2003, 'Development of Side Impact Thoracic Injury Criteria and Their Application to the Modified ES-2 Dummy with Rib Extensions (ES-2re)', *Stapp Car Crash J*, vol. 47, pp. 189-210, NLM, item: 17096250.

Lau, IV, Horsch, JD, Viano, Da & Andrzejak, DV 1993, 'Mechanisms of injury from air bag deployment loads', *Accid Anal Prev*, vol. 25, no. 1, pp. 29-45.

Lau, VK & Viano, DC 1986, 'The Viscous Criterion -Bases and Applications of an Injury Serverity Index for Soft Tissues', in Proceedings of the Thirtieth Stapp Car Crash Conference *proceedings of theProceedings of the Thirtieth Stapp Car Crash Conference* Warrendale, PA, USA, pp. 123-42.

Lawrence, G & Hardy, B 1992, 'Vehicle Crash Bars-Assessment of Pedestrian Injury Potential', *TRL WORKING PAPER*, no. WP/VS/225.

Link, MS 2003, 'Mechanically induced sudden death in chest wall impact (commotio cordis)', *Progress in Biophysics and Molecular Biology*, vol. 82, no. 1–3, pp. 175-86, viewed 2003/7//.

Link, MS & Estes Iii, NAM 2007, 'Mechanically induced ventricular fibrillation (commotio cordis)', *Heart Rhythm*, vol. 4, no. 4, pp. 529-32.

Link, MS, Maron, BJ, Wang, PJ, VanderBrink, BA, Zhu, W & Estes Iii, NAM 2003, 'Upper and lower limits of vulnerability to sudden arrhythmic death with chest-wall impact (commotio cordis)', *J Am Coll Cardiol*, vol. 41, no. 1, pp. 99-104.

Link, MS, Maron, BJ, Wang, PJ, VanderBrink, BA, Zhu, W & Estes, NA, 3rd 2003, 'Upper and lower limits of vulnerability to sudden arrhythmic death with chest-wall impact (commotio cordis)', *J Am Coll Cardiol*, vol. 41, no. 1, pp. 99-104, Nlm, item: 12570951.

Link, MS, Wang, PJ, VanderBrink, BA, Avelar, E, Pandian, NG, Maron, BJ & Estes, NAM 1999, 'Selective Activation of the K+ATP Channel Is a Mechanism by Which Sudden Death Is Produced by Low-Energy Chest-Wall Impact (Commotio Cordis)', *Circulation*, vol. 100, no. 4, pp. 413-8.

Link, MS, Maron, BJ, VanderBrink, BA, Takeuchi, M, Pandian, NG, Wang, PJ & Estes, IIINAM 2001, 'Impact directly over the cardiac silhouette is necessary to produce ventricular fibrillation in an experimental model of commotio cordis', *J Am Coll Cardiol*, vol. 37, no. 2, pp. 649-54.

Link, MS, Wang, PJ, Pandian, NG, Bharati, S, Udelson, JE, Lee, M-Y, Vecchiotti, MA, VanderBrink, BA, Mirra, G, Maron, BJ & Estes, NAM 1998, 'An Experimental Model of Sudden Death Due to Low-Energy Chest-Wall Impact (Commotio Cordis)', *New England Journal of Medicine*, vol. 338, no. 25, pp. 1805-11, item: 9632447.

Lyon, DH 1997, 'Development of a 40mm nonlethal catridge', *Defense Technology Federal Laboratories Research Journal*, pp. 64-78.

Lyon, DH, Bir, CA & Patton, BJ 1999, *Injury Evaluation Techniques for Non-Lethal Kinetic Energy Munitions*, DTIC Document.

Madias, C, Maron, BJ, Weinstock, J, Estes, NA, 3rd & Link, MS 2007, 'Commotio cordis--sudden cardiac death with chest wall impact', *J Cardiovasc Electrophysiol*, vol. 18, no. 1, pp. 115-22, NLM, item: 17229310.

Madias, C, Maron, BJ, Weinstock, J, Estes, N & Link, MS 2007, 'Commotio cordis—sudden cardiac death with chest wall impact', *Journal of Cardiovascular Electrophysiology*, vol. 18, no. 1, pp. 115-22.

Madias, C, Maron, BJ, Weinstock, J, Estes, NAM & Link, MS 2007, 'Commotio Cordis—Sudden Cardiac Death with Chest Wall Impact', *Journal of Cardiovascular Electrophysiology*, vol. 18, no. 1, pp. 115-22.

Maguire, K, Hughes, DM, Fitzpatrick, MS, Dunn, F, Rocke, LG & Baird, CJ 2007, 'Injuries caused by the attenuated energy projectile: the latest less lethal option', *Emergency Medicine Journal*, vol. 24, no. 2, pp. 103-5.

Mahajna, A, Aboud, N, Harbaji, I, Agbaria, A, Lankovsky, Z, Michaelson, M, Fisher, D & Krausz, MM 2002, 'Blunt and penetrating injuries caused by rubber bullets during the Israeli-Arab conflict in October, 2000: a retrospective study', *The Lancet*, vol. 359, no. 9320, pp. 1795-800.

Mancini, MC 2012, *Blunt Chest Trauma*, 428723, Medscape Reference, http://emedicine.medscape.com, 13 Aug 2012.

Maron, BJ & Estes III, NM 2010, 'Commotio cordis', *New England Journal of Medicine*, vol. 362, no. 10, pp. 917-27.

Maron, BJ, Poliac, LC, Kaplan, JA & Mueller, FO 1995, 'Blunt impact to the chest leading to sudden death from cardiac arrest during sports activities', *N Engl J Med*, vol. 333, no. 6, pp. 337-42, Nlm, item: 7609749.

Maron, BJ, Gohman, TE, Kyle, SB, Estes, IN & Link, MS 2002, 'CLinical profile and spectrum of commotio cordis', *Jama*, vol. 287, no. 9, pp. 1142-6.

Maron, BJ, Doerer, JJ, Haas, TS, Estes Iii, NAM & Link, MS 2006, 'Historical observation on commotio cordis', *Heart Rhythm*, vol. 3, no. 5, pp. 605-6.

Maron, BJ, Doerer, JJ, Haas, TS, Estes, NM, Hodges, JS & Link, MS 2009, 'Commotio cordis and the epidemiology of sudden death in competitive lacrosse', *Pediatrics*, vol. 124, no. 3, pp. 966-71.

McGrath, AC & Finch, CF 1996, *Bowling cricket injuries over: A review of the literature*, Monash University Accident Research Centre.

Millar, R, Rutherford, W, Johnston, S & Malhotra, V 1975, 'Injuries caused by rubber bullets: a report on 90 patients', *British Journal of Surgery*, vol. 62, no. 6, pp. 480-6.

Morgan, RM, Marcus, JH & Eppinger, RH 1986, 'Side impact - The biofidelity of NHTSA's proposed ATD and efficacy of TTI', Society of Automotive Engineers, SAE paper no. 861877, Warrendalte, PA, USA, pp. 27-40.

Morris, A, Barnes, J, Fildes, B, Bentivegna, F & Seyer, K 2001, 'Effectiveness of ADR 69: a case-control study of crashed vehicles equipped with airbags'.

Munroe, BJ & Sherwood, JA 2012, 'Finite Element Modeling of a Baseball', *Procedia Engineering*, vol. 34, no. 0, pp. 610-5.

Murray, YD, Reid, J, Faller, R, Bielenberg, B & Paulsen, T 2005, *Evaluation of LS-DYNA Wood Material Model 143*, FHWA-HRT-04-096, Turner-Fairbank Highway Research Center, http://www.fhwa.dot.gov/publications/research/safety/04096/>.

Mustone, TJ & Sherwood, JA 1998, 'Using LS-DYNA to characterize the performance of baseball bats', in 5th International LS-DYNA Users Conference, September: *proceedings of the5th International LS-DYNA Users Conference, September* pp. 21-2.

Nahum, AM, Kroell, CK & Schneider, DC 1973, 'The biomechanical basis of chest impact protection. II. Effects of cardiovascular pressurization', *J Trauma*, vol. 13, no. 5, pp. 443-59, Nlm, item: 4701840.

National Institute of Justice, 2008, *Ballistic Resistance of Personal Body Armor NIJ Standard–0101.04*, US Department of Justice, USA.

Nicholls, RL, Miller, K & Elliott, BC 2005, 'A numerical model for risk of ball-impact injury to baseball pitchers', *Medicine and science in sports and exercise*, vol. 37, no. 1, pp. 30-8.

Nicholls, RL, Miller, K & Elliott, BC 2006, 'Numerical analysis of maximal bat performance in baseball', *J Biomech*, vol. 39, no. 6, pp. 1001-9.

Nicholls, RL, Elliott, BC, Miller, K & Koh, M 2003, 'Bat Kinematics in Baseball: Implications for Ball Exit Velocity and Player Safety', *Journal of Applied Biomechanics*, vol. 19, no. 4.

Nsiampa, N, Robbe, C, Oukara, A & Papy, A 2012, 'Comparison of less lethal 40 mm sponge projectile and the 37 mm projectile for injury assessment on human thorax', in EPJ Web of Conferences: *proceedings of theEPJ Web of Conferences* EDP Sciences, p. 03002.

Pang, TY, Subic, A & Takla, M 2011, 'Finite element analysis of impact between cricket ball and cantilever beam', *Procedia Engineering*, vol. 13, pp. 258-64.

Papy, A, Robbe, C, Nsiampa, N, Oukara, A & Goffin, J 2012, 'Definition of a standardized skin penetration surrogate for blunt impacts', in Proceedings of the International Research Council on the Biomechanics of Injury conference: *proceedings of theProceedings of the International Research Council on the Biomechanics of Injury conference* International Research Council on Biomechanics of Injury, pp. 486-93.

Patrick, LM, Kroell, CK & Mertz, H 1965, 'Forces on the human body in simulated crashes', in Proceedings of the 9th Stapp Car Crash Conference: *proceedings of theProceedings of the 9th Stapp Car Crash Conference* pp. 237-60.

Pintar, FA, Yoganandan, N, Stemper, BD, Bostrom, O, Rouhana, SW, Digges, KH & Fildes, BN 2007, 'Comparison of PMHS, WorldSID, and THOR-NT responses in simulated far side impact', *Stapp Car Crash J*, vol. 51, pp. 313-60, Nlm, item: 18278603.

Rezende-Neto, J, Silva, FD, Porto, LB, Teixeira, LC, Tien, H & Rizoli, SB 2009, 'World Journal of Emergency Surgery', *World Journal of Emergency Surgery*, vol. 4, p. 26.

Ritchie, A 1992, 'Plastic bullets: significant risk of serious injury above the diaphragm', *Injury*, vol. 23, no. 4, pp. 265-6.

Ritchie, A & Gibbons, J 1990, 'Plastic bullets in Northern Ireland', *BMJ: British Medical Journal*, vol. 301, no. 6764, p. 1332.

Roberts, JC, O'Connor, JV & Ward, EE 2005, 'Modeling the effect of non-penetrating ballistic impact as a means of detecting behind armor blunt trauma', *J Trauma*, vol. 58, no. 6, pp. 1241-51, Nlm, item: 15995477.

Roberts, JC, Ward, EE, Merkle, AC & O'Connor, JV 2007, 'Assessing behind armor blunt trauma in accordance with the National Institute of Justice Standard for Personal Body Armor Protection using finite element modeling', *J Trauma*, vol. 62, no. 5, pp. 1127-33, Nlm, item: 17495712.

Rocke, L 1983, 'Injuries caused by plastic bullets compared with those caused by rubber bullets', *Lancet*, vol. 1, no. 8330, pp. 919-20, NLM, item: 6132230.

Rowden, P, Steinhardt, D & Sheehan, M 2008, 'Road crashes involving animals in Australia', *Accident Analysis & Prevention*, vol. 40, no. 6, pp. 1865-71.

Scaling, AAfAMCoI 1985, *Abbreviated Injury Scale 1985 Revision*, AAAM.

Schuster, PJ 2006, 'Current trends in bumper design for pedestrian impact', in Proceedings from 2006 SAE World Congress: Detroit, Michigan: *proceedings of theProceedings from 2006 SAE World Congress: Detroit, Michigan*.

Shaw, J 1972, 'Pulmonary contusion in children due to rubber bullet injuries', *British medical journal*, vol. 4, no. 5843, p. 764.

Sheridan, SM & Whitlock, RI 1983, 'Plastic baton round injuries', *Br J Oral Surg*, vol. 21, no. 4, pp. 259-67, NLM, item: 6580913.

Sheridan, SM & Whitlock, RI 1983, 'Plastic baton round injuries', *British Journal of Oral Surgery*, vol. 21, no. 4, pp. 259-67.

Shigeta, K, Kitagawa, Y & Yasuki, T 2009, 'Development of next generation human FE model capable of organ injury prediction', in 21st International Technical Conference on the Enhanced Safety of Vehicles: *proceedings of the21st International Technical Conference on the Enhanced Safety of Vehicles* pp. 09-0111.

Smith, L 2001, 'Evaluating baseball bat performance', *Sports Engineering*, vol. 4, no. 4, pp. 205-14.

Smith, L, Shenoy, M & Axtell, J 2000, 'Simulated composite baseball bat impacts using numerical and experimental techniques', *Proceedings of the Society of Experimental Mechanics, Orlando, FL, Society for Experimental Mechanics Inc., Bethal, CT*, pp. 5-8.

Song, E, Lecuyer, E & Trosseille, X 2011, 'Development of Injury Criteria for Frontal Impact Using a Human Body FE Model', in Proceedings of the 22nd Int. Tech. Conf. on the Enhanced Safety of Vehicles: *proceedings of theProceedings of the 22nd Int. Tech. Conf. on the Enhanced Safety of Vehicles*.

Sredojevic, B & Zivkovic, G 1998, *Vehicle front protection systems (Bull Bars) : Airbag Compatibility Tests*, Automotive Safety Engineering Pty Ltd, Australia,<.

Stapp, JP 1951a, *Human Exposure to Linear Deceleration. Part 2: the Forward-facing Position and the Development of a Crash Harness*.

Stahlschmidt, S, D'Souza, R, Franz, U, Burger, M & Maurath, CA 2010, *LSTC EuroSID-2re Finite Element Model*, Livermore Softwre Technology Corporation, Livermore, CA, USA.

Stahlschmidt, S, Gromer, A, Huang, Y & Franz, U 2012, 'Dummy Model Validation and its Assessment'.

Stapp, JP 1951b, 'Human tolerance to deceleration; summary of 166 runs', *Journal of Aviation Medicine*, vol. 22, no. 1, pp. 42-5; passim.

Stapp, JP 1955, 'Effects of mechanical force on living tissues. I. Abrupt deceleration and windblast', *The Journal of aviation medicine*, vol. 26, no. 4, p. 268.

Stapp, JP 1970a, 'Voluntary human tolerance levels', *Impact Injury and Crash Protection*, pp. 308-49.

Stapp, JP (ed.) 1970b, *Voluntary human tolerance levels*, in Impact Injury and Crash Protection, Springfield, IL, USA.

States, JD 1969, 'The Abbreviated and the Comprehensive Research Injury Scales', *SAE Technical Paper 690810*.

States, JD, Fenner, HA, Flamboe, EE, Nelson, WD & Hames, LN 1971, 'Field Application and Research Development of the Abbreviated Injury Scale,' *SAE Technical Paper 710873*.

Steele, JA, McBride, SJ, Kelly, J, Dearden, CH & Rocke, LG 1999, 'Plastic bullet injuries in Northern Ireland: experiences during a week of civil disturbance', *J Trauma*, vol. 46, no. 4, pp. 711-4, NLM, item: 10217239.

Sturdivan, LM, Viano, DC & Champion, HR 2004, 'Analysis of injury criteria to assess chest and abdominal injury risks in blunt and ballistic impacts', *J Trauma*, vol. 56, no. 3, pp. 651-63, Nlm, item: 15128140.

Tanaka, K, Sato, F, Oodaira, H, Teranishi, Y & Ujihashi, S 2006, 'Construction of the finite-element models of golf balls and simulations of their collisions', *Proceedings of the Institution of Mechanical Engineers, Part L: Journal of Materials Design and Applications*, vol. 220, no. 1, pp. 13-22.

Thota, NM, Eepaarachchi, JA & Lau, KT 2012, 'Develop and validate a biomechanical surrogate of the human thorax using corrugated sheets: a feasibility study', in Proceedings of the 7th Australasian Congress on Applied Mechanics (ACAM 7): *proceedings of theProceedings of the 7th Australasian Congress on Applied Mechanics (ACAM 7)* Engineers Australia.

Thota, NM, Eepaarachchi, JA & Lau, KT 2013a, 'Effect of the energy absorbing mechanisms on the blunt thoracic trauma caused by a typical foam projectile', *International Journal of Engineering Research and Technology*, vol. 6, no. 5, pp. 37-42, Nlm.

Thota, NM, Eepaarachchi, JA & lau, KT 2013b, 'Important aspects of finite element modelling of low density thermo plastic closed cell foams', *International journal of Mechanical Engineering Research*, vol. 3, pp. 291-4, Nlm.

Thota, NM, Eepaarachchi, JA & Lau, KT 2013c, 'Effect of the foam embellishments on the pedestrian safety of the vehicle front protection systems', *International Journal of Engineering Research and Technology*, vol. 6, no. 5, pp. 11-4, Nlm.

Ueyama, M, Ogawa, S, Chikasue, H & Muramatu, K 1998, 'Relationship between driving behaviour and traffic accidents-accident data recorder and driving monitor recorder', in 16th International Technical Conference on the Enhanced Safety of Vehicles: *proceedings of the16th International Technical Conference on the Enhanced Safety of Vehicles*.

Viano, DC & Lau, IV 1988, 'A viscous tolerance criterion for soft tissue injury assessment', *J Biomech*, vol. 21, no. 5, pp. 387-99, NLM, item: 3417691.

Viano, DC & Lau, IV 1988, 'A viscous tolerance criterion for soft tissue injury assessment', *J Biomech*, vol. 21, no. 5, pp. 387-99.

Viano, DC, Lau, IV, Andrzejak, DV & Asbury, C 1989, 'Biomechanics of injury in lateral impacts', *Accid Anal Prev*, vol. 21, no. 6, pp. 535-51, Nlm, item: 2629762.

Viano, DC, Bir, CA, Cheney, AK & Janda, DH 2000, 'Prevention of commotio cordis in baseball: an evaluation of chest protectors', *J Trauma*, vol. 49, no. 6, pp. 1023-8, NLM, item: 11130483.

Vlessis, AA & Trunkey, DD 1997, 'Non-penetrating injury of the thorax', in GJ Cooper, et al. (eds), *Scientific foundation of trauma*, Butterworth-Heinemann, Oxford, pp. 127-43.

Volokh, E 2009, 'Nonlethal Self-Defense,(Almost Entirely) Nonlethal Weapons, and the Rights to Keep and Bear Arms and Defend Life', *Stan. L. Rev.*, vol. 62, p. 199.

Walker, HL, Carr, DJ, Chalmers, DJ & Wilson, CA 2010, 'Injury to recreational and professional cricket players: Circumstances, type and potential for intervention', *Accident Analysis & Prevention*, vol. 42, no. 6, pp. 2094-8.

Wang, HC 1995, 'Development of a side impact finite element human thoracic model ', Wayne State University, Detroit, Michigan, USA.

Wang, JT 1989, 'Analytical Studies of Injury Criteria for the Thorax', *J Biomech Eng*, vol. 111, no. 2, pp. 128-35.

Widder, J, Perhala, C & Rascoe, J 2003, 'Caseless, Variable Velocity Systems for Precision Non-Lethal Fires to beyond 100 Meters. Part-II: Terminal effects Study, Selection of Projectile Parameters', *AMMTIAC-WSTIAC Journal*, vol. 1, no. 2, pp. 13-6.

Widder, JM, Butz, DJ & Milosh, JM 1997, *Assessing the Blunt Trauma Potential of Free Flying Projectiles for Development and Safety Certification of Non-Lethal Impactors*, Battelle Columbus Operations, Columbus, OH 43201, USA,<.

Yang, KH & King, AI 2004, 'Development of an anthropomorphic numerical surrogate for injury reduction (ANSIR)', *Journal of Mechanics in Medicine and Biology*, vol. 4, no. 04, pp. 447-61.

Zhao, J & Narwani, G 2005, 'Development of a human body finite element model for restraint system R&D applications', in 19th ESV Conference: *proceedings of the19th ESV Conference* TAKATA-Automotive system laboratory.

APPENDIX – I

List of publications (technical papers published in the peer-reviewed conference proceedings and international journals)

1. Thota, N, Epaarachchi, J & Lau, KT 2013, 'CAE Simulation Based Methodology for Airbag Compliant Vehicle Front Protection System Development', *2013*.

2. Thota, N, Epaarachchi, J & Lau, KT 2014, 'Development and validation of a thorax surrogate FE model for assessment of trauma due to high speed blunt impacts', *Journal of Biomechanical Science and Engineering*, vol. 9, no. 1, pp. JBSE0008-JBSE.

3. Thota, NM, Eepaarachchi, JA & Lau, KT 2012, 'Develop and validate a biomechanical surrogate of the human thorax using corrugated sheets: a feasibility study', in Proceedings of the 7th Australasian Congress on Applied Mechanics (ACAM 7): *proceedings of theProceedings of the 7th Australasian Congress on Applied Mechanics (ACAM 7)* Engineers Australia.

4. Thota, NM, Eepaarachchi, JA & Lau, KT 2013, 'Effect of the energy absorbing mechanisms on the blunt thoracic trauma caused by a typical foam projectile', *International Journal of Engineering Research and Technology*, vol. 6, no. 5, pp. 37-42, Nlm.

5. Thota, NM, Eepaarachchi, JA & Lau, KT 2013, 'Effect of the foam embellishments on the pedestrian safety of the vehicle front protection systems', *International Journal of Engineering Research and Technology*, vol. 6, no. 5, pp. 11-4, Nlm.

6. Thota, NM, Eepaarachchi, JA & lau, KT 2013, 'Important aspects of finite element modelling of low density thermo plastic closed cell foams', *International journal of Mechanical Engineering Research*, vol. 3, pp. 291-4, Nlm.

7. Thota, NM, Eepaarachchi, JA & Lau, KT 2014, 'Effect of energy absorbing mechanisms on the blunt thoracic trauma caused by ballistic impacts', in Proceedings of the 8th Australasian Congress on Applied Mechanics (ACAM 8): *proceedings of theProceedings of the 8th Australasian Congress on Applied Mechanics (ACAM 8)* Engineers Australia, Melbourne Convention Centre, Melbourne, Victoria, Ausralia.

8. Thota, NM, Eepaarachchi, JA & Lau, KT 2014, 'Evaluation of the blunt thoracic trauma due to baseball impacts - Review of the blunt criterion', in Proceedings of the 8th Australasian Congress on Applied Mechanics (ACAM 8): *proceedings of theProceedings of the 8th Australasian Congress on Applied Mechanics (ACAM 8)* Engineers Australia, Melbourne Convention Centre, Melbourne, Victoria, Ausralia.

9. Thota, NM, Eepaarachchi, JA & Lau, KT 2014, 'Review of anthropomorphic test dummies for the evaluation of thoracic trauma due to blunt ballistic impacts', in Proceedings of the 8th Australasian Congress on Applied Mechanics (ACAM 8): *proceedings of theProceedings of the 8th Australasian Congress on Applied Mechanics (ACAM 8)* Engineers Australia, Melbourne Convention Centre, Melbourne, Victoria, Ausralia.

10. Thota, NM, Eepaarachchi, JA & Lau, KT 2014, 'Viscous criterion and its relation with the projectile-thorax energy interactions', in Proceedings of the 8th Australasian Congress on Applied Mechanics (ACAM 8): *proceedings of theProceedings of the 8th Australasian Congress on Applied Mechanics (ACAM 8)* Engineers Australia, Melbourne Convention Centre, Melbourne, Victoria, Ausralia.

Technical papers under consideration for publication by peer reviewed conferences and international journals

11. Thota, N, Epaarachchi, J & Lau, KT , 'Evaluation of the blunt thoracic trauma caused by solid sports balls', is under consideration for the publication in the *Journal of Biomechanical Science and Engineering*. Final review was also completed.

12. Thota, NM, Eepaarachchi, JA & Lau, KT, 'Evaluation of the performance of three elastomers for non-lethal projectile applications', is under consideration for the publication in the proceedings of the 11th International DYMAT Conference, scheduled to be held in September 2015 at Leguna, Switzerland.

13. Thota, NM, Eepaarachchi, JA & Lau, KT, 'Evaluation of the performance of a rubber like elastomer and two high energy absorbing foams as chest protectors for baseball players', is under review for the publication in the European Physical Journal (special edition) by the organizing committee of the DYMAT-2015 international conference